TECHNICAL REPORT N-71-2

DYNAMIC TESTS OF LARGE REINFORCING BAR SPLICES

by

W. J. Flathau

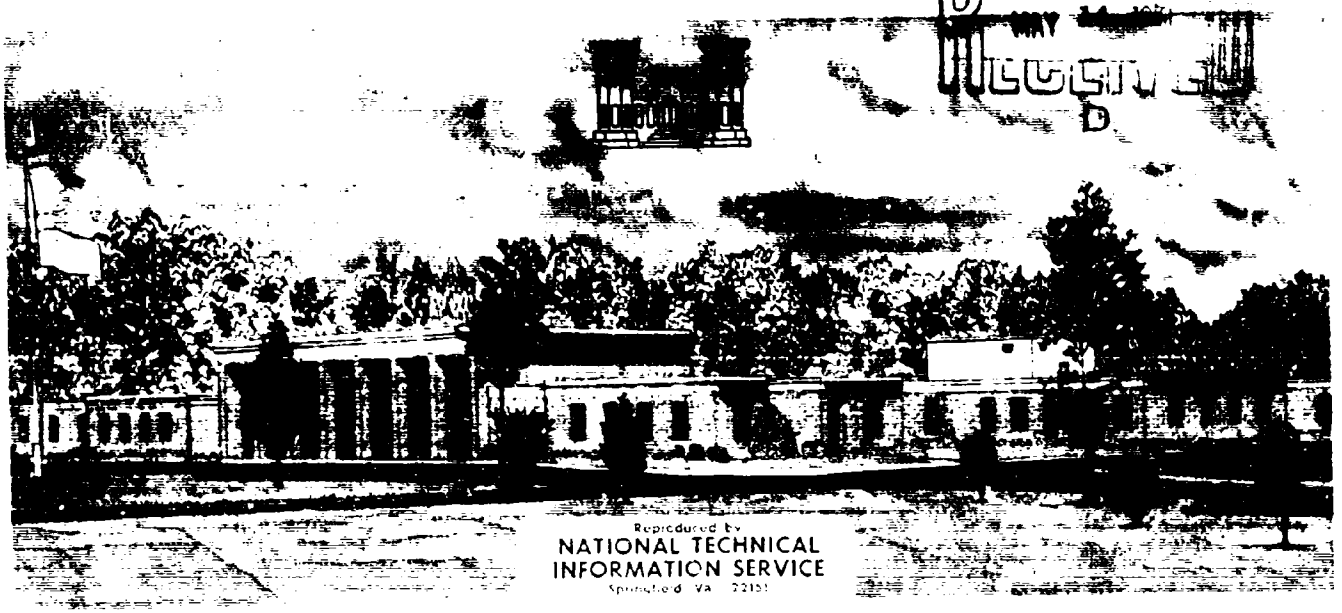

April 1971

Sponsored by U. S. Army Engineer Division, Huntsville

Conducted by U. S. Army Engineer Waterways Experiment Station, Vicksburg, Mississippi

183

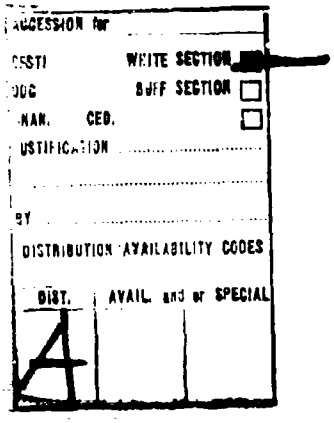

Destroy this report when no longer needed. Do not return it to the originator.

The findings in this report are not to be construed as an official Department of the Army position unless so designated by other authorized documents.

TECHNICAL REPORT N-71-2

DYNAMIC TESTS OF LARGE REINFORCING BAR SPLICES

by

W. J. Flathau

April 1971

Sponsored by U. S. Army Engineer Division, Huntsville

Conducted by U. S. Army Engineer Waterways Experiment Station, Vicksburg, Mississippi

FOREWORD

This report was prepared in the Nuclear Weapons Effects Division (NWED), U. S. Army Engineer Waterways Experiment Station (WES), under the sponsorship of the U. S. Army Engineer Division, Huntsville. The work was accomplished during the period March through December 1970. During this time, Mr. G. L. Arbuthnot, Jr., was Chief of NWED.

This report was prepared by Mr. William J. Flathau, Chief, Protective Structures Branch, NWED, and is essentially a thesis submitted in partial fulfillment of the requirements for the degree of Master of Science in Civil Engineering to the Mississippi State University, State College, Mississippi.

Directors of WES during the preparation and publication of this report were COL Levi A. Brown, CE, and COL Ernest D. Peixotto, CE. Technical Director was Mr. F. R. Brown.

ACKNOWLEDGEMENT

In accomplishing any research effort, the energies and contributions of many are usually involved. Consequently, the author would like to mention a few who contributed and to thank them as well as others who are not mentioned by name.

Special acknowledgement is given to Mr. Guy L. Arbuthnot, Jr., Chief of the Nuclear Weapons Effects Division (NWED) of U. S. Army Engineer Waterways Experiment Station (WES) for his encouragement and for providing the environment in which to pursue the research task. Greatly appreciated is the support of COL Levi A. Brown, CE, and COL Ernest D. Peixotto, CE, the former and current Directors of WES, through whose efforts a graduate center with Mississippi State University (MSU) was established and is being maintained. Invaluable discussions were held with Messrs. Bob Walker, Jim Balsara, and Tom Kennedy of the Protective Structures Branch (PSB) of the NWED. It would not have been possible to conduct the experimental portion of the effort without the expert help of Messrs. Jim Hossley and Billy Benson of the Operations Group of the PSB and Messrs. Nick Lavecchia, Jim Pickens, and Jerry Graham of the Instrumentation Services Division.

The effort was part of a research program sponsored by the U. S. Army Engineer Division, Huntsville, and monitored by Messrs. M. Dembo and M. Jones.

The interest of Professor Walter Carnes, the Director of the graduate center, is also recognized. The review and guidance of Professors Charles Ivy, Keith Denson, and Ralph Sinno of the Civil Engineering Department of MSU are appreciated.

Special thanks are extended to Mrs. F. Ellison, Mrs. M. Cheney, and Mrs. N. Denmon, all of the PSB, who typed portions of the manuscript. The excellent support from numerous people in the Reproduction and Reports Office of WES is also appreciated.

The interest and assistance of Messrs. Bob Smith and Leonard Gelfand, representatives of ERICO Products, the manufacturer of the Cadweld splice, are acknowledged. The assistance of Mr. Bob Longstreet, a representative of Thermex Metallurgical, Inc., the manufacturer of the Thermit splice, is also acknowledged.

Conversations with Professors Bill Hall and Mete Sozen of the University of Illinois concerning certain aspects of this study are also appreciated.

Last, but not least, the patience of an understanding wife and son cannot be forgotten.

TABLE OF CONTENTS

FOREWORD v

ACKNOWLEDGEMENT. vii

LIST OF TABLES xi

LIST OF FIGURES. xii

LIST OF SYMBOLS. xix

ABSTRACT xxi

CHAPTER 1 INTRODUCTION. 1

1.1 Background. 1

1.2 Objective 3

1.3 Scope 3

1.4 Previous Work 4

CHAPTER 2 PROCEDURES. 9

2.1 Preparation of Specimens. 9

2.1.1 As-Rolled Bars. 10

2.1.2 Machined Bars 10

2.1.3 Butt-Welded Splice. 10

2.1.4 Thermit-Welded Splice 11

2.1.5 Cadweld Splice. 13

2.1.6 Method of Gripping Specimens. 15

2.2 Instrumentation 16

2.2.1 Load. 17

2.2.2 Strain. 18

2.2.3 Acceleration. 20

2.2.4 Optical Tracker 21

2.2.5 Recording Instrumentation 23

TABLE OF CONTENTS--Continued

2.3 Test Device 23

2.4 Load Analysis and Data Reduction. 25

CHAPTER 3 RESULTS 53

3.1 Tabulated Results 53

3.2 Posttest Photographs. 53

3.3 Stress-Strain Plots 53

CHAPTER 4 DISCUSSION OF RESULTS 120

4.1 Spliced Bars. 120

4.1.1 Butt-Welded Splices 122

4.1.2 Thermit Splices 122

4.1.3 Cadweld Splices 122

4.2 Dynamic Strength Characteristics. 124

4.2.1 Grade 60 Bars 126

4.2.2 Grade 75 Bars 127

4.3 Load Analysis 128

4.3.1 Rapid Load Tests. 128

4.3.2 Machined Specimens. 129

CHAPTER 5 SUMMARY OF RESULTS, CONCLUSIONS, AND RECOMMENDATIONS. . 140

5.1 Summary of Results. 140

5.2 Conclusions 140

5.3 Recommendations 141

BIBLIOGRAPHY 143

APPENDIX A TEST RECORDS 147

LIST OF TABLES

Tables

2.1 Mill Report for No. 11 Deformed Steel Reinforcing Bars. . . 28

2.2 Results of Independent Chemical Analysis. 29

2.3 Summary of Test Numbers and Weights for Various Specimens . 30

2.4 Geometric Properties of Some Reinforcing Bars Tested. . . . 31

2.5 Results of X-Ray Tests of Butt-Welded Specimens 32

2.6 Summary of Measurements for All Tests 33

3.1 Summary of Test Results, As-Rolled Bars, Grade 60 55

3.2 Summary of Test Results, Machined Bars. 56

3.3 Summary of Test Results, Butt-Welded Splices. 56

3.4 Summary of Test Results, Thermit-Welded Splices 57

3.5 Summary of Test Results, Cadweld Splices. 57

4.1 Comparative Effectiveness of the Various Spliced Bars . . . 130

4.2 Approximate Relation of Rockwell Hardness Numbers to Tensile Strength 131

4.3 Loads Corrected for Inertial Effects on Machined-Bar Specimens 132

4.4 Upper and Lower Loads Determined from Strain Gage Readings on Machined-Bar Specimens 134

LIST OF FIGURES

Figures

1.1	Test schedule	8
2.1	Specimen types tested	34
2.2	Schematic and dimensions for machined-bar specimens	35
2.3	Butt-welded splice	36
2.4	Thermit splicing kit and rebar to be spliced	36
2.5	Thermit process, placing molds	37
2.6	Thermit process, positioning molds	37
2.7	Thermit process, placing tapping disk	37
2.8	Thermit process, adding Thermit	37
2.9	Thermit process, adding starting Thermit	38
2.10	Thermit process, ignition	38
2.11	Thermit process, postignition	38
2.12	Cadweld splicing kit	39
2.13	Cadweld process, placing metal sleeve	40
2.14	Cadweld process, end-alignment fittings	40
2.15	Cadweld process, horizontal packing clamp	40
2.16	Cadweld process, ceramic insert	40
2.17	Cadweld process, seating of pouring basin	41
2.18	Cadweld process, crucible and addition of Cadweld powder	41
2.19	Cadweld process, ignition	41
2.20	Cadweld process, crucible and other fittings removed	41
2.21	Poured-metal gripper	42
2.22	Alignment jig for poured-type grippers	42
2.23	Pouring molten babbitt metal into gripper	43

LIST OF FIGURES--Continued

Figures

2.24 End view of poured-type gripper 44

2.25 Gripper for machined bars 44

2.26 Bar with poured-type grippers ready for testing 45

2.27 Machined bar with one gripper attached. 45

2.28 Gage locations and identifications for all specimen types . 46

2.29 Instrumented specimen in place ready for testing. 47

2.30 Marking strain gage locations 48

2.31 Strain gages applied to metal surface 49

2.32 Pressing gages to bar 49

2.33 Wire attached between gage tab and terminal strip 50

2.34 Lead wires attached 50

2.35 200-kip-capacity dynamic loading device 51

2.36 Spring-mass model of test configuration 52

3.1 Posttest, as-rolled bars, Grade 60. 58

3.2 Posttest, machined bars, Grade 60 58

3.3 Posttest, machined bars, Grade 75 59

3.4 Posttest, butt-welded splices, Grade 60 60

3.5 Posttest, Thermit splices, Grade 60 61

3.6 Posttest, Cadweld splices, Grade 60 62

3.7 Posttest, intermediate load rate, Grade 75. 63

3.8 Posttest, intermediate load rate, Grade 75, bars with "X" deformations. 63

3.9 As-rolled bar, Grade 60, Test No. 144 64

3.10 As-rolled bar, Grade 60, Test No. 172 64

LIST OF FIGURES--Continued

Figures

3.11 As-rolled bar, Grade 60, Test No. 199 66

3.12 Machined bar, Grade 60, Test No. 145. 66

3.13 Machined bar, Grade 60, Test No. 148. 68

3.14 Machined bar, Grade 60, Test No. 152. 68

3.15 Machined bar, Grade 60, Test No. 161. 70

3.16 Machined bar, Grade 60, Test No. 164. 70

3.17 Machined bar, Grade 60, Test No. 167. 72

3.18 Machined bar, Grade 60, Test No. 188. 72

3.19 Machined bar, Grade 60, Test No. 191. 74

3.20 Machined bar, Grade 60, Test No. 194. 74

3.21 Machined bar, Grade 75, Test No. 155. 76

3.22 Machined bar, Grade 75, Test No. 170. 76

3.23 Machined bar, Grade 75, Test No. 173. 78

3.24 Machined bar, Grade 75, Test No. 176. 78

3.25 Machined bar, Grade 75, Test No. 180. 80

3.26 Machined bar, Grade 75, Test No. 185. 80

3.27 Machined bar, Grade 75, Test No. 197. 82

3.28 Machined bar, Grade 75, Test No. 200. 82

3.29 Butt-welded splice, Grade 60, Test No. 146. 84

3.30 Butt-welded splice, Grade 60, Test No. 150. 84

3.31 Butt-welded splice, Grade 60, Test No. 159. 86

3.32 Butt-welded splice, Grade 60, Test No. 163. 86

3.33 Butt-welded splice, Grade 60, Test No. 168. 88

3.34 Butt-welded splice, Grade 60, Test No. 186. 88

LIST OF FIGURES--Continued

Figures

3.35 Butt-welded splice, Grade 60, Test No. 190. 90

3.36 Butt-welded splice, Grade 60, Test No. 195. 90

3.37 Butt-welded splice, Grade 75, Test No. 174. 92

3.38 Butt-welded splice, Grade 75, Test No. 178. 92

3.39 Butt-welded splice, Grade 75, Test No. 182. 94

3.40 Thermit-welded splice, Grade 60, Test No. 149 94

3.41 Thermit-welded splice, Grade 60, Test No. 153 96

3.42 Thermit-welded splice, Grade 60, Test No. 157 96

3.43 Thermit-welded splice, Grade 60, Test No. 162 98

3.44 Thermit-welded splice, Grade 60, Test No. 166 98

3.45 Thermit-welded splice, Grade 60, Test No. 171 100

3.46 Thermit-welded splice, Grade 60, Test No. 189 100

3.47 Thermit-welded splice, Grade 60, Test No. 193 102

3.48 Thermit-welded splice, Grade 60, Test No. 198 102

3.49 Thermit-welded splice, Grade 75, Test No. 177 104

3.50 Thermit-welded splice, Grade 75, Test No. 181 104

3.51 Thermit-welded splice, Grade 75, Test No. 184 106

3.52 Cadweld splice, Grade 60, Test No. 147. 106

3.53 Cadweld splice, Grade 60, Test No. 151. 108

3.54 Cadweld splice, Grade 60, Test No. 156. 108

3.55 Cadweld splice, Grade 60, Test No. 160. 110

3.56 Cadweld splice, Grade 60, Test No. 169. 110

3.57 Cadweld splice, Grade 60, Test No. 187. 112

3.58 Cadweld splice, Grade 60, Test No. 192. 112

LIST OF FIGURES--Continued

Figures

3.59	Cadweld splice, Grade 60, Test No. 196.	114
3.60	Cadweld splice, Grade 75, Test No. 175.	114
3.61	Cadweld splice, Grade 75, Test No. 179.	116
3.62	Cadweld splice, Grade 75, Test No. 183.	116
3.63	Cadweld splice, Grade 75 ("X" ribs), Test No. 201	118
3.64	Cadweld splice, Grade 75 ("X" ribs), Test No. 202	118
4.1	Composite stress-strain curves, butt-welded splices . . .	134
4.2	Composite stress-strain curves, Thermit splices	135
4.3	Composite stress-strain curves, Cadweld splices	136
4.4	Yield stress versus strain rate, Grade 60 bars.	137
4.5	Yield stress versus strain rate, Grade 75 bars.	138
4.6	Yield stress versus strain rate, machined bars, Grade 75.	139
A.1	As-rolled bar, Grade 60, intermediate load rate, Test 172.	148
A.2	Machined bar, Grade 60, rapid load rate, Test 148	149
A.3	Machined bar, Grade 60, intermediate load rate, Test 167.	151
A.4	Machined bar, Grade 75, intermediate load rate, Test 180.	152
A.5	Machined bar, Grade 60, slow load rate, Test 191.	153
A.6	Butt-welded splice, Grade 60, rapid load rate, Test 159 .	154
A.7	Butt-welded splice, Grade 60, intermediate load rate, Test 163.	155
A.8	Butt-welded splice, Grade 75, intermediate load rate, Test 174.	156

LIST OF FIGURES--Continued

Figures

A.9 Thermit splice, Grade 60, rapid load rate, Test 157 . . . 157

A.10 Thermit splice, Grade 60, slow load rate, Test 198. . . . 158

A.11 Cadweld splice, Grade 60, rapid load rate, Test 156 . . . 159

A.12 Cadweld splice, Grade 60, intermediate load rate, Test 169. 160

A.13 Cadweld splice, Grade 75, intermediate load rate, Test 179. 161

A.14 Cadweld splice, Grade 75, intermediate load rate, Test 202. 162

LIST OF SYMBOLS

a_ℓ	Lower acceleration	LT^{-2}
a_u	Upper acceleration	LT^{-2}
A_1	Area under stress-strain curve bounded by $1.05\sigma_y$	$FL^{-2}LL^{-1}$
A_2	Total area under stress-strain curve	$FL^{-2}LL^{-1}$
E	Young's modulus of elasticity	FL^{-2}
F	Fundamental unit of force	F
F(t)	The applied time-dependent force	F
k_1	The spring constant of the upper reaction member	FL^{-1}
k_2	The spring constant of the test specimen	FL^{-1}
k_3	The spring constant of the loading ram	FL^{-1}
L	Fundamental unit of length	L
M_1	Mass of half the test specimen and all of the upper gripper	$FL^{-1}T^2$
M_2	Mass of half the test specimen and all of the lower gripper	$FL^{-1}T^2$
M_3	Mass of the loading ram	$FL^{-1}T^2$
P_ℓ	Lower load	F
$\dot{P}_\ell$	Loading rate, lower load	FT^{-1}
P_u	Upper load	F
$\dot{P}_u$	Loading rate, upper load	FT^{-1}
t_ℓ	Time to peak lower load	T
t_u	Time to peak upper load	T
t_y	Average time to yield strain	T
T	Fundamental unit of time	T
T_ℓ	Lower reference line for optical tracker	-
T_u	Upper reference line for optical tracker	-

x_1	The displacement of M_1	L
x_2	The displacement of M_2	L
x_3	The displacement of M_3	L
$\ddot{x}_1$	The acceleration of M_1	LT^{-2}
$\ddot{x}_2$	The acceleration of M_2	LT^{-2}
$\ddot{x}_3$	The acceleration of M_3	LT^{-2}
ϵ	Strain	LL^{-1}
ϵ_a	Average strain	LL^{-1}
ϵ_c	Center strain	LL^{-1}
ϵ_ℓ	Lower strain	LL^{-1}
ϵ_m	Strain at maximum stress	LL^{-1}
ϵ_u	Upper strain	LL^{-1}
ϵ_y	Strain at yield	LL^{-1}
$\dot{\epsilon}$	Average strain rate	$LL^{-1}T^{-1}$
σ	Stress	FL^{-2}
σ_{dy}	Dynamic yield stress	FL^{-2}
σ_m	Maximum stress	FL^{-2}
σ_y	Yield stress	FL^{-2}

ABSTRACT

Dynamic tensile tests were conducted at rapid, intermediate, and slow rates of strain on specimens of No. 11 reinforcing bars of Grades 60 and 75 A615 billet steel. As-rolled bars, machined bars, butt-welded splices, Thermit splices, and Cadweld splices were prepared. The as-rolled and machined specimens were tested primarily to determine the tensile strength characteristics of the Grades 60 and 75 bars for use when assessing how effective the various spliced specimens were when tested. All tests were conducted in a 700,000-pound-capacity dynamic loader.

Under all loading rates, the breaking strength for all three splice types was greater than the 125 percent of nominal yield required by standards set forth by the American Concrete Institute, the American Welding Society, and the Concrete Reinforcing Steel Institute. Apparently, however, the heat produced by the three splicing methods appreciably reduced the ductility of all spliced bars. The strains in the bars when any of the splice types failed were generally less than 25 percent of the maximum strain achieved by the as-rolled or machined bars at rupture. Very few of the spliced bars met ASTM standards for minimum elongations of 7 and 5 percent, respectively, for Grades 60 and 75 bars. The butt-welded splices, Thermit splices, and Cadweld splices all performed satisfactorily under rapid rates of loading. However, it is believed that better quality control can be achieved at a lesser cost using either a Thermit or Cadweld splice in lieu of a butt-welded splice.

The Grade 60 bars were more ductile than the Grade 75 bars and were

also more sensitive to the influence of the strain rate on the dynamic strength of the bars tested.

An optical tracker was used to measure postyield strains for all the specimen types. This device made it possible, especially in the rapid strain rate tests, to measure successfully the strains across the various spliced specimens.

CHAPTER 1

INTRODUCTION

1.1 BACKGROUND

In the design of reinforced concrete structures to resist dynamic forces such as those produced by earthquakes or blasts from nuclear detonations, the loading rate influences the magnitude of the yield strength[1-5] of the steel reinforcement as well as the compressive strength of the concrete. Hence, an increase in yield strength means an increase in the energy-absorbing capacity, i.e. resistance, of the reinforced concrete structural system. Economic considerations necessitate designing blast-resistant structures to respond in the inelastic range of response to take full advantage of the energy-absorbing capacity of the system instead of designing a system well within the elastic range of response as is done for conventional design. In most large structures, it is necessary to splice reinforcing bars; hence, it is essential that the connection be capable of transferring at least as much load as the bar itself is able to sustain. Bars greater than size No. 11 should be spliced either by mechanical means or by welding; codes (ACI, AWS, and CRSI)[6-9] require that these spliced joints be able to withstand a stress greater than 125 percent of the nominal yield strength of the grade bar being used.

From a search of the literature, it appears that only a limited number of studies (Keenan, Siess, and Cowell),[10-12] primarily of small-sized bars, have been conducted to determine the increase in yield strength of steel reinforcing bars with increases in loading rates. Only one study examined the influence of rapid loads on the response of

reinforcing bars that had been spliced by a butt-welding technique; no other references were found describing dynamic tests of bars spliced by use of other techniques. In all these referenced studies, the main reason for conducting tests on small-sized reinforcing bars was the limited capacity of available dynamic loading equipment. Available at the U. S. Army Engineer Waterways Experiment Station (WES) is a dynamic ram loader[13] that can apply 200,000 pounds of force within 1-1/2 msec, thus making it possible to test large-sized steel reinforcing bars at very rapid loading rates. Information derived from such tests would be very useful to designers of structures to resist dynamic loads. However, static tests[14] have been conducted for large-sized reinforcing bars that were spliced by use of four different techniques, i.e. the butt-weld, Thermit, Cadweld, and Howlett techniques.

There are essentially three types[9] of steel (i.e. billet steel, A615; axle steel, A617; and rail steel, A616) used in making deformed reinforcing bars. Of the three types, the billet-steel bars are most commonly used. Within the billet-steel bar types are three grades, i.e. 40, 60, and 75. The minimum tensile strength and minimum yield point for these grades, respectively, are 70,000 and 40,000 psi; 90,000 and 60,000 psi; and 100,000 and 75,000 psi. The Grades 60 and 75 bars are being found more useful as a building material for strategic structures designed to resist dynamic loads and, consequently, were considered in this study. The ASTM specifications for these two grade bars are described in References 15 and 16, respectively. The ASTM specifications for deformation requirements and mechanical testing of steel products are given in References 17 and 18, respectively.

1.2 OBJECTIVE

The primary objective of this study was to determine the effectiveness of three different splicing techniques (butt-weld, Thermit, and Cadweld techniques) for No. 11 reinforcing bars made of billet steel, A615, for Grades 60 and 75 when stressed in tension at various loading rates.

Secondary objectives included:

1. A determination of the dynamic strength characteristics of the two grades of steel used.

2. An investigation to verify the magnitude of loads applied to the test specimens.

3. A measurement of postyield strain using an optical tracker.

1.3. SCOPE

A total of 59 tests were conducted at three different general rates of strain (rapid, intermediate, and slow) on 2-1/2-foot-long specimens of No. 11 reinforcing bars of Grades 60 and 75, both grades being of the same type, i.e. billet steel, A615. The deformations on all bars were of the barrel rib type except for two special Cadweld specimens that had "X" type deformations. The bars were spliced according to specifications stipulated by the Concrete Reinforcing Steel Institute as well as by instructions from the suppliers of the Cadweld and Thermit splices. Manufacturers' representatives prepared the specimens using both Cadweld and Thermit splices. Machined and as-rolled bars were also tested to determine the basic tensile strength characteristics of the Grades 60 and 75 steel bars. A schedule of tests for the various types of specimens is shown in Figure 1.1. All tests were conducted with the WES 200-kip-capacity loader.

All specimens were instrumented with strain gages in an attempt to determine the state of strain at various locations on the test bars. Accelerometers were attached to the grippers holding the bars in order to determine the acceleration-time histories of the mass at the ends of the bars for use in assessing the influence of inertial effects. Two optical trackers were used to measure strain over an 8-inch gage length for spliced bars and over a 3-inch gage length for machined bars. The trackers were especially useful in determining strain across the three types of splices tested. A three-degree-of-freedom mathematical spring-mass model of the loading system was formulated by lumping the mass of the upper and lower grips, the test specimen, and loading ram. By using this formulation, it was possible to determine the true load applied to the test specimens during rapid loading tests.

1.4 PREVIOUS WORK

The most recent and perhaps most pertinent work related to this study is described in References 10, 11, 12, and 14. In only one study[10] did the author attempt to determine the influence that the inertial forces of the grip and load cell would have on the load applied to the specimen; for these tests it appeared that such forces were negligible. However, for rates of strain greater than were considered, the influence of inertia could become significant. A brief summary of References 10, 11, 12, and 14 follows.

1. Reference 10 (Keenan and Feldman). A total of 34 tests were conducted using intermediate-grade (A15) steel reinforcing bars of sizes 6, 7, and 9. In most tests, the maximum stress level was reached in a time of 6 msec and then held constant until yielding was complete. If

the peak stress level was slightly greater than the static yield strength, the delay time to reach yield was long (up to several seconds), but if the peak stress was much greater, the delay time was short (i.e. several milliseconds). The authors believed that even though these tests were not conducted at a constant strain rate, the results were reliable. The static yield strengths ranged from 40,500 to 48,900 psi, and the dynamic yield strengths varied from 102 to 149 percent of the static yield value, depending on the strain rate.

2. Reference 11 (Siess). A total of 59 tests were conducted, 35 rapid and 24 static load tests, using No. 6 bars of two types of steel, i.e. intermediate grade (A15) and high strength (A431). The main purpose of this study was to determine the effectiveness of intermediate-grade and high-strength bars that had been butt welded. The tests were about equally divided between butt-welded and as-rolled specimens. The time to maximum load for the high-strength bars ranged from 0.005 to 0.013 sec. The time to yield for the intermediate-grade bars ranged from about 0.003 to 0.004 sec. In these tests, the dynamic yield strengths were only slightly greater (up to 5 percent) than the static strengths for both the high- and low-strength steels. Also, the welded bars performed about the same as the as-rolled bars except in the cases of poor welds.

3. Reference 12 (Cowell). A total of 94 tests were conducted using No. 8 reinforcing steel bars of four different types, i.e., A15 (intermediate grade), A15 (hard grade), A431 (75,000-psi minimum yield), and A432 (40,000-psi minimum yield). The effects of strain rate (up to 1.7 in/in/sec) and machine testing speed (up to 30 in/sec) on the upper

yield stress and tensile strength of each steel were determined. At the maximum strain rate, the percentage increases in upper yield stress over the static values were 53, 40, and 18 and the percentage increases in lower yield stresses were 29, 27, and 11 for the A15 intermediate, A15 hard, and A432 grades of steel, respectively. The increase in yield stress was 9 percent at the maximum strain rate for the A431 steel. The yield and tensile stresses for machined bars were slightly higher than the values obtained for the as-rolled bars for all four types of steel.

4. Reference 14 (Holt). A total of 98 static tensile tests were conducted using No. 9, 11, 14, and 18 reinforcing steel bars all classed as intermediate-grade steel (A15). Tested were butt-welded, Thermit, Cadweld, and Howlett splices along with as-rolled bars to determine the basic strength characteristics of the various bars. The static yield strengths for the four bar types ranged from 40,000 to 60,000 psi, and the static tensile strengths ranged from 53,000 to 103,000 psi. All spliced rebar specimens developed tensile strengths that were greater than 125 percent of the nominal yield strength of 40,000 psi. Stress-strain data for each specimen are presented in graphical and tabular form in Reference 14. An extensometer using a linear variable differential transformer (LVDT) was used to measure the deflection across the various splices during each test for the purpose of determining strain across a spliced joint.

5. References 19 through 26. Other pertinent references dealing primarily with the strength characteristics of steel as influenced by strain rate and temperature effects are listed. The results from these

studies were widely used in the studies described in the preceding paragraphs.

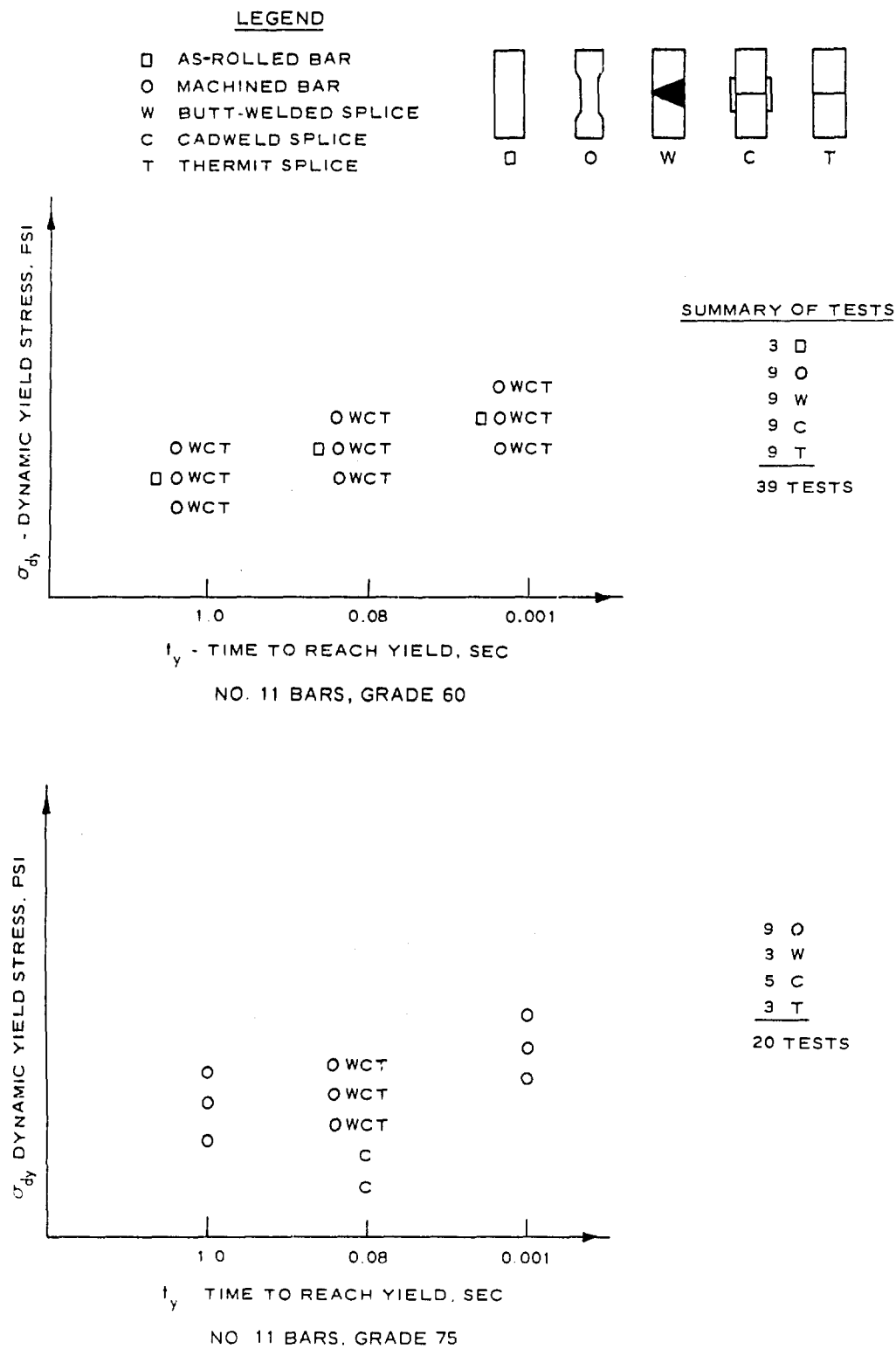

Figure 1.1 Test Schedule

CHAPTER 2

PROCEDURES

A total of seven No. 11 bars of Grade 60 and four No. 11 bars of Grade 75 all having barrel-type deformations were procured. The original length of all bars was approximately 20 feet. Shown in Table 2.1 are the chemical and physical properties of the bars according to the mill report provided by the manufacturer. Since five different types of specimens, i.e., as-rolled bars, machined bars, butt-welded splices, Thermit-welded splices, and Cadweld splices, were prepared, they were randomly selected from the various bars so that all of one type would not be prepared from only one or two bars (see Figure 2.1). Two special specimens (Tests 201 and 202) made from Grade 75 bars having "X" deformations were prepared with Cadweld splices. This type bar is not shown in Figure 2.1 but can be seen in Figure 3.8. An independent chemical analysis was made for the special bar (Test 201), the weld material in a butt-welded splice, and the Grades 60 and 75 bars. Results of this analysis are summarized in Table 2.2.

2.1 PREPARATION OF SPECIMENS

The specimen selection for the various Grades 60 and 75 bars, including the numbering system used as well as the weight of each bar with upper and lower grippers attached, is shown in Table 2.3. The geometric properties (bar diameter, deformation spacing, gap, etc.) of the reinforcing bars used are summarized in Table 2.4. The measured diameters (and hence areas) were less than nominal values but were within tolerable limits (CRSI and ASTM).[9, 15, 16] The measured areas were

within the 6 percent difference allowed. The spacing and measurements of deformations met all specifications. The total gap thickness is the sum of thicknesses of longitudinal ribs. For Grade 60 bars, there are three ribs; for Grade 75 bars, there are four ribs. The standards do not stipulate any minimum width for deformations.

2.1.1 As-Rolled Bars. These specimens (Figure 2.1) were saw cut from the reinforcing bars and were each 2-1/2 feet long. The ends were threaded so that a special nut could be placed when the ends of the bars were inserted in the wedge-type grippers used to hold the specimens during a test.

2.1.2 Machined Bars. These bars were also 2-1/2 feet long but were prepared with a double necked-down section that was carefully machined. A drawing showing the dimensions for these bar types is presented in Figure 2.2. The necked-down portions were very carefully machined so that the diameters of the cross sections were within 0.0005 inch for those lengths of machined section.

2.1.3 Butt-Welded Splice. Specimens 2-1/2 feet long were first cut from the various rebars and sawed in half at an angle of about 23 degrees to the centerline of the bar. The bevel on one of the halves was then saw cut so that when the bars were butt together the interior angle that was formed ranged from 46 to 50 degrees to conform to recommendations in Reference 7 (AWS). A cut specimen and a completed splice of a single-bevel groove weld are shown in Figure 2.3.

The welding techniques used conform to the practices described in Reference 7. For welding both the Grades 60 and 75 bars, 5/32-inch-diameter, low-hydrogen electrodes (E7018) were used. These electrodes

conform to the American Welding Society Classification E70XX. Only the Grade 75 bars were preheated to a temperature of 450 F. Preheating was done with a torch, and the temperature was measured with a thermocouple. The unwelded Grade 75 bars were first positioned in a steel angle prior to heat treating in order to maintain proper alignment. The angle not only served as an alignment jig but also as a heat sink that helped to maintain even preheat temperatures for the bar. Welding was accomplished by qualified welders with a dc manual electric arc welding unit operating at 140 amps dc. All welded specimens were X-rayed by the Mid-South X-Ray Company of Jackson, Mississippi, and it was determined that all welded butt joints were satisfactory (see Table 2.5).

2.1.4 Thermit-Welded Splice. Used in this process are various mixtures of metal oxides and metallic reducing agents that, upon ignition, react to produce heat. During welding, the reaction produces so much heat that it leaves the products of the reaction in a superheated molten state. The Thermit mixture for welding reinforcing bars produces superheated molten welding steel of the following typical analysis: carbon (C), 0.42 percent; manganese (Mn), 0.54 percent; phosphorus (P), 0.04 percent; and sulphur (S), 0.04 percent. Additional information is presented in the manufacturer's brochure (Reference 27). A complete splicing kit and a rebar to be spliced are shown in Figure 2.4. The bars were spliced according to the following step-by-step procedure under the supervision of a representative from the manufacturer of the Thermit kits.

1. Step 1, Alignment of Bars. All bars to be spliced were aligned

in a jig made of structural steel angles so that each bar was on the same centerline and maintained in this geometry for the entire welding cycle. In all cases, the vertical gap between bars was not less than 1/2 inch nor more than 5/8 inch.

2. Step 2, Placing Molds. Half molds were attached to the bars and temporarily held in place using a pair of spring clamps (see Figure 2.5). Bolts were then inserted through the three holes in the mold below the bar and through the two above the bar. The bolts were tightened, and the spring clamps removed.

3. Step 3, Positioning Molds. The molds were then moved along the bars until the pouring gate was centered over the gap between the bars. Holding the molds in a vertical position, wedges were slipped into cavities on each side of the mold between the bar and the mold to prevent sliding or rotation (see two molds on the left in Figure 2.6).

4. Step 4, Luting the Molds. Asbestos cord approximately equal in length to the circumference of the bar was placed around the bar and firmly pushed into the bell-shaped cavities on each side of the mold. The bell-shaped cavities were next filled with a special mixture of sand and clay (No. 2 luting material) that was very permeable. The mixture was carefully pressed into the deepest recesses of the flare, taking care not to slide the mold along the bar during the process (see two molds on the right in Figure 2.6).

5. Step 5, Placing Tapping Disk. One 10-gage steel tapping disk 1-1/4 inches in diameter was then dropped into the small well, called the tap well, at the bottom of the large cavity (see Figure 2.7). A screwdriver was used to tap the disk firmly into place.

6. Step 6, Addition of Thermit. The entire bag of Thermit was added on top of the disk (see Figure 2.8).

7. Step 7, Ignition of Thermit Reaction. A half teaspoon of starting Thermit, which is an exothermic mixture with a very low ignition point, was placed at the top center of the Thermit mixture that was placed in the crucible section of the mold during Step 6 (see Figure 2.9). A long match was then used to ignite the starting Thermit, which, in turn, ignited the main body of Thermit (see Figure 2.10). The superheated molten metal, with slag floating on the top, melted through the 1-1/4-inch tapping disk. The molten metal then flowed through the gap between the bars, with some of the hot fluid entering the discharge cavity after transferring a considerable amount of heat to the bars. By the time the discharge cavity had been filled according to manufacturer's instructions, the bars were completely fused.

8. Step 8, Disassembling and Finishing the Weld. Disassembly of the welding unit was begun approximately 10 min after ignition. The mold as it appeared after the molten metal had cooled somewhat is shown at the upper center in Figure 2.11. A view of a bar with the used mold removed is shown at the lower left in Figure 2.11.

2.1.5 Cadweld Splice. The bars to be spliced were connected by a loosely fitting metal sleeve. A graphite crucible was placed over the sleeve and filled with Cadweld powdered metal. The powder was ignited, and the ensuing exothermic reaction produced a molten metal that flowed through an opening in the metal sleeve and filled the cavity between the outside surface of the rebar and the inside surface of the metal sleeve. Under tension, the bar transferred load in shear to the Cadweld metal which in turn transferred the load to the internally

grooved splice sleeve. The contents of a rebar splicing kit are shown in Figure 2.12. Additional information about the process is presented in a brochure published by the manufacturer (Reference 28). The Cadweld material produces metal having the following typical analysis: carbon (C), 0.43 percent; manganese (Mn), 0.86 percent; chromium (Cr), 0.87 percent; and molybdenum (Mo), 0.21 percent. The bars were spliced according to the following step-by-step procedure under the supervision of the manufacturer's representative.

1. Step 1, Alignment of Bars. All bars to be spliced were aligned in a jig made of structural steel angles so that each bar was on the same centerline and maintained in this geometry for the entire welding cycle. In all cases, the vertical gap between bars was about 1/4 inch. The ends of the bars to be spliced were inspected to insure that they were clean and dry before placement of the metal sleeve.

2. Step 2, Placing Metal Sleeve. The sleeve was positioned with the top hole directly over the gap between the bar ends. Asbestos packing was then wrapped (two turns) around the rebar and against each end of the sleeve (see Figure 2.13). The packing was not forced into the sleeve.

3. Step 3, End-Alignment Fittings. These fittings were placed on the rebar at each end of the sleeve. They were then slid over the packing and snugly locked in place over the sleeve (see Figure 2.14).

4. Step 4, Horizontal Packing Clamp. This clamp was placed in position and tightened by turning a hand knob in order to squeeze the end-alignment fittings toward the sleeve, thus wedging the packing securely against the sleeve and rebar to prevent leaking (see Figure 2.15).

5. Step 5, Guide Tube and Ceramic Insert. The guide tube (see Figure 2.15) was placed in the hole in the top of the sleeve and then a ceramic insert was positioned around the guide tube (see Figure 2.16).

6. Step 6, Seating of Pouring Basin. The pouring basin was placed over the ceramic insert and secured to the sleeve by tightening a chain attached to the pouring basin (see Figure 2.17). The chain was tightened just enough to keep the assembly from tipping.

7. Step 7, Crucible Attachment and Addition of Cadweld Powder. The graphite crucible was attached, and then a steel disk was placed over the top hole of the pouring basin. The Cadweld powder was added, and starting powder was placed evenly over the top surface (see Figure 2.18). The crucible extension was then placed on top of the graphite crucible.

8. Step 8, Ignition. The starting powder was ignited with a flint gun (Figure 2.19).

9. Step 9, Removal of Crucible and Other Fittings. Approximately 1 min after the filler metal had solidified, the crucible and other fittings were removed. The splice with the residue riser composed of slag and metal can be seen in Figure 2.20.

2.1.6 Method of Gripping Specimens. Special care was given to using a gripping system that would not slip under load or cause high stress concentrations to the specimen. All specimens except the machined-bar specimens were anchored in wedge-shaped holders filled with babbitt metal. A detailed drawing of one of these holders is shown in Figure 2.21.

A special angle jig was used to hold the grippers with a test bar

in place (see Figure 2.22). Molding clay was packed around the intersection of the bar with the grippers. The entire assembly was raised to a vertical position, and then molten babbitt metal was poured into the end of the gripper to a prescribed height (see Figure 2.23). Sheet-metal inserts were used to protect the threaded portions of the gripper and test bar during the pouring operation. An end view of one of the grippers showing the solidified metal in the well is shown in Figure 2.24. The end nut also shown in the figure was then attached, and the bar was ready for testing.

The grippers for the machined-bar specimens were much simpler in design, as the ends of the bars could be threaded and screwed into the two grippers. A detailed drawing of this gripper is shown in Figure 2.25.

A bar in place in a poured gripper ready for testing is shown in Figure 2.26, and a machined bar with one gripper attached is shown in Figure 2.27. The two holes visible in the gripper on the right were used for attaching an accelerometer. The weights for all the test bars including the weight of the grippers are summarized in Table 2.3.

2.2 INSTRUMENTATION

The bars with end grips attached were screwed into the upper and lower connections of the 200-kip-capacity loader. Load cells were integral parts of the connections, the lower cell measuring the applied load and the upper cell measuring the reactive load.

All specimens were instrumented with strain gages in an attempt to determine the state of strain at various locations on the test bars. Accelerometers were attached to the upper and lower grippers holding

the bars in order to determine the acceleration-time histories of the mass at the ends of the bars for use in assessing the influence of inertial effects. An optical tracker was used to measure strain over an 8-inch gage length for all specimens except machined bars, for which strains were measured over a 3-inch gage length; this device was especially useful in determining strain across the three types of splices tested. On certain machined bars, high-speed movies were taken in an attempt to study the development of failure. The gage locations for the five types of specimens considered are shown in Figure 2.28, and the measurements made for each test are presented in Table 2.6. An instrumented machined specimen in place and ready for testing is shown in Figure 2.29. The two optical trackers used to measure primarily posttest yield strain can be seen in the foreground.

2.2.1 Load. Load cells, or dynamometers, having a maximum capacity greater than 200 kips were attached to the grippers at each end of a test bar in order to measure the applied and reactive forces during a test. The cells were carefully machined from 4130 steel quenched and tempered to produce a minimum yield strength of 100,000 psi. Four 120-ohm strain gages were mounted on the surface at the midheight of each gage. One set of two strain gages mounted 180 degrees apart sensed vertical strains, and two gages that formed the second set (also 180 degrees apart) were mounted to sense circumferential strains. The gages were connected electrically to form a wheatstone bridge, with strain gages in each set as opposite arms of the bridge. In this configuration, the net contribution to the electrical imbalance of the bridge, whether the cell is strained in tension or compression, is

always additive. When the load cell is in tension, the vertical strain gages elongate, resulting in an increase in gage resistance. At the same time, the circumferential strain gages are compressed, resulting in a decrease in gage resistance. Ideally, each strain gage of a set contributes equally to the bridge imbalance; the circumferential set contributes less by a factor μ (Poisson's ratio for steel). Consequently, the output of the cell is not four times that of a bridge containing a single active gage but rather $2(1 + \mu)$ times that output. For each gage, the applied load versus indicated strain remained linear up to a maximum load of 200 kips. Both load cells were calibrated before and after the test series was completed, with no differences noted.

2.2.2 Strain. All strain gages applied to the test specimens were 1/4-inch-long, foil-type gages with gage factors of 2.095 $\pm$ 0.5 percent at 75 F. A wheatstone bridge circuit with three dummy gages was used with each active gage. Step-by-step procedures for attaching a typical strain gage are as follows:

1. Step 1. The surface where the gage was to be attached was roughened with 320 emery cloth. Then the test bar was placed in a pair of V-cut wood blocks. A ball-point pen was used to inscribe horizontal and circumferential lines to mark gage locations (see Figure 2.30).

2. Step 2. Two separate cleaning operations were performed. Feron TF Degreaser was first used to remove ink and other foreign material; however, the lines inscribed in Step 1 were still visible. A cotton swab was then saturated with M-Prep Neutralizer 5 and rubbed over the bar to remove all traces of grease. The treatment was

repeated until no discoloration occurred on a white paper tissue that was rubbed over the bar.

3. Step 3. Epoxy EIY 150 made by Baldwin Lima Hamilton was prepared and applied to the surfaces that were to receive strain gages. (If the metal is not clean the epoxy will form beads.) Each strain gage was placed on a strip of Mylar tape and then pressed on the metal surface that was previously prepared with epoxy (see Figure 2.31). The Milar tape was then gently pressed with fingers to remove air bubbles underneath; excess tape was then cut off.

4. Step 4. A strip of Teflon and a strip of Scotch 88 electrical tape were then wrapped around the bar (see Figure 2.32). The purpose of the Teflon was to eliminate slippage and the possibility of pulling as well as to prevent the electrical tape from sticking to the gage later when the tape was removed. Additional electrical tape was then tightly wrapped around the bar to develop a clamping pressure of 5 to 15 psi. The gages were then allowed to cure for at least 12 hours at a temperature of 75 F.

5. Step 5. The electrical tape, Teflon strip, and Mylar tape directly over the gage were then removed. Paper masking tape was then applied to cover only the gage grid to avoid accidental damage during the soldering operation.

6. Step 6. Resin flux was then applied to the gage tabs and terminal strips. Solder drops were then applied to the gage tabs (two on tabs) and the terminal strip (four on strip). Thin copper wire having a coating of tin was then attached between each gage tab and terminal strip (two wires per gage, see Figure 2.33). The wires were

looped to allow for movement later when the bars were tested.

7. Step 7. Two braided-shield, vinyl-covered conductor lead wires were next attached to the terminal strips (see Figure 2.34). These wires were also looped to allow for stretching. Electrical tape was then wrapped around the wires to secure them to the reinforcing steel bar so they would not be accidentally pulled from the soldered connection on the terminal.

8. Step 8. Resin solvent was brushed on not only to make removing the masking tape easier but also to clean the gage and leads (see Figure 2.34). Excess solvent was gently blotted off with soft paper tissue. The electrical resistance of the gage was then checked to insure that it had not shorted out.

9. Step 9. An air-drying polyurethane coating (M-Coat A) was then brushed over the gage to protect it from moisture. A water-resistant silicon resin (Gagekote No. 3) was next applied and allowed to dry for 30 min. The assembly was then ready for testing.

2.2.3 Acceleration. Two 10,000-g, piezoresistive-type accelerometers manufactured by ENDEVCO were used to measure the vertical acceleration on the upper and lower grippers, respectively. They were attached to the grippers with screws; however, a Teflon sheet was placed between the underside of the gage and the surface of the grippers.

The accelerometers comprise a mass attached to a cantilever element. When in motion, the mass exerts a force on each of the piezoresistive sensing elements connected in a wheatstone bridge configuration. The resulting imbalance of the bridge is proportional to the

acceleration sensed by the gage. These gages were calibrated using a centrifuge up to 1,000 g's. The gages are linear to ±2 percent for the full range of 10,000 g's specified by the manufacturer.

2.2.4 Optical Tracker. Two optical trackers (Physitech, Inc., Model 39A Electrooptical tracking system) were used to measure the change in axial displacement between two points on the surface of the reinforcing bars when they were stressed in tension. In order for the point to be discernible when tracked, a prescribed target was painted on the surface of the reinforcing bars. The prescribed target is any two color interfaces providing appropriate contrast. The color combination used on the test specimens was white on top and black on bottom, with the reference point lying on the interface formed by the two colors. It is this optical discontinuity that is tracked. The color scheme can be seen on the bar in Figure 2.29. Each target was illuminated using a 5,000-watt incandescent lamp placed at a distance of approximately 7 feet.

The electrooptical tracking system consists of an optical head with lens system, an optical calibrator, and a control unit connected by a cable. The optical head, lens, and optical calibrator are mounted on a tripod as shown in Figure 2.29. The tripod is in turn shock mounted. The optical head has a reflex viewer which is used to adjust the focus of the lens system. An oscilloscope is used in the critical alignment of the optical head with the target.

The optical head contains an image analyzer tube which converts the light image focused on a photocathode tube into an electron image focused on an aperture plate. The electrons entering the aperture are

multiplied in number by a photoelectron multiplier tube. It is the output of this tube that provides the input to the control unit at any instant in time. The magnitude of this input is related to the position of the image in the aperture and, therefore, the position of the target with respect to the field of view of the optical head.

The electron image is scanned once every 40 μsec, or 25,000 times a second. For example, if a welded bar tested dynamically broke within 3 msec, it would be possible to record 75 images with the optical tracker. Also, if the targets displaced uniformly with time during this interval the distance between images can be proportionately determined. For instance, if the top target moved 0.263 inch, an image would be taken approximately every 0.003 inch. If the bottom target moved 0.474 inch, an image would be taken approximately every 0.006 inch.

System linearity over this range is easily checked using the optical calibrator (Physitech Model No. CX-500). The calibrator is capable of displacing the optical image of the target presented to the optical head. The optical calibrator is present in the optical path throughout the test. This device has a range of $\pm$0.5 inch. It utilizes two prisms, one stationary and one movable. The optical image of the target is displaced precisely the same distance that the movable prism is displaced. The movement of the image by a precise amount simulates the movement of the target by the same amount. The displacement of the prism is made continuously variable by rotating a screw mechanism which is coupled to a dial gage that indicates the travel of the prism in marked increments of thousandths of an inch.

2.2.5 Recording Instrumentation. The output of the control unit is a varying dc voltage of a magnitude great enough not to require amplification before being fed to the frequency-modulated record electronics of the analog tape machine, which was an Ampex Model FR-100. The outputs of the other transducers and single-element strain gages are amplified by a factor of approximately 200 before being fed to the tape machine. Amplification was accomplished using WES-constructed dc amplifiers. A dc excitation of 4 volts was used for all transducers and strain sensing networks. The instrumentation tape recorders used were Ampex Model FR-100 operated at 60 in/sec. The Inter-Range Instrumentation Group (IRIG) specifies that the frequency response of instrumentation tape machines operating at 60 in/sec be flat out to 20,000 Hz. This is equivalent to the capability of recording rise times on the order of 12 μsec without distortion. This easily satisfies the requirements of recording all signals generated during the tests including loads, strains, accelerations, and optical tracker outputs. Playback of the data from magnetic tape to paper was accomplished using a Sangamo 4700 tape machine and a Consolidated Electrodynamics Data Graph 5-133 direct-write oscillograph. Playback of the data in digital format was achieved directly from the magnetic tape using an analog-to-digital converter system.

2.3 TEST DEVICE

All tests were conducted in the WES 200-kip-capacity dynamic loader, which is a large, hydraulically actuated device with a rigid support system (see Figure 2.35). At maximum loading rates, the loader

is capable of applying a 200-kip force to a stiff specimen within a time span of 1.5 msec. The maximum stroke of the loading ram is 4 inches.

The device is pressurized with a low-volume, high-pressure multiplier and is triggered by a ruptured-disk valve. Basically, the actuator has three pressure chambers: one above the piston (upper chamber); one below the piston (lower chamber); and one between the two rupture disks. The machine is cocked by a slow buildup of pressure below and above the piston while a slight preload on the specimen is maintained (approximately 1 to 2 kips). Concurrently, pressure is built up in the oil volume between the two rupture disks; the pressure between the rupture disks is maintained at approximately half the pressure of the oil in the lower chamber, thereby allowing containment of half the total pressure below the piston by the first rupture disk and the remaining half by the second rupture disk. To trigger the machine, the pressure between the rupture disks is suddenly reduced, allowing the total fluid pressure in the lower chamber to be exerted on the first rupture disk, thus causing it to fail. When the second disk ruptures, the pressure below the ram is rapidly exhausted, and the ram is rapidly accelerated by the pressurized oil above the piston. The specimen that is positioned above or below the ram is thus loaded. Rise times to full load of 1.5 to approximately 100 msec can be achieved by placing the proper orifice plate on the upstream side of the rupture disk assembly. Rise times from 100 msec to 1 sec are produced by replacing the rupture disk assembly with a 1/2-inch-diameter solenoid valve to control flow rates. Orifices are also used with the solenoid valve to produce desired rise times.

During the cocking operation, the load signal is split from the top load cell and displayed on a highly sensitive digital voltmeter. This voltmeter records the small preload pressure that is maintained on the specimen to remove any slack from the load column and to seat the ball-swivel joint located at the top of the load column.

2.4 LOAD ANALYSIS AND DATA REDUCTION

For rapidly applied loads, inertial forces can exist that will influence the response of the loading system. Consequently, the acceleration of the rather massive loading ram and that of the upper and lower grippers need to be considered in order to determine what load was delivered to the test specimen. A cutaway view of the loading device and the associated lumped spring-mass model are shown in Figure 2.36.

The symbols are defined as follows:

Symbol	Definition	Dimension
k_1	The spring constant of the upper reaction member	FL^{-1}
M_1	Mass of half the test specimen and all of the upper gripper	$FL^{-4}T^2$
x_1	The displacement of M_1	L
$\ddot{x}_1$	The acceleration of M_1	LT^{-2}
k_2	The spring constant of the test specimen	FL^{-1}
M_2	Mass of half the test specimen and all of the lower gripper	$FL^{-4}T^2$
x_2	The displacement of M_2	L
$\ddot{x}_2$	The acceleration of M_2	LT^{-2}

(Continued)

Symbol	Definition	Dimension
k_3	The spring constant of the loading ram	FL^{-1}
M_3	Mass of the loading ram	$FL^{-4}T^2$
x_3	The displacement of M_3	L
$\ddot{x}_3$	The acceleration of M_3	LT^{-2}
F(t)	The applied time-dependent force	F

The masses shown in the mathematical model were uncoupled, and equations of motion and equilibrium were written.

$$k_2(x_2 - x_1) = M_1\ddot{x}_1 + k_1x_1 \qquad (2.1)$$

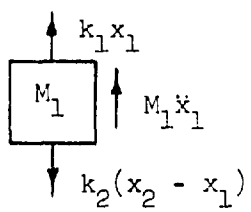

$$k_3(x_3 - x_2) = M_2\ddot{x}_2 + k_2(x_2 - x_1) \qquad (2.2)$$

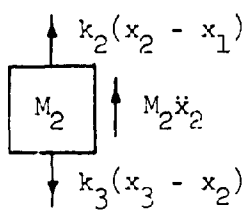

$$F(t) = M_3\ddot{x}_3 + k_3(x_3 - x_2) \qquad (2.3)$$

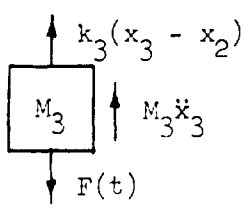

Substituting Equation 2.2 into Equation 2.1,

$$k_3(x_3 - x_2) - M_2\ddot{x}_2 = M_1\ddot{x}_1 + k_1x_1 \qquad (2.4)$$

The quantity $k_3(x_3 - x_2)$ represents the load measured by the lower load cell, and the quantity k_1x_1 represents the load measured by the upper load cell. Both M_1 and M_2 are measured, and the accelerations of M_1 and M_2 were recorded respectively by the upper and lower accelerometers. It was therefore possible to calculate Equation 2.4 and determine if equilibrium was achieved using measured quantities. The equilibrium load is the actual load $k_2(x_2 - x_1)$ applied to the test specimen and is the one used in determining states of stress. Where acceleration values are very small or nonexistent, it is obvious that the load measured by the upper load cell k_1x_1 should be the same as that recorded by the lower load cell $k_3(x_3 - x_2)$.

The analog records were digitized, and a computer routine was utilized to determine stress-strain relationships with time. The tabulated data were then processed so that they were electronically plotted for rapid and intermediate load rate tests. The slow load rate data were hand-digitized and plotted.

TABLE 2.1 MILL REPORT FOR NO. 11 DEFORMED STEEL REINFORCING BARS

Grade	Heat No.	Chemical Composition of Steel Bars				Physical Properties			
						Strength		Elongation in 8 inches	Nominal Area
		C	Mn	P	S	Yield	Tensile		
		pct	pct	pct	pct	kips/in^2	kips/in^2	pct	in^2
60	20775	0.35	0.63	0.033	0.049	66.45	96.12	18.0	--
75	84542	0.41	0.87	0.009	0.034	87.00	118.70	10.94	1.56

TABLE 2.2 RESULTS OF INDEPENDENT CHEMICAL ANALYSIS

Element	Chemical Composition of Indicated Bar Types			
	Grade 60	Grade 75	Grade 75[a]	Butt-Welded Splice
	pct	pct	pct	pct
Carbon	0.41	0.40	0.41	0.08
Manganese	0.70	0.93	1.15	1.07
Phosphorus	0.019	0.017	0.017	0.013
Sulfur	0.040	0.029	0.027	0.022
Silicon	0.19	0.32	0.48	0.57
Nickel	0.05	0.07	0.10	<0.05
Chromium	0.10	0.88	0.14	0.05
Molybdenum	<0.05	0.13	<0.05	<0.05
Copper	0.30	0.28	0.15	<0.05

[a] Results of Test 201, which was a test of a special specimen having "X" deformations (see Figure 3.8) and prepared with a Cadweld splice.

TABLE 3.4 SUMMARY OF TEST NUMBERS AND WEIGHTS FOR VARIOUS SPECIMENS

Test No.	Load Rate[a]	Bar No.	Grade	Splice Type[b]	Total Weight of Bar and Grippers
					pounds
154	Rapid	1	60	AR	69.5
155	Rapid	1	60	M	25.2
156	Rapid	2	60	W	68.0
157	Rapid	2	60	C	73.5
158	Rapid	2	60	M	25.2
159	Rapid	4	60	T	69.0
160	Intermediate	3	60	W	68.0
161	Rapid	3	60	C	73.5
162	Rapid	4	60	M	25.2
163	Rapid	3	60	T	69.0
164	Rapid	4	60	W	68.0
165	Rapid	1	75	M	25.2
166	Rapid	4	60	C	73.5
167	Rapid	3	60	T	69.0
168	Rapid	2	75	M	25.2
169	Rapid	1	60	W	68.0
170	Intermediate	4	60	C	73.5
171	Intermediate	4	60	M	25.2
172	Intermediate	1	60	T	69.0
173	Intermediate	2	60	W	68.0
174	Intermediate	3	60	M	25.2
175	Intermediate	3	60	C	73.5
176	Intermediate	4	60	T	69.0
177	Intermediate	4	60	M	25.2
178	Intermediate	3	60	W	68.0
179	Intermediate	4	60	C	73.5
180	Intermediate	3	60	M	25.2
181	Intermediate	2	60	T	69.0
182	Intermediate	3	60	W	68.0
183	Intermediate	3	60	C	73.5
184	Intermediate	3	60	T	69.0
185	Slow	1	75	M	25.0
186	Slow	5	60	W	68.0
187	Slow	1	60	C	74.0
188	Slow	4	60	M	25.5
189	Slow	2	60	T	69.0
190	Slow	3	60	W	68.5
191	Slow	2	60	M	25.0
192	Slow	3	60	C	74.0
193	Slow	5	60	T	69.0
194	Slow	6	60	M	25.0
195	Slow	4	60	W	68.0
196	Slow	4	60	C	74.0
197	Slow	2	75	M	25.0
198	Slow	2	60	T	70.0
199	Slow	2	60	AR	68.0
200	Slow	1	75	M	24.6
201[c]	Intermediate	--	75	C	72.5
202[c]	Intermediate	--	75	C	72.5

[a] Rapid - approximately 0.001 msec to peak load; Intermediate - approximately 0.06 msec to peak load; Slow - approximately 1 second to peak load.

[b] AR - as-rolled bar; M - machined bar; W - butt-welded splice; T - Thermit splice; C - Cadweld splice.

[c] Tests 201 and 202 were tests of special bars with "S" deformations (see Figure 3.8).

TABLE 2.4 GEOMETRIC PROPERTIES OF SOME REINFORCING BARS TESTED

Test No.	Steel Grade	Bar No.	Diameter		Area		Deformations						
			Nominal	Measured	Nominal	Measured	Average Spacing	Height				Width at Base	Total Gap Thickness[a]
								Minimum	Intermediate	Maximum	Average		
			inches	inches	in^2	in^2	inches	inches	inches	inches	inches	inches	inches
167	60	5	1.410	1.367	1.560	1.467	0.936	0.072	0.070	0.091	0.078	0.21	0.72
169	60	6	1.410	1.366	1.560	1.465	0.928	0.060	0.080	0.087	0.076	0.21	0.72
160	60	4	1.410	1.370	1.560	1.474	0.933	0.065	0.086	0.086	0.079	0.21	0.73
196	60	4	1.410	1.372	1.560	1.478	0.932	0.066	0.080	0.088	0.078	0.22	0.72
165	60	3	1.410	1.366	1.560	1.466	0.934	0.065	0.077	0.091	0.078	0.22	0.72
192	60	3	1.410	1.367	1.560	1.467	0.934	0.063	0.062	0.090	0.072	0.21	0.72
187	60	1	1.410	1.368	1.560	1.469	0.930	0.052	0.081	0.076	0.070	0.23	0.71
175	75	1	1.410	1.357	1.560	1.446	0.954	0.062	0.100	0.102	0.088	0.26	0.81
179	75	2	1.410	1.356	1.560	1.443	0.956	0.077	0.078	0.079	0.078	0.28	0.85
183	75	3	1.410	1.355	1.560	1.441	0.950	0.061	0.064	0.079	0.068	0.26	0.85
201	75	X[b]	1.410	1.338	1.560	1.405	--	0.084	0.091	0.101	0.079	0.30	0.95
202	75	X[b]	1.410	1.342	1.560	1.413	--	0.085	0.085	0.099	0.076	0.30	0.96

[a] Sum of thicknesses of longitudinal ribs.
[b] Special bar with "X" deformation (see Figure 3.8).

TABLE 2.5 RESULTS OF X-RAY TESTS OF BUTT-WELDED SPECIMENS

Film used was X-ray film No. I-V2.

Test No.	Bar No.	Remarks
146	2	Satisfactory
150	3	Satisfactory
154	6	Satisfactory
159	1	Light porosity; satisfactory
163	2	Light porosity; satisfactory
168	5	Satisfactory
174	1	Light to moderate porosity; satisfactory
178	2	Light to moderate porosity; satisfactory
182	3	Satisfactory
186	5	Light porosity
190	3	Light to moderate porosity; satisfactory
195	4	Moderate porosity; satisfactory
--	7	Light porosity
--	5	Satisfactory
--	4	Satisfactory

TABLE 3.- SUMMARY OF MEASUREMENTS FOR ALL TESTS

See Figure 3.11 for gage locations.

Test No.	Load		Strain			Optical Tracker		Acceleration		High-Speed Movie
	Lower F_l	Upper F_u	Lower ϵ_l	Center ϵ_c	Upper ϵ_u	8-Inch Gage Length	3-Inch Gage Length	Lower a_l	Upper a_u	
144	X	X		X		X		X	X	X
145	X	X	X	X	X		X	X	X	X
146	X	X	X			X		X	X	
147	X	X	X			X		X	X	
148	X	X	X	X	X		X	X	X	
149	X	X	X			X		X	X	
150	X	X	X			X		X	X	
151	X	X	X					X	X	
152	X	X	X	X	X		X	X	X	
153	X	X	X			X		X	X	
154	Lost									
155	X	X	X	X	X		X	X	X	
156	X	X	X			X		X	X	
157	X	X	X			X		X	X	
158	Lost									
159	X	X	X			X		X	X	
160	X	X	X			X		X	X	
161	X	X	X	X	X		X			
162	X	X		X		X				
163	X	X	X			X				
164	X	X	X	X	X		X			
165	Lost									
166	X	X	X			X		X	X	
167	X	X	X	X	X		X			
168	X	X	X			X				
169	X	X	X			X				
170	X	X	X	X	X[a]		X	X		
171	X	X	X			X		X		
172	X	X	X			X		X		
173	X	X		X			X	X		

Test No.	Load		Strain			Optical Tracker		Acceleration		High-Speed Movie
	Lower F_l	Upper F_u	Lower ϵ_l	Center ϵ_c	Upper ϵ_u	8-Inch Gage Length	3-Inch Gage Length	Lower a_l	Upper a_u	
174	X	X	X			X		X		
175	X	X	X			X		X		
176	X	X		X			X	X		
177	X	X	X			X		X		
178	X	X	X			X				
179	X	X	X			X				
180	X	X		X			X			X
181	X	X	X			X				
182	X	X	X			X				
183	X	X	X			X				
184	X	X	X			X				
185	X	X		X			X			
186	X	X	X			X				
187	X	X	X			X				
188	X	X	X	X	X		X			
189	X	X	X			X				
190		X	X			X				
191	X	X		X			X			
192	X	X	X			X				
193	X	X	X			X				
194	X	X		X			X			
195	X	X	X			X				
196	X	X	X			X				
197	X	X		X			X			
198	X	X	X			X				
199	X	X		X			X			
200	X	X		X						
201	X	X	X[b]			X				
202	X	X	X[b]			X				

[a] One strain gage.
[b] Two strain gages.

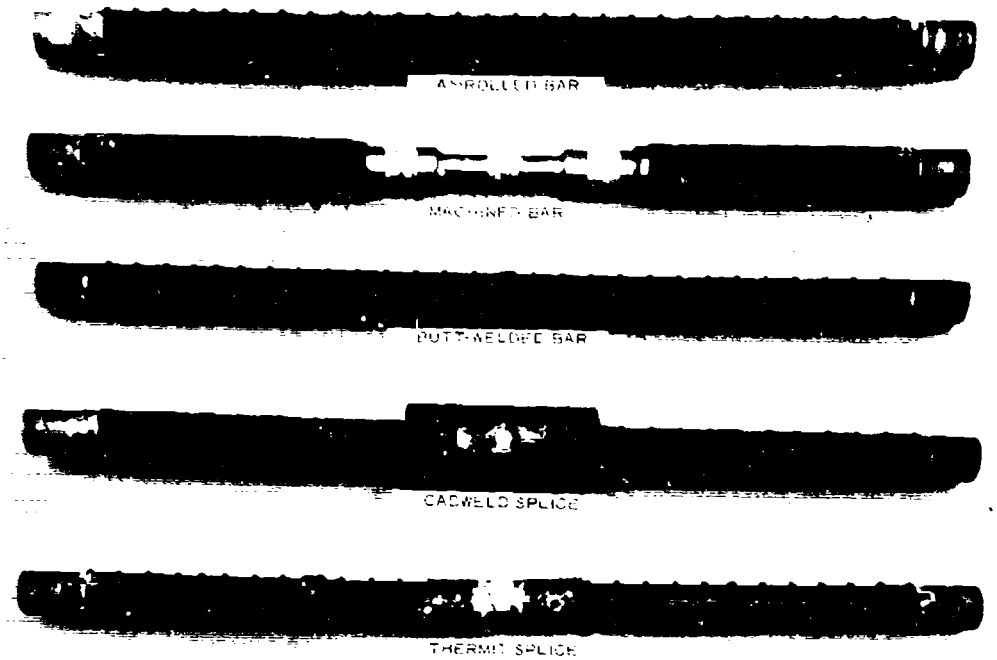

Figure 2.1 Specimen types tested.

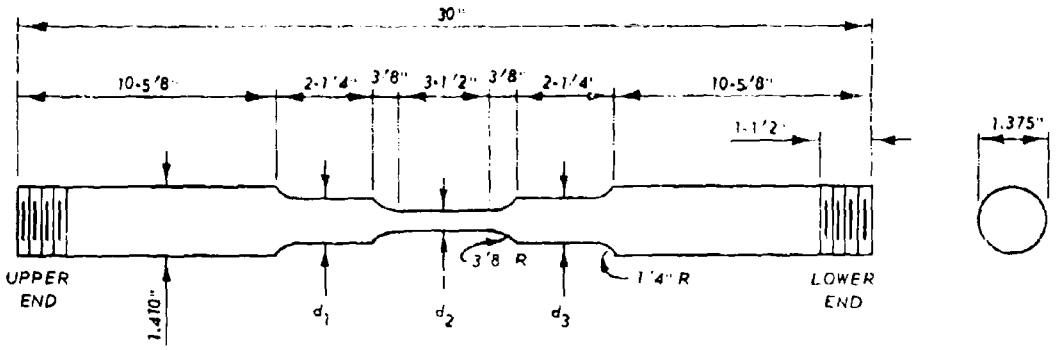

TEST NO.	DIAM d_1	AREA A_1	DIAM d_2	AREA A_2	DIAM d_3	AREA A_3
	INCHES	IN^2	INCHES	IN^2	INCHES	IN^2
145	1.1245	0.9926	0.7495	0.4410	1.1250	0.9935
148	1.1290	1.0006	0.7505	0.4422	1.1310	1.0040
152	1.1280	1.0006	0.7490	0.4404	1.1285	0.9997
161	1.1490	1.0364	0.7495	0.4410	1.1490	1.0364
164	1.1255	0.9944	0.7515	0.4433	1.1256	0.9946
167	1.1200	0.9847	0.7460	0.4369	1.1200	0.9847
188	1.1245	0.9926	0.7500	0.4416	1.1245	0.9926
191	1.1250	0.9935	0.7510	0.4427	1.1250	0.9935
194	1.1250	0.9935	0.7500	0.4416	1.1250	0.9935
155	1.1255	0.9944	0.7490	0.4404	1.1255	0.9944
158	1.1250	0.9935	0.7490	0.4404	1.1250	0.9935
170	1.1180	0.9912	0.7500	0.4416	1.1180	0.9812
173	1.1250	0.9935	0.7500	0.4416	1.1250	0.9935
176	1.1240	0.9918	0.7495	0.4410	1.1240	0.9918
180	1.1235	0.9909	0.7500	0.4416	1.1235	0.9909
185	1.1260	0.9953	0.7510	0.5527	1.1265	0.9962
197	1.1250	0.9935	0.7490	0.4404	1.1250	0.9935
200	1.1250	0.935	0.7500	0.4416	1.1250	0.9935

Figure 2.2 Schematic and dimensions for machined-bar specimens.

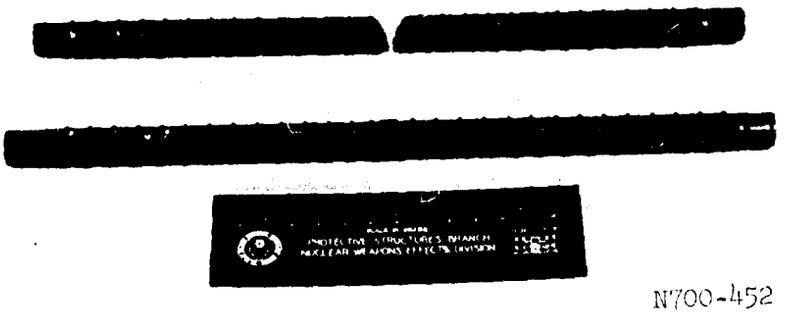

Figure 2.3 Butt-welded splice.

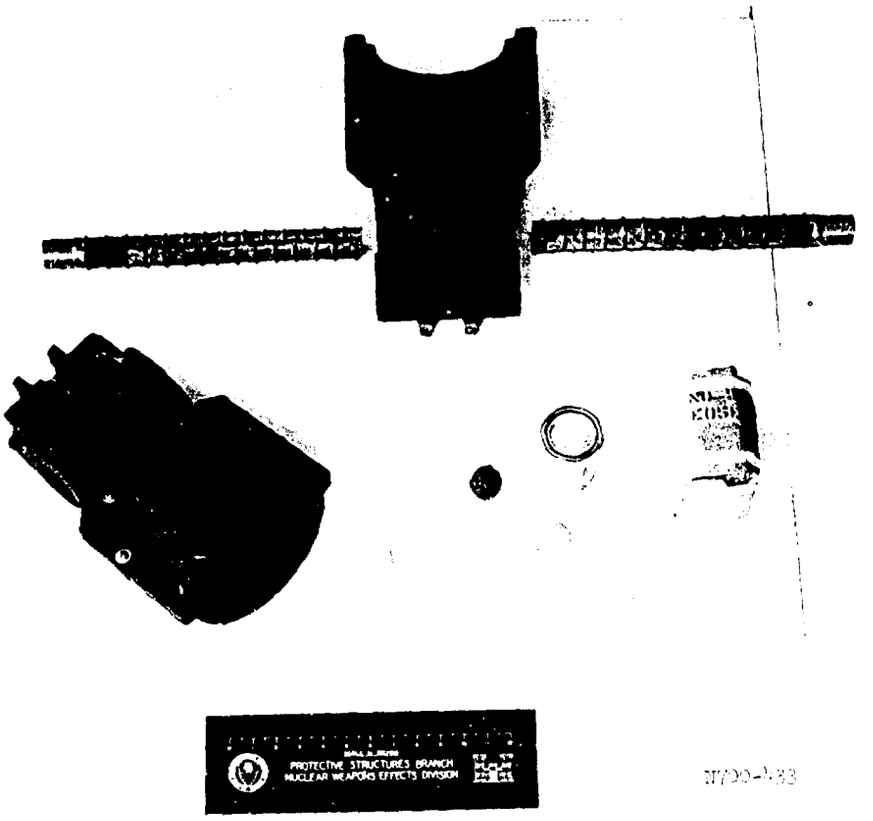

Figure 2.4 Thermit splicing kit and rebar to be spliced.

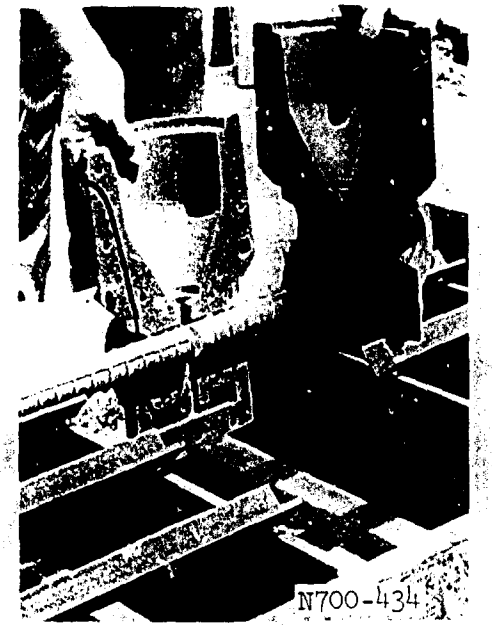

Figure 2.5 Thermit process, placing molds.

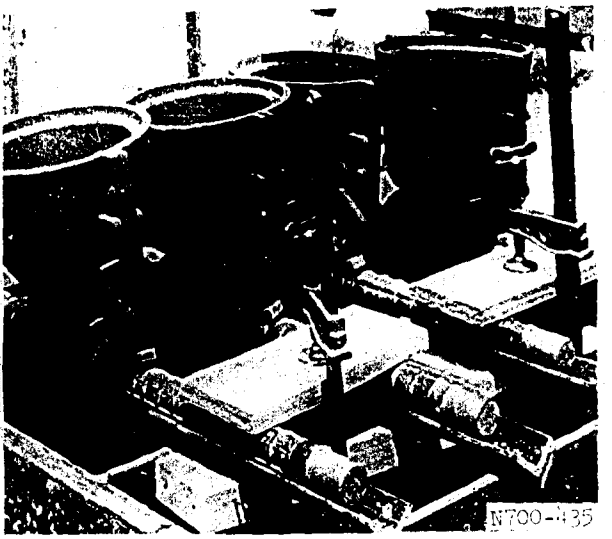

Figure 2.6 Thermit process, positioning molds.

Figure 2.7 Thermit process, placing tapping disk.

Figure 2.8 Thermit process, adding Thermit.

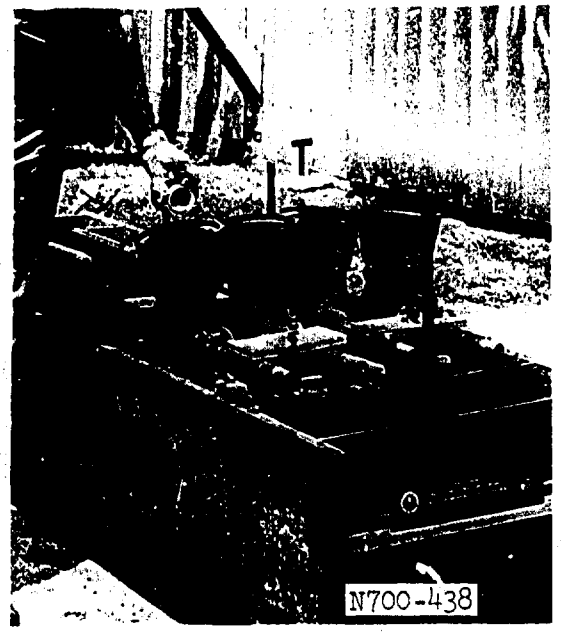

Figure 2.9 Thermit process, adding starting Thermit.

Figure 2.10 Thermit process, ignition.

Figure 2.11 Thermit process postignition.

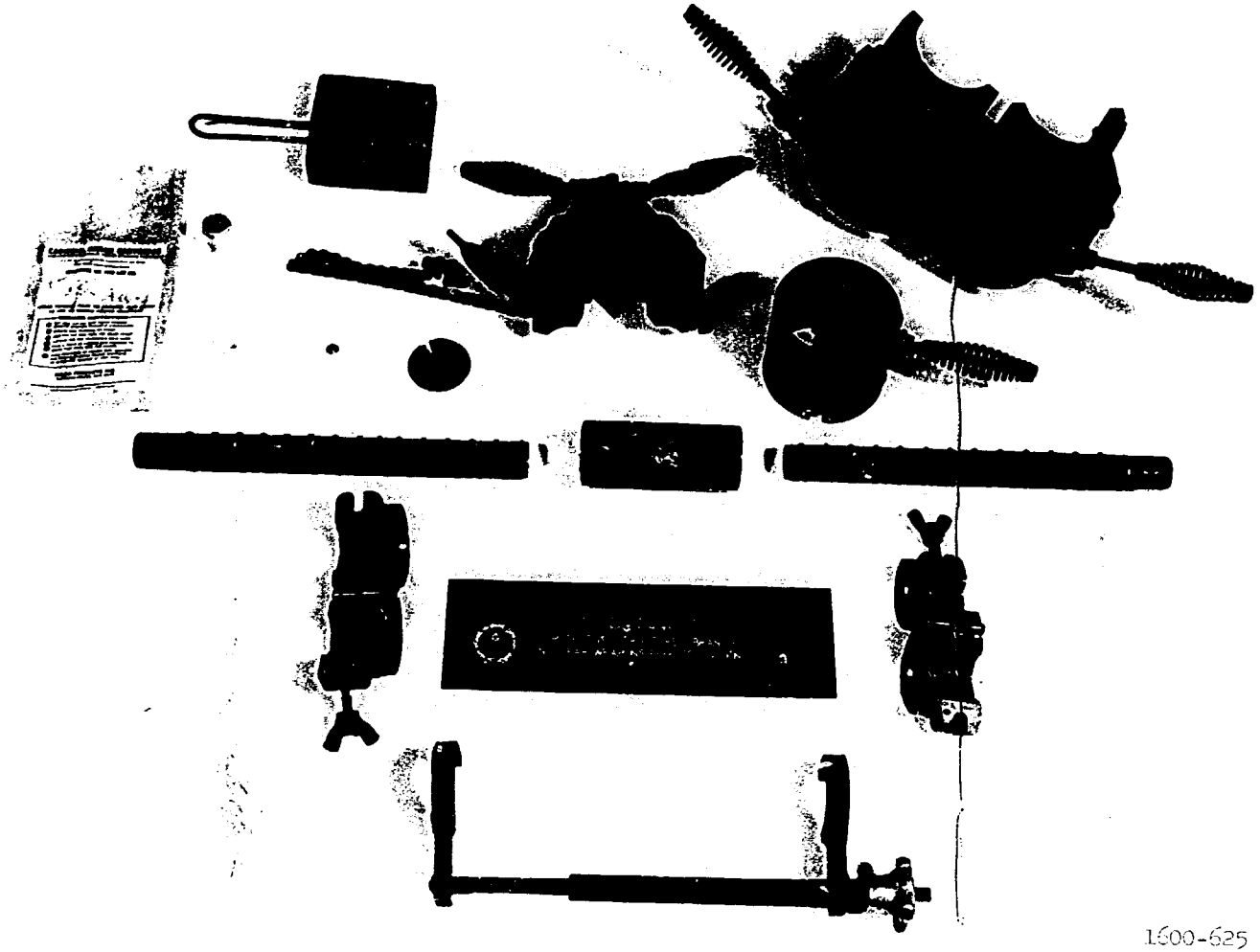

1600-625

Figure 2.12 Cadweld splicing kit.

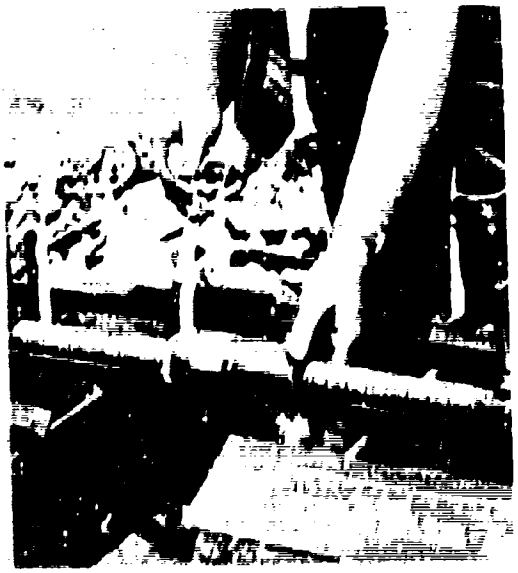

Figure 2.13 Cadweld process, placing metal sleeve.

Figure 2.14 Cadweld process, end-alignment fittings.

Figure 2.15 Cadweld process, horizontal packing clamp.

Figure 2.16 Cadweld process, cermide inserts.

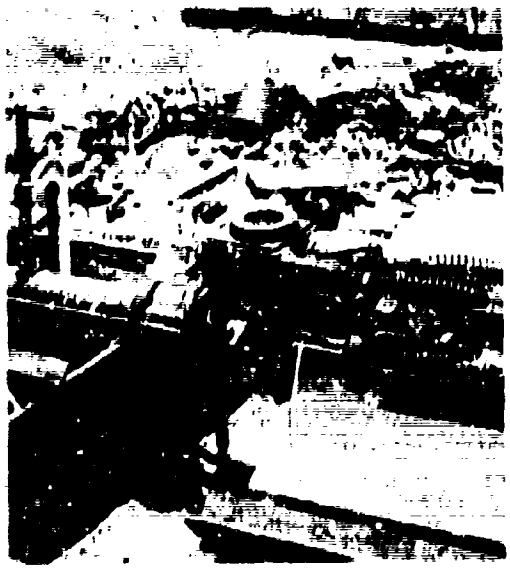

Figure 2.17 Cadweld process, heating of pouring basin.

Figure 2.18 Cadweld process, crucible and addition of Cadweld powder.

Figure 2.19 Cadweld process, ignition.

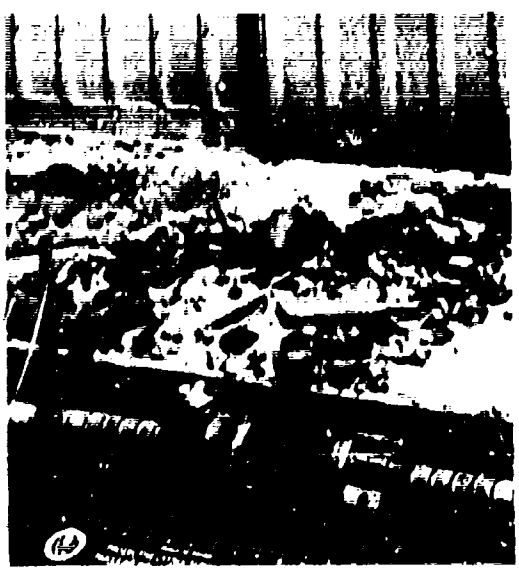

Figure 2.20 Cadweld process, crucible and other fittings removed.

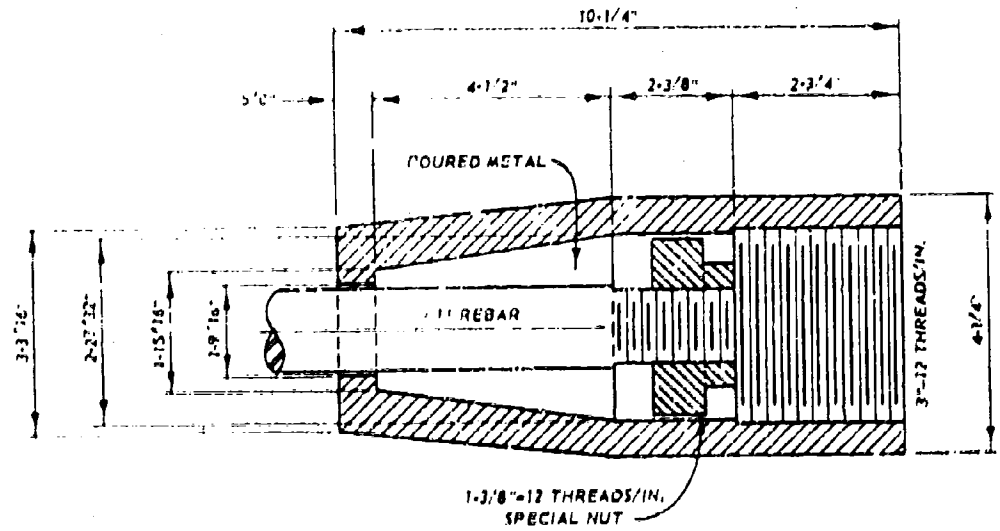

Figure 2.21 Poured-metal gripper.

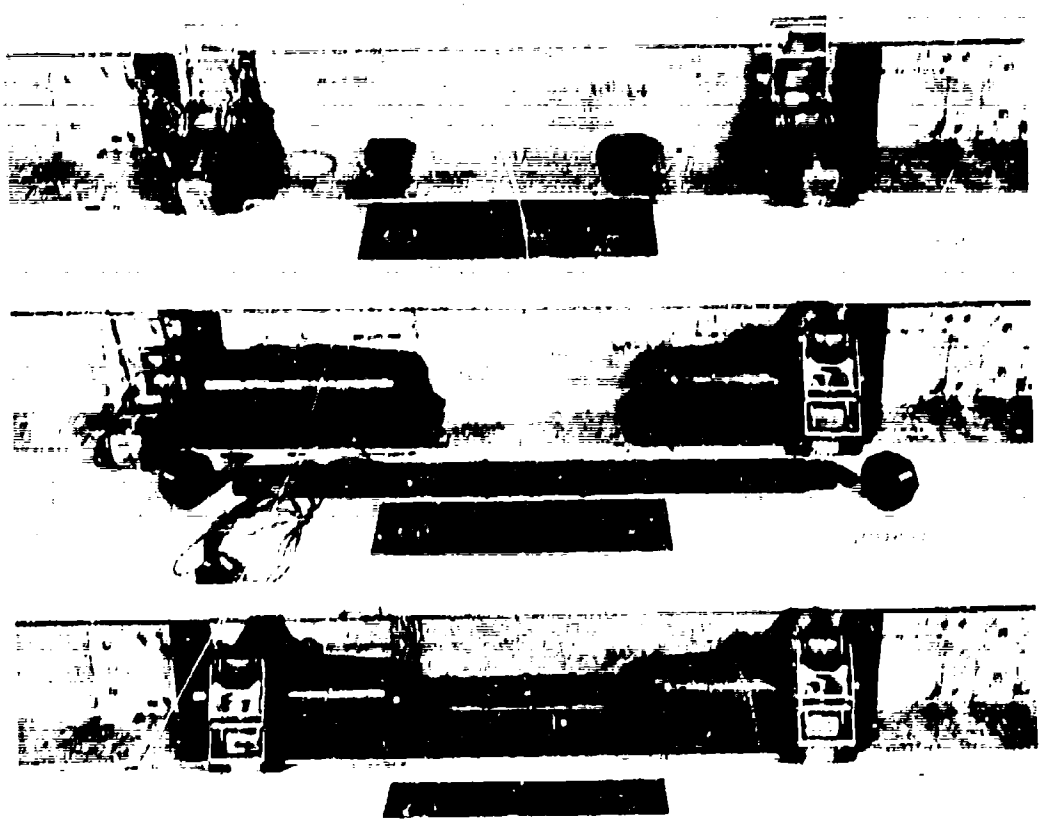

Figure 2.22 Alignment jig for poured-type grippers.

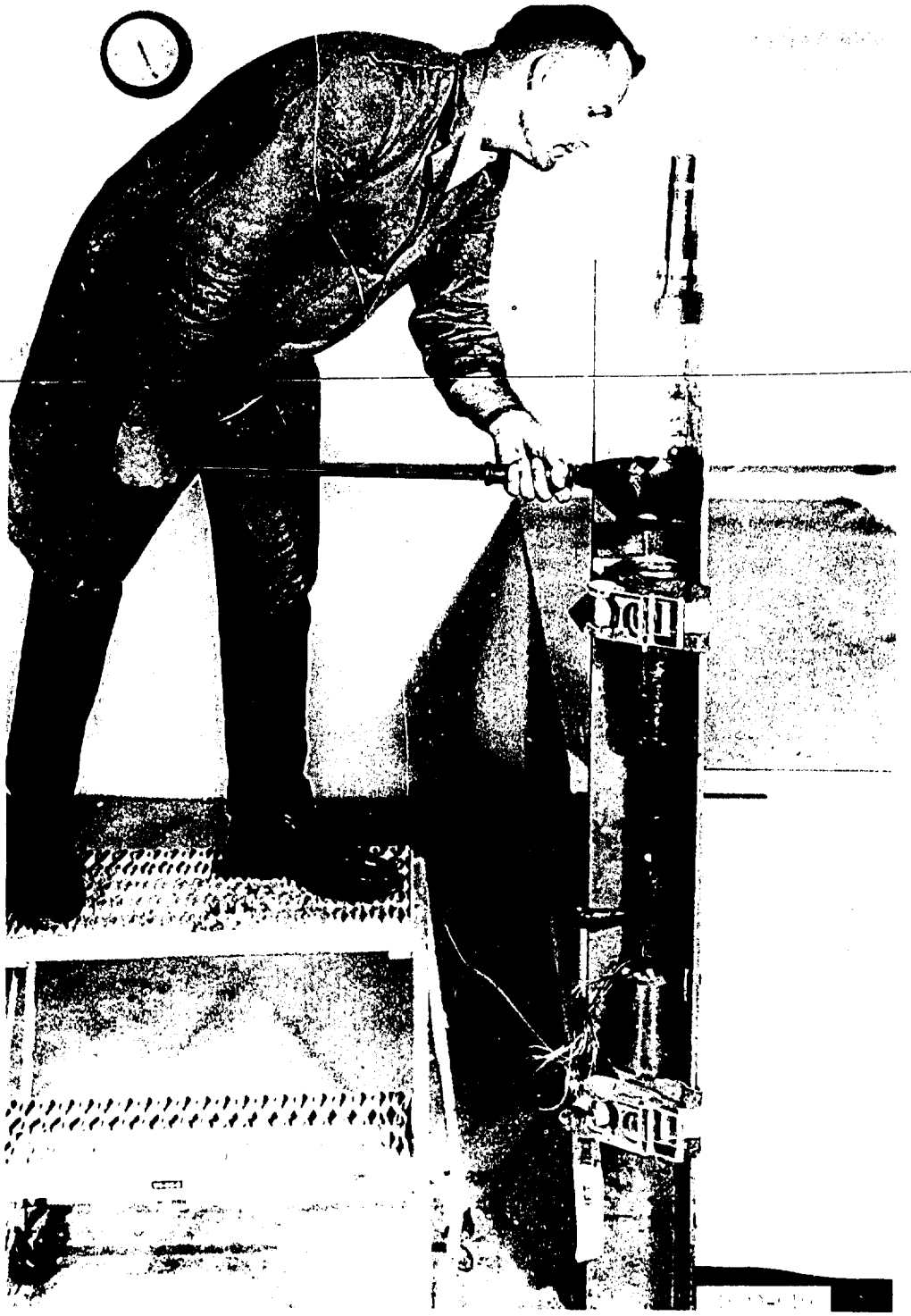

Figure 2.23 Pouring molten babbitt metal into gripper.

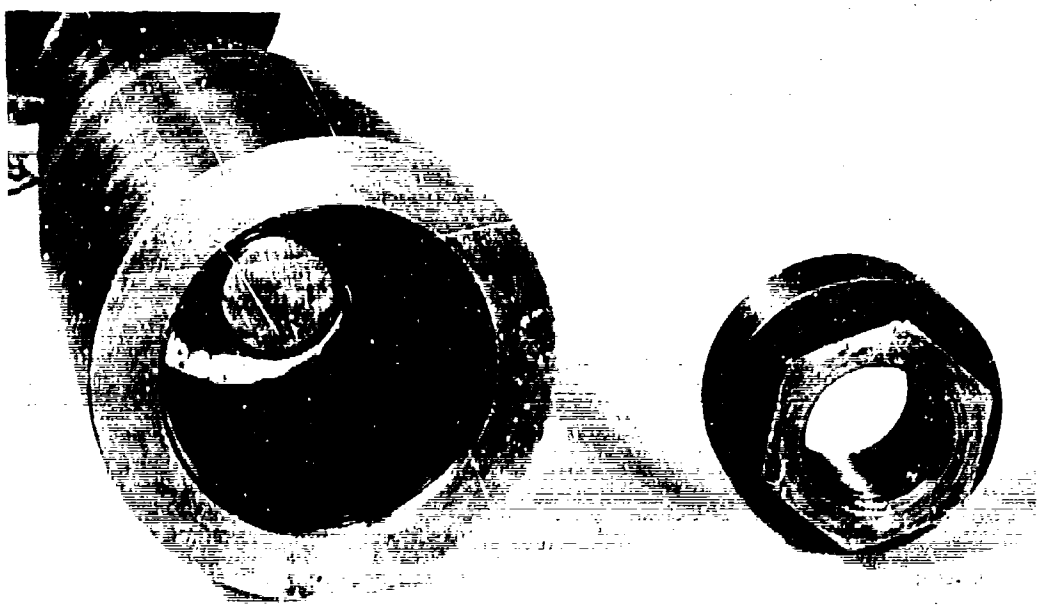

Figure 2.24 End view of poured-type gripper.

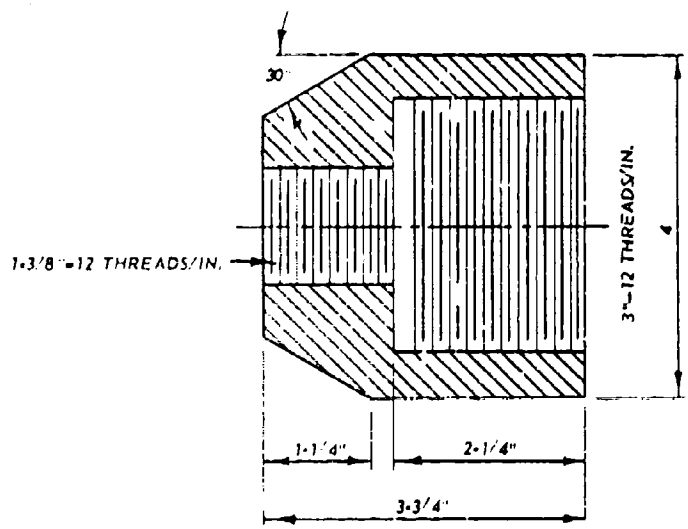

Figure 2.25 Gripper for machined bars.

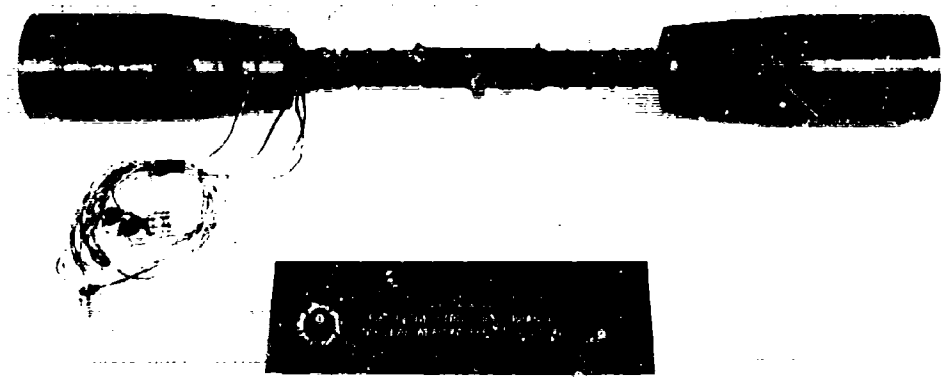

Figure 2.26 Bar with poured-type grippers ready for testing.

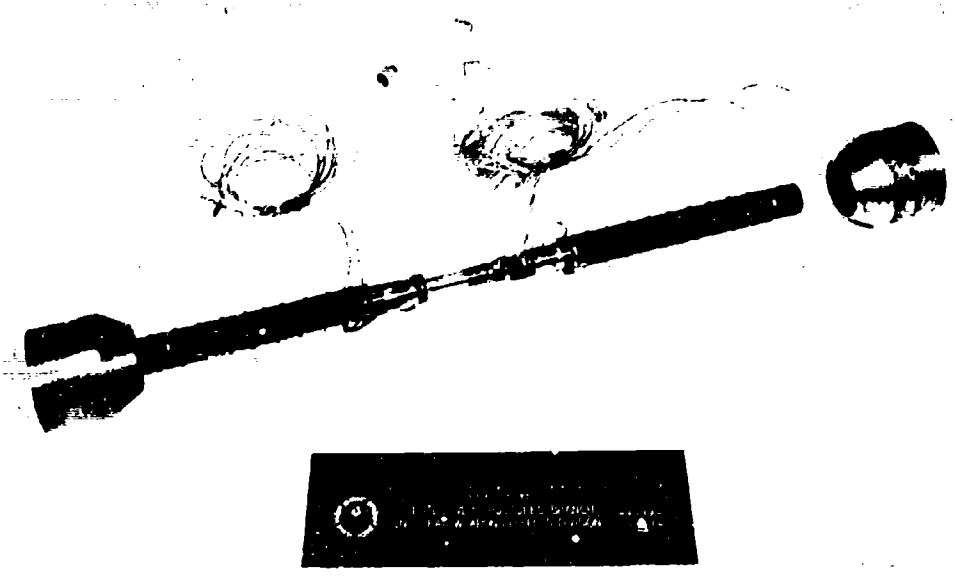

Figure 2.27 Machined bar with one gripper attached.

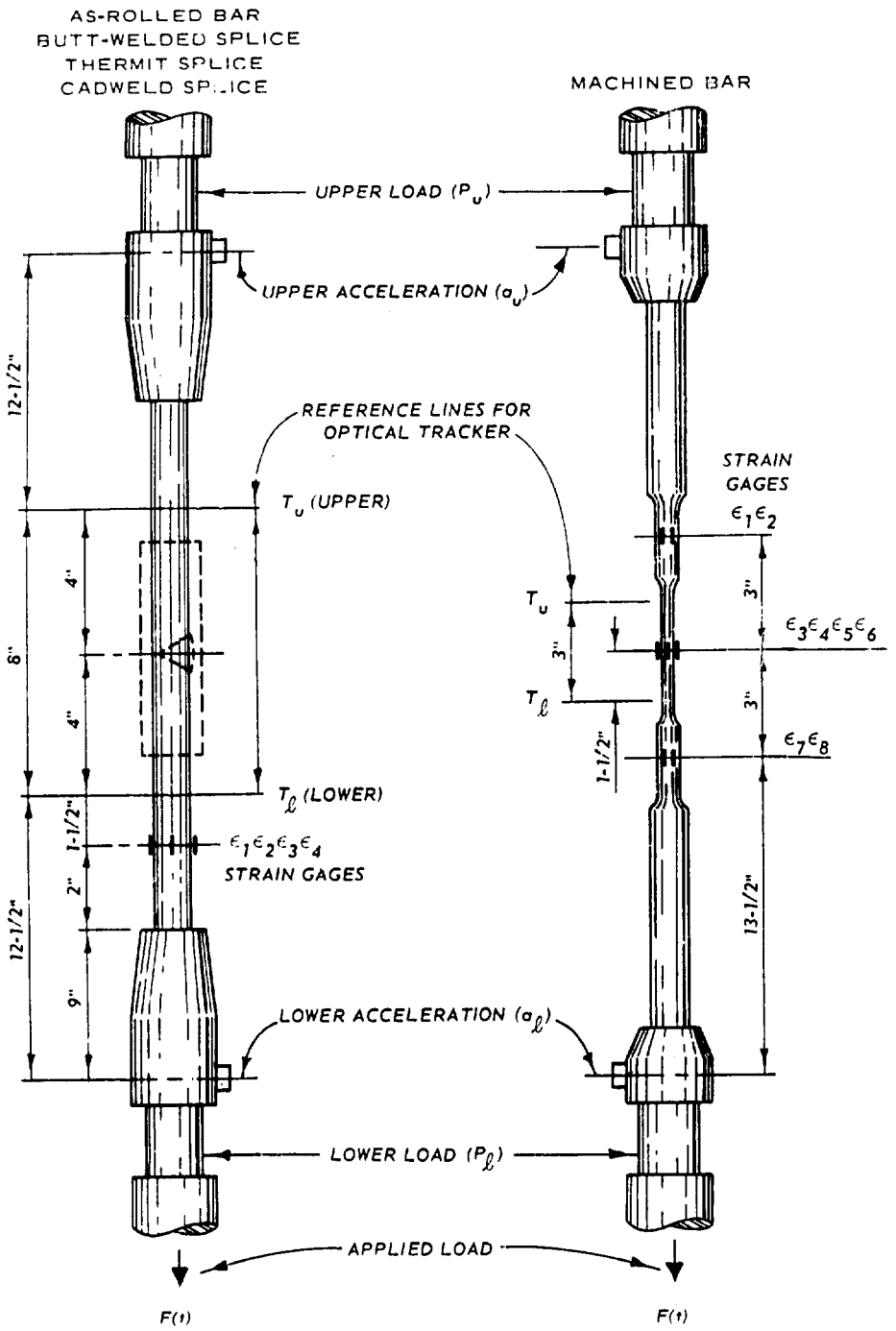

Figure 2.28 Gage locations and identifications for all specimen types.

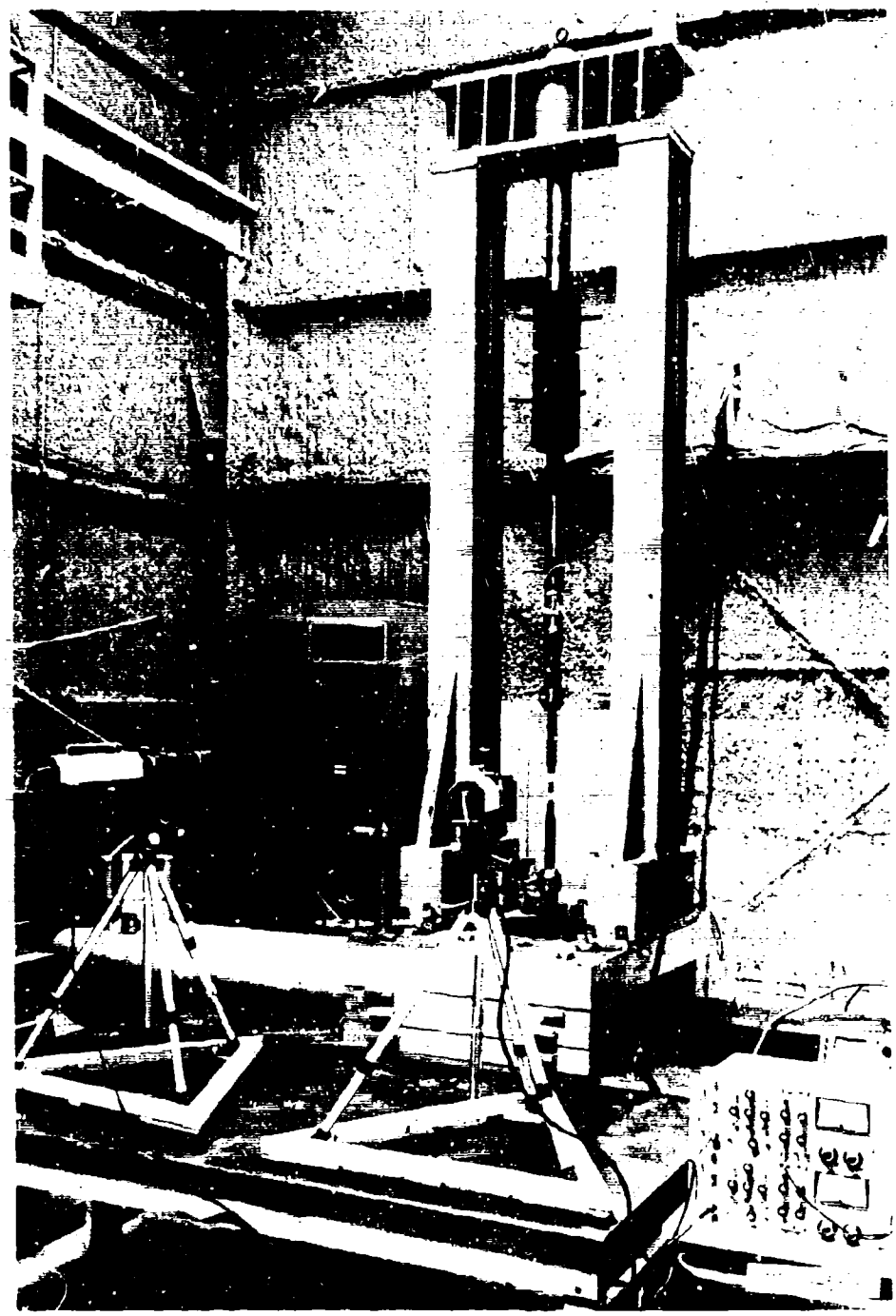

Figure 2.29 Instrumented specimen in place ready for testing.

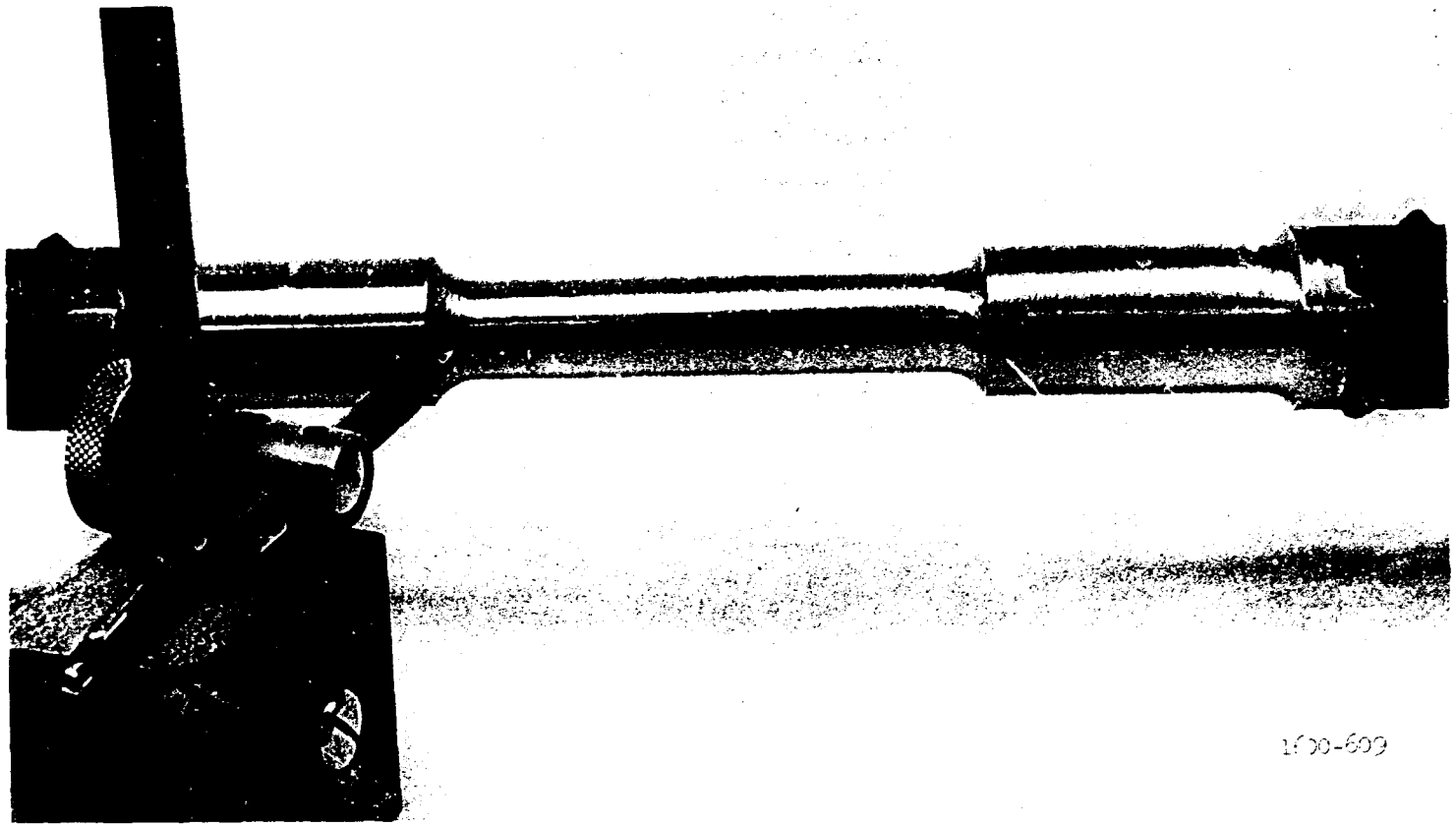

Figure 2.30 Marking strain gage locations.

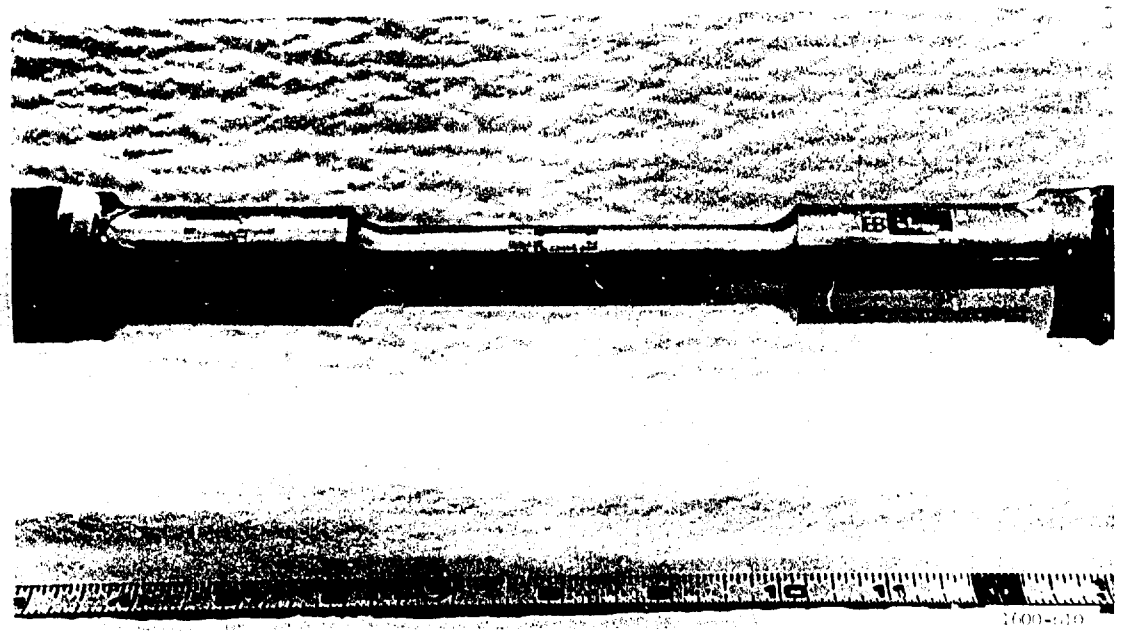

Figure 2.31 Strain gages applied to metal surface.

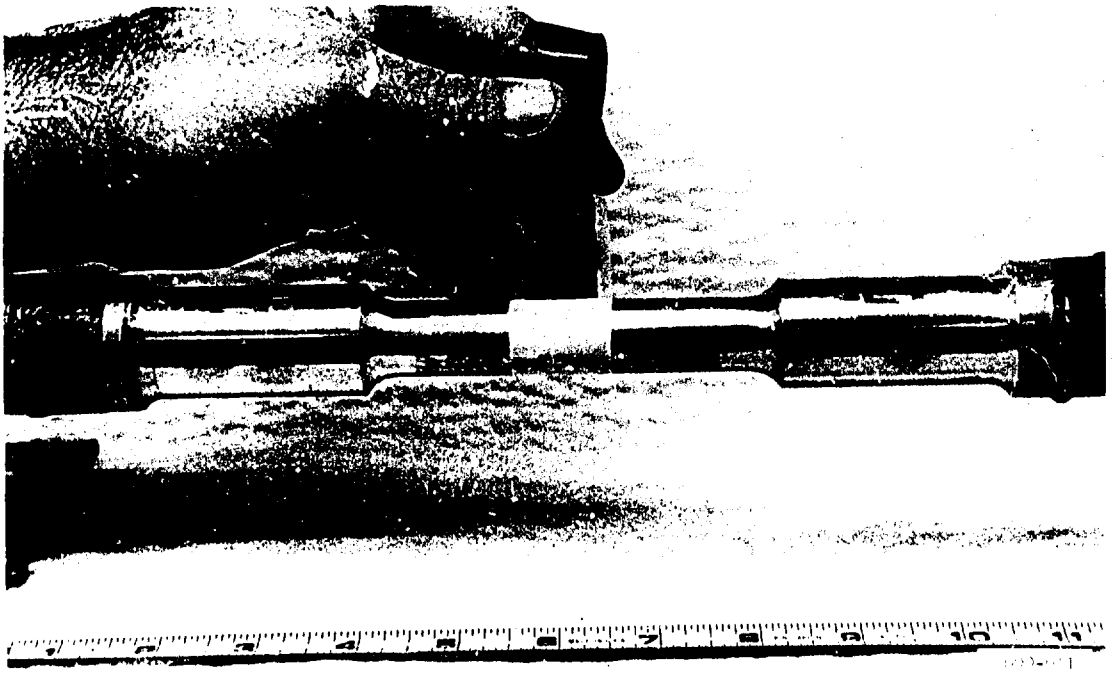

Figure 2.32 Pressing gages to bar.

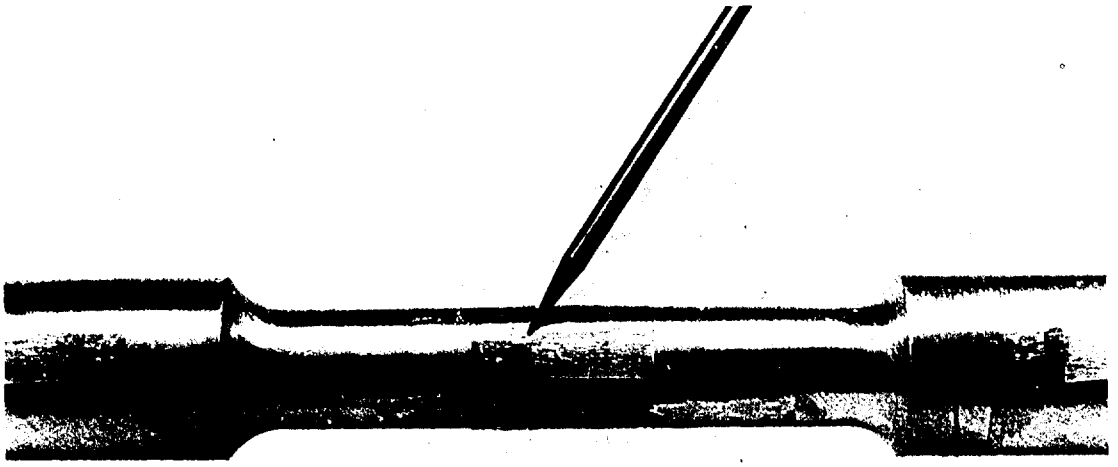

Figure 2.33 Wire attached between gage tab and terminal strip.

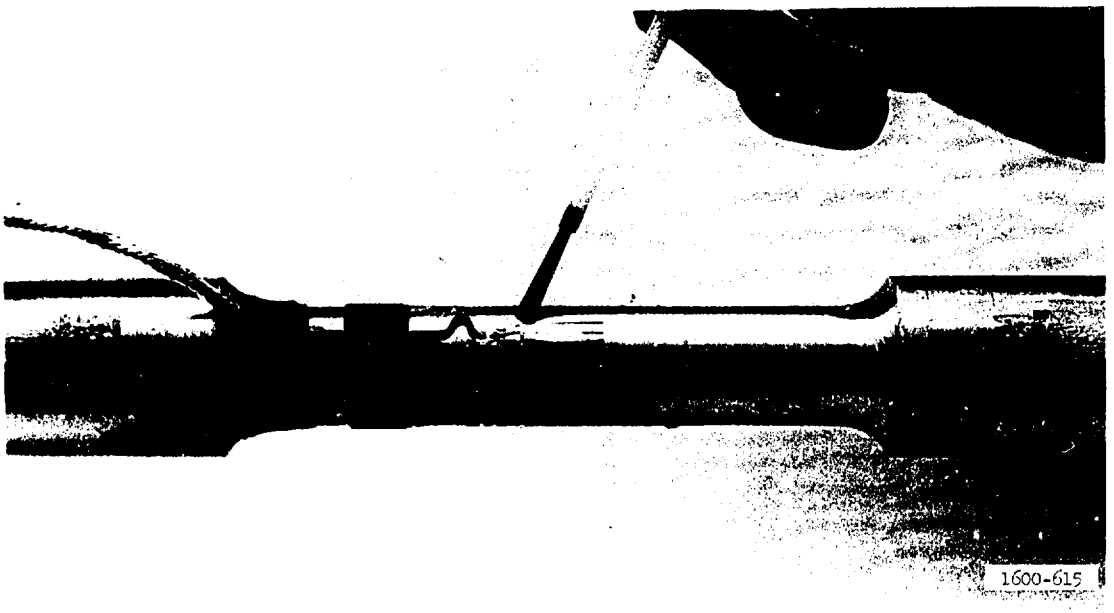

Figure 2.34 Lead wires attached.

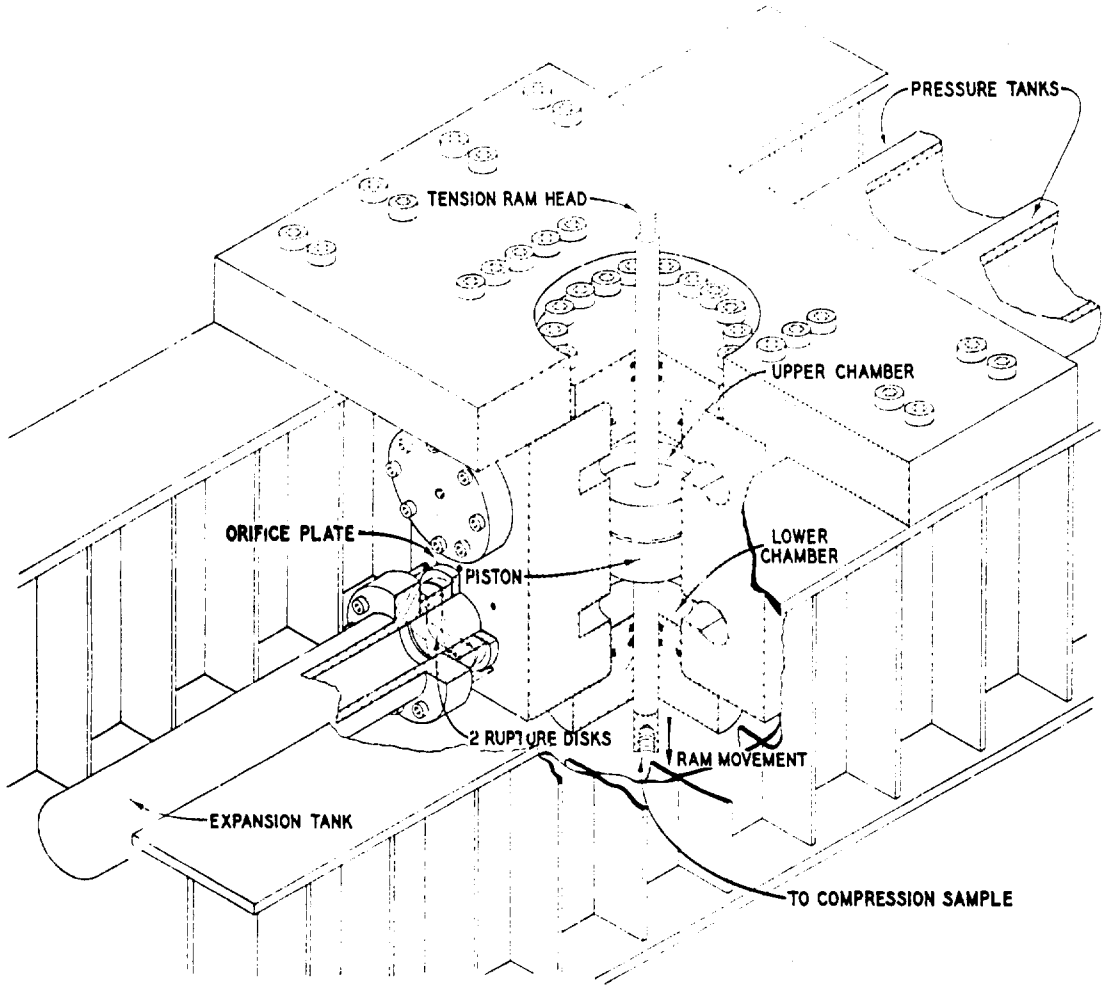

CHARACTERISTICS

1. PEAK DYNAMIC LOAD: 200,000 LB IN LESS THAN 2 MSEC.
2. RISE TIME: 1 TO 200 MSEC.
3. HOLD TIME: 0 TO 200 MSEC.
4. DELAY TIME: 15 TO 500 MSEC.

Figure 2.35 200-kip-capacity dynamic loading device.

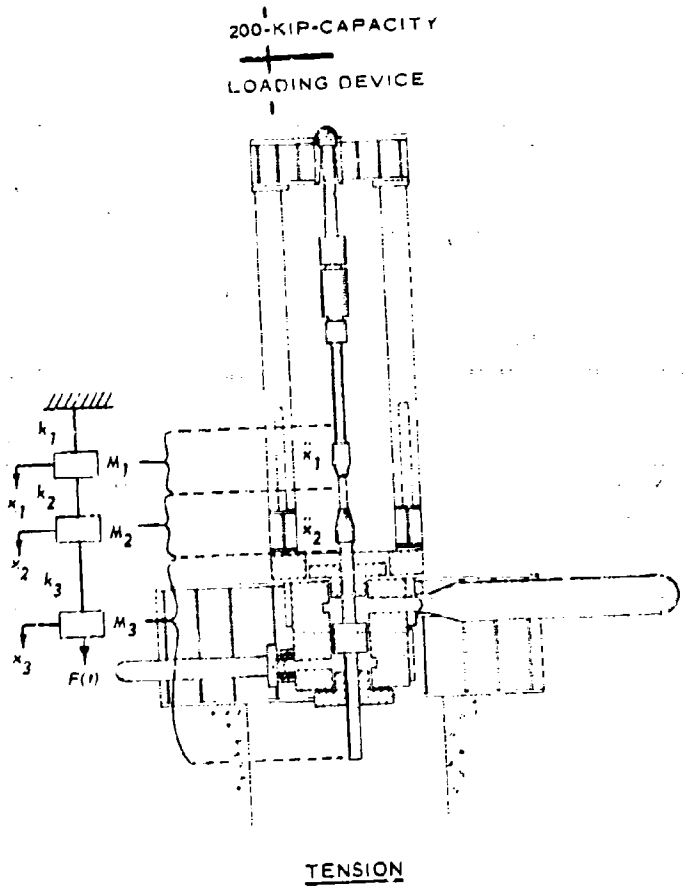

Figure 2.36 Spring-mass model of test configuration.

CHAPTER 3

RESULTS

3.1 TABULATED RESULTS

Copies of the analog records of fourteen tests that are representative of the various specimen types tested are presented in Appendix A. From these data, Tables 3.1 through 3.5 were prepared. Included in the tables are the peak upper and lower loads determined from load cell readings, time to peak load, loading rate, yield strain measurements, average time to yield strain, average strain rate, final elongation of the specimen, and total reduction in area in percent. For the Grade 75 bars, in which no definite yield point existed, the strain rates were not determined until stress-strain plots were prepared and the yield stress for a 0.2 percent offset modulus was determined. Then using the strain determined for the offset yield strength, the analog records were utilized to determine the strain rates for this value of strain. For the Grade 75 machined bars (Table 3.2) only, the offset yield load, time to peak load, and loading rate were also determined from the analog records at the time dictated by the offset yield strain. This type of information was not included in Tables 3.3 through 3.5.

3.2 POSTTEST PHOTOGRAPHS

Posttest photographs of all specimens are shown in Figures 3.1 through 3.8.

3.3 STRESS-STRAIN PLOTS

The analog records for the rapid and intermediate rates of strain

were digitized, electronically operated upon to take account of inertial effects, and electronically plotted. The stress-strain curves for the slow load rate test were hand-digitized and hand-plotted. All these curves are summarized in Figures 3.9 through 3.64. The curves are presented in two parts for two different strain scales. The curves are shown first for strains up to 20,000 μin/in; then each curve is continued on the subsequent page for strains up to 200,000 μin/in. The continued portions of the curves were plotted using optical tracker data except for the elastic portion of each curve. For cases in which the optical tracker exceeded its calibrated range prior to rupture of the bar, the curve was estimated (dashed line) and continued to a strain value at rupture that was measured after the test (see final elongation column in Tables 3.1 through 3.5 for a summary of such values). For static tests, stress-strain values obtained from the optical tracker (shown as open points in the figures) were also plotted on the curves plotted to the 20,000 μin/in scale in order to compare tracker data with those obtained from strain gage results. For the Grade 75 bars that did not have a definite yield point, a 0.2 percent offset modulus was drawn and the intersection of this line with the stress-strain curve established the offset yield strength of the specimen. For rapid load tests, the method described in Section 2.4 was used to determine the true load applied to the test specimen, which was then converted to stress by dividing this quantity by the cross-sectional area of the bar. Sample calculations outlining the procedure to determine the true load for actual tests at a particular time are discussed in Chapter 4.

TABLE 4.1 SUMMARY OF TEST RESULTS, BUTT-WELDED SPLICES

All bars broke in weld.

Test No.	Peak Yield Load		Time to Peak Load		Loading Rate		Yield Strain (Lower Position)					Average Time to Yield Strain	Average Strain Rate $\dot{\epsilon}$	Final Elongation[a]	Reduction in Area[b]
	Upper P_u	Lower P_ℓ	Upper t_u	Lower t_ℓ	Upper $\dot{P}_u$	Lower $\dot{P}_\ell$	ϵ_1	ϵ_2	ϵ_3	ϵ_4	Average	t_y			
	kips		sec		kips/sec		1,000 μin/in					sec	in/in/sec	pct	pct
Grade 60:															
146	150.0	179.0	0.00083	0.00140	180,700	127,900	3.39	2.32	3.19	3.38	3.07	0.0009	3.25	5.9	3.6
150	113.7	120.3	0.4055	0.4258	280	283	3.04	3.26	2.75	2.79	2.96	0.5164	0.0057	8.6	4.3
154	Bad test.													6.5	4.9
159	160.2	161.6	0.001	0.00138	160,200	117,100	3.13	3.12	2.88	2.88	3.00	0.0011	2.69	7.4	5.5
163	116.5	114.9	0.0495	0.475	2,354	2,418	2.49	2.78	3.00	2.87	2.78	0.0480	0.0579	8.2	5.0
168	114.0	114.0	0.0540	0.0553	2,111	2,061	2.40	2.80	2.75	2.60	2.638	0.05672	0.0465	9.8	7.8
186	98.0	99.0	0.958	0.980	102.3	101.0	2.20	2.40	2.30	2.20	2.275	0.9497	0.0024	4.7	3.6
190	97.0	--	0.993	--	97.7	--	2.10	2.40	2.35	2.00	2.213	1.003	0.0022	3.1	3.0
195	97.0	99.0	0.978	0.968	99.2	102.3	2.20	2.20	2.10	2.10	2.15	0.967	0.0022	6.0	3.6
Grade 75:															
174	--	--	--	--	--	--	--	--	--	--	5.50	0.083	0.066	3.9	0.4
178	--	--	--	--	--	--	--	--	--	--	5.25	0.088	0.060	4.7	0.3
182	--	--	--	--	--	--	--	--	--	--	5.15	0.081	0.064	6.6	0.3

[a] Over 8-inch gage length; posttest measurements.
[b] Measured on bar, not in splice; gage locations are shown in Figure 2.28.

[illegible] OF TEST RESULTS, [illegible] SPLICES

Test	Peak Load Upper	Peak Load Lower	Time to Peak Load Upper t_u	Time to Peak Load Lower t_l	Loading Rate Upper $\dot{F}_u$	Loading Rate Lower $\dot{F}_l$	Yield Strain (Lower Position) ϵ_1	ϵ_2	ϵ_3	ϵ_4	Average	Average Time to Yield Strain t_y	Average Strain Rate $\dot{\epsilon}$	Final Elongation[a]	Reduction in Area[b]	Remarks
	kips		sec		kips/sec		1,000 µin/in					sec	in/in/sec	pct	pct	
[illegible]																
[illegible]	[illegible]	[illegible]	[illegible]	[illegible]	[illegible]	117,500	2.73	3.16	3.41	2.74	3.02	0.0012	2.51	3.7	[illegible]	Bar broke 1 inch above splice
[illegible]	[illegible]	[illegible]	[illegible]	0.0014	[illegible]	115,200	[illegible]	2.91	2.96	3.18	[illegible]	0.0011	2.83	10.7	12.1	Bar broke 1 inch below splice
[illegible]	[illegible]	[illegible]	[illegible]	[illegible]	[illegible]	[illegible]	[illegible]	2.80	3.10	2.95	[illegible]	0.000935	3.10	7.0	[illegible]	Bar broke 1 inch above splice
[illegible]	[illegible]	[illegible]	[illegible]	[illegible]	[illegible]	[illegible]	[illegible]	[illegible]	3.07	3.03	[illegible]	0.060	0.0542	6.2	[illegible]	Bar broke 1 inch below splice
[illegible]	[illegible]	[illegible]	[illegible]	[illegible]	[illegible]	[illegible]	2.70	[illegible]	2.65	2.65	2.675	[illegible]	0.0434	6.6	7.5	Bar did not break
[illegible]	[illegible]	[illegible]	[illegible]	[illegible]	[illegible]	[illegible]	[illegible]	[illegible]	2.60	2.50	2.725	0.0550	0.0495	8.6	9.8	Bar did not break
[illegible]	[illegible]	[illegible]	[illegible]	[illegible]	[illegible]	111.1	2.45	2.45	2.35	2.40	2.413	[illegible]	0.0026	0.79	0.3	Bar broke in splice but did not yield
[illegible]	[illegible]	[illegible]	[illegible]	[illegible]	[illegible]	107.9	2.20	2.45	[illegible]	2.20	[illegible]	[illegible]	0.0024	5.1	[illegible]	Bar broke 1 inch above splice
[illegible]	[illegible]	[illegible]	[illegible]	[illegible]	110.5	[illegible]	2.30	2.45	2.25	2.15	[illegible]	[illegible]	0.0024	5.5	[illegible]	Bar broke 1/2 inch above splice
[illegible]																
[illegible]	--	--	--	--	--	--	--	--	--	--	5.00	[illegible]	0.075	0.79	0.3	Bar broke in splice
[illegible]	--	--	--	--	--	--	--	--	--	--	5.20	[illegible]	[illegible]	2.4	[illegible]	Bar broke 1 inch above splice
[illegible]	--	--	--	--	--	--	--	--	--	--	[illegible]	[illegible]	0.077	1.95	[illegible]	Bar broke 1/4 inch below splice

[a] [illegible]-inch gage length.
[b] [illegible] are shown in Figure 2.28.

[illegible] OF TEST RESULTS, [illegible] SPLICES

Test	Peak Load Upper	Peak Load Lower	Time to Peak Load Upper t_u	Time to Peak Load Lower t_l	Loading Rate Upper $\dot{F}_u$	Loading Rate Lower $\dot{F}_l$	Yield Strain (Lower Position) ϵ_1	ϵ_2	ϵ_3	ϵ_4	Average	Average Time to Yield Strain t_y	Average Strain Rate $\dot{\epsilon}$	Final Elongation[a]	Reduction in Area[b]	Remarks
	kips		sec		kips/sec		1,000 µin/in					sec	in/in/sec	pct	pct	
[illegible]																
[illegible]	[illegible]	[illegible]	[illegible]	[illegible]	[illegible]	[illegible]	[illegible]	[illegible]	2.65	[illegible]	[illegible]	0.0012	2.2	[illegible]	0.05	Lower bar pulled out (2 deformations)
[illegible]	[illegible]	[illegible]	[illegible]	0.00130	[illegible]	[illegible]	3.11	[illegible]	3.32	[illegible]	[illegible]	0.0013	2.6	3.1	[illegible]	Lower bar pulled out (3 deformations)
[illegible]	[illegible]	[illegible]	0.00115	0.00135	[illegible]	[illegible]	--	[illegible]	3.00	[illegible]	[illegible]	0.0012	2.6	1.8	3.4	Upper bar pulled out (2-1/2 deformations)
[illegible]	[illegible]	[illegible]	[illegible]	[illegible]	[illegible]	2,140	[illegible]	2.94	2.97	[illegible]	2.51	[illegible]	0.0502	4.7	[illegible]	Upper bar pulled out (2-1/2 deformations)
[illegible]														2.7	3.6	Upper bar pulled out (2 deformations)
[illegible]	[illegible]	[illegible]	[illegible]	[illegible]	[illegible]	[illegible]	[illegible]	2.50	[illegible]	[illegible]	2.713	[illegible]	0.0412	2.3	[illegible]	Lower bar pulled out (2-1/2 deformations)
[illegible]	[illegible]	[illegible]	[illegible]	[illegible]	[illegible]	[illegible]	2.20	2.40	2.50	2.10	2.30	[illegible]	0.0024	[illegible]	[illegible]	Lower bar pulled out (3 deformations)
[illegible]	[illegible]	[illegible]	[illegible]	[illegible]	[illegible]	[illegible]	2.30	2.20	2.40	2.20	[illegible]	1.059	0.0021	[illegible]	[illegible]	Upper bar pulled out (2-1/2 deformations)
[illegible]	[illegible]	[illegible]	[illegible]	1.11	[illegible]	[illegible]	2.40	2.40	[illegible]	2.20	[illegible]	[illegible]	0.0022	[illegible]	[illegible]	Lower bar pulled out (2-1/2 deformations)
[illegible]																
[illegible]	--	--	--	--	--	--	--	--	--	--	[illegible]	[illegible]	[illegible]	1.95	[illegible]	Upper bar pulled out (2 deformations)
[illegible]	--	--	--	--	--	--	--	--	--	--	5.20	[illegible]	0.055	3.9	3.4	Bar did not break
[illegible]	--	--	--	--	--	--	--	--	--	--	[illegible]	[illegible]	[illegible]	[illegible]	[illegible]	Lower bar pulled out (2 deformations)
[illegible]	[illegible]	[illegible]	[illegible]	[illegible]	[illegible]	[illegible]	[illegible]	[illegible]	--	--	[illegible]	[illegible]	0.049	[illegible]	9.5	Bar did not break
[illegible]	[illegible]	[illegible]	[illegible]	[illegible]	[illegible]	[illegible]	[illegible]	[illegible]	--	--	[illegible]	[illegible]	0.052	[illegible]	[illegible]	Splice failed

[a] [illegible] gage length.
[b] [illegible] are shown in Figure 2.28.

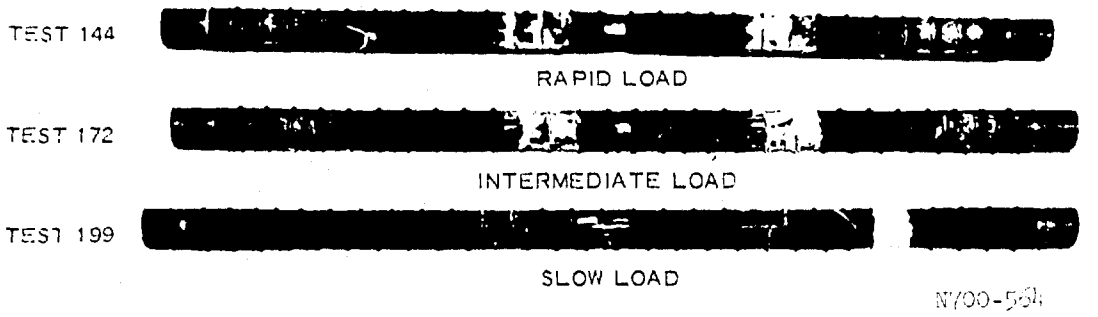

Figure 3.1 Posttest, as-rolled bars, Grade 60.

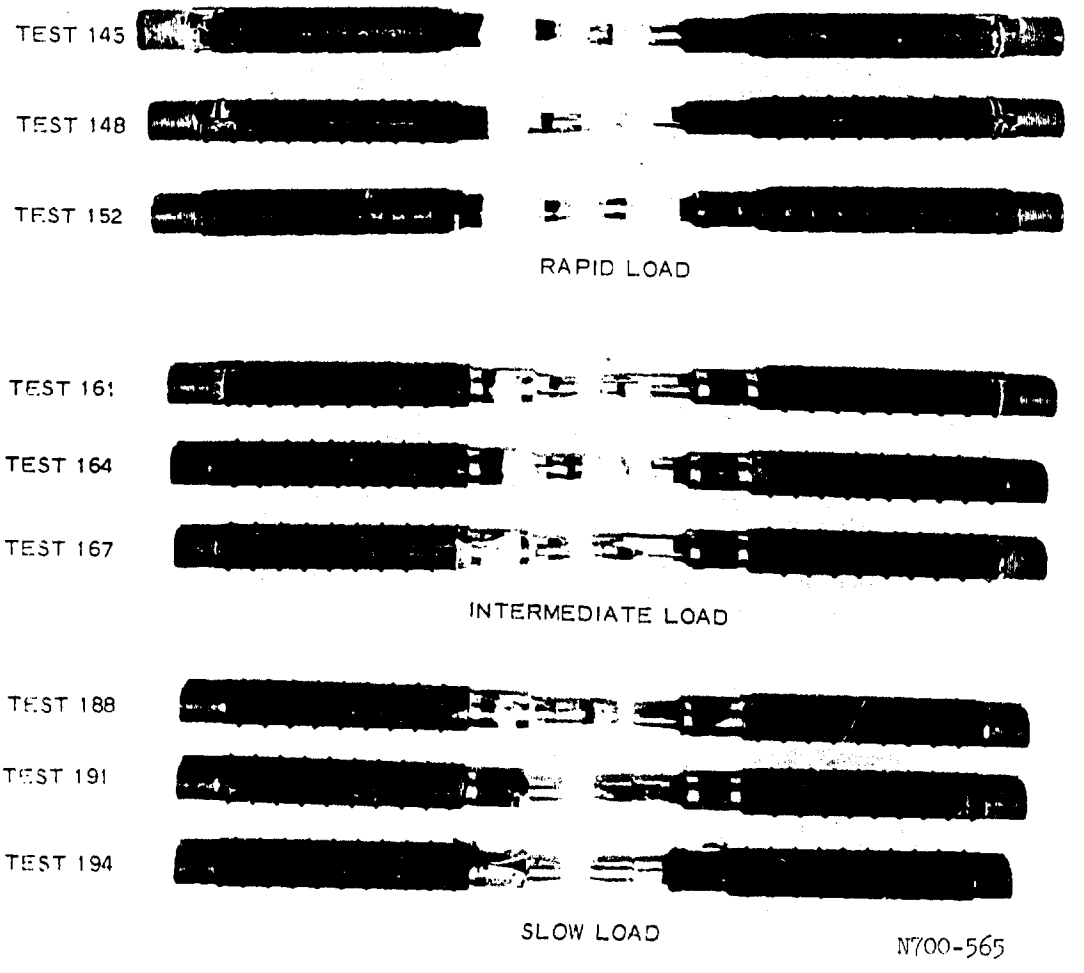

Figure 3.2 Posttest, machined bars, Grade 60.

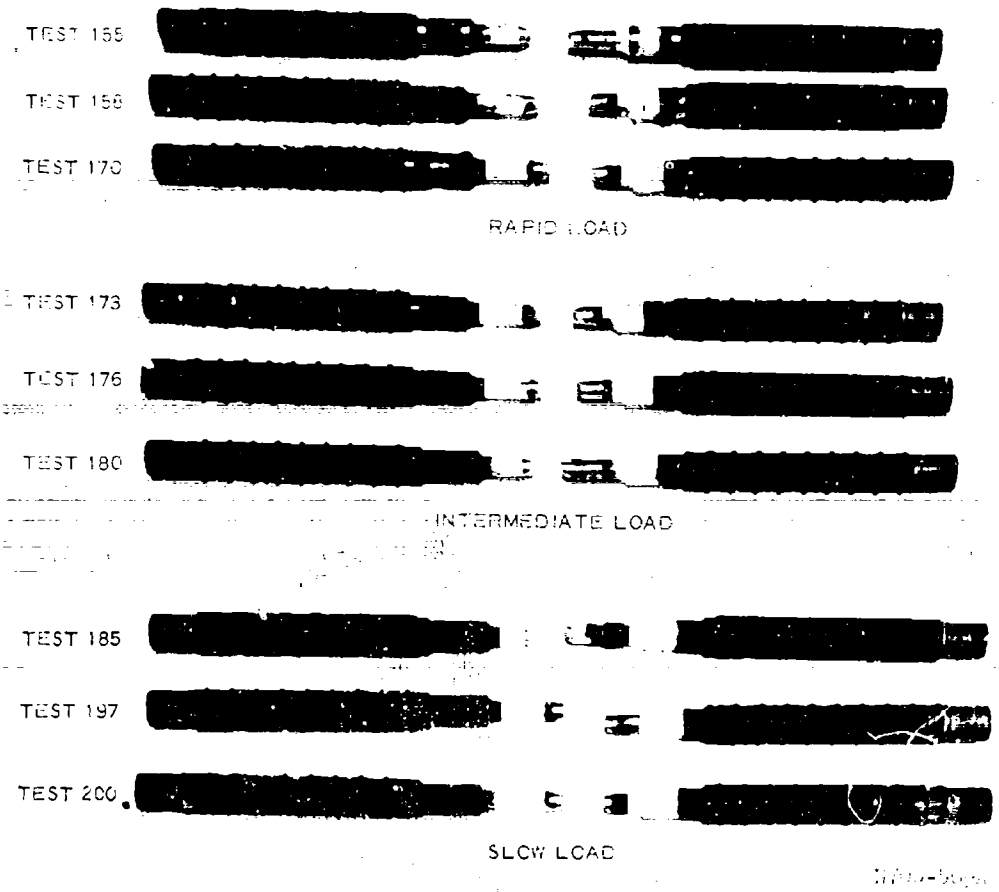

Figure 3.3 Posttest, machined bars, Grade 75.

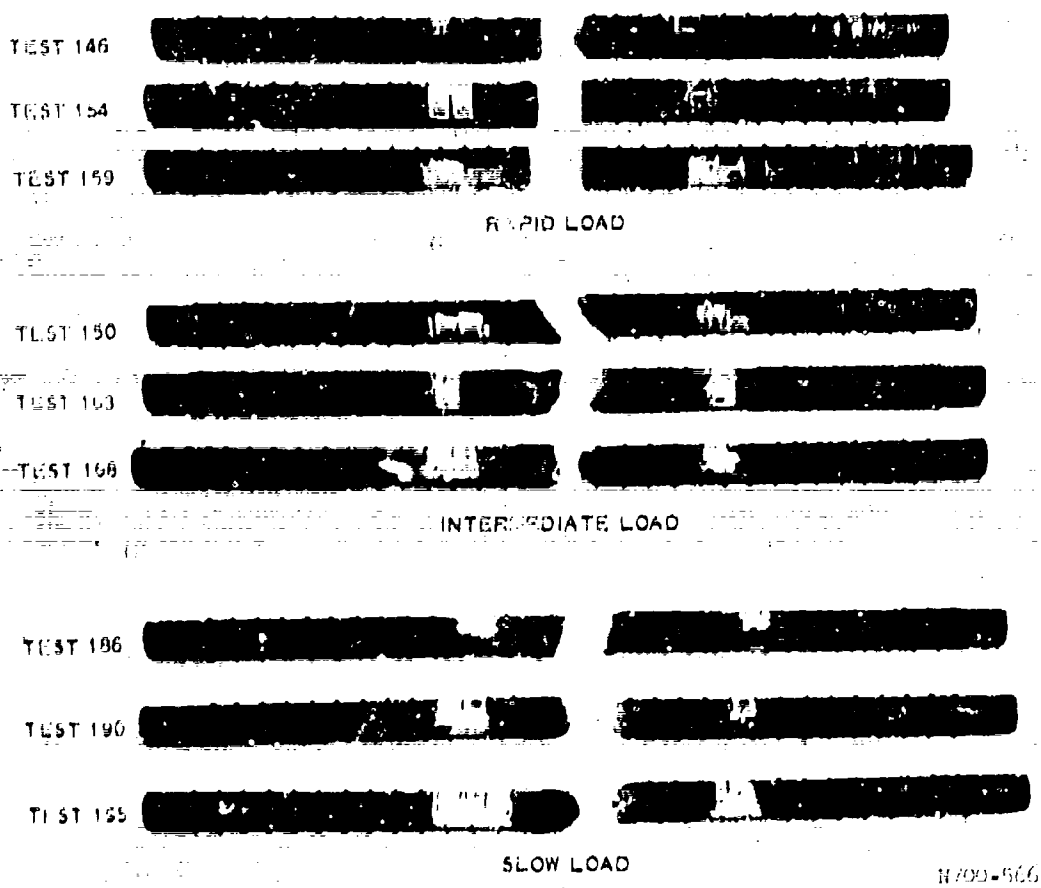

Figure 4.4 Restitent, butt-welded splices, Grade 60.

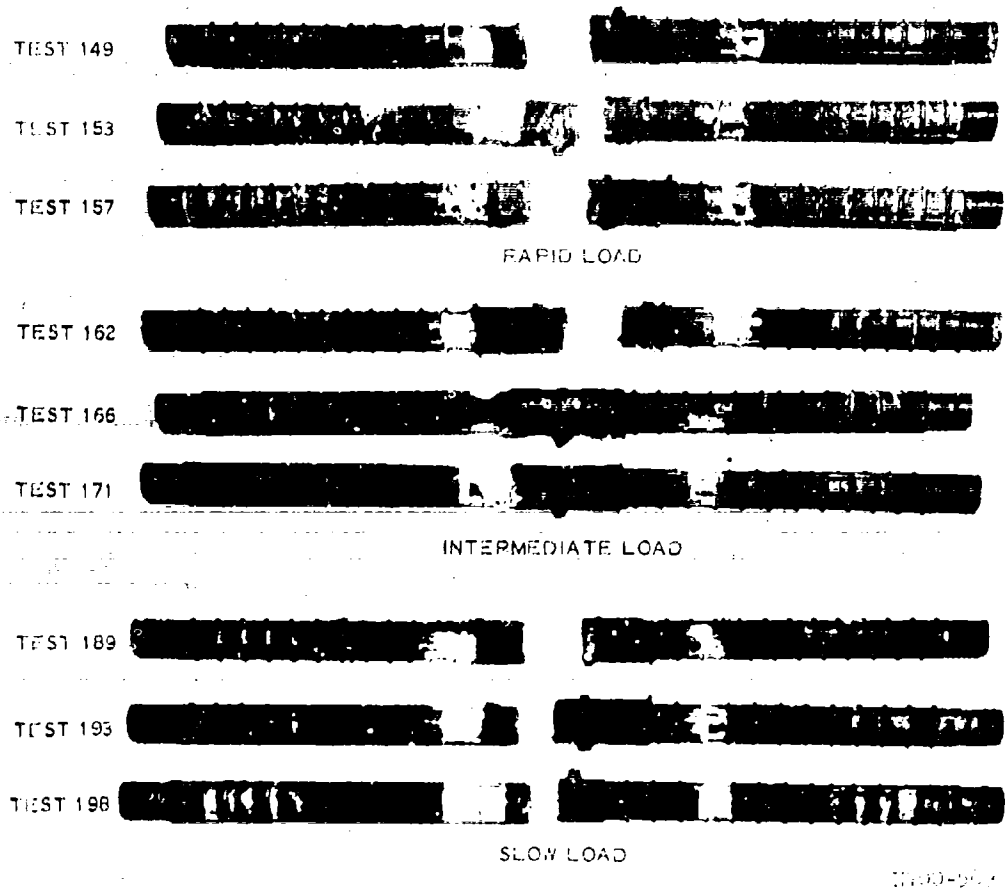

Figure 3.5 Posttest, Thermit splices, Grade 60.

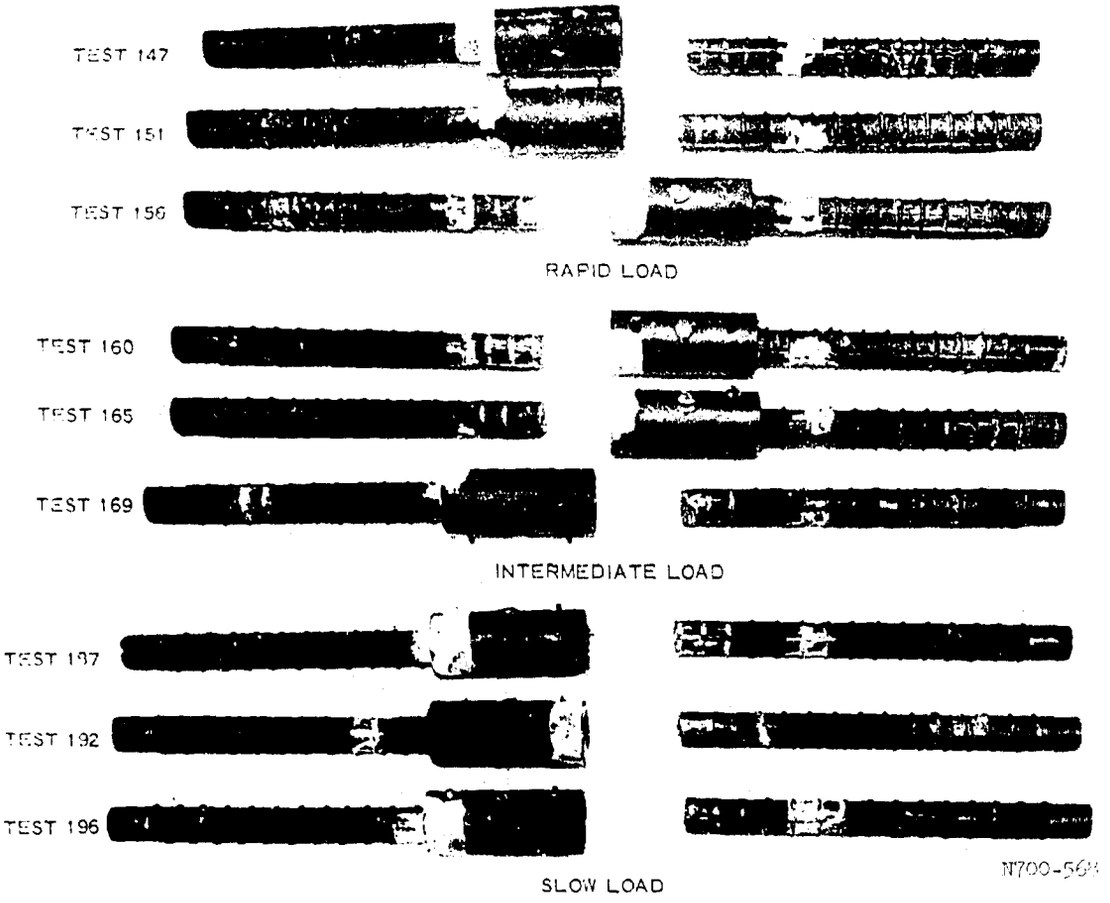

Figure 3.6 Posttest, Cadweld splices, Grade 60.

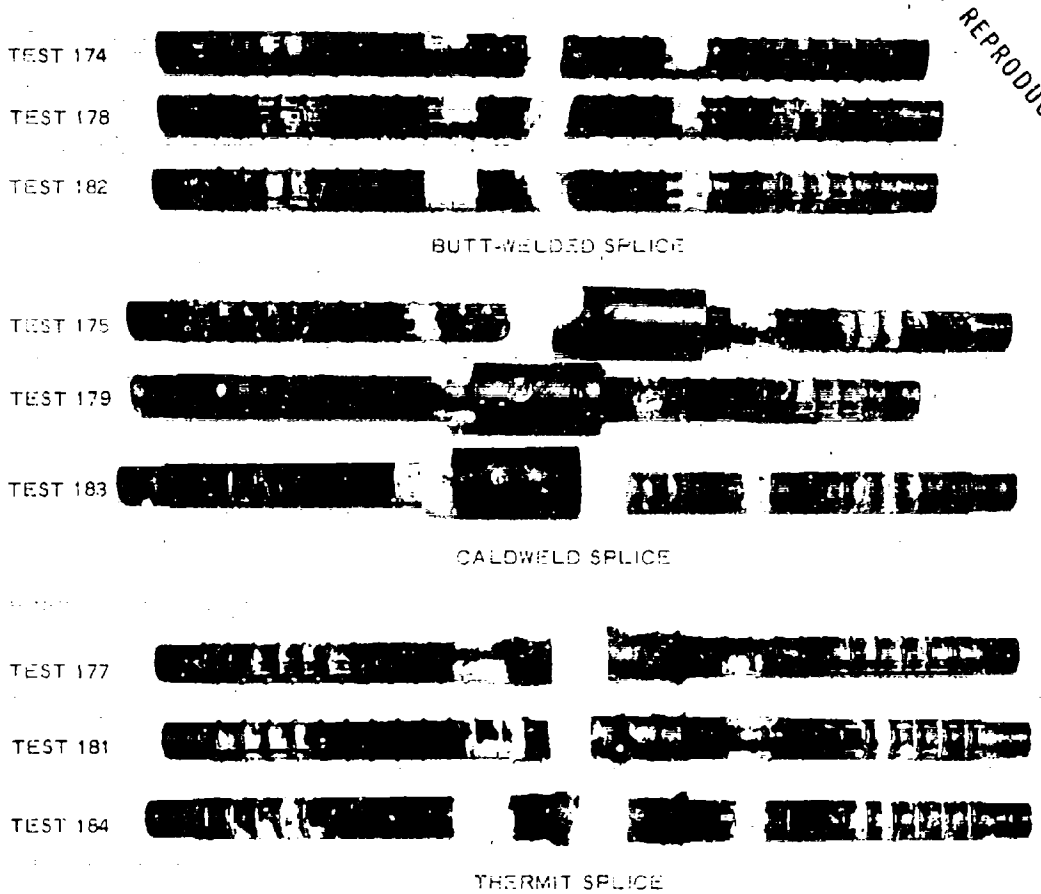

Figure 3.7 Posttest, intermediate load rate, Grade 75.

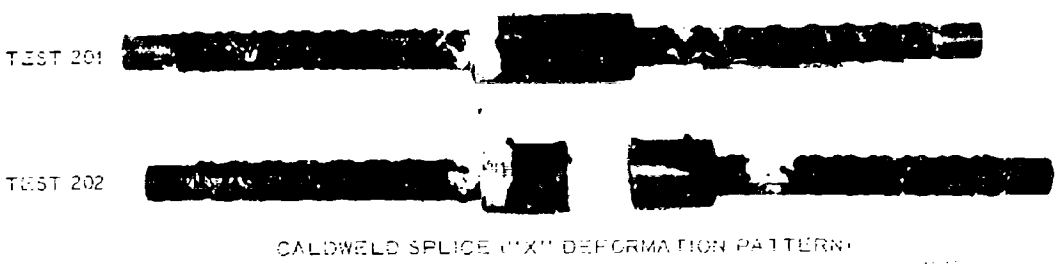

Figure 3.8 Posttest, intermediate load rate, Grade 75, bars with "X" deformations.

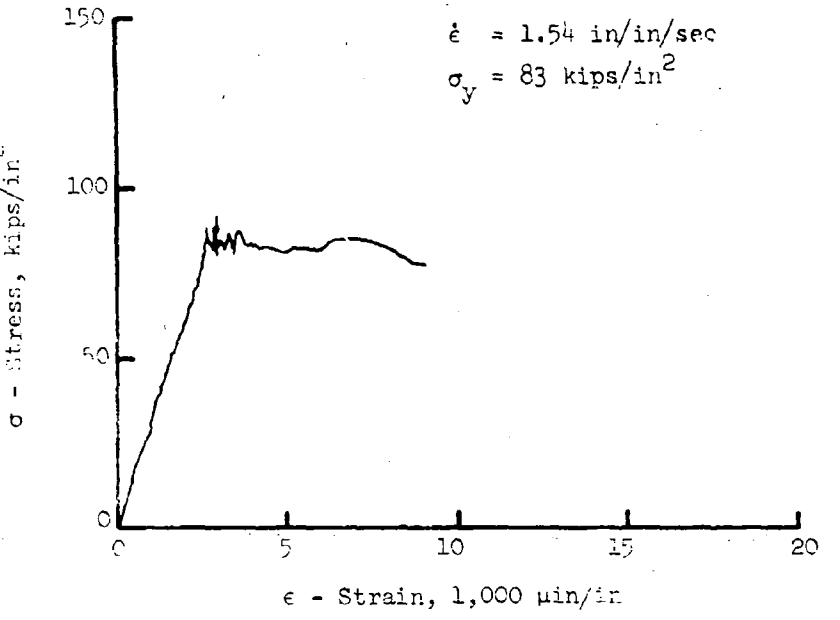

Figure 3.9 As-rolled bar, Grade 60, Test No. 144.

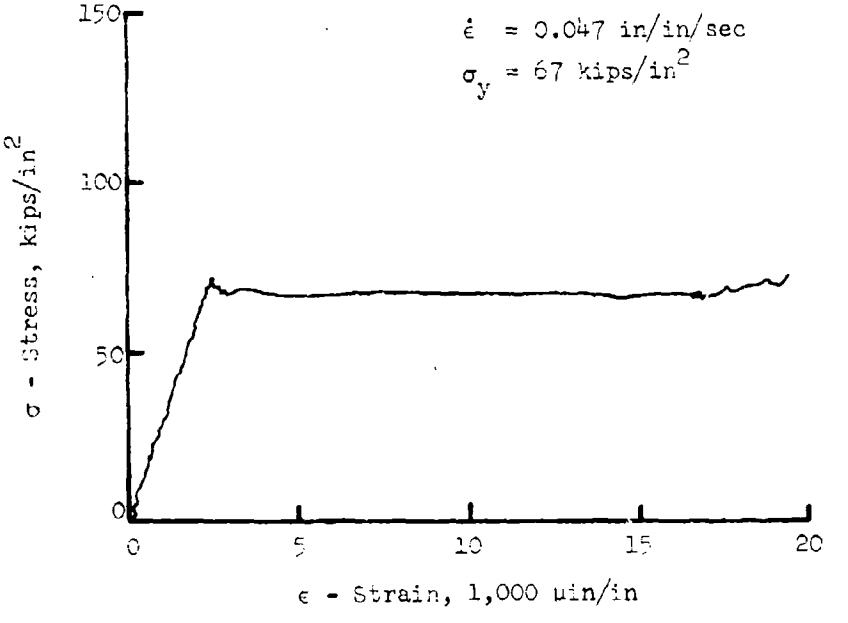

Figure 3.10 As-rolled bar, Grade 60, Test No. 172.

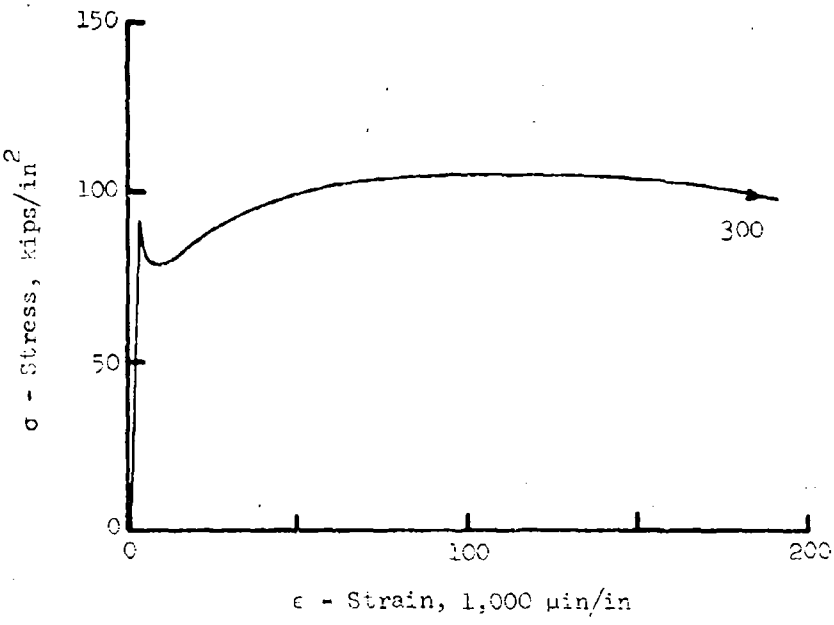

Figure 3.9 (Continued) Test No. 1[illegible].

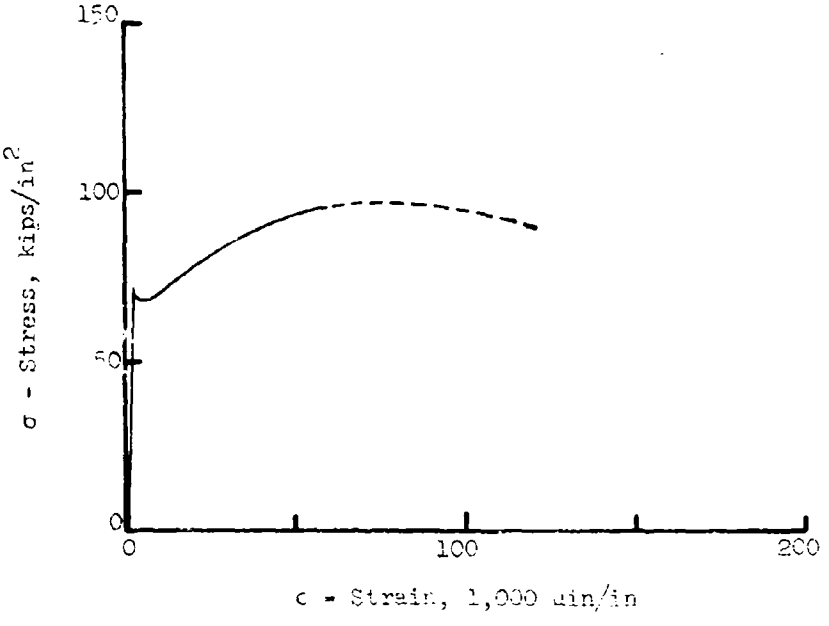

Figure 3.10 (Continued) Test No. 1T2.

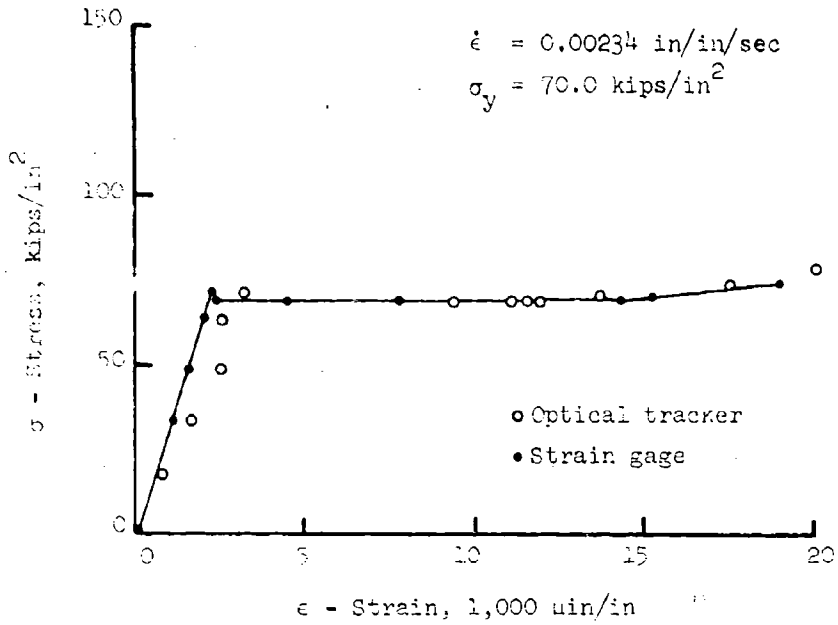

Figure 3.11 As-rolled bar, Grade 60, Test No. 199.

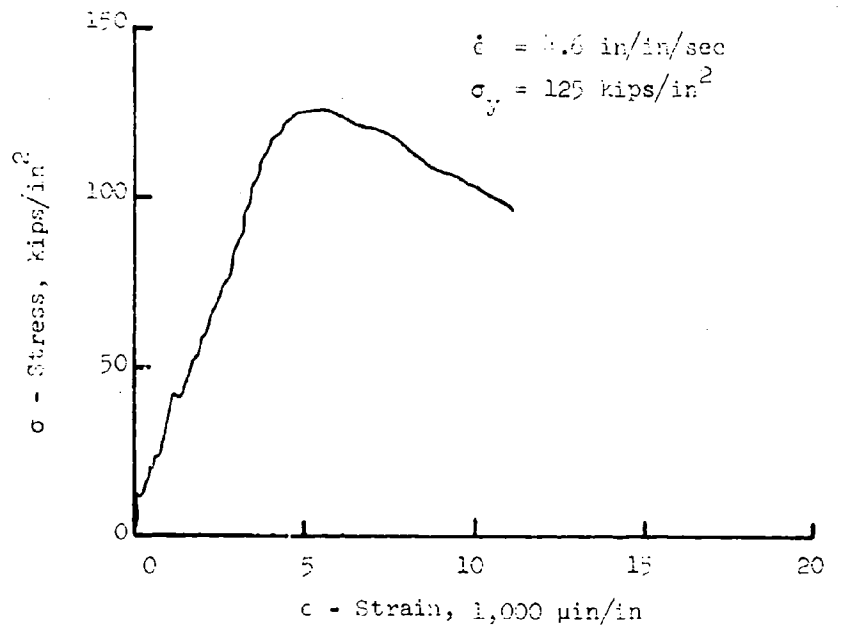

Figure 3.12 Machined bar, Grade 60, Test No. 149.

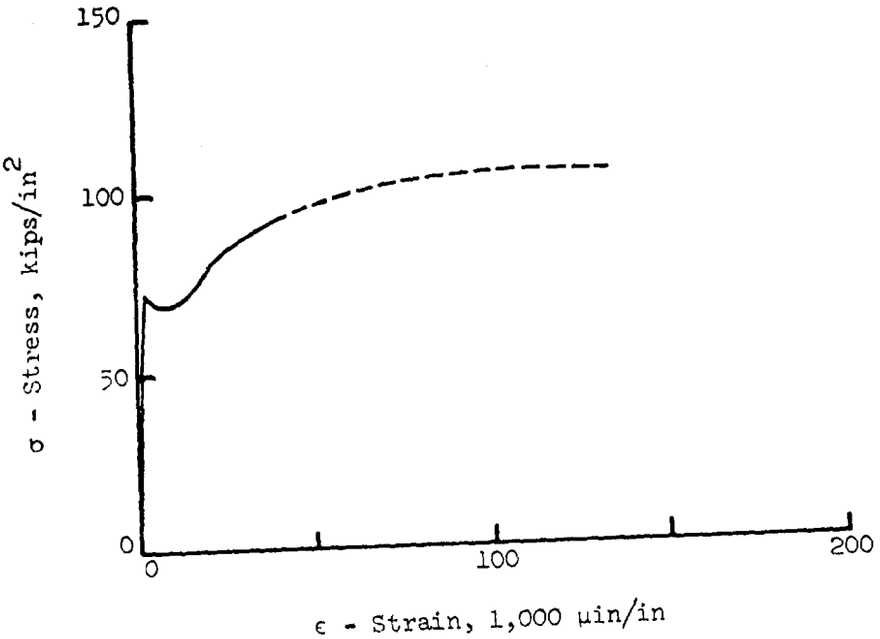

Figure 3.11 (Continued) Test No. 199.

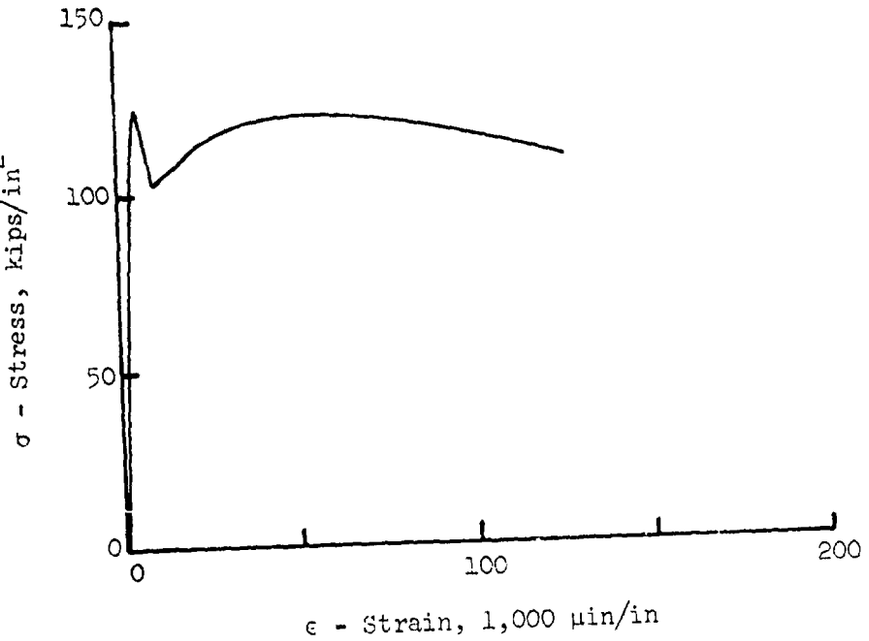

Figure 3.12 (Continued) Test No. 145.

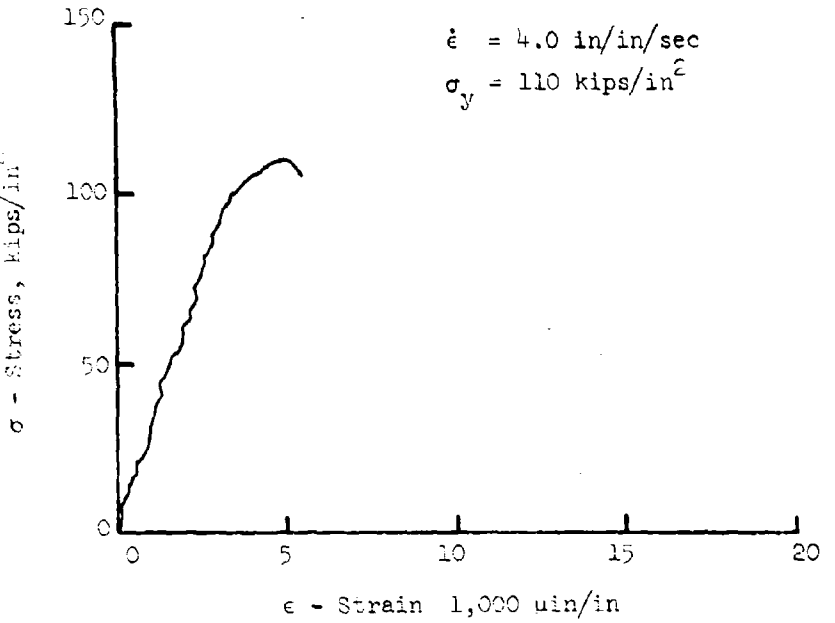

Figure 3.13 Machined bar, Grade 60, Test No. 148.

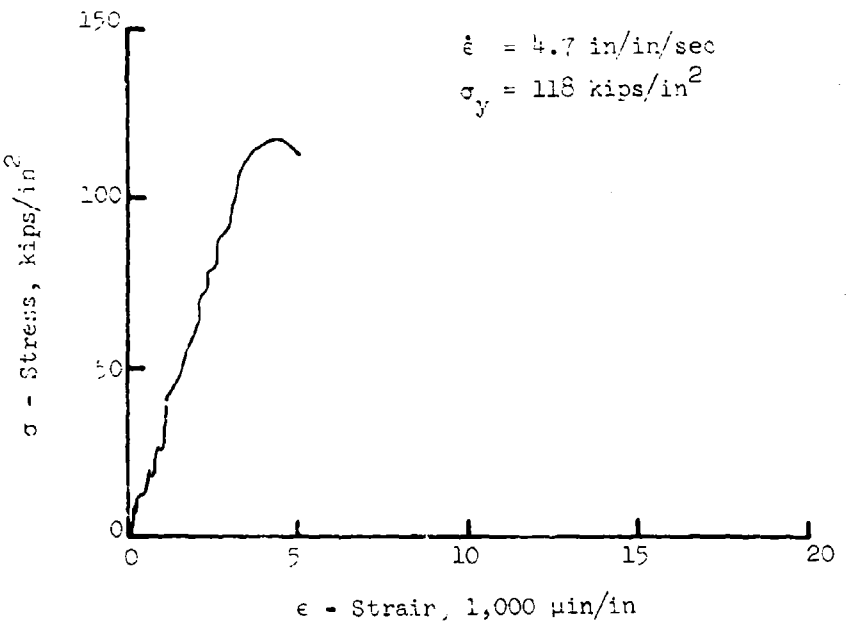

Figure 3.14 Machined bar, Grade 60, Test No. 152.

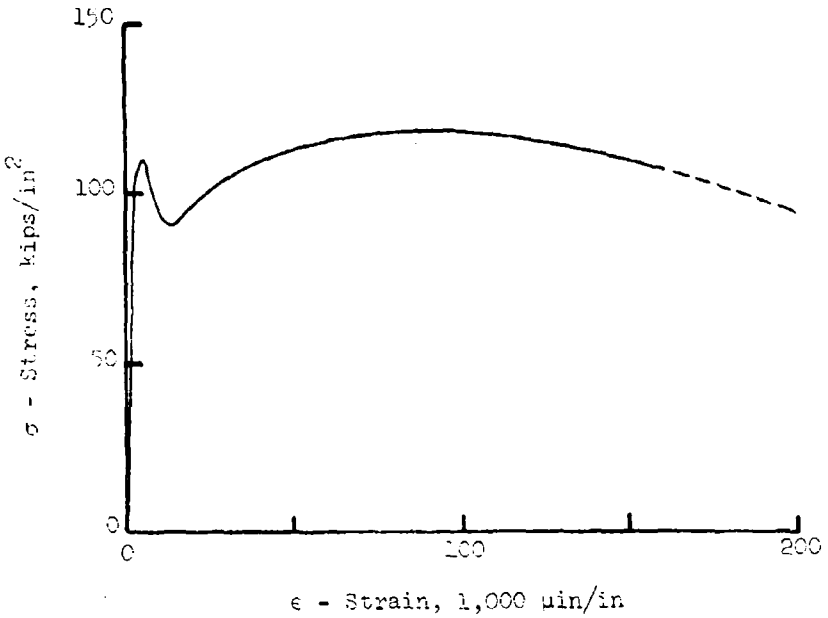

Figure 3.13 (Continued) Test No. 148.

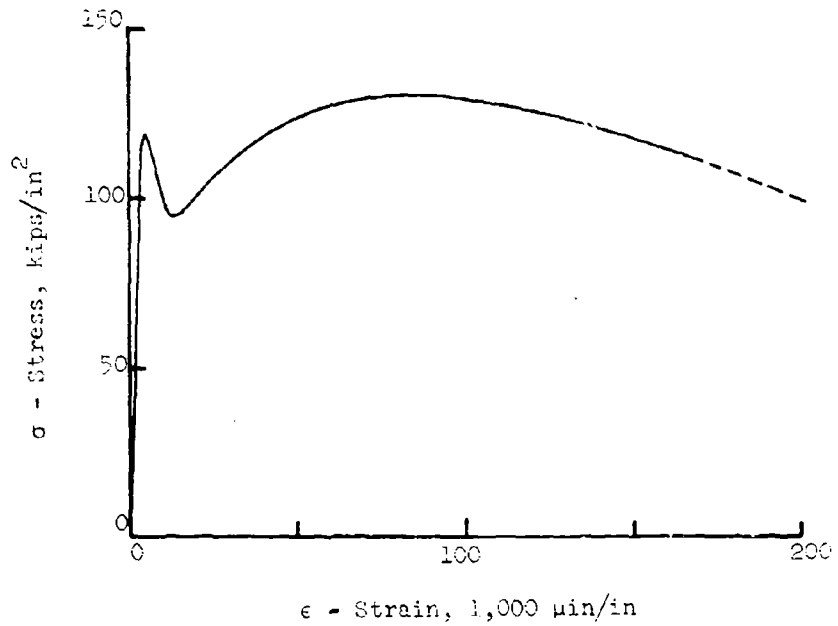

Figure 3.14 (Continued) Test No. 152.

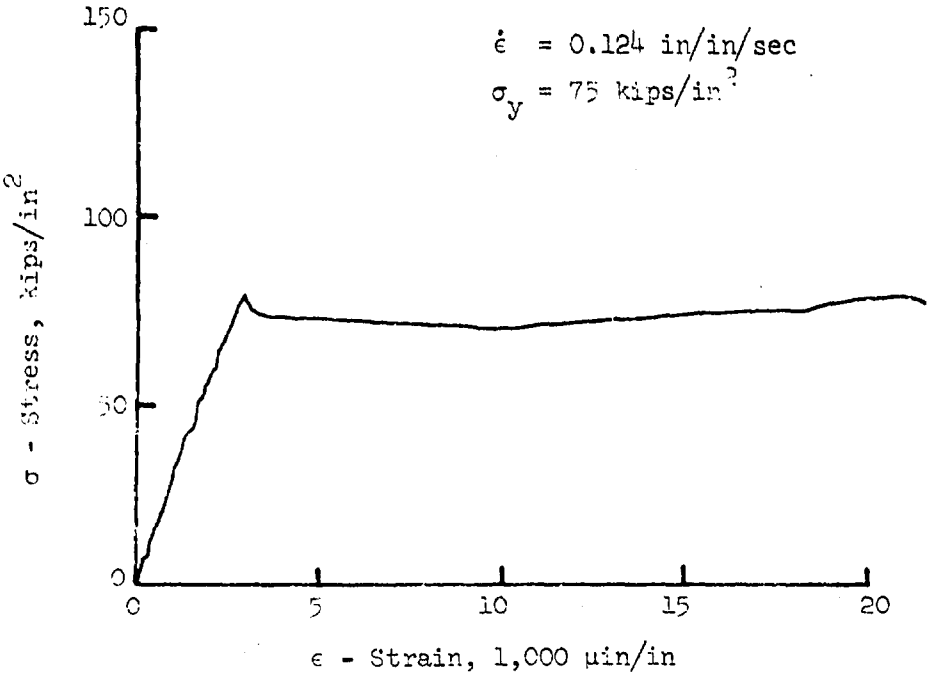

Figure 3.15 Machined bar, Grade 60, Test No. 161.

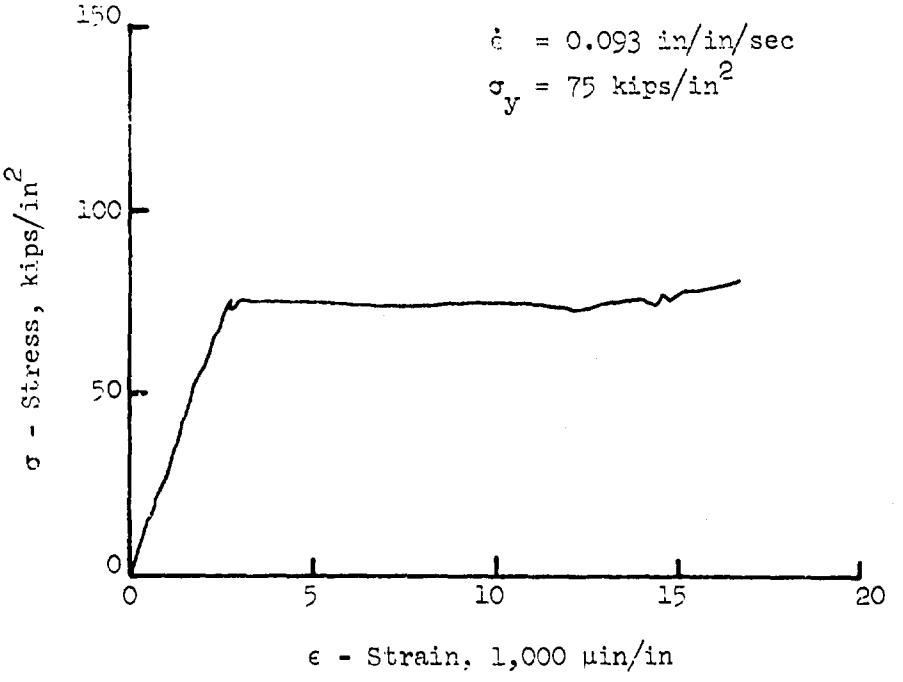

Figure 3.16 Machined bar, Grade 60, Test No. 164.

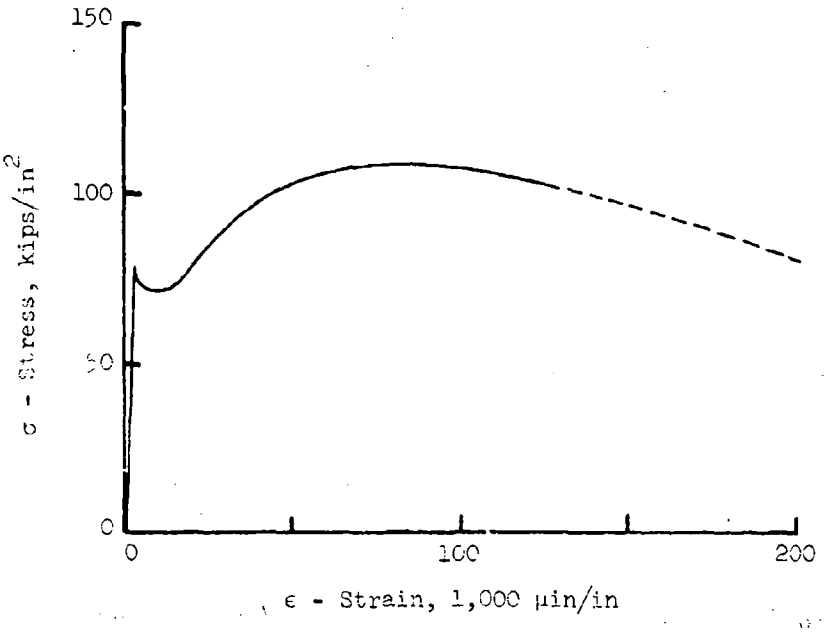

Figure 3.15 (Continued) Test No. 161.

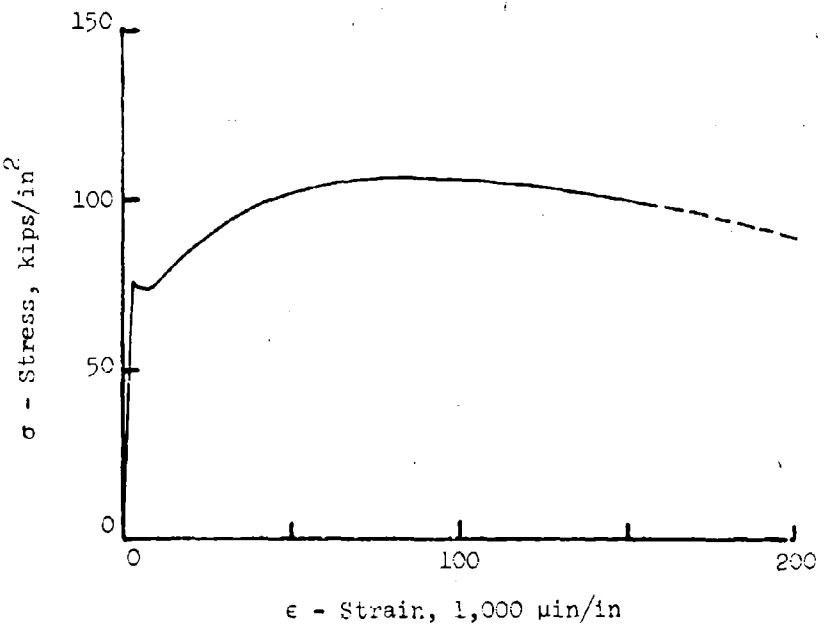

Figure 3.16 (Continued) Test No. 164.

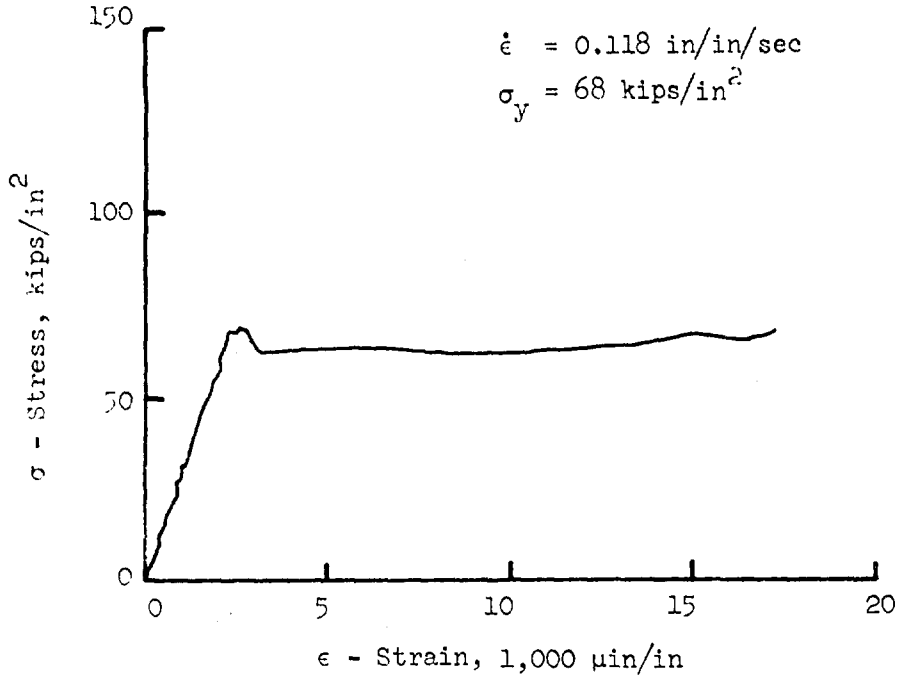

Figure 3.17 Machined bar, Grade 60, Test No. 167.

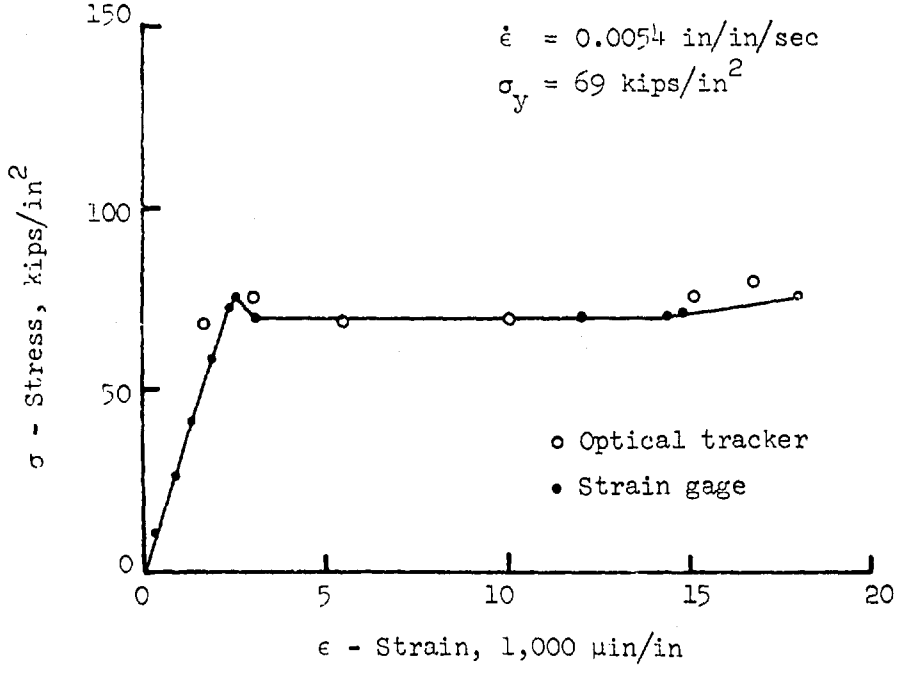

Figure 3.18 Machined bar, Grade 60, Test No. 188.

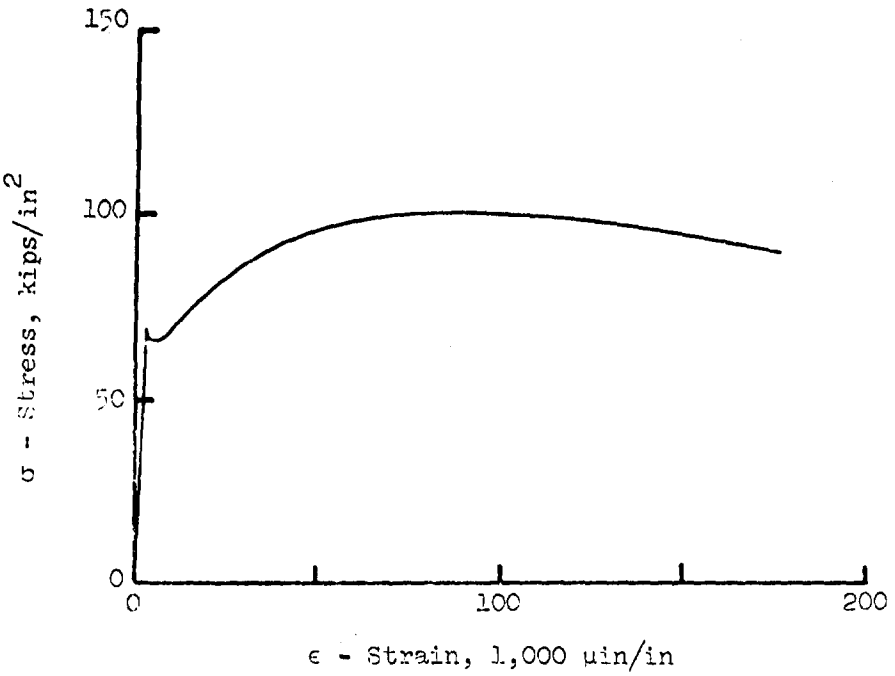

Figure 3.17 (Continued) Test No. 167.

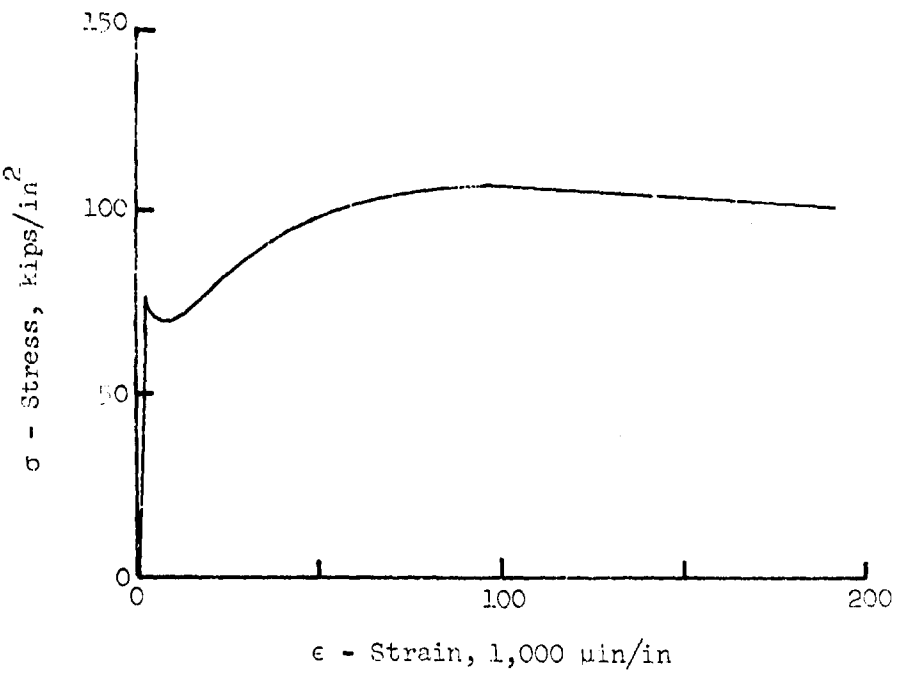

Figure 3.18 (Continued) Test No. 188.

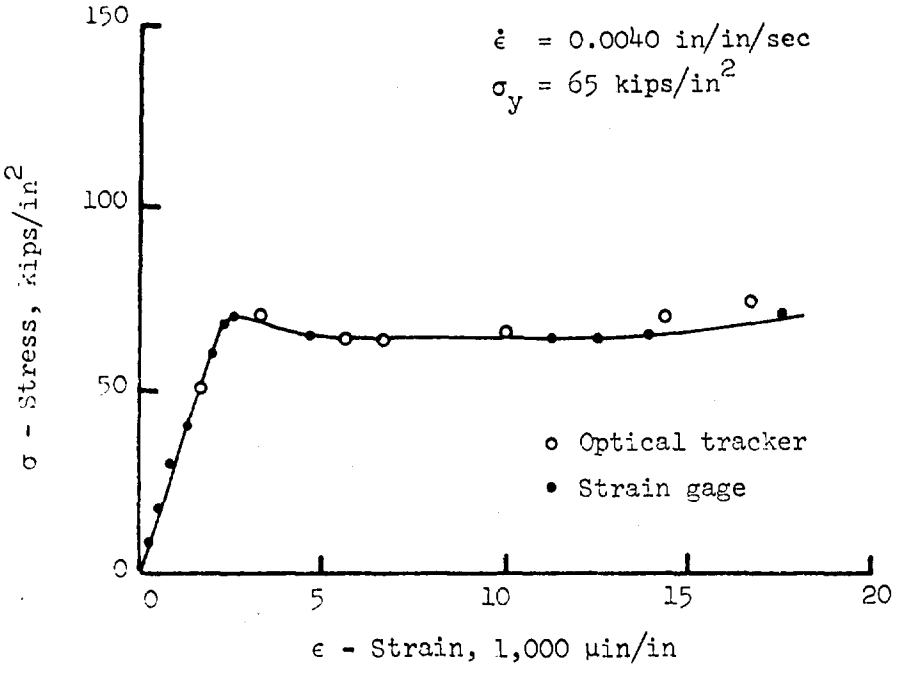

Figure 3.19 Machined bar, Grade 60, Test No. 191.

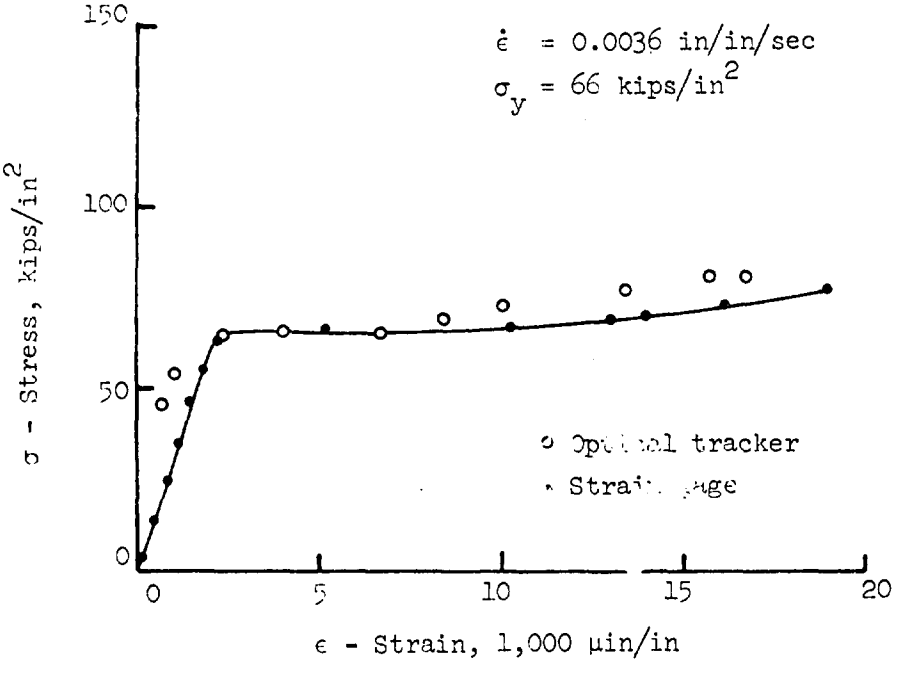

Figure 3.20 Machined bar, Grade 60, Test No. 194.

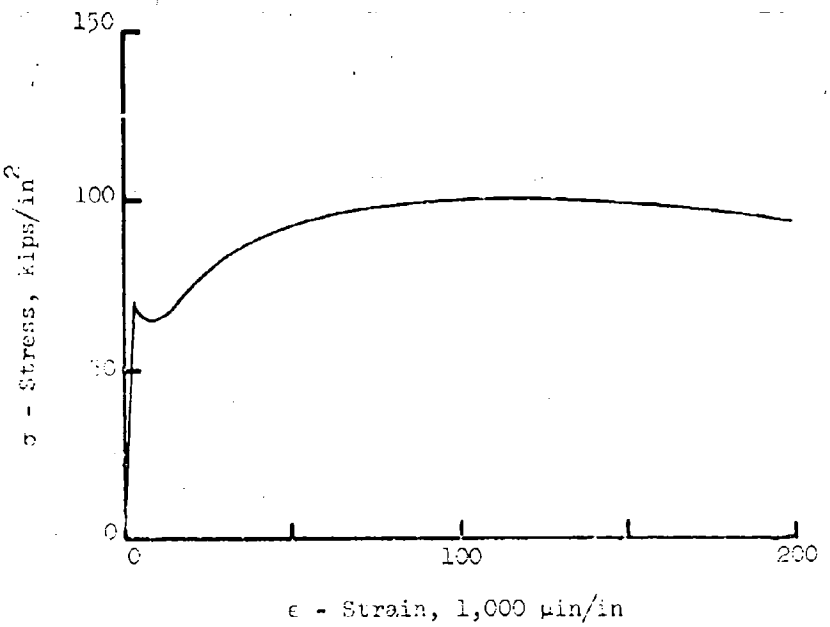

Figure 3.19 (Continued) Test No. 19L.

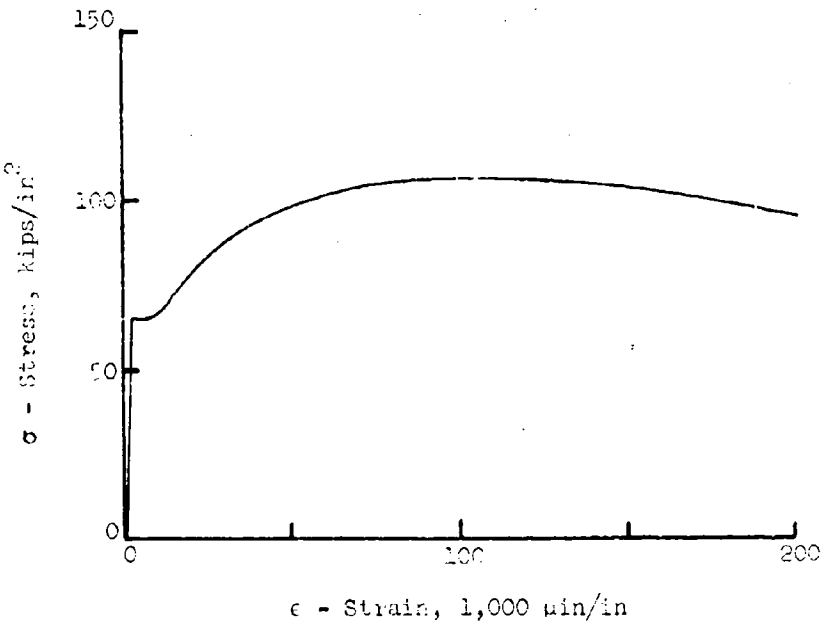

Figure 3.20 (Continued) Test No. 19M

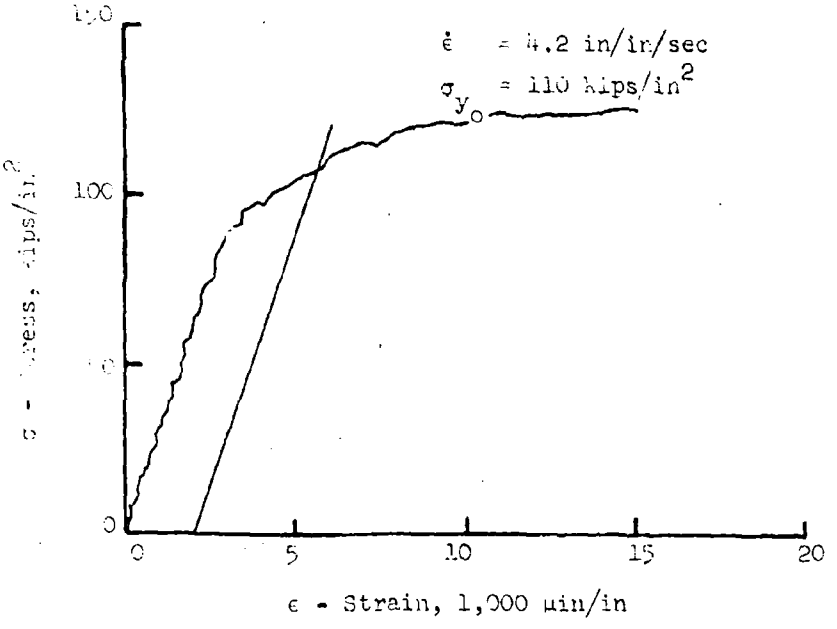

Figure 3.21 Machined bar, Grade 75, Test No. 135.

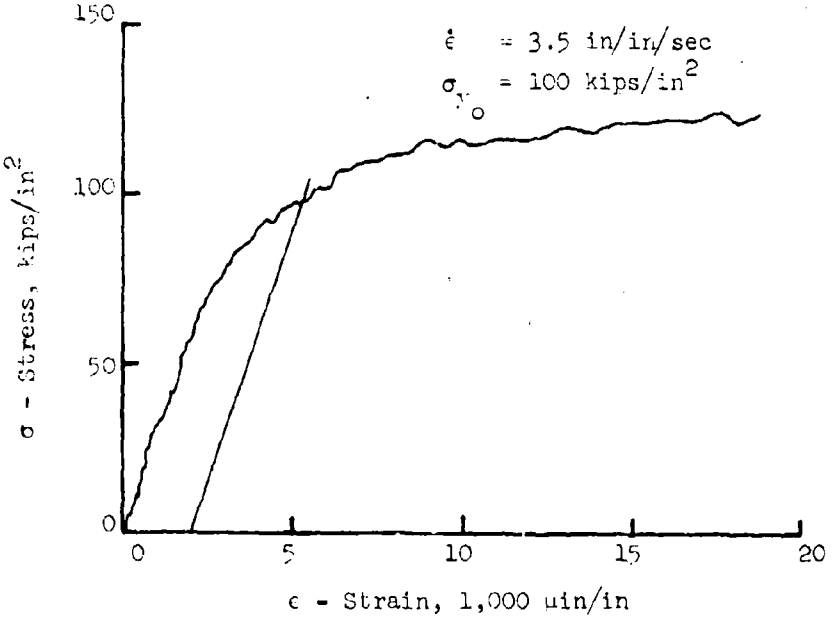

Figure 3.22 Machined bar, Grade 75, Test No. 170.

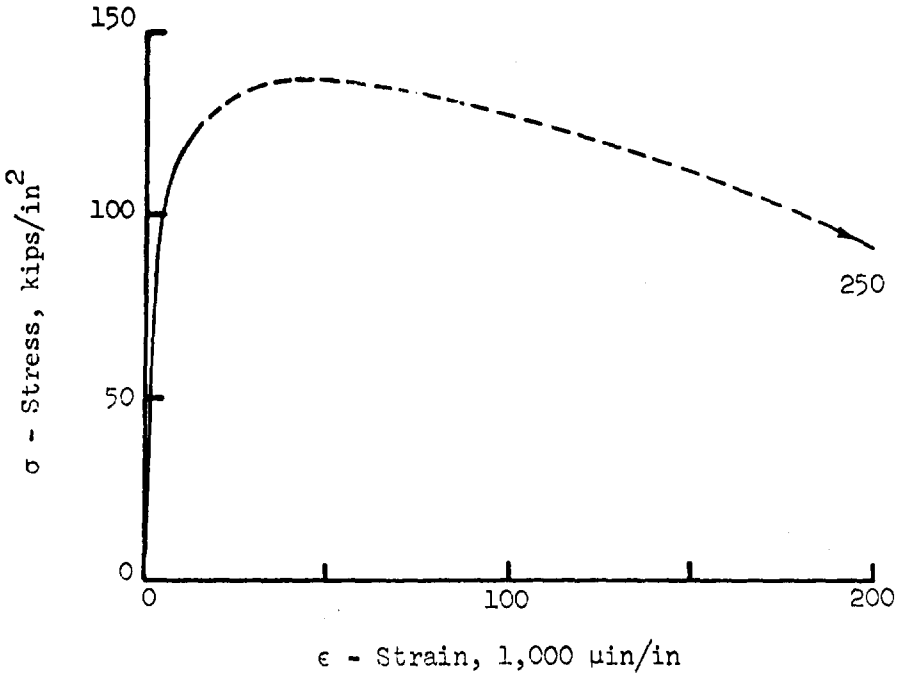

Figure 3.21 (Continued) Test No. 155.

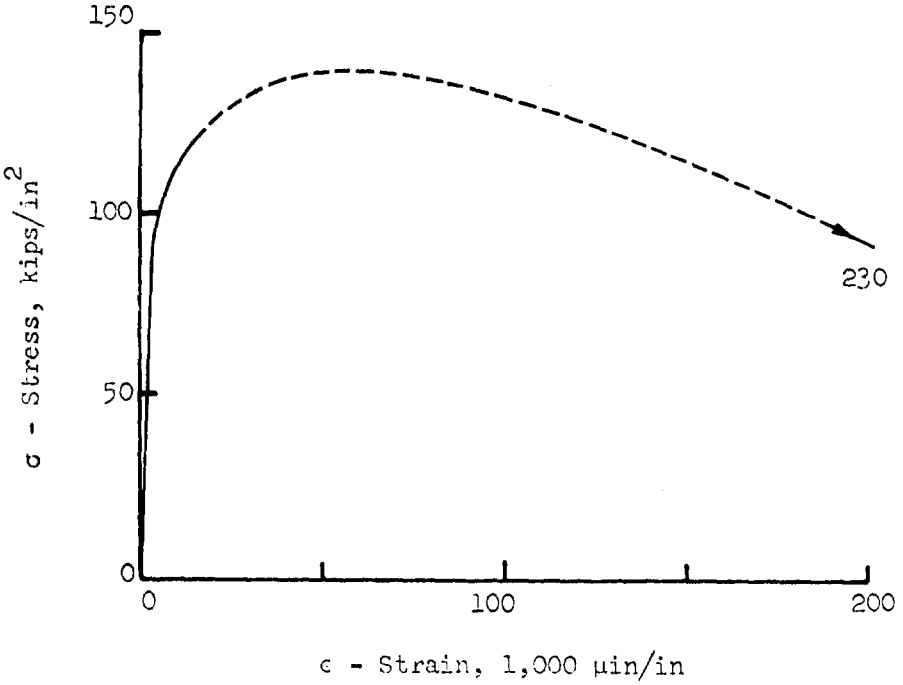

Figure 3.22 (Continued) Test No. 170.

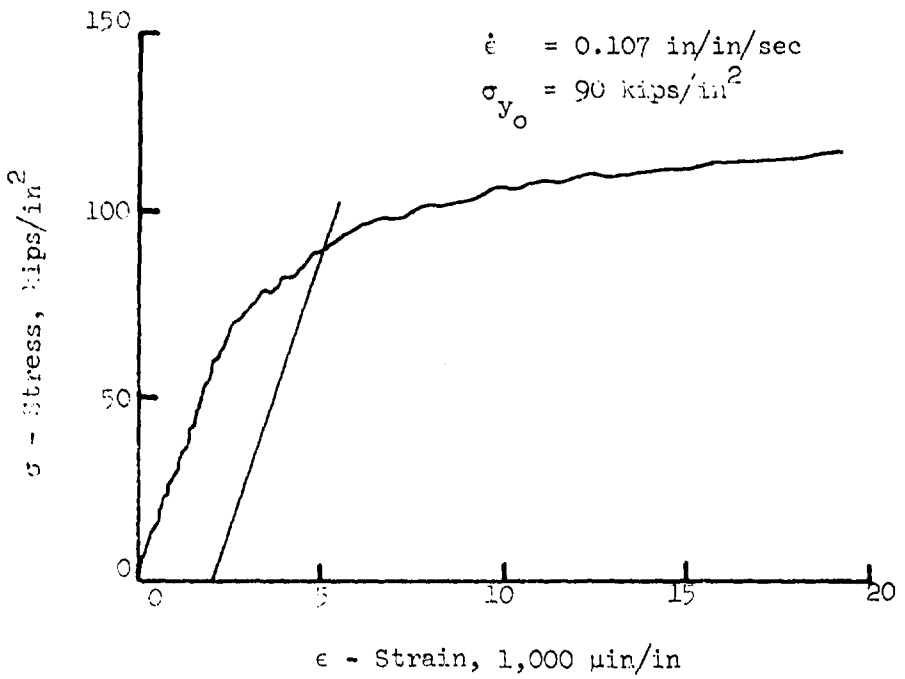

Figure 3.23 Machined bar, Grade 75, Test No. 173.

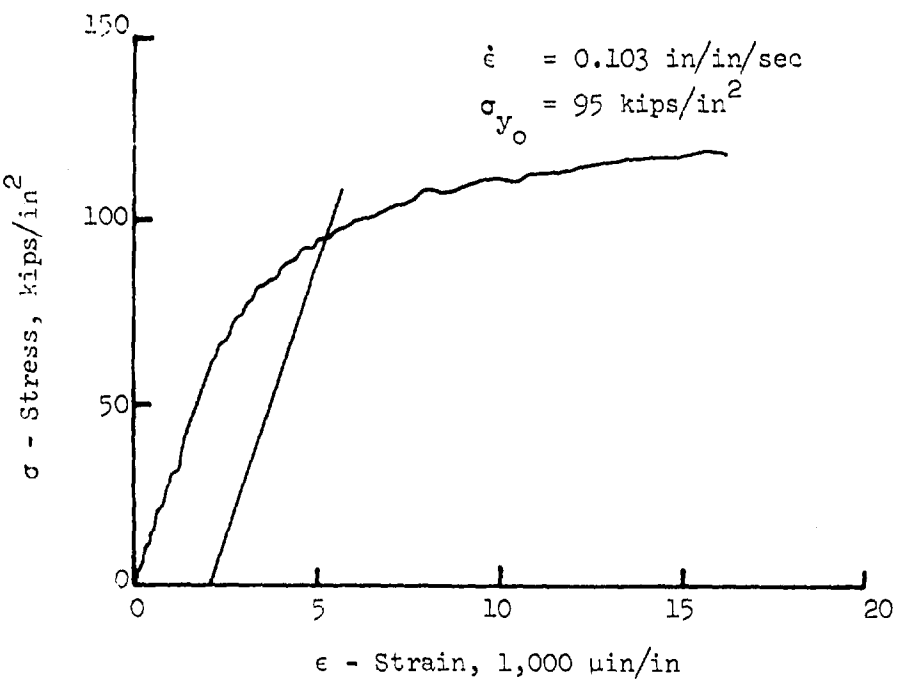

Figure 3.24 Machined bar, Grade 75, Test No. 176.

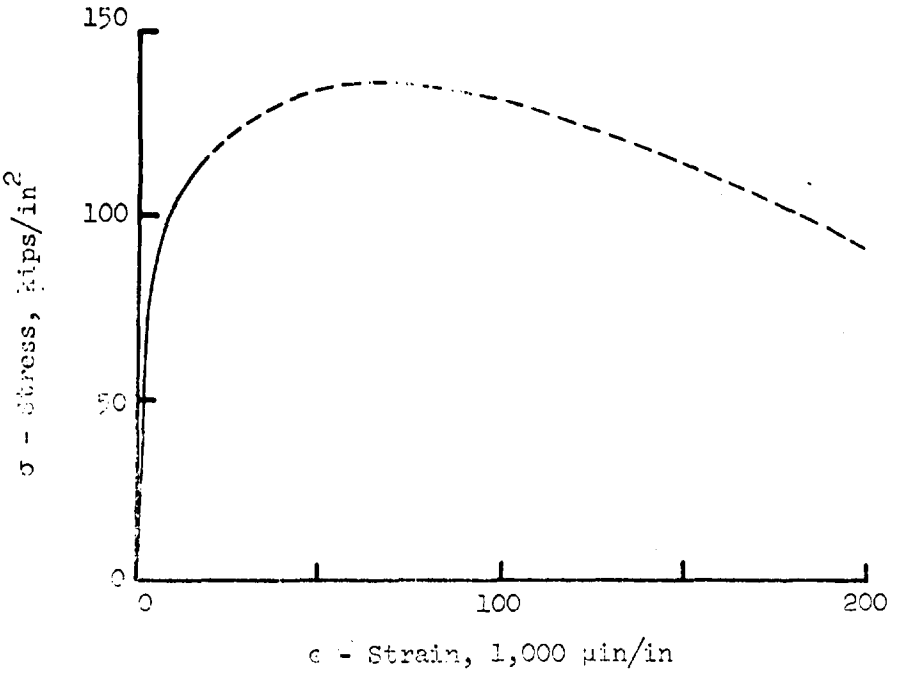

Figure 3.23 (Continued) Test No. 173.

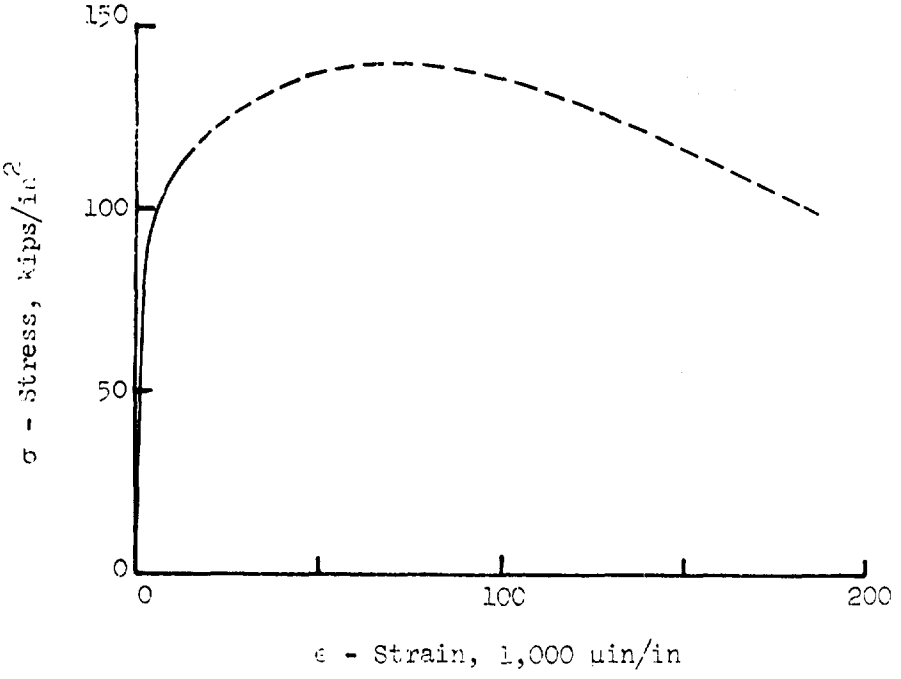

Figure 3.24 (Continued) Test No. 176.

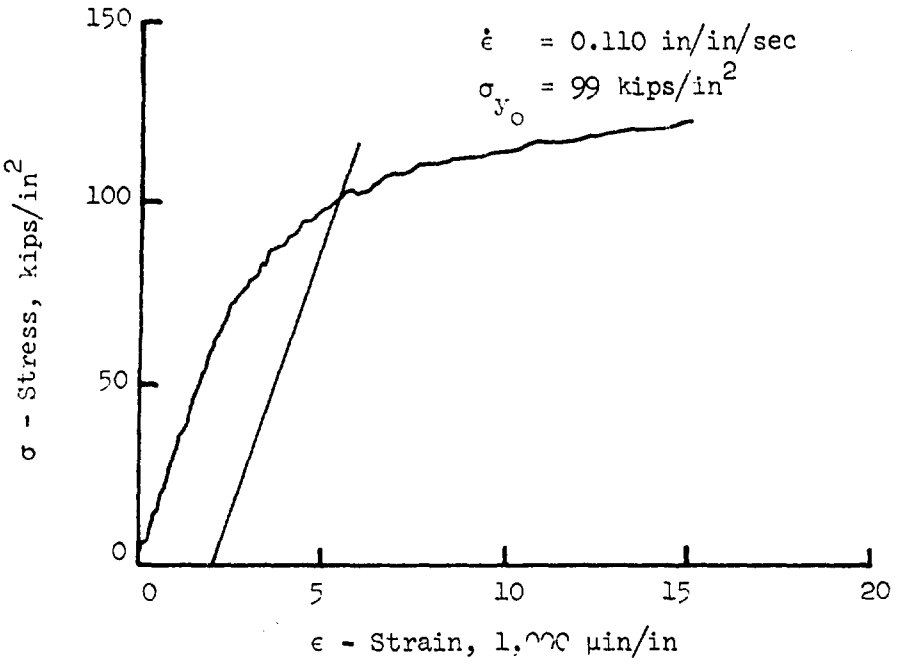

Figure 3.25 Machined bar, Grade 75, Test No. 180.

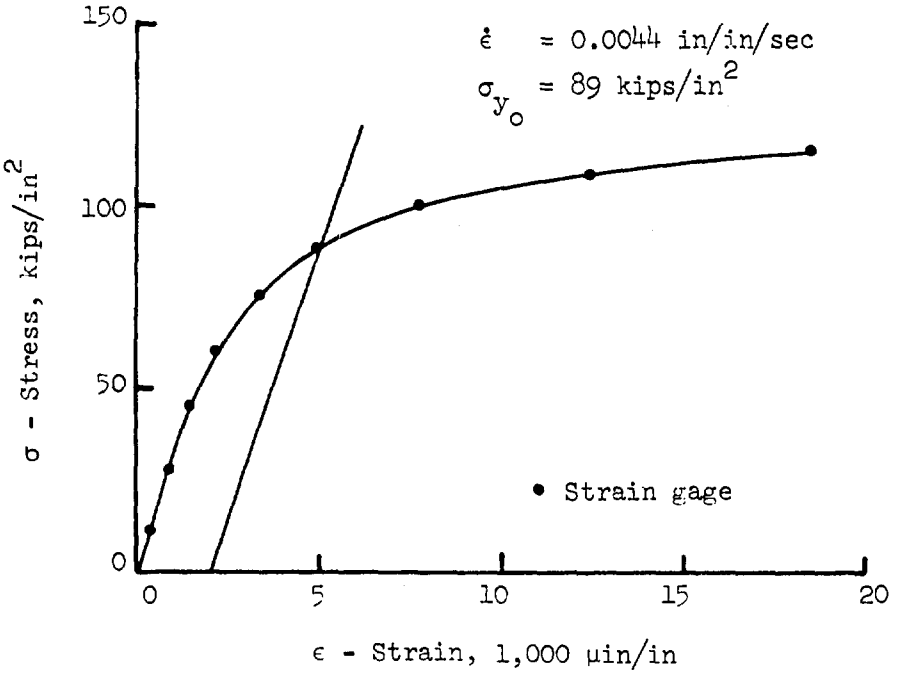

Figure 3.26 Machined bar, Grade 75, Test No. 185

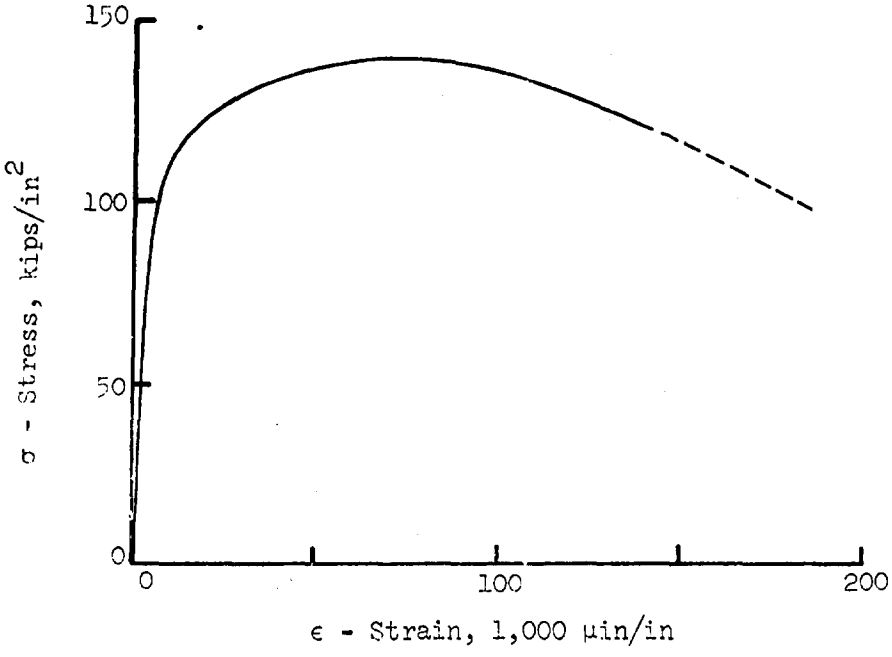

Figure 3.25 (Continued) Test No. 180.

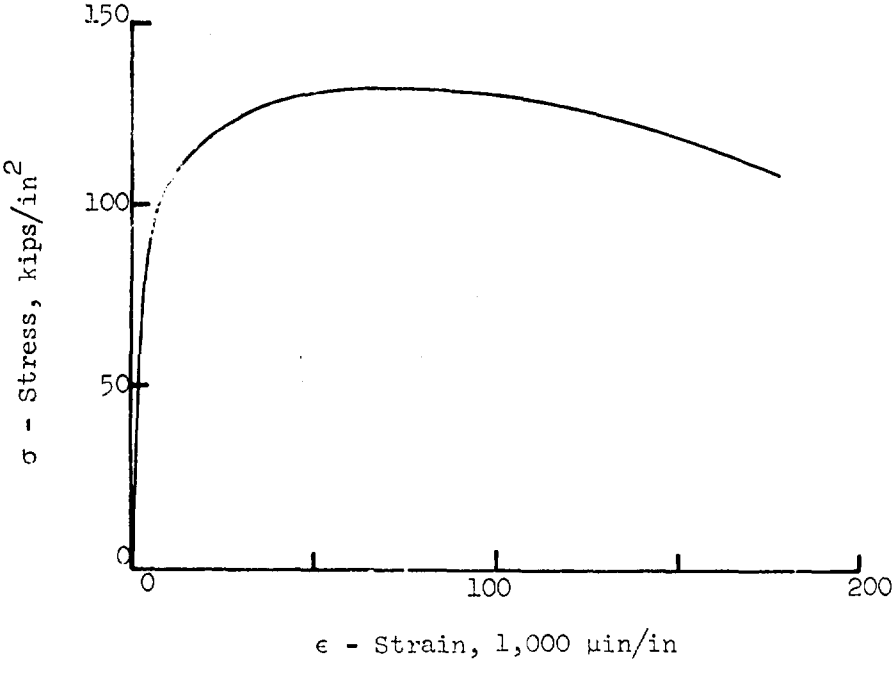

Figure 3.26 (Continued) Test No. 185.

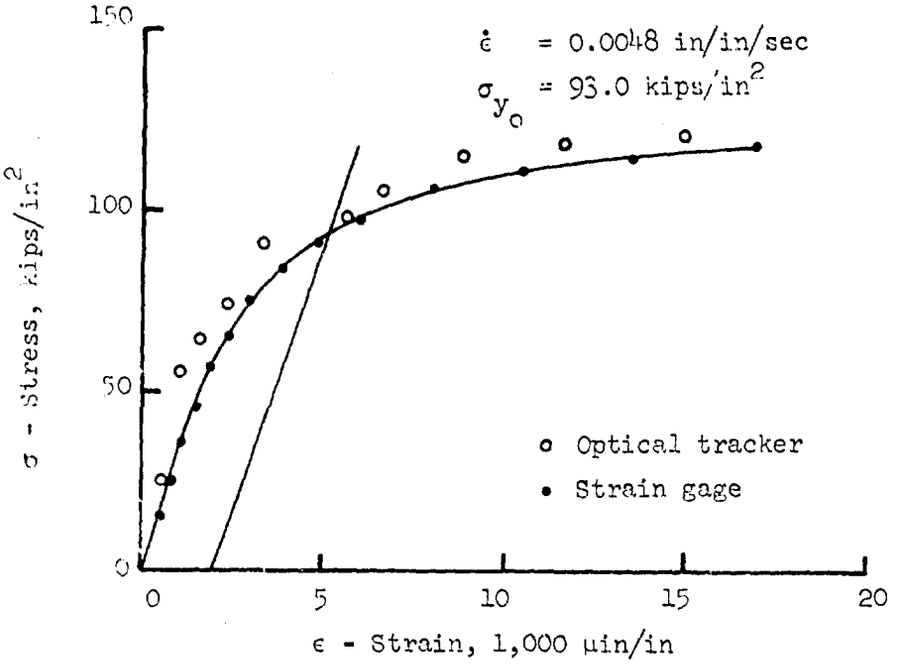

Figure 3.27 Machined bar, Grade 75, Test No. 197.

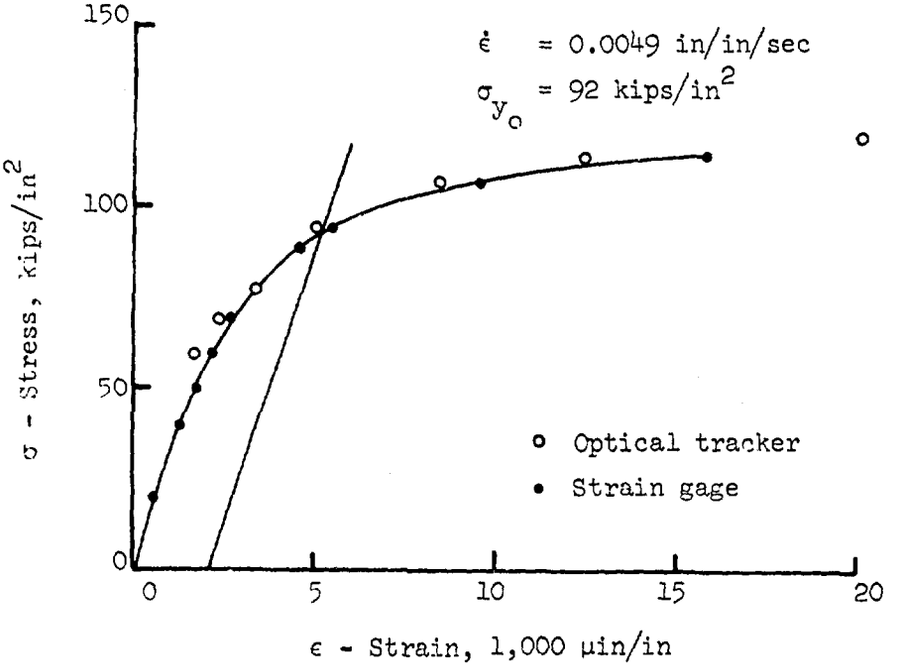

Figure 3.28 Machined bar, Grade 75, Test No. 200.

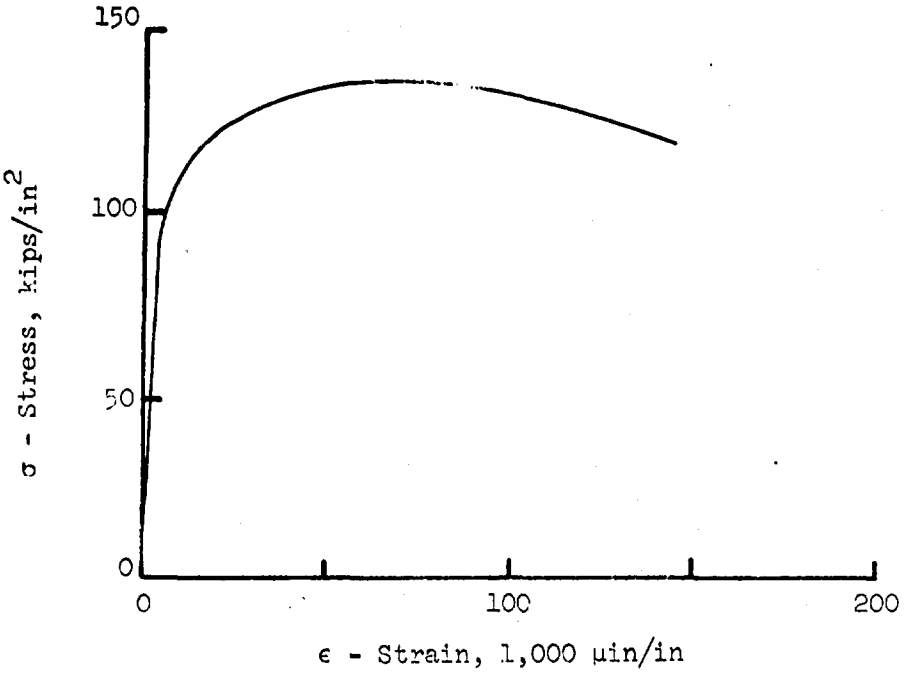

Figure 3.27 (Continued) Test No. 197.

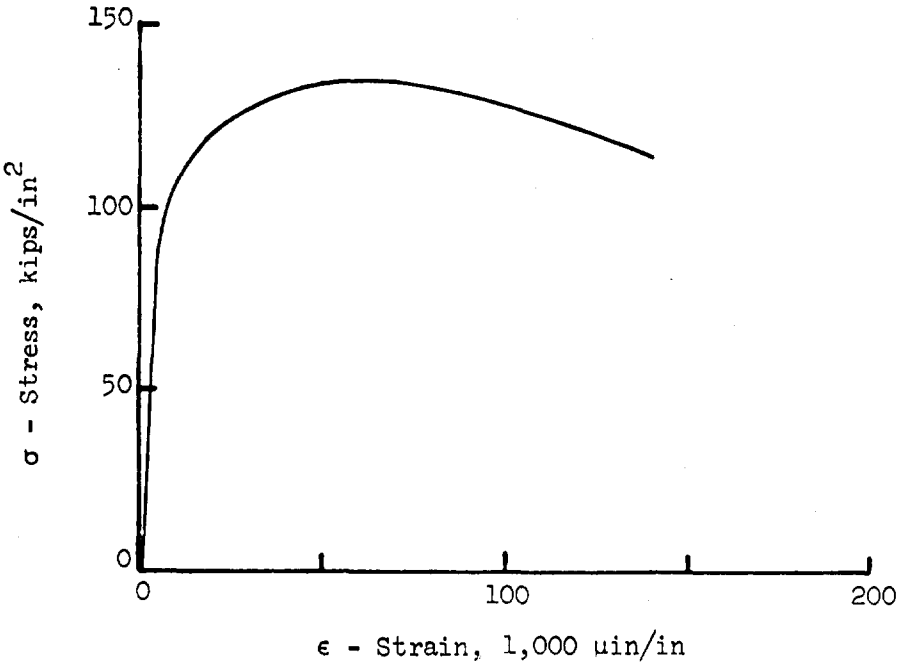

Figure 3.28 (Continued) Test No. 200.

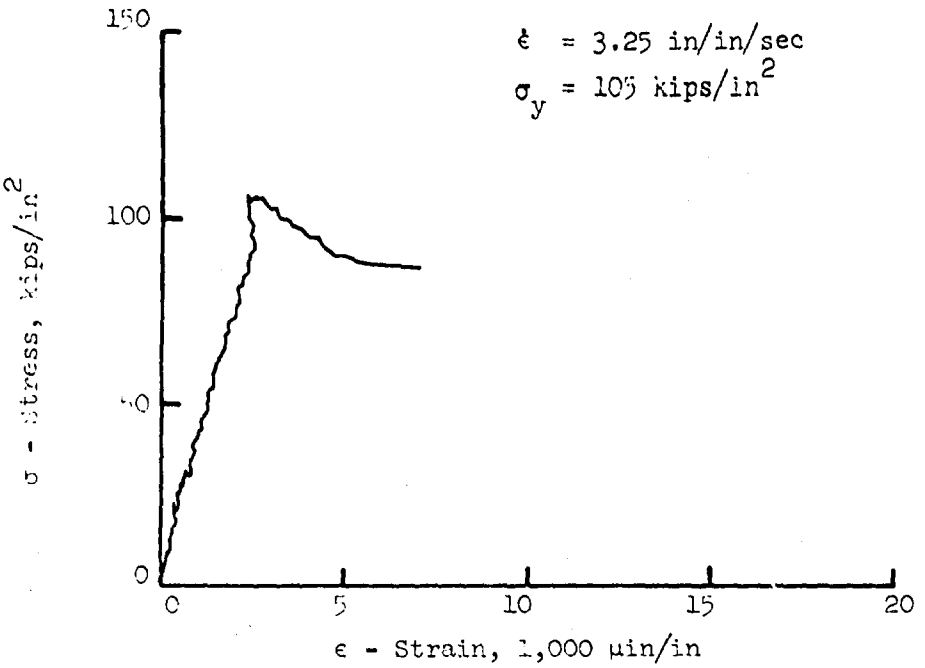

Figure 3.29 Butt-welded splice, Grade 60, Test No. 146.

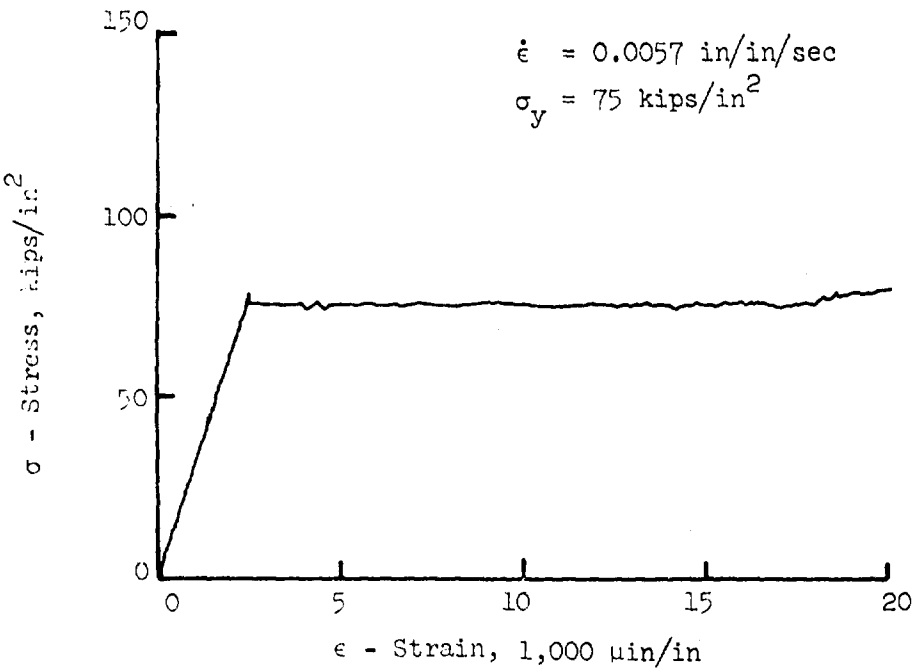

Figure 3.30 Butt-welded splice, Grade 60, Test No. 150.

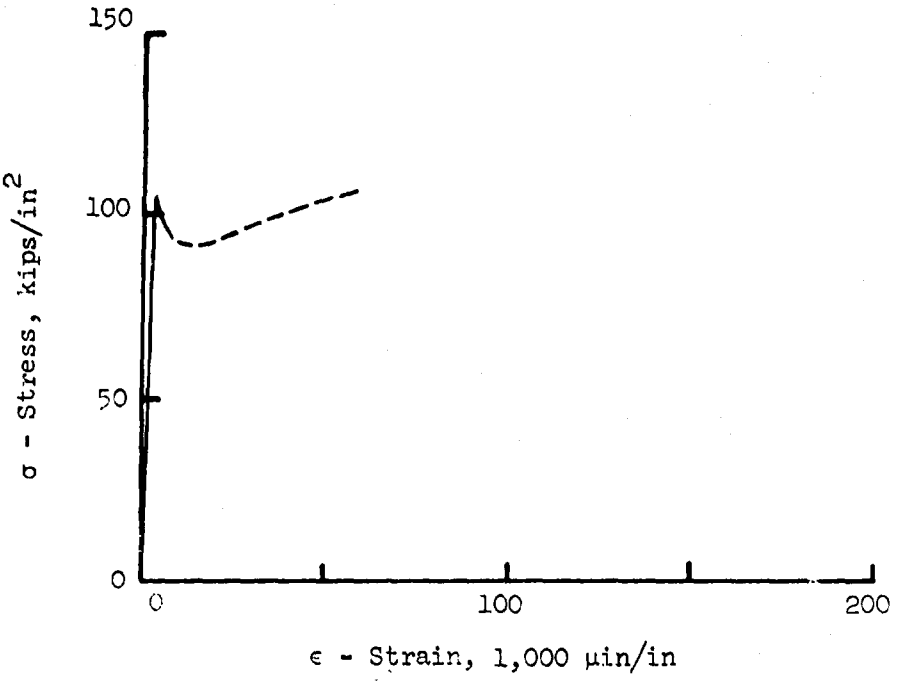

Figure 3.29 (Continued) Test No. 146.

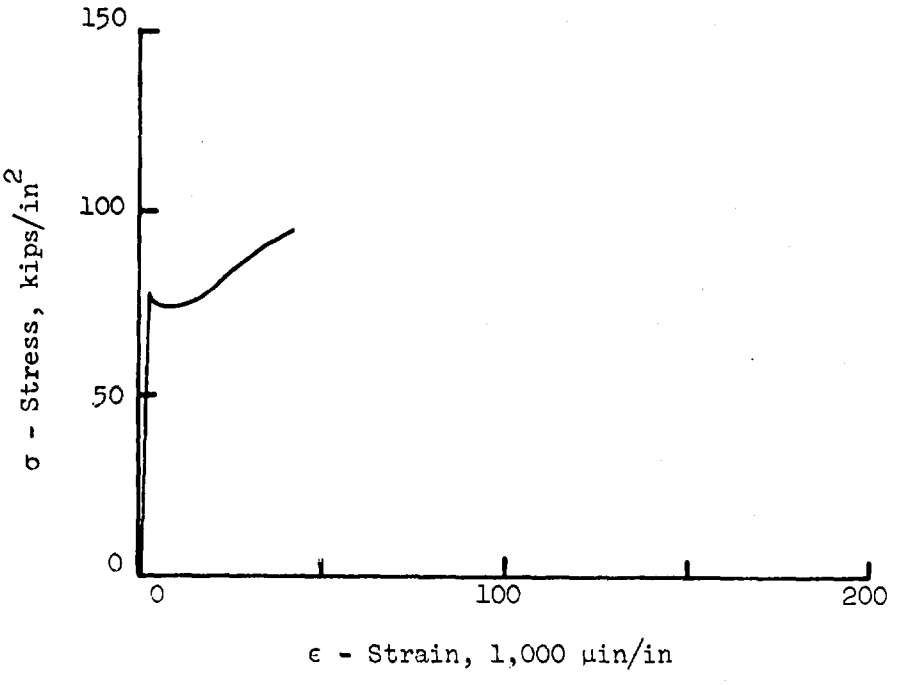

Figure 3.30 (Continued) Test No. 150.

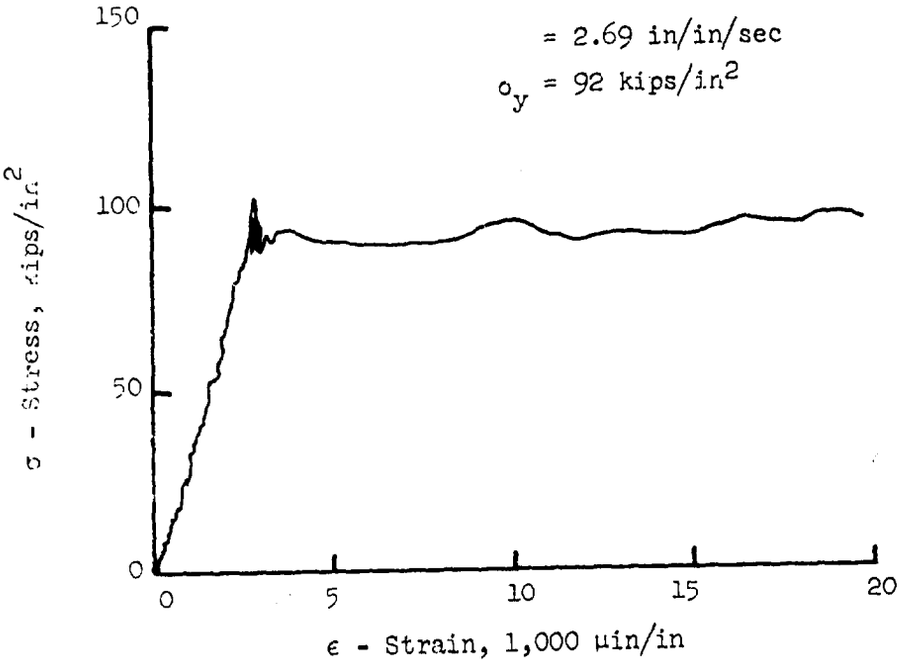

Figure 3.31 Butt-welded splice, Grade 60, Test No. 159.

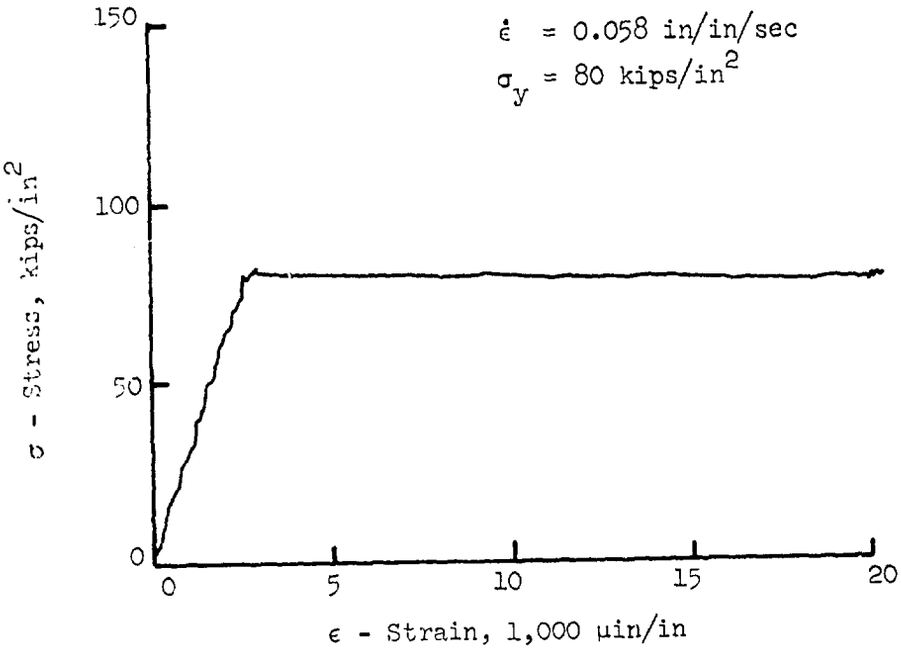

Figure 3.32 Butt-welded splice, Grade 60, Test No. 163.

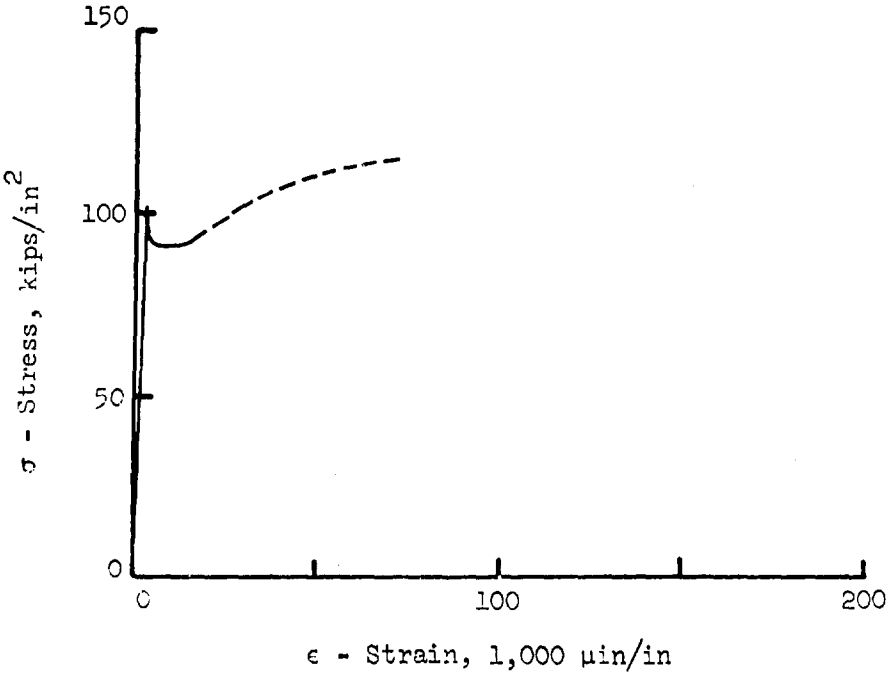

Figure 3.31 (Continued) Test No. 159.

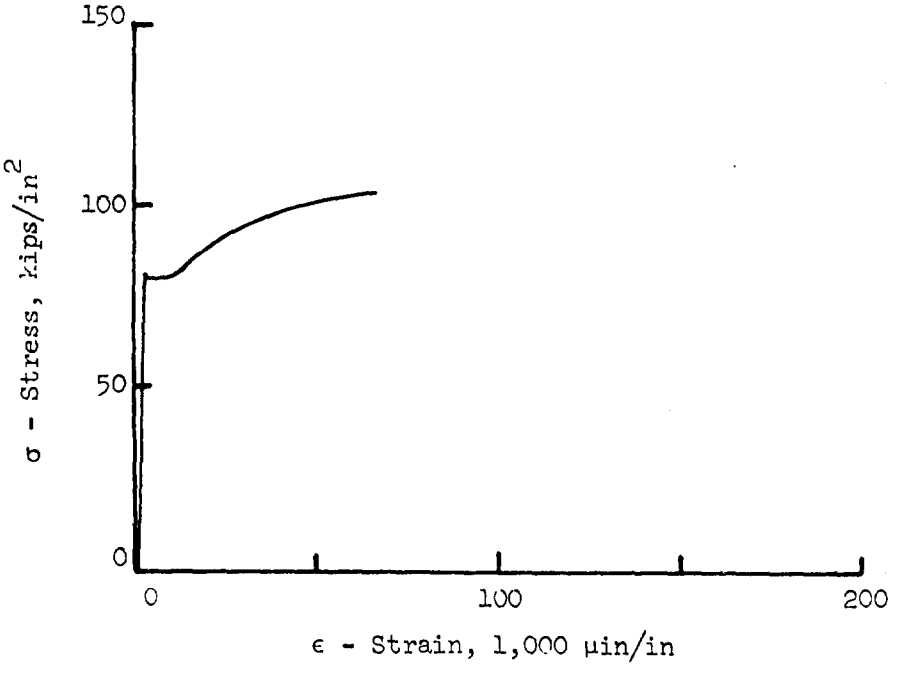

Figure 3.32 (Continued) Test No. 163.

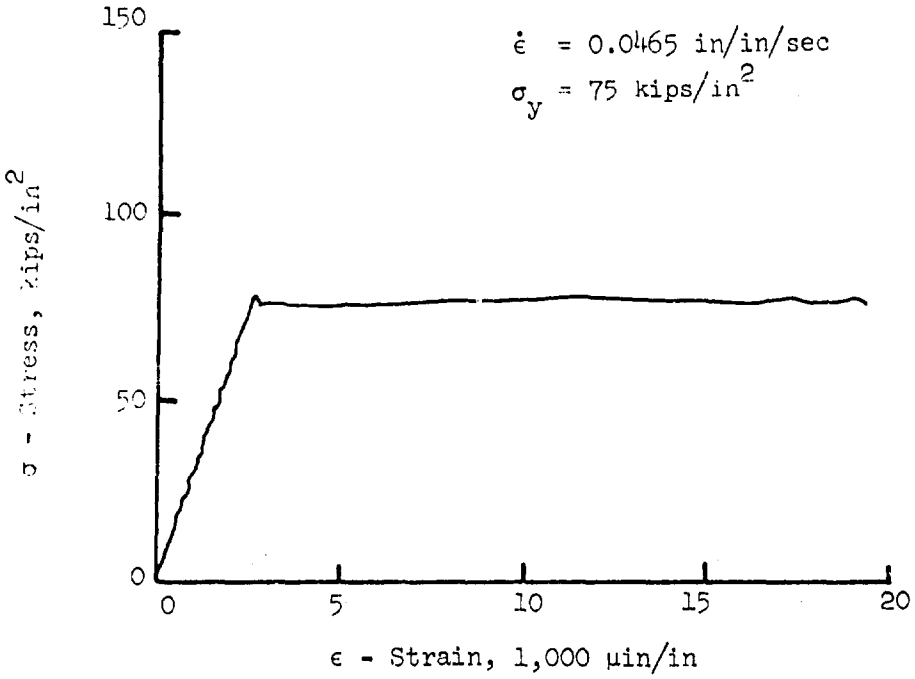

Figure 3.33 Butt-welded splice, Grade 60, Test No. 168.

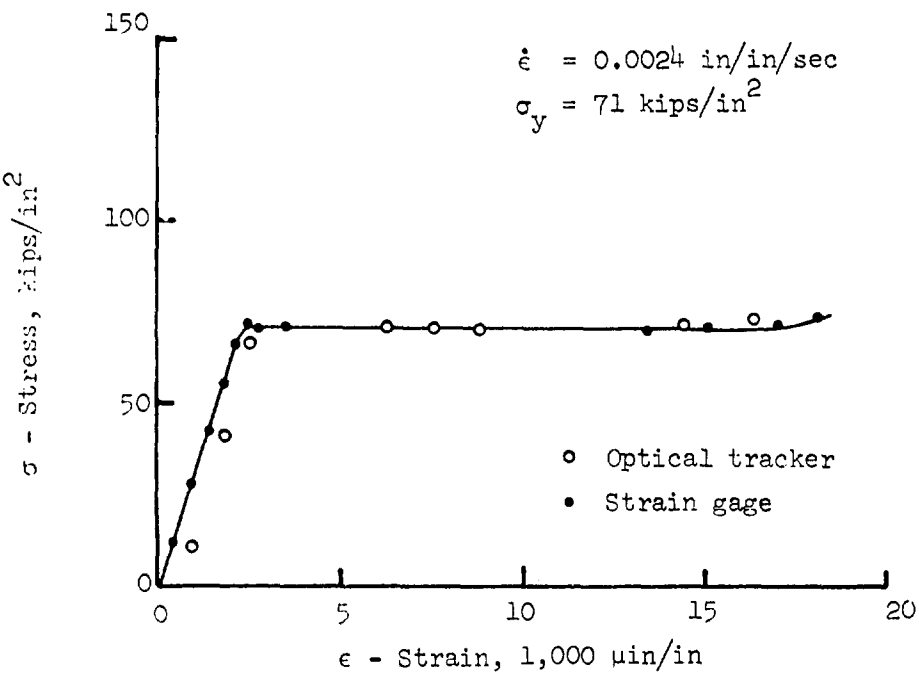

Figure 3.34 Butt-welded splice, Grade 60, Test No. 186.

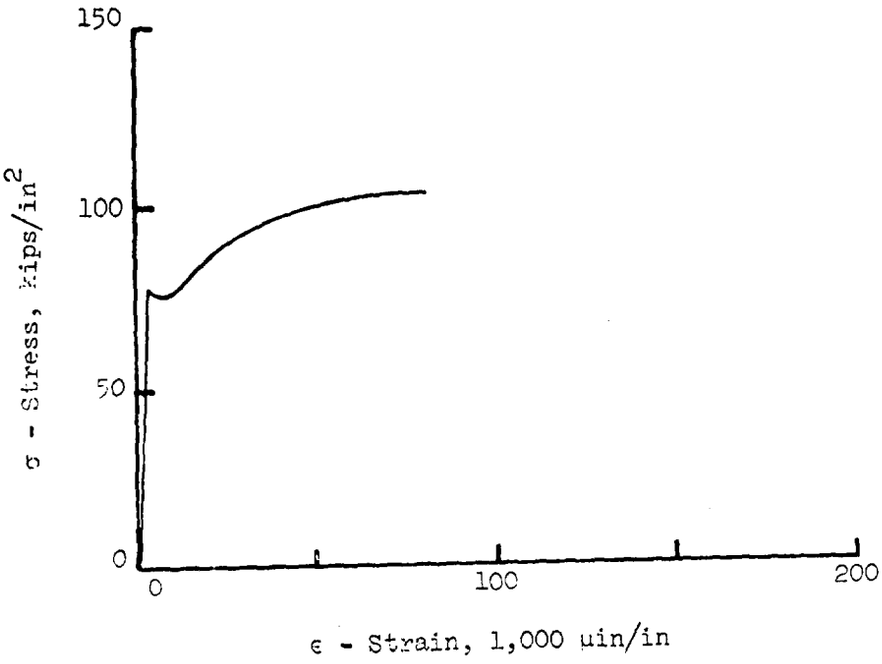

Figure 3.33 (Continued) Test No. 168.

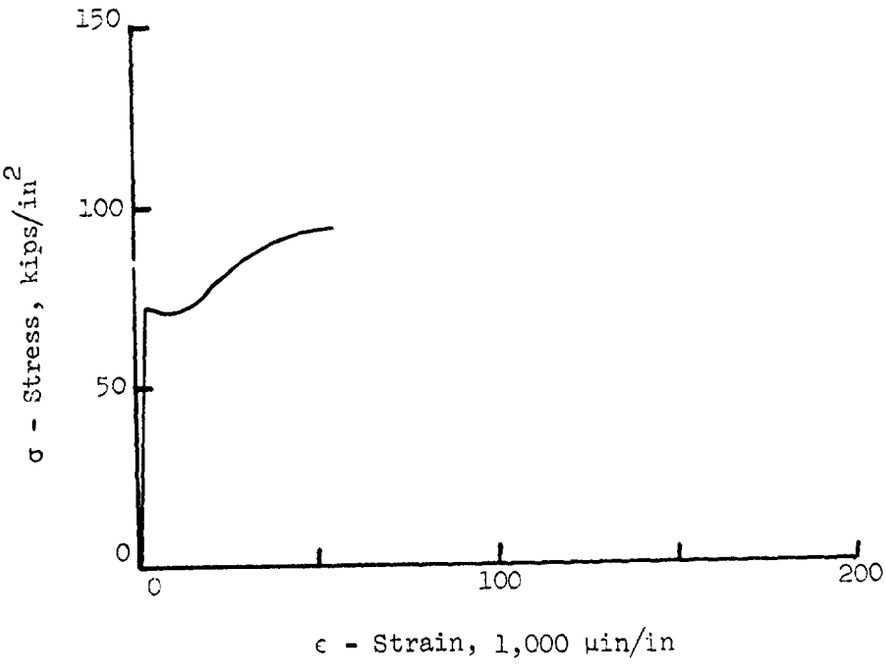

Figure 3.34 (Continued) Test No. 186.

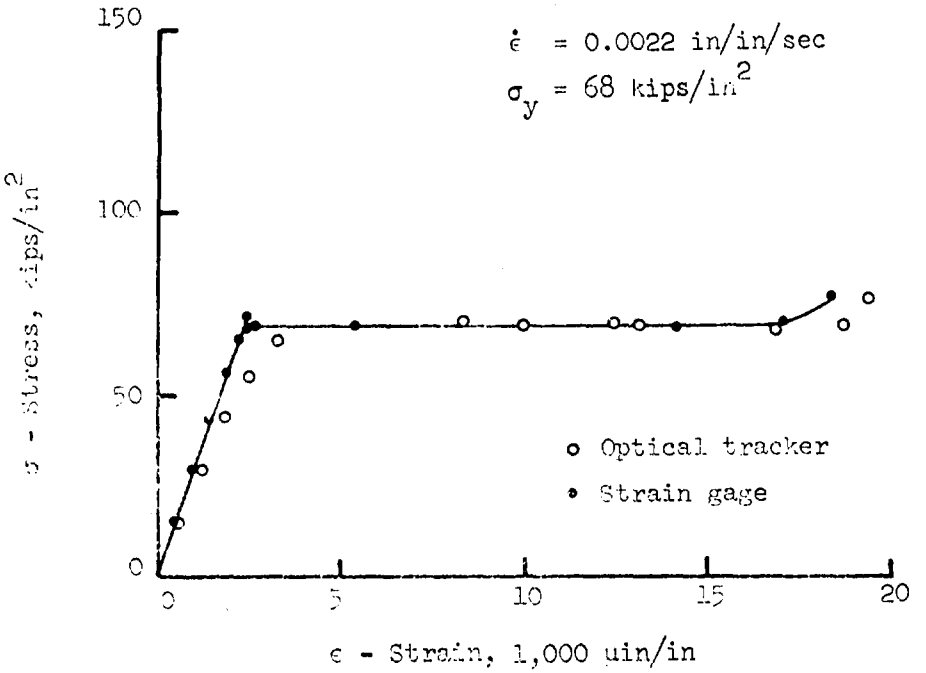

Figure 3.35 Butt-welded splice, Grade 60, Test No. 190.

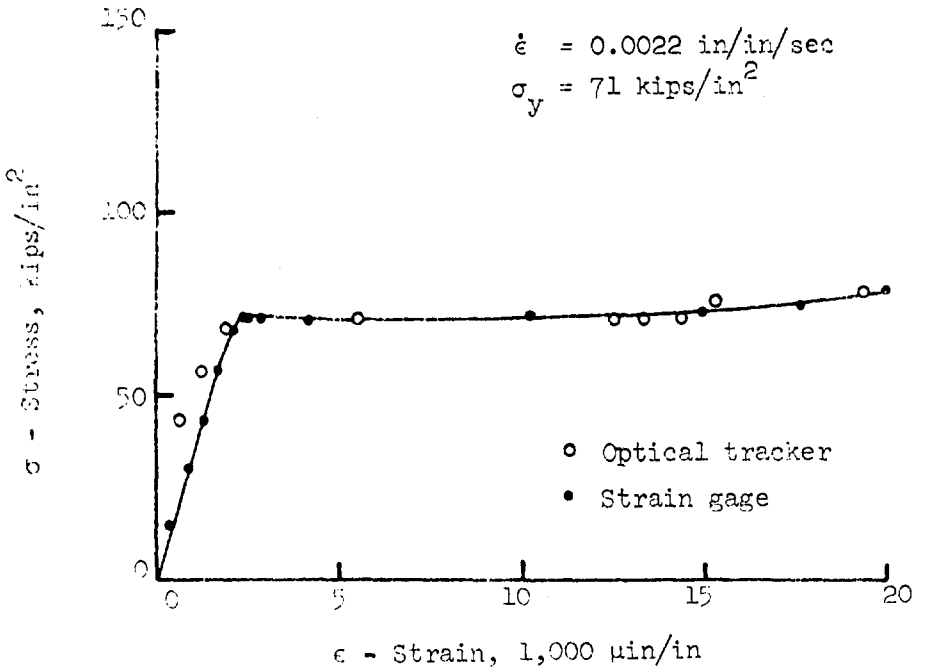

Figure 3.36 Butt-welded splice, Grade 60, Test No. 195.

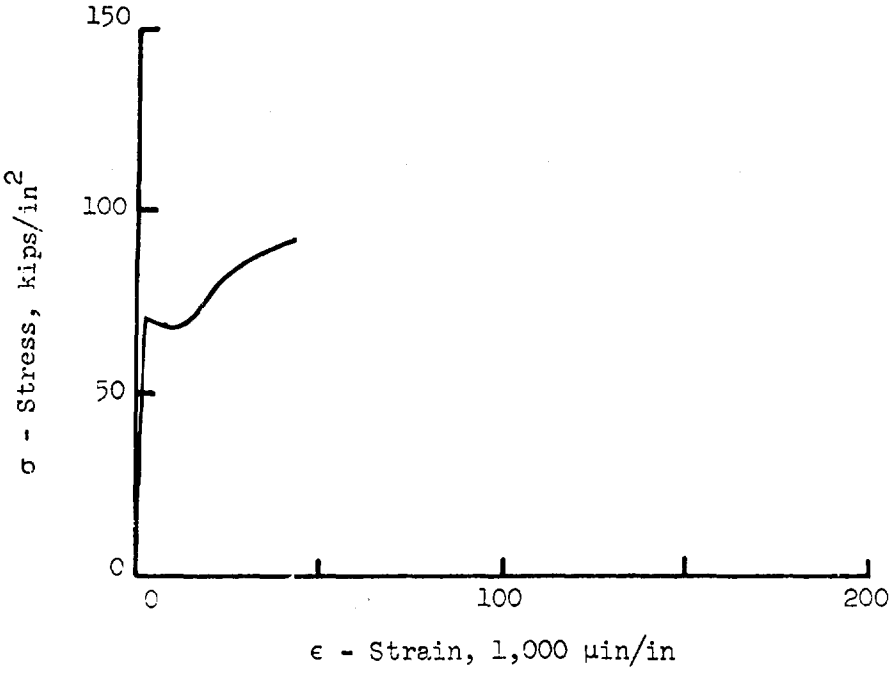

Figure 3.35 (Continued) Test No. 190.

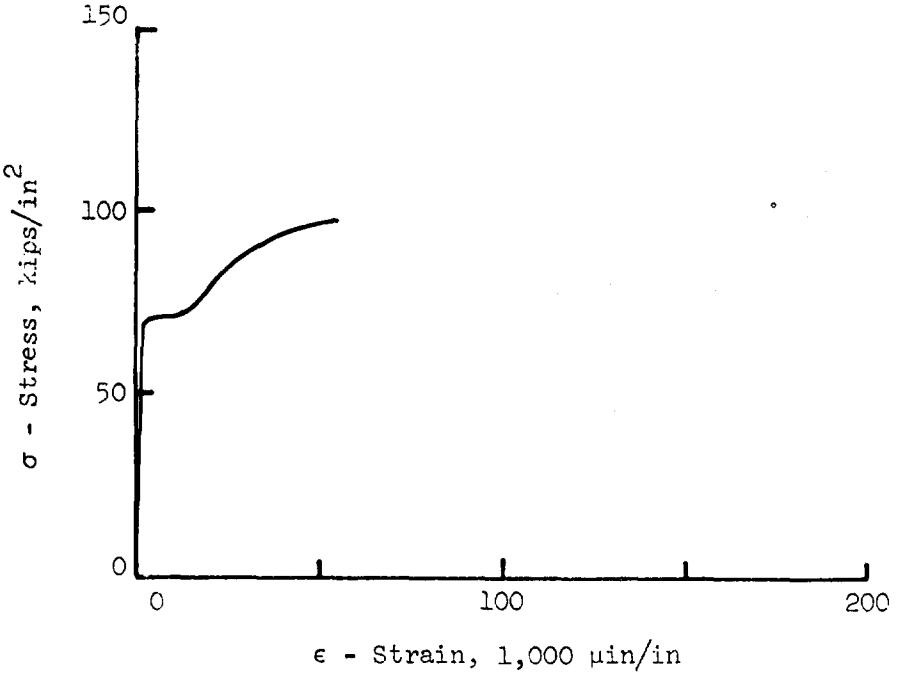

Figure 3.36 (Continued) Test No. 195.

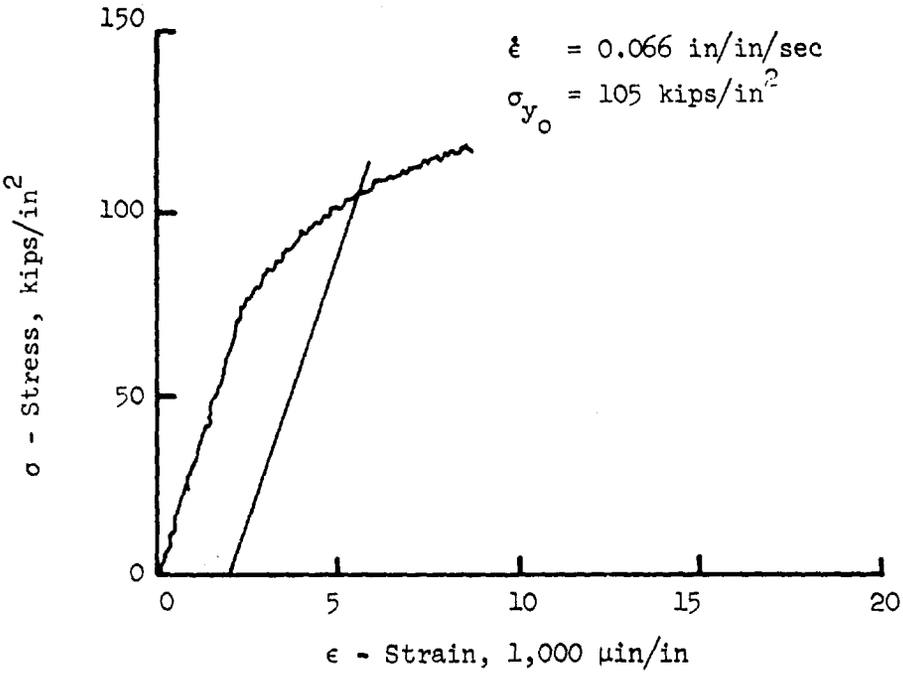

Figure 3.37 Butt-welded splice, Grade 75, Test No. 174.

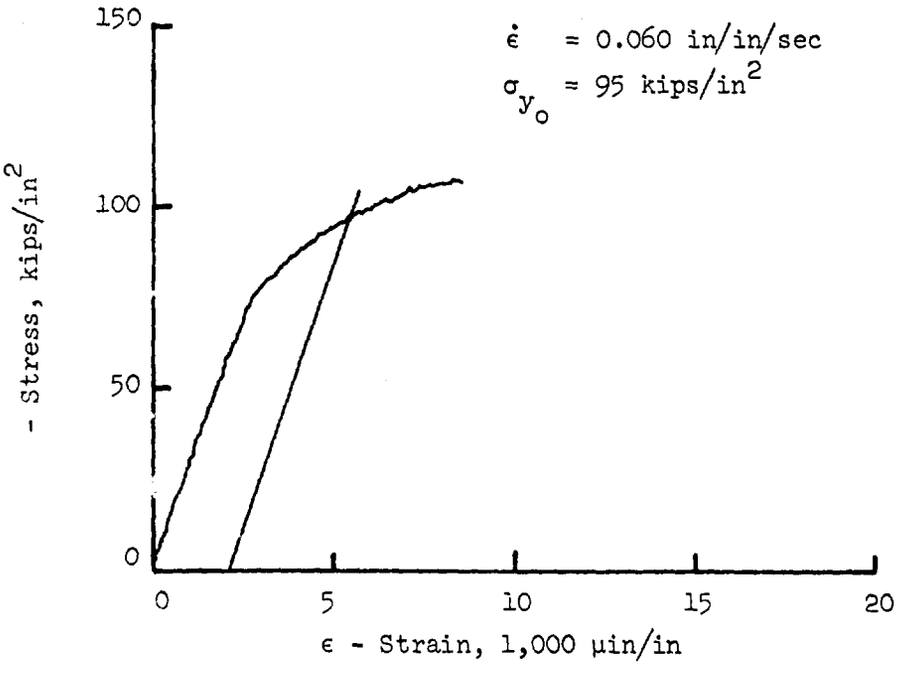

Figure 3.38 Butt-welded splice, Grade 75, Test No. 178.

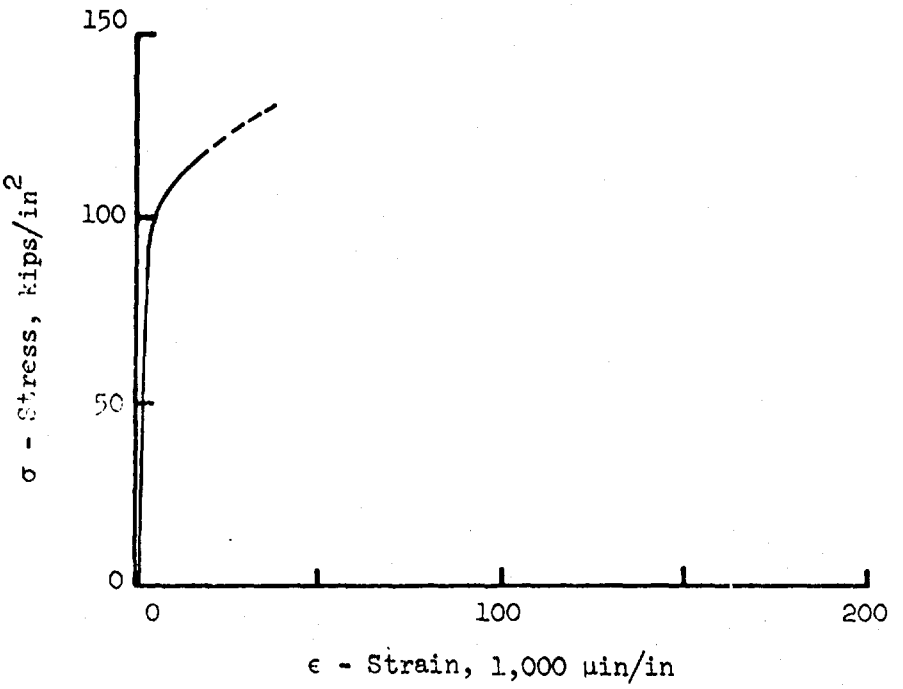

Figure 3.37 (Continued) Test No. 174.

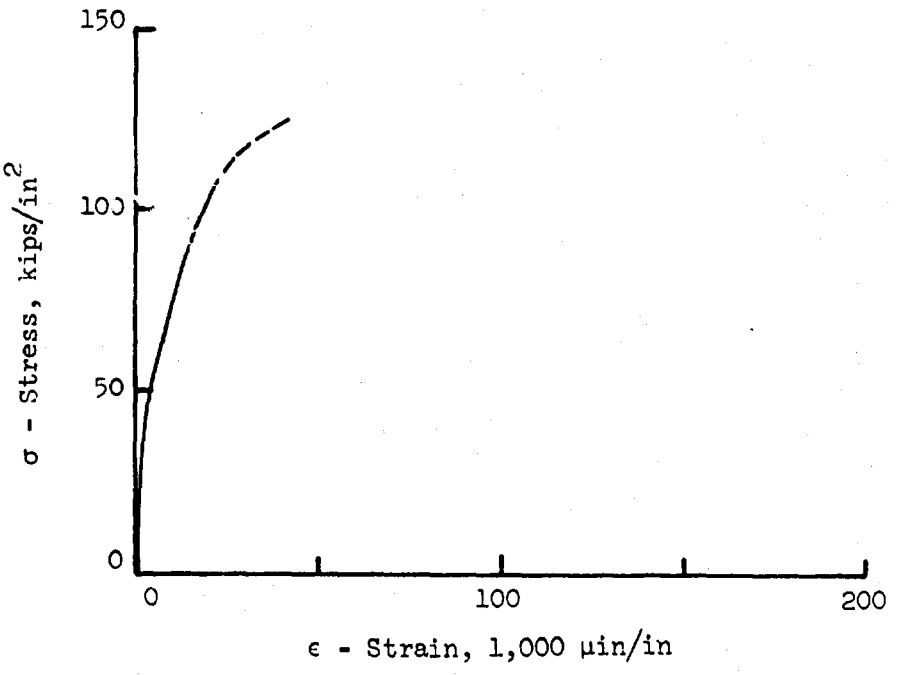

Figure 3.38 (Continued) Test No. 178.

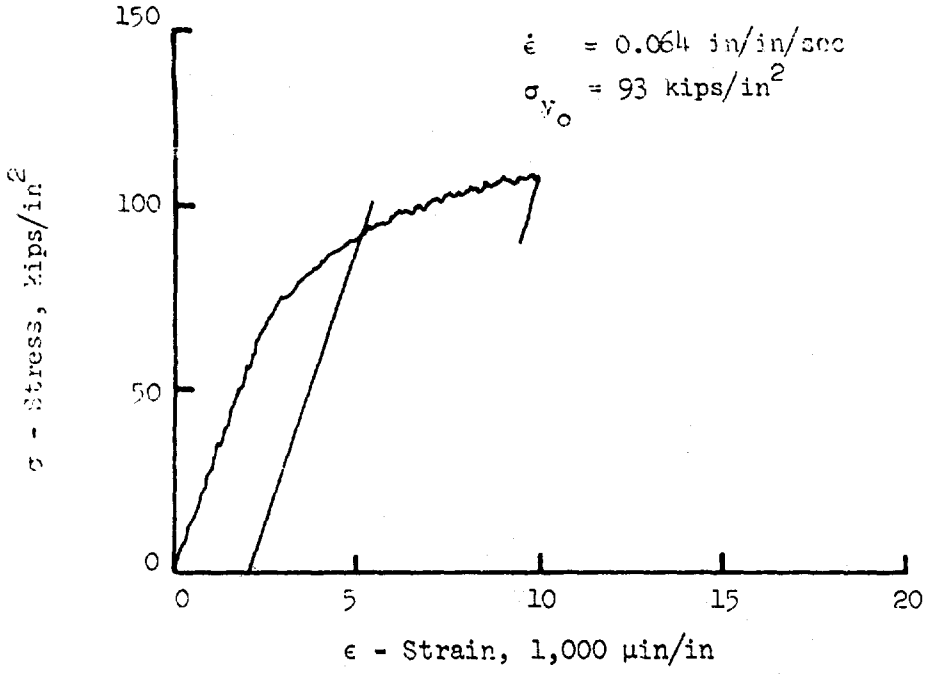

Figure 3.39 Butt-welded splice, Grade 75, Test No. 182.

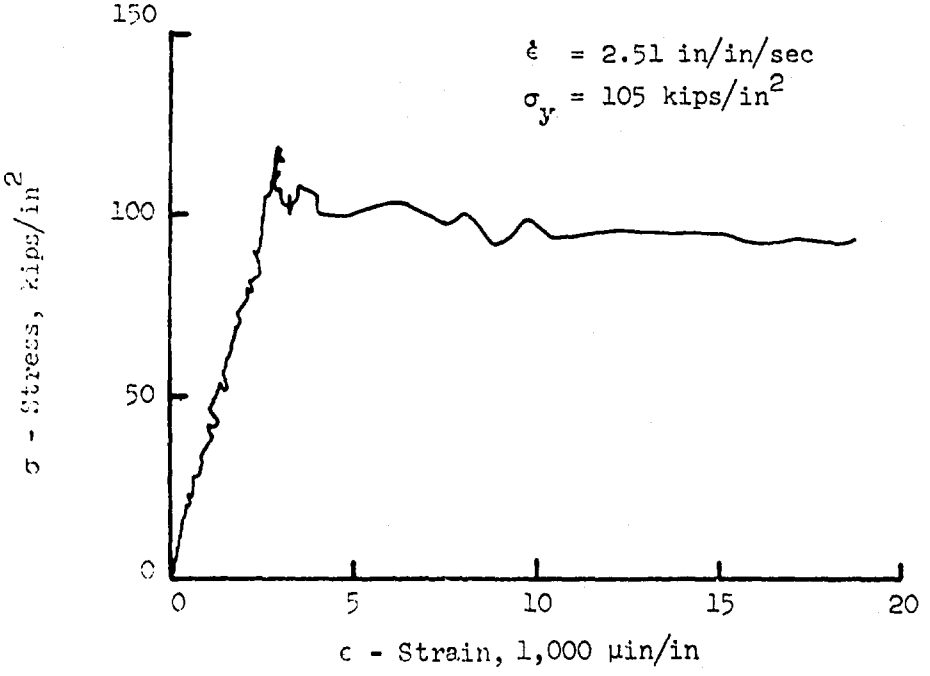

Figure 3.40 Thermit-welded splice, Grade 60, Test No. 149.

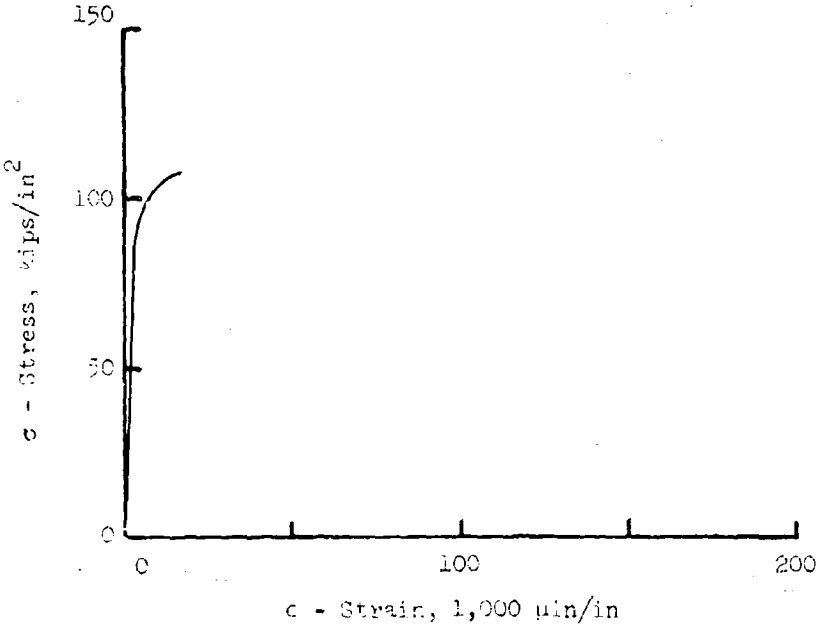

Figure 3.39 (Continued) Test No. 182.

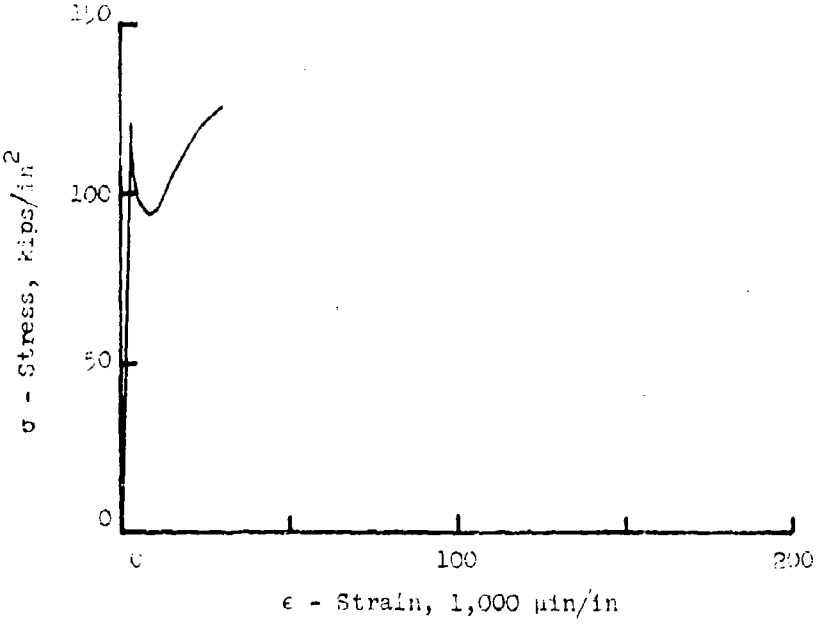

Figure 3.40 (Continued) Test No. 189

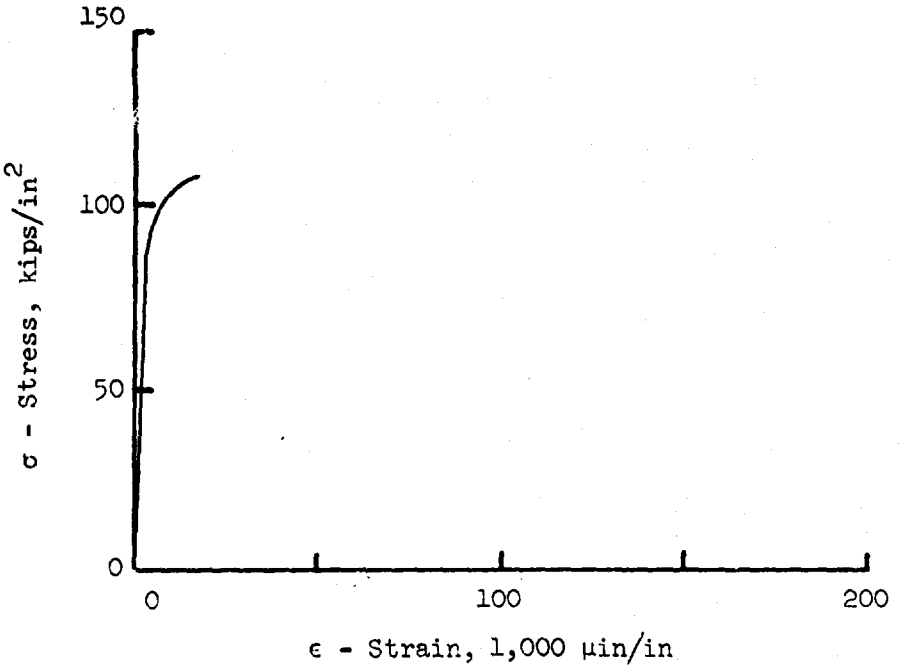

Figure 3.39 (Continued) Test No. 182.

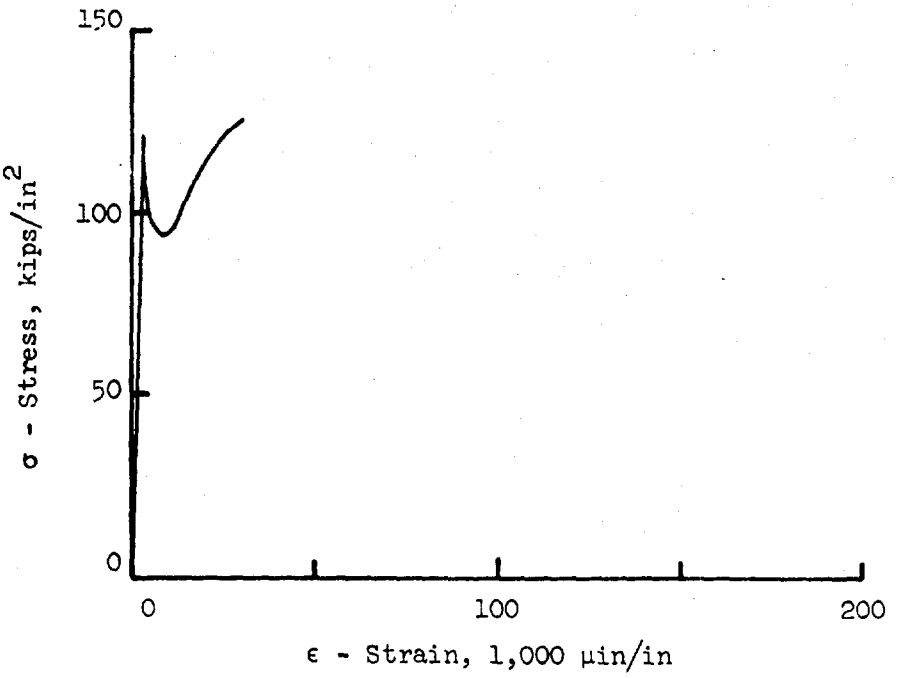

Figure 3.40 (Continued) Test No. 149

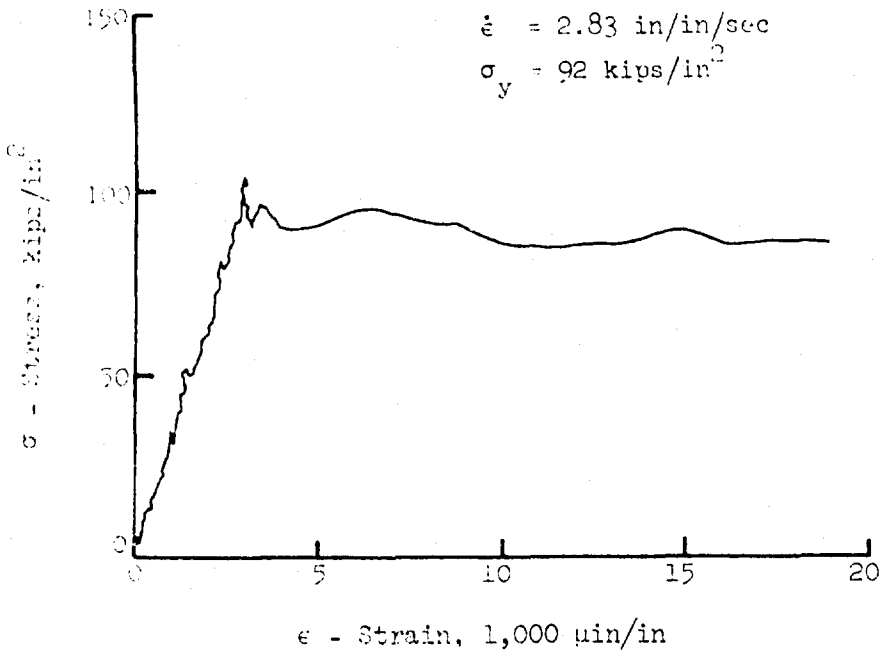

Figure 3.41 Thermit-welded splice, Grade 60, Test No. 153.

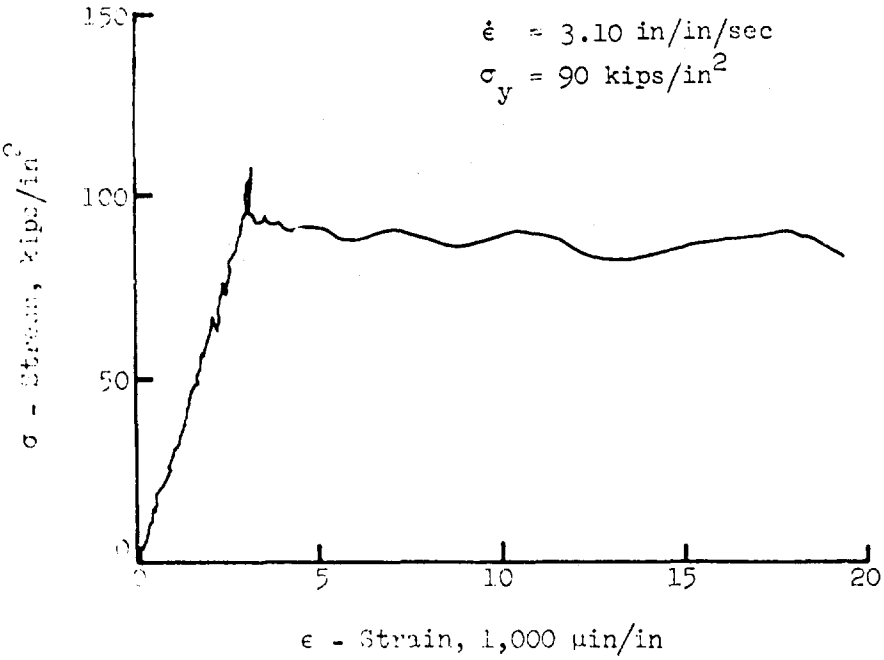

Figure 3.42 Thermit-welded splice, Grade 60, Test No. 157.

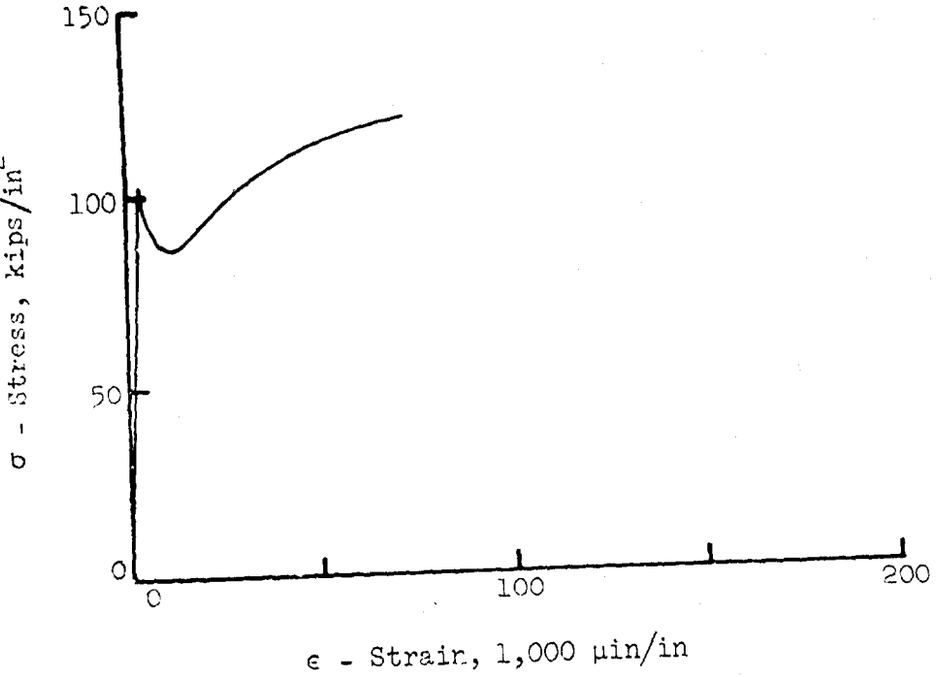

Figure 3.41 (Continued) Test No. 153.

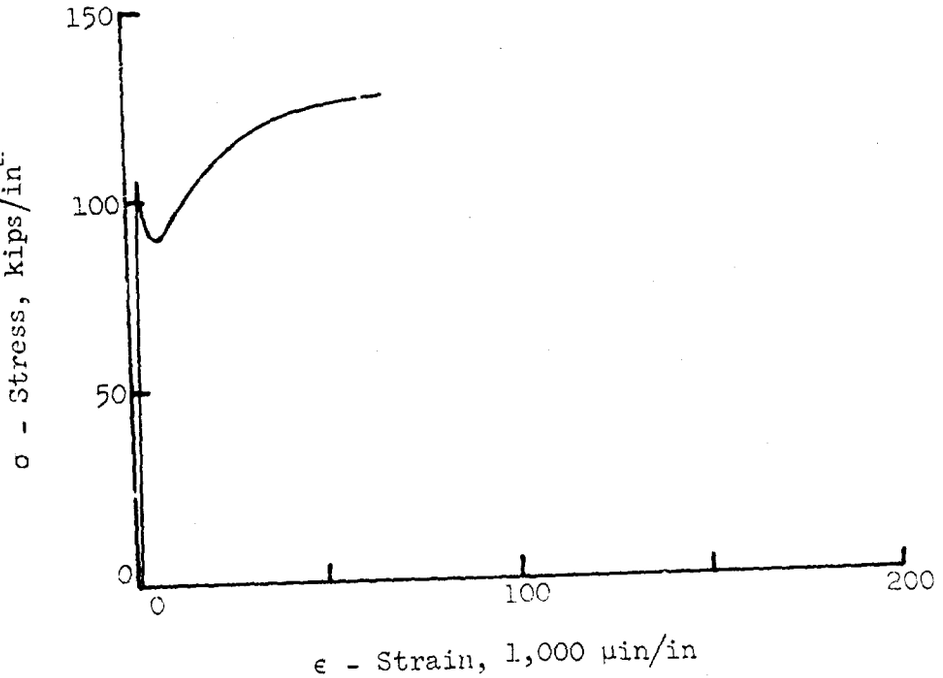

Figure 3.42 (Continued) Test No. 157.

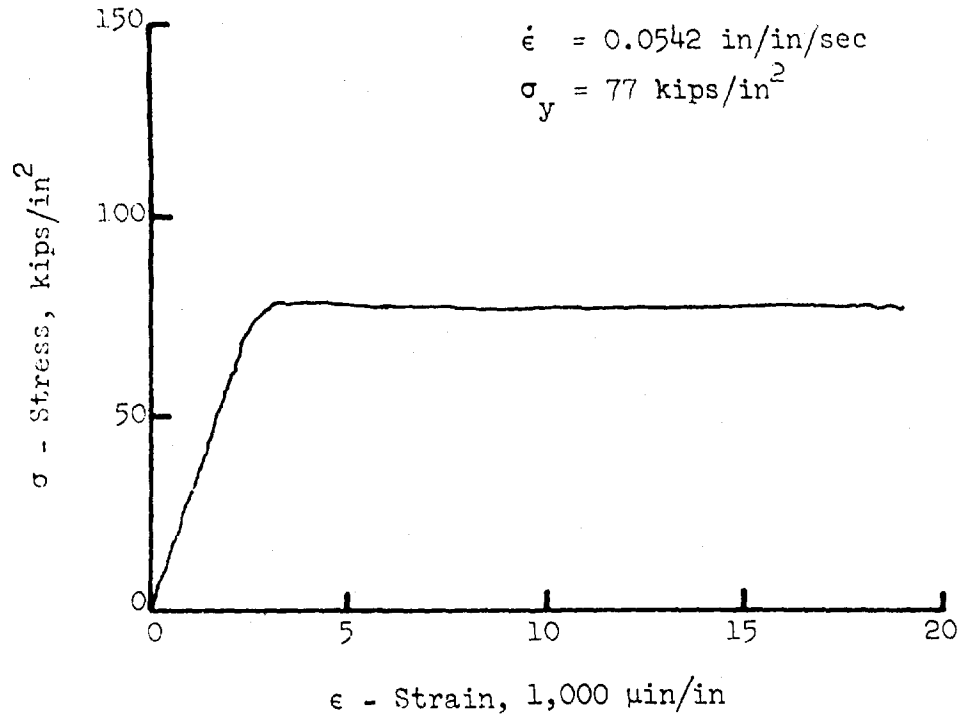

Figure 3.43 Thermit-welded splice, Grade 60, Test No. 162.

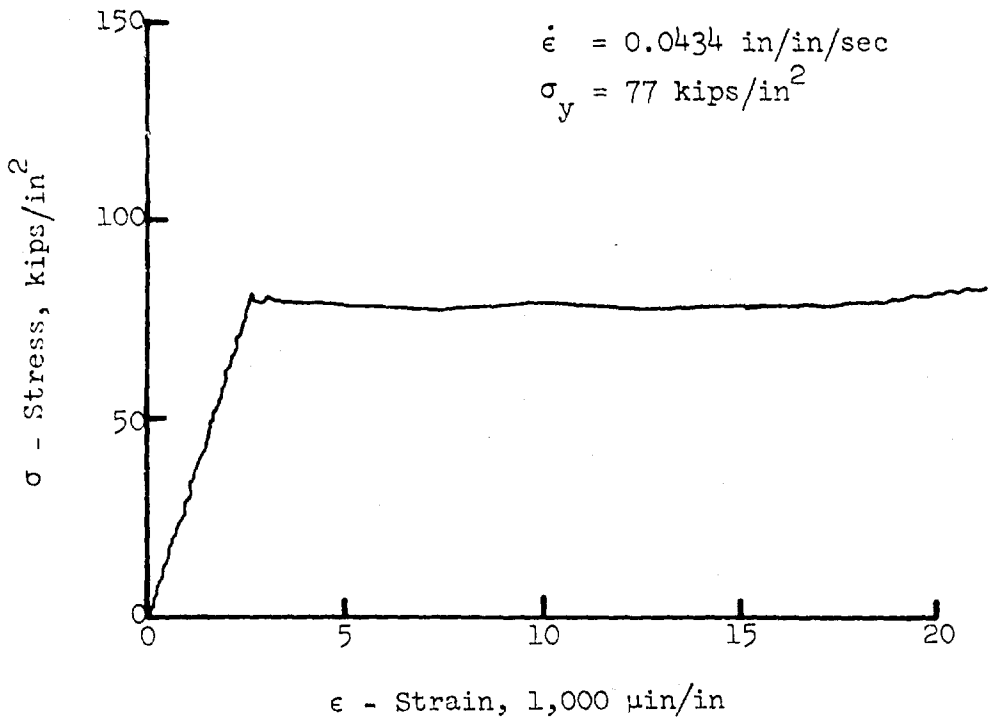

Figure 3.44 Thermit-welded splice, Grade 60, Test No. 166.

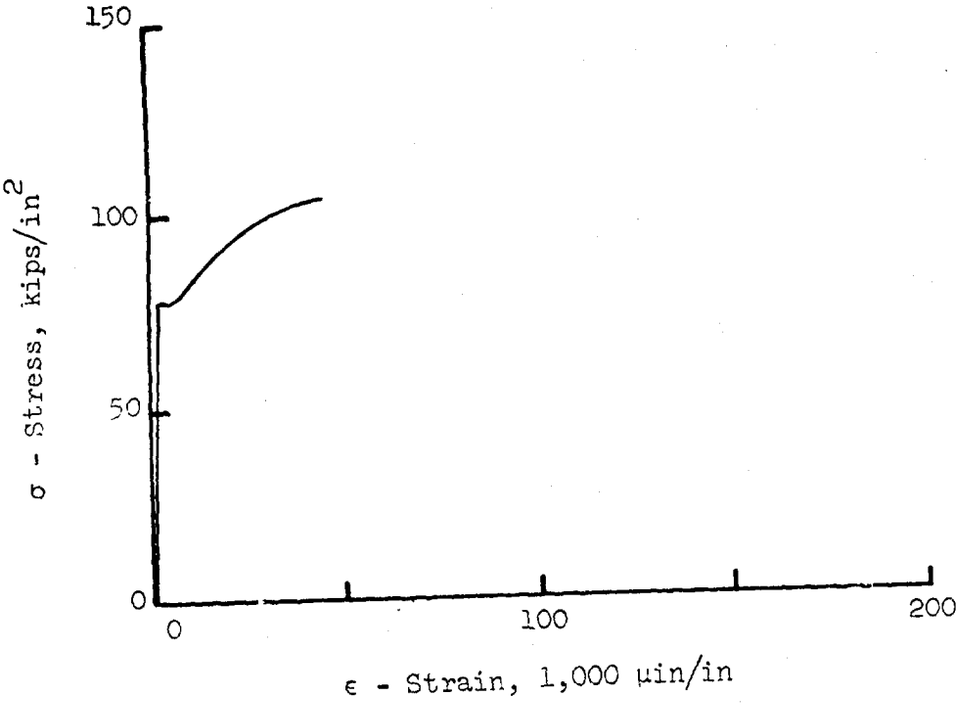

Figure 3.43 (Continued) Test No. 162.

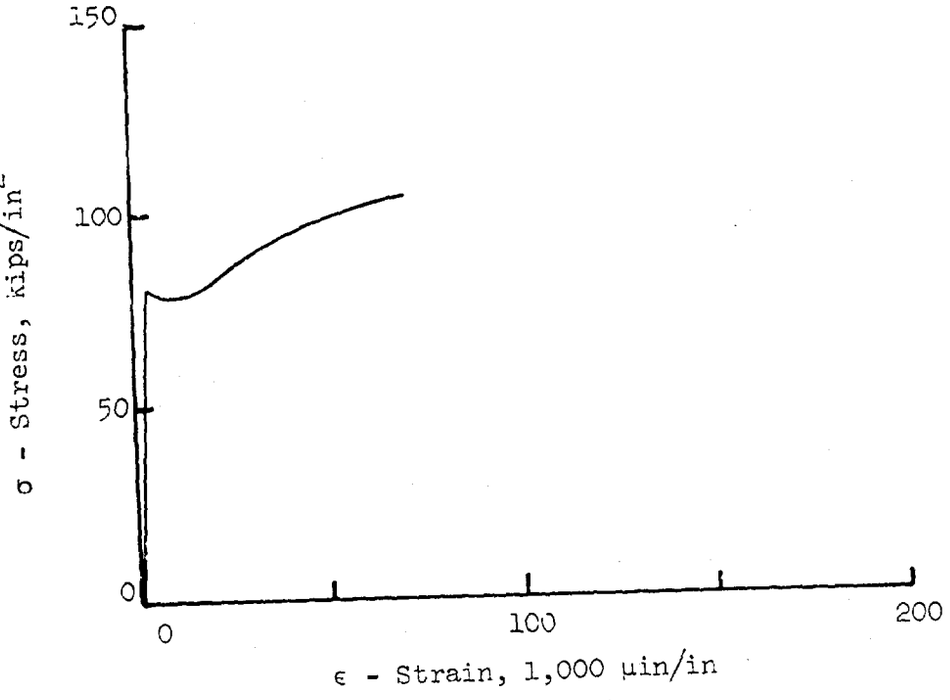

Figure 3.44 (Continued) Test No. 166.

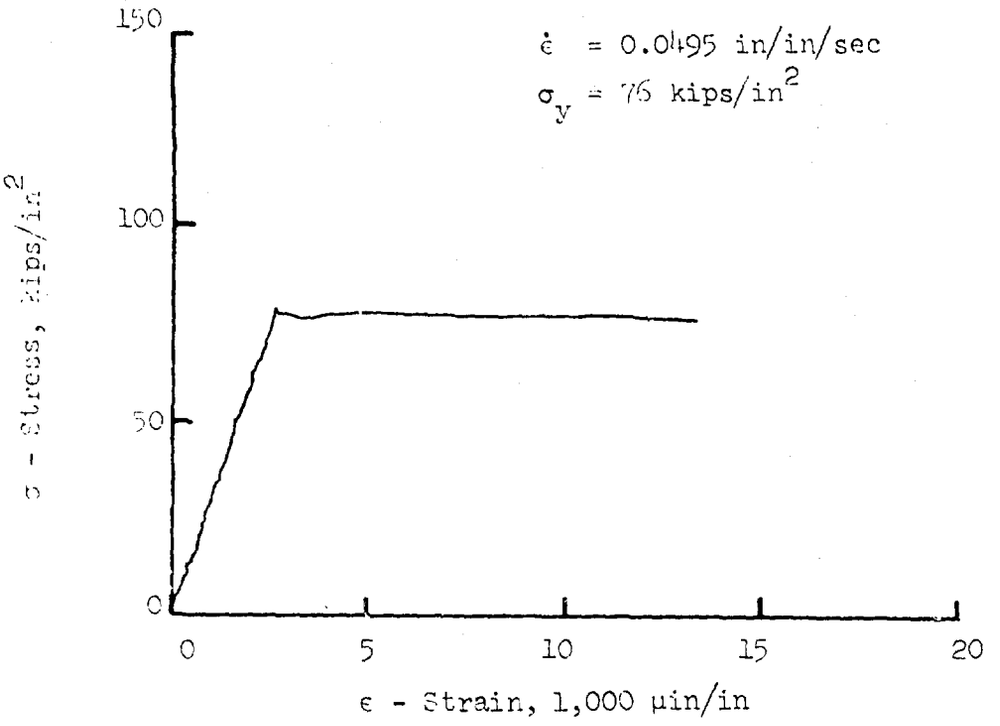

Figure 3.45 Thermit-welded splice, Grade 60, Test No. 171.

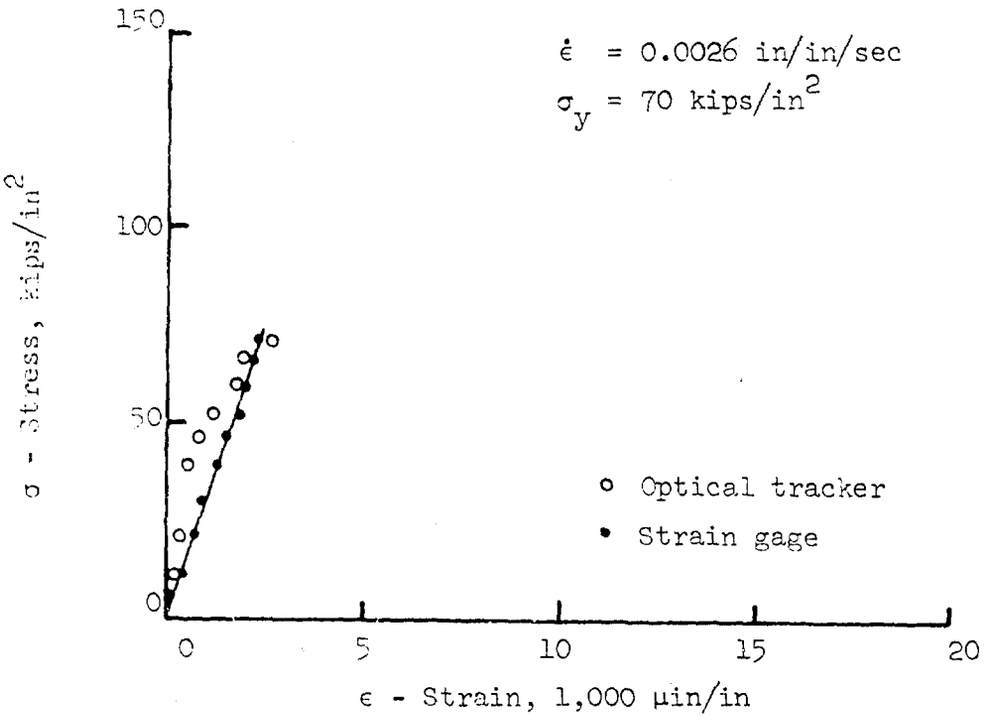

Figure 3.46 Thermit-welded splice, Grade 60, Test No. 189.

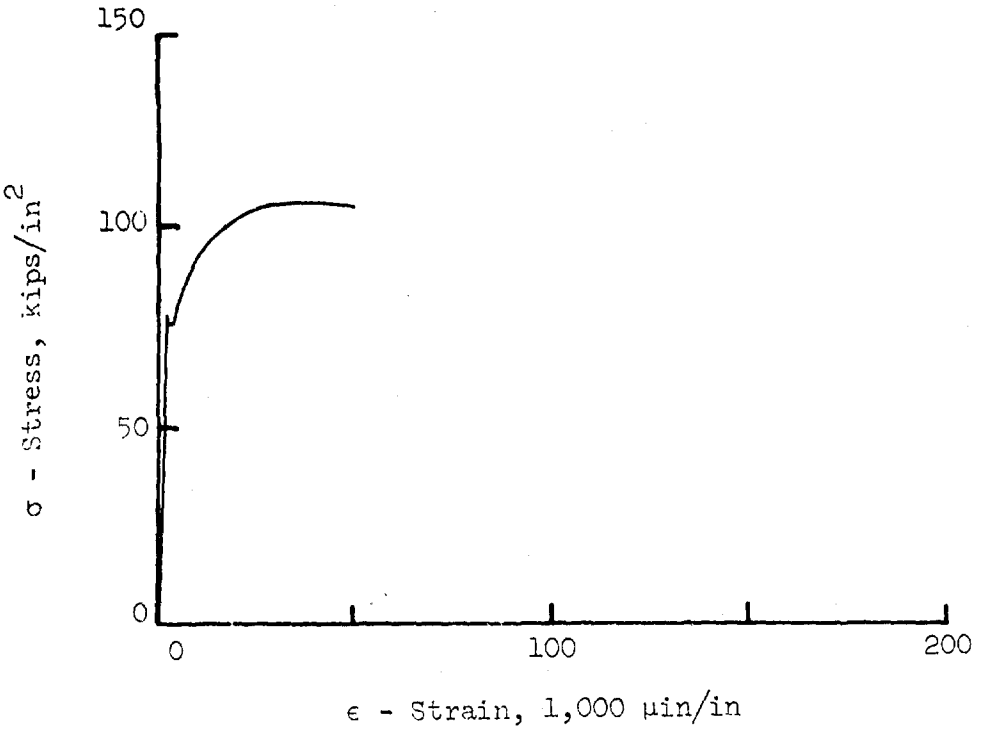

Figure 3.45 (Continued) Test No. 171.

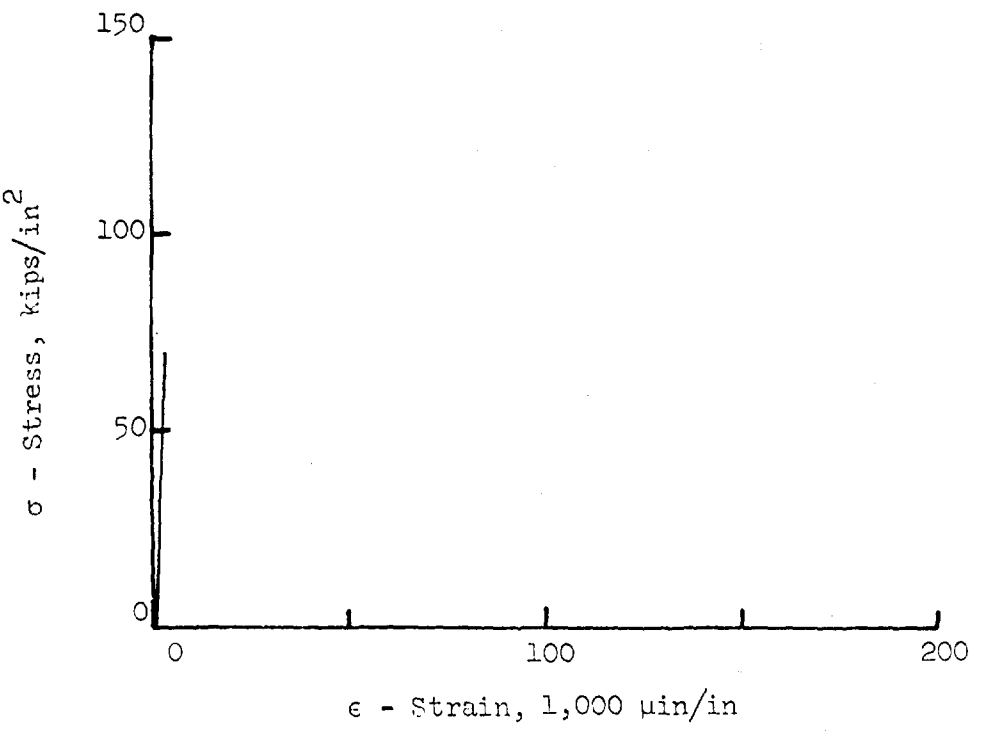

Figure 3.46 (Continued) Test No. 189.

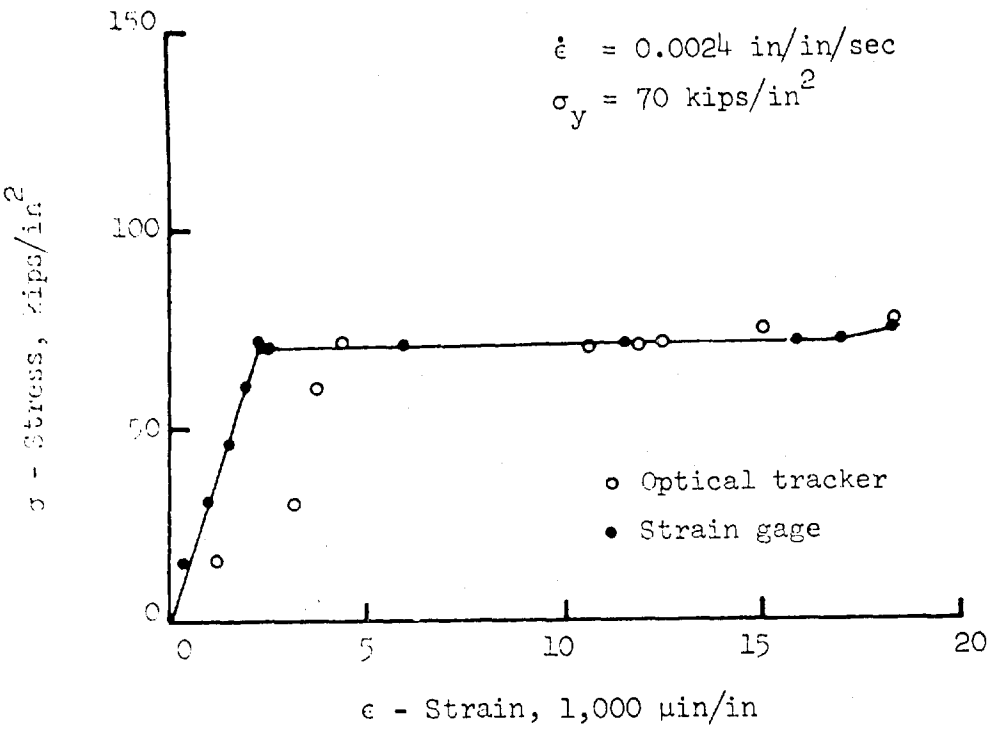

Figure 3.47 Thermit-welded splice, Grade 60, Test No. 193.

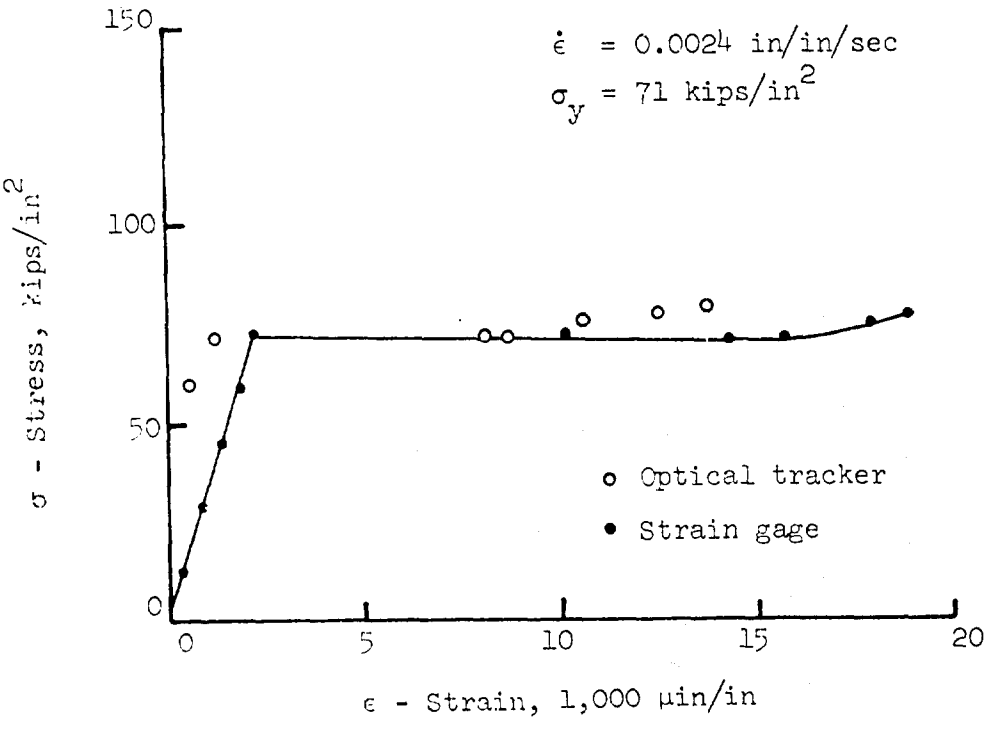

Figure 3.48 Thermit-welded splice, Grade 60, Test No. 198.

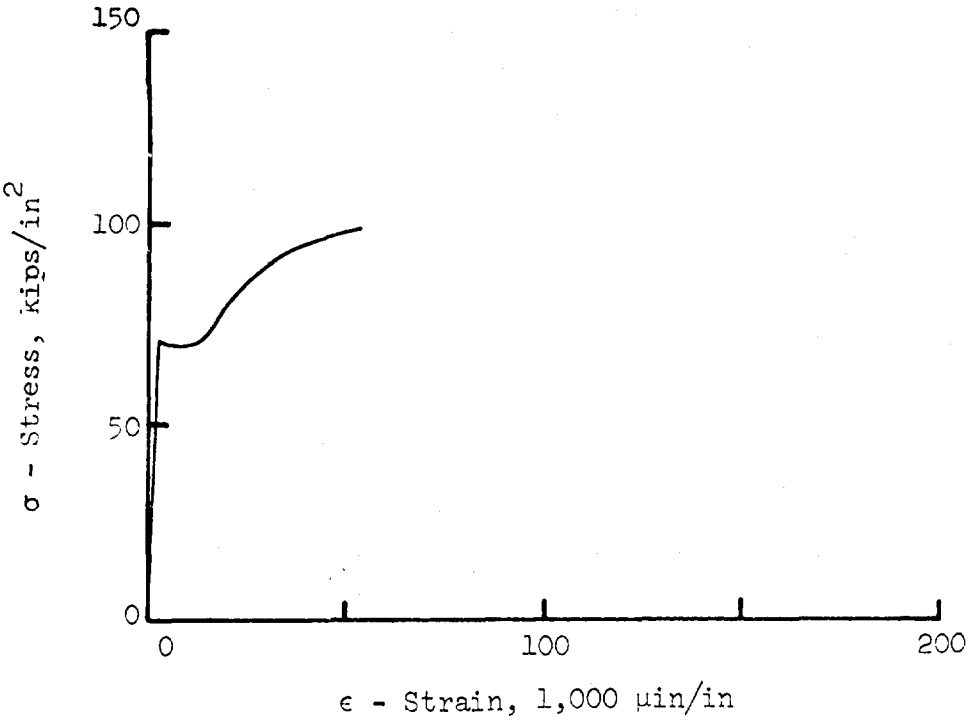

Figure 3.47 (Continued) Test No. 193.

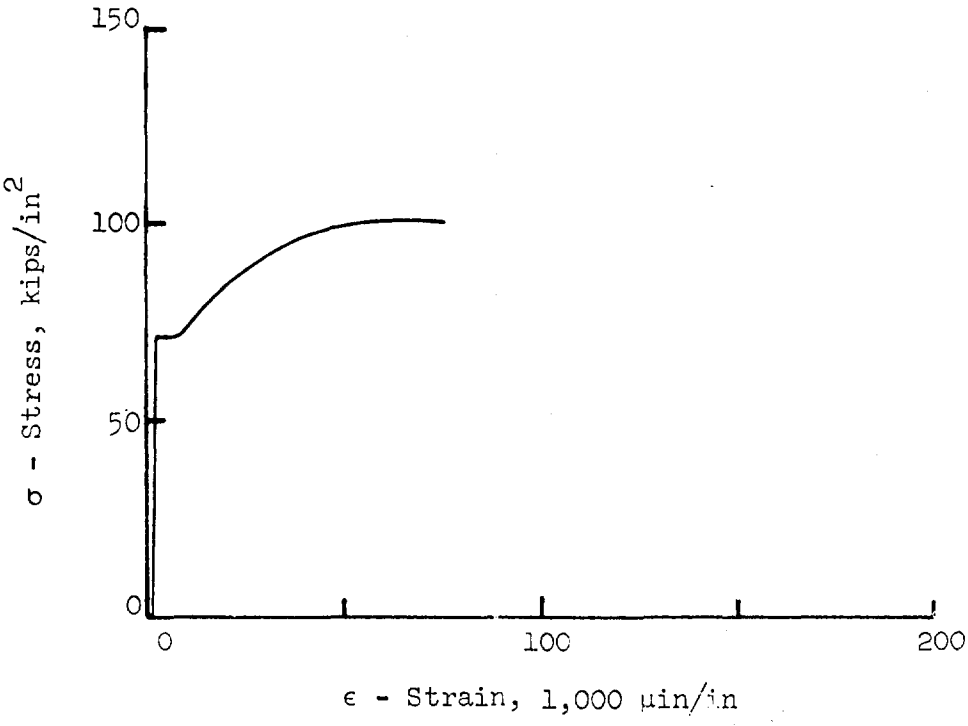

Figure 3.48 (Continued) Test No. 198.

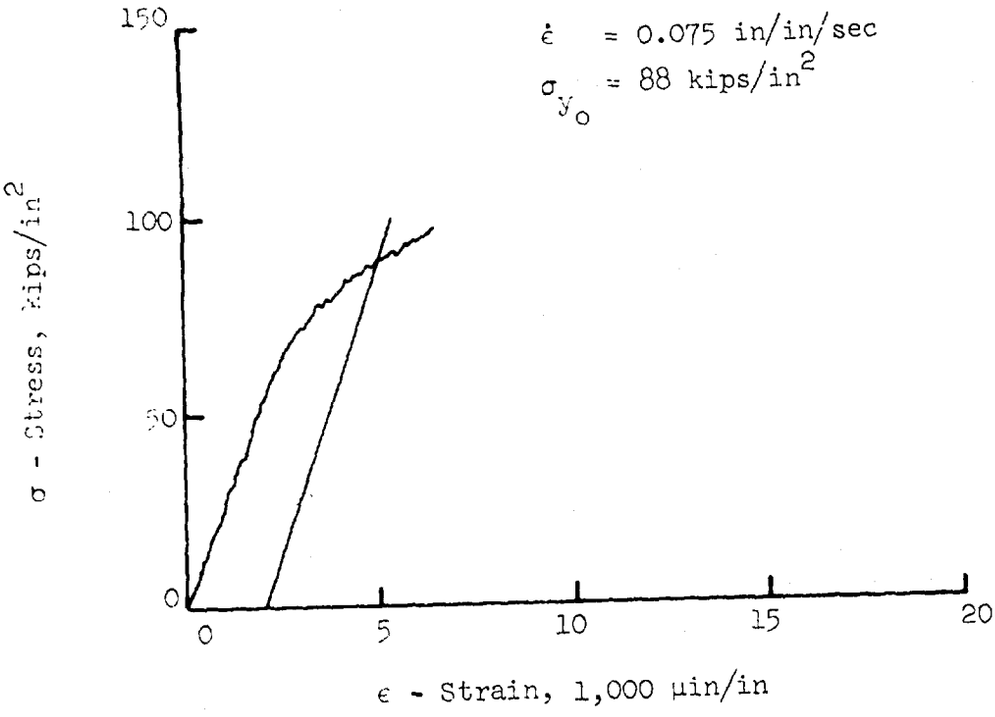

Figure 3.49 Thermit-welded splice, Grade 75, Test No. 177.

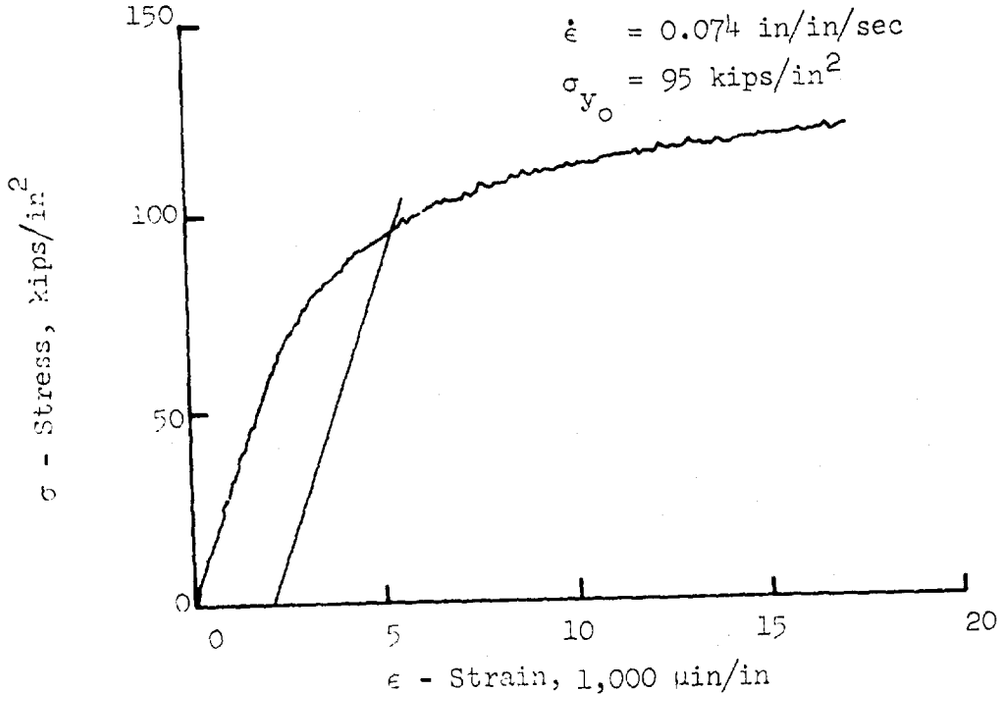

Figure 3.50 Thermit-welded splice, Grade 75, Test No. 181.

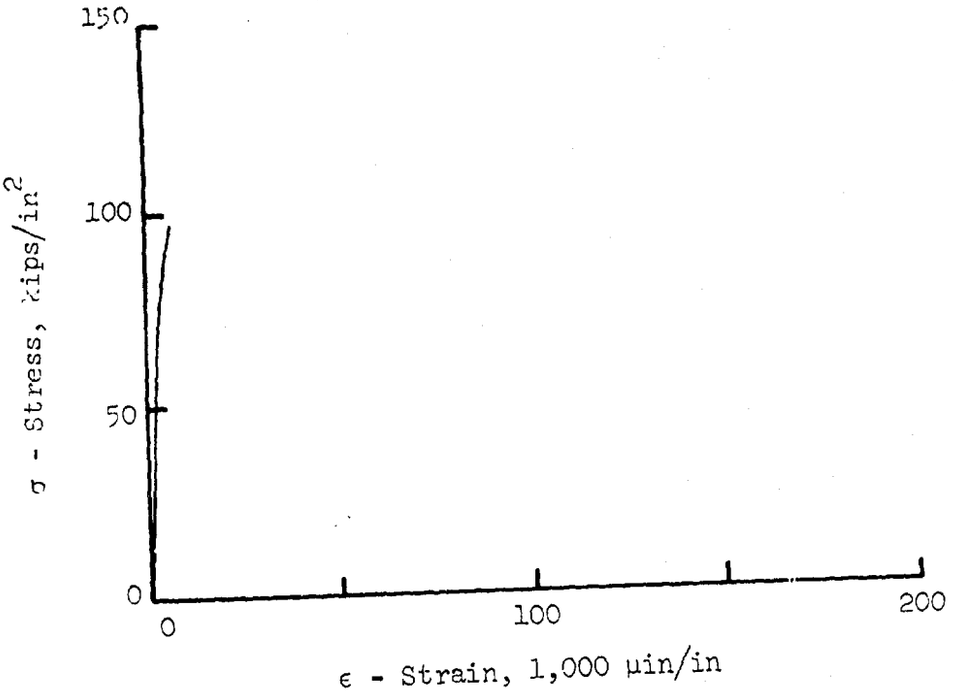

Figure 3.49 (Continued) Test No. 177.

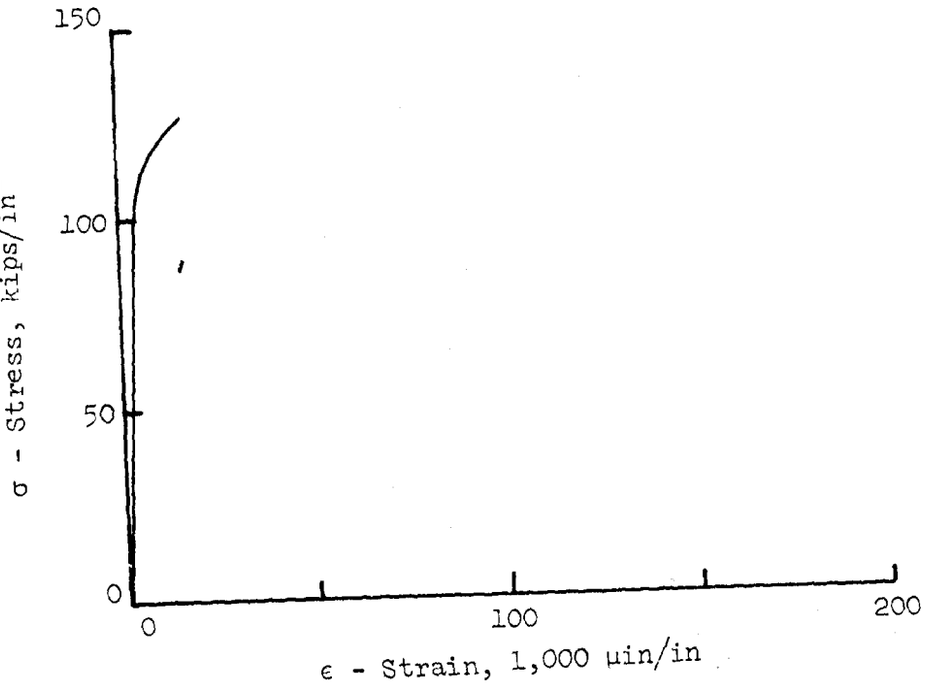

Figure 3.50 (Continued) Test No. 181.

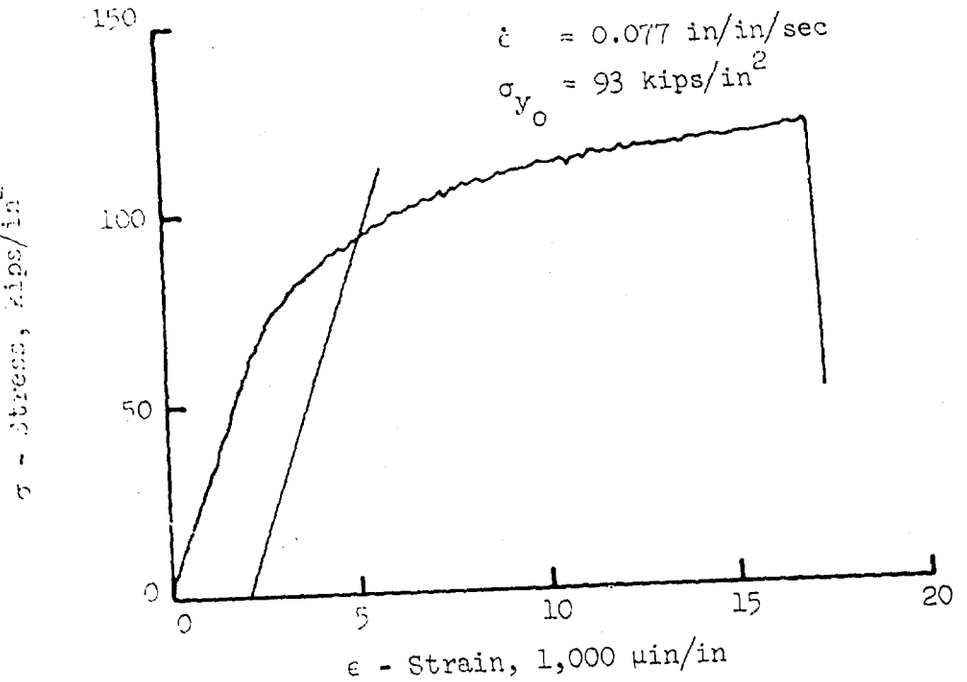

Figure 3.51 Thermit-welded splice, Grade 75, Test No. 184.

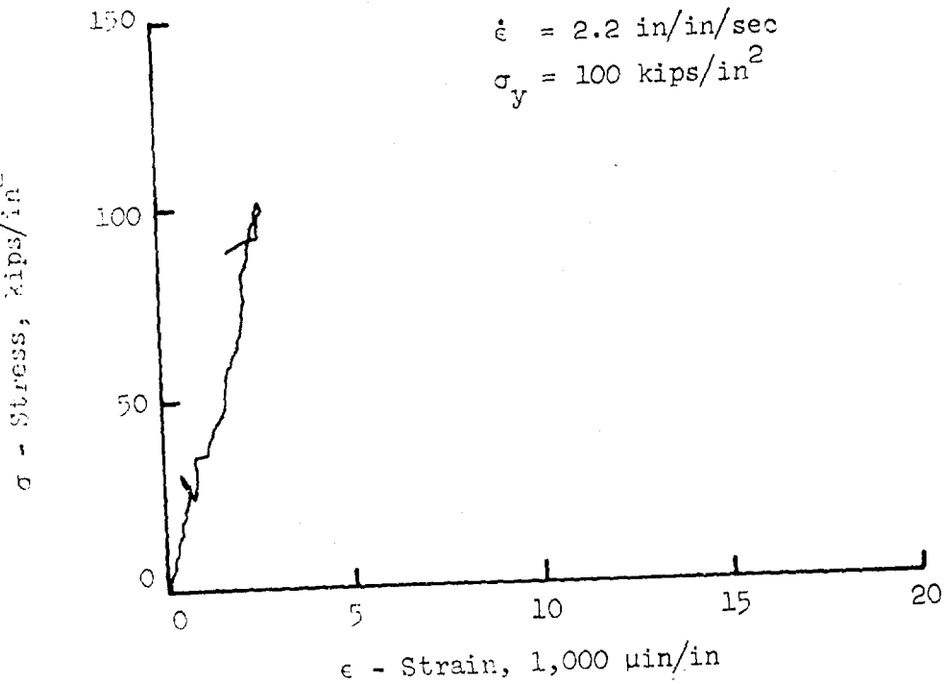

Figure 3.52 Cadweld splice, Grade 60, Test No. 147.

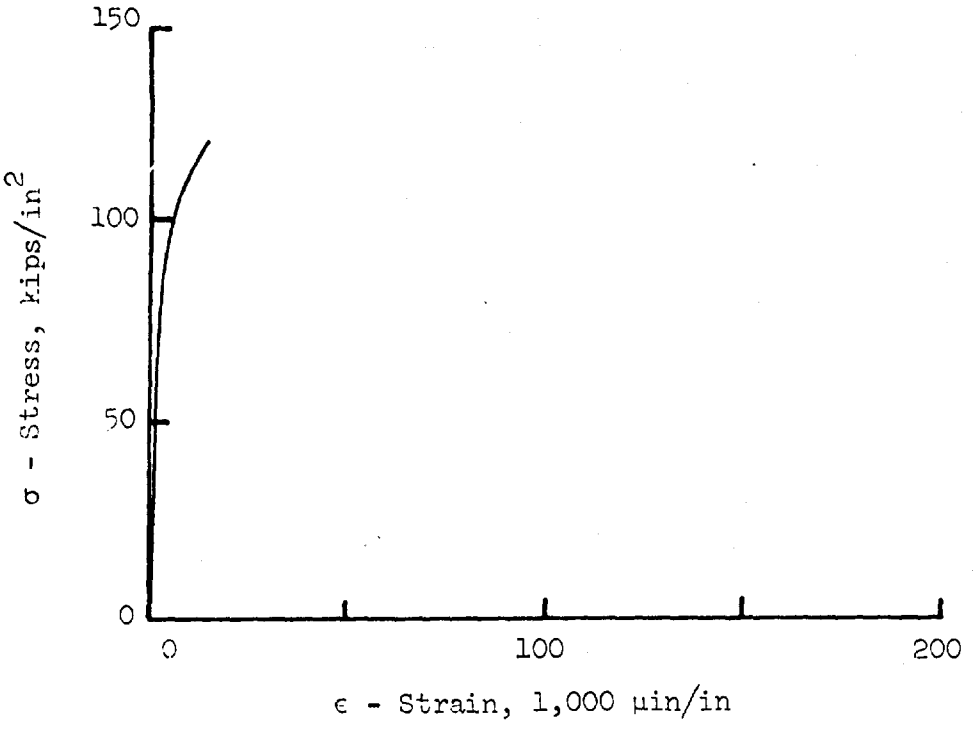

Figure 3.51 (Continued) Test No. 184.

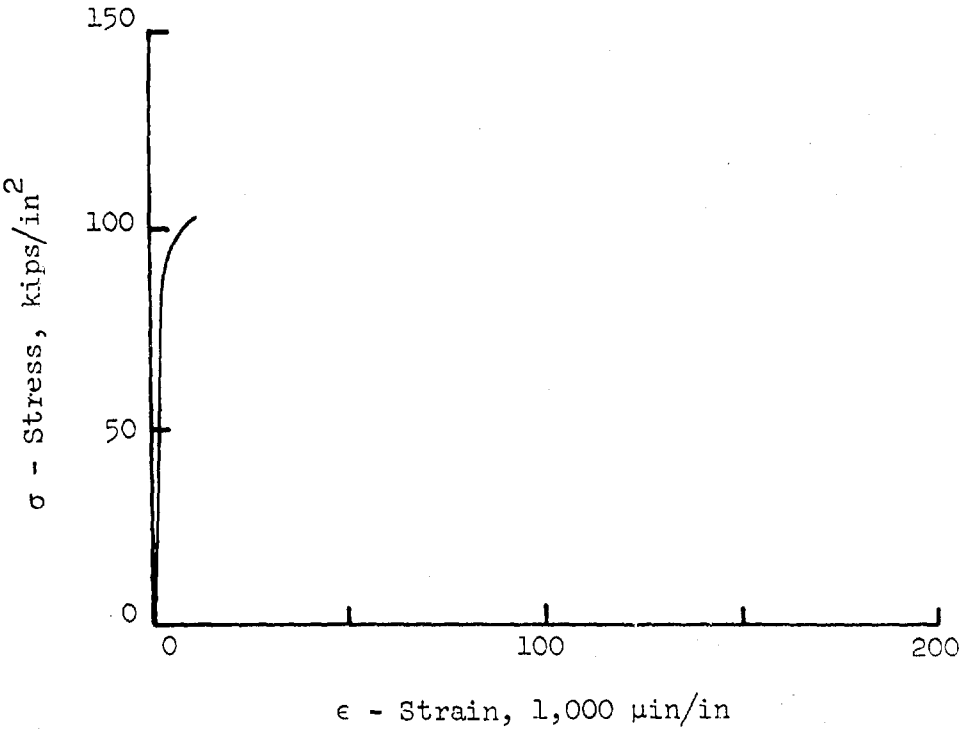

Figure 3.52 (Continued) Test No. 147.

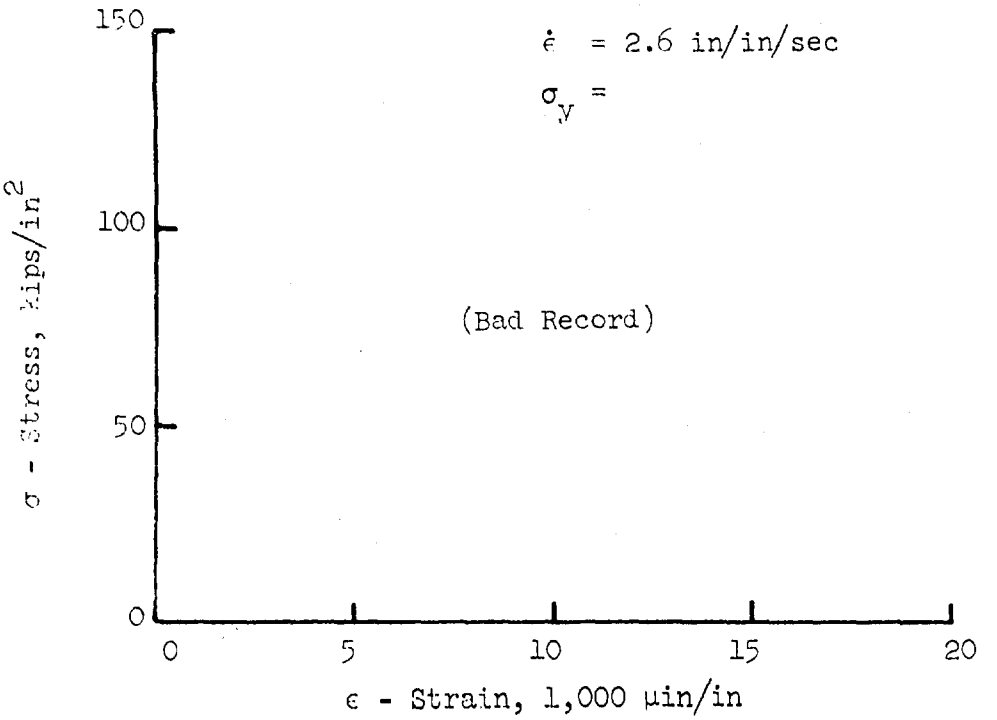

Figure 3.53 Cadweld splice, Grade 60, Test No. 151.

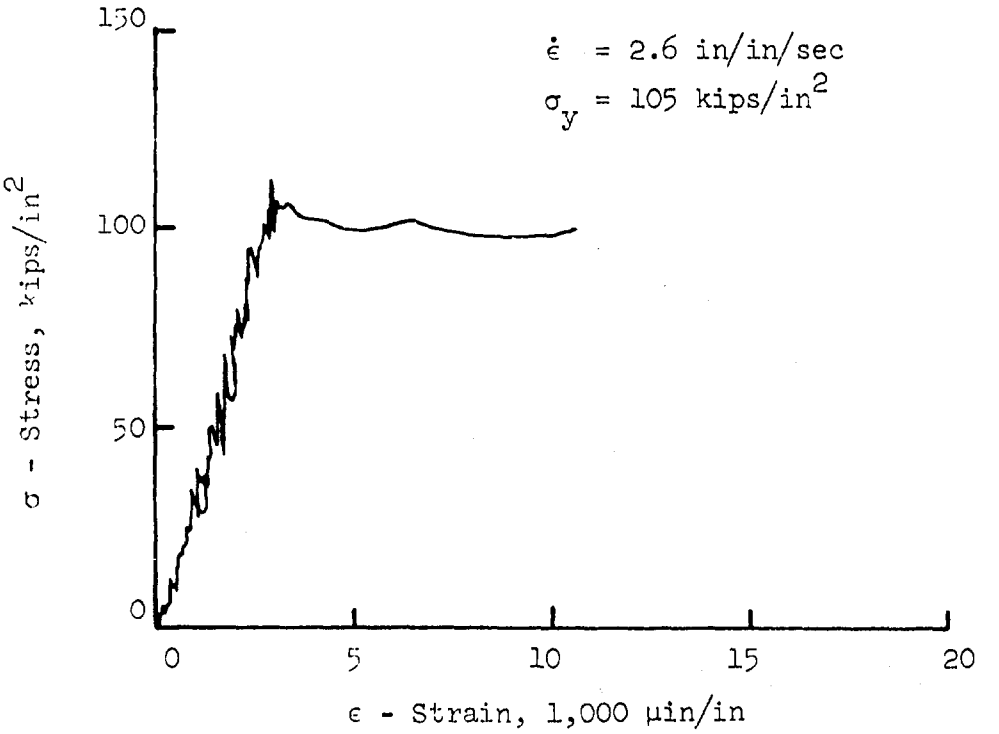

Figure 3.54 Cadweld splice, Grade 60, Test No. 156.

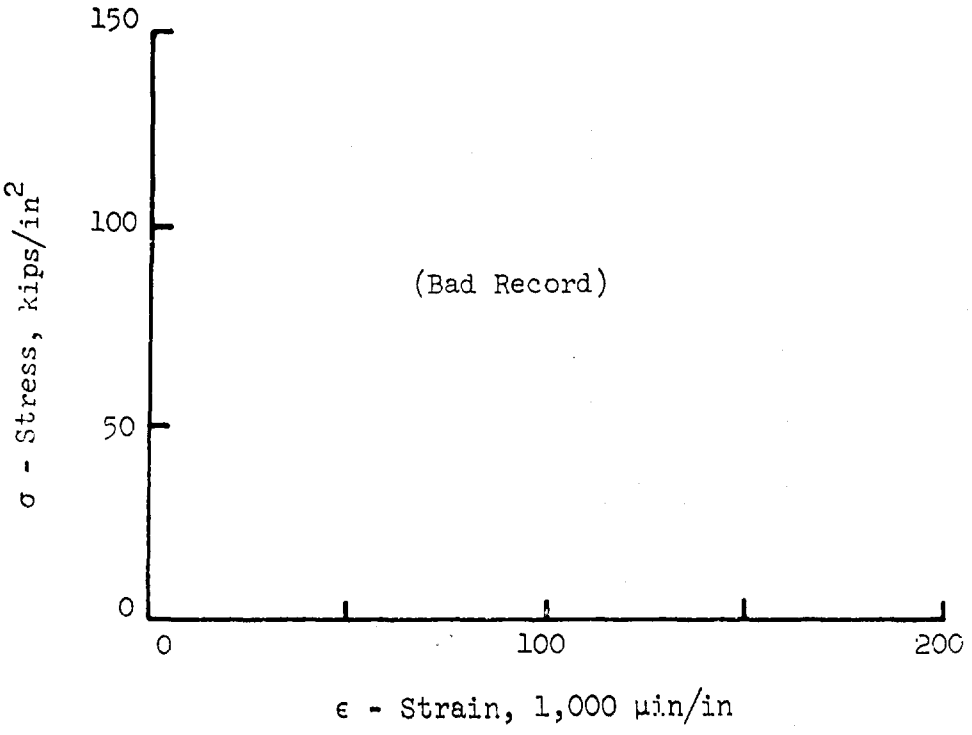

Figure 3.53 (Continued) Test No. 151.

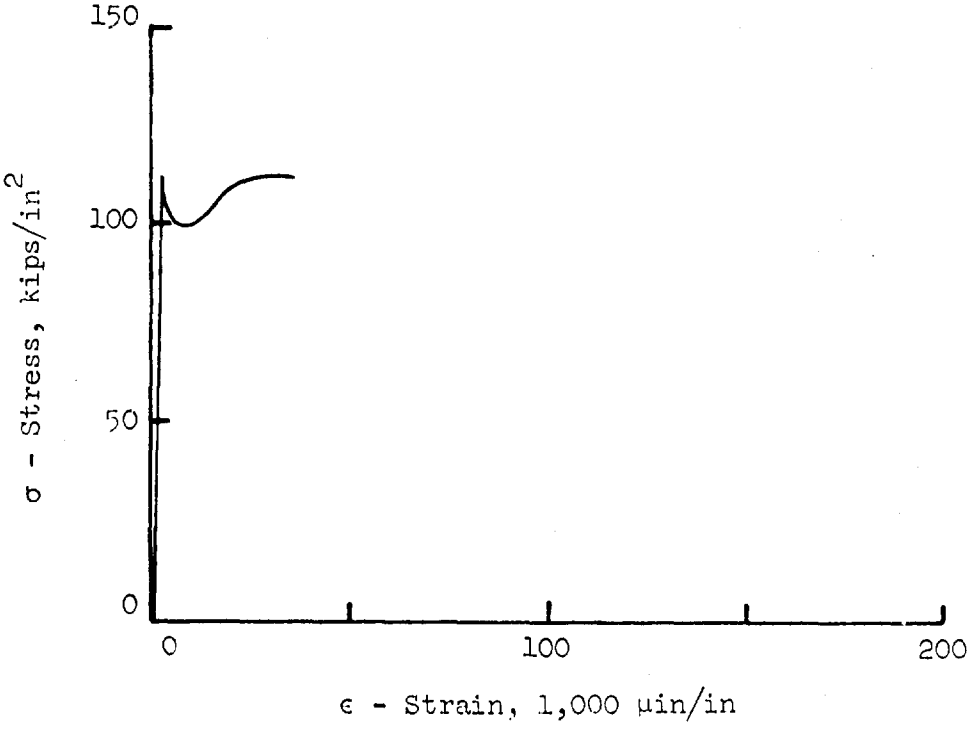

Figure 3.54 (Continued) Test No. 156.

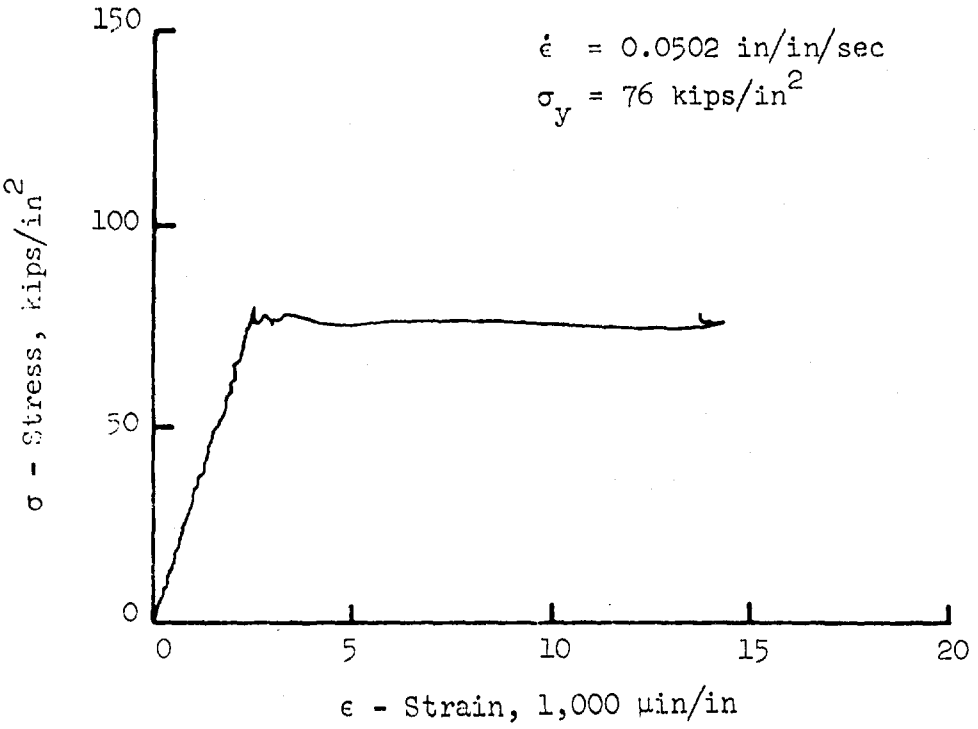

Figure 3.55 Cadweld splice, Grade 60, Test No. 160.

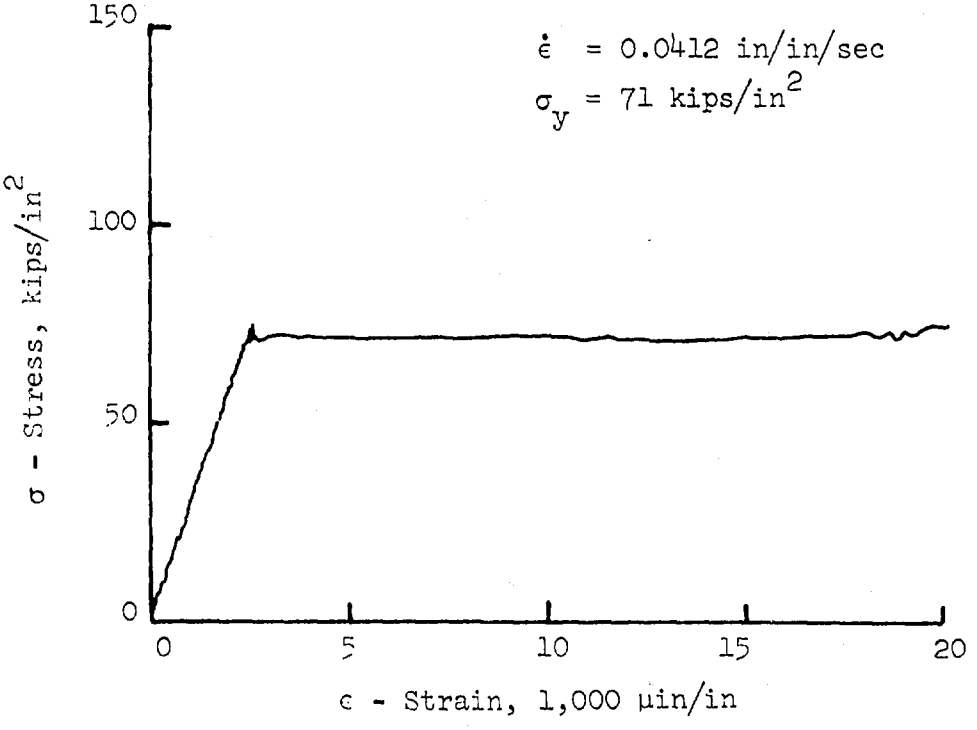

Figure 3.56 Cadweld splice, Grade 60, Test No. 169.

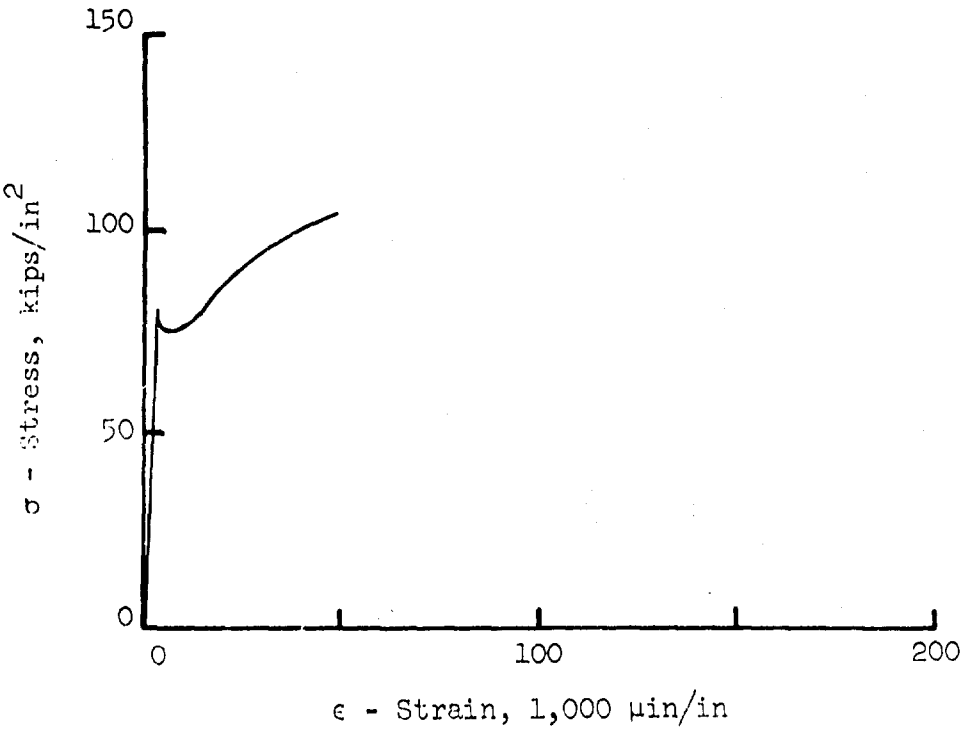

Figure 3.55 (Continued) Test No. 160.

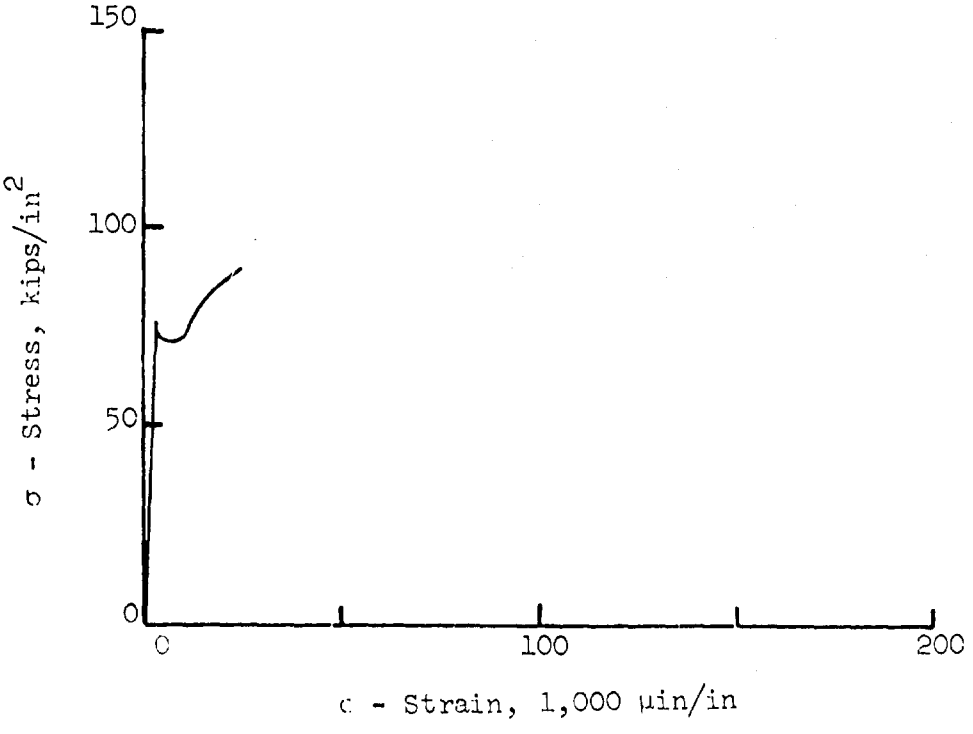

Figure 3.56 (Continued) Test No. 169.

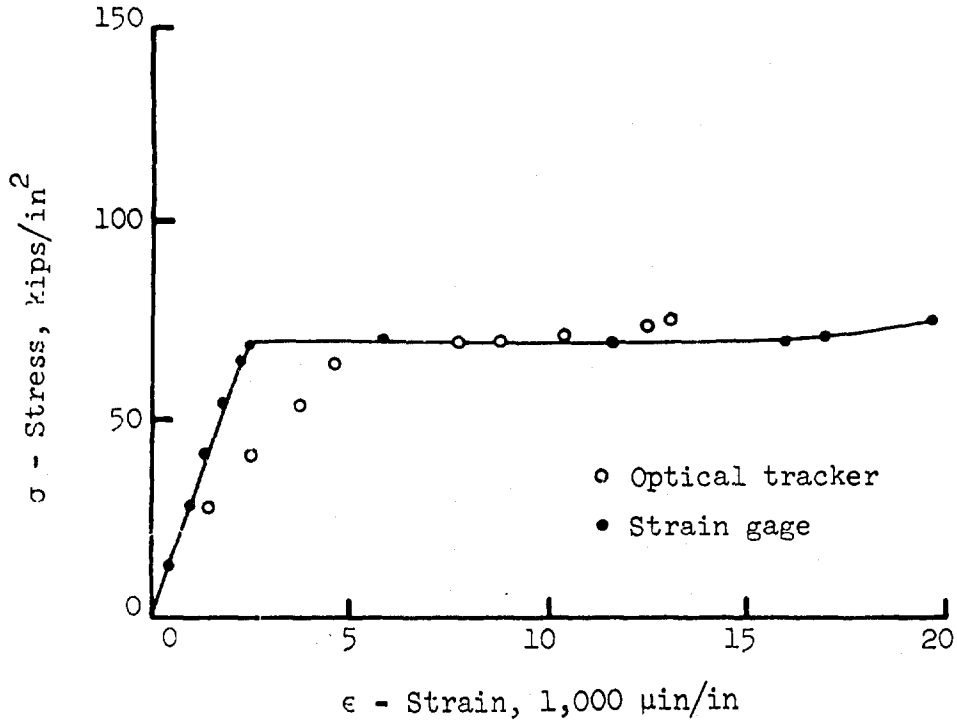

Figure 3.57 Cadweld splice, Grade 60, Test No. 187.

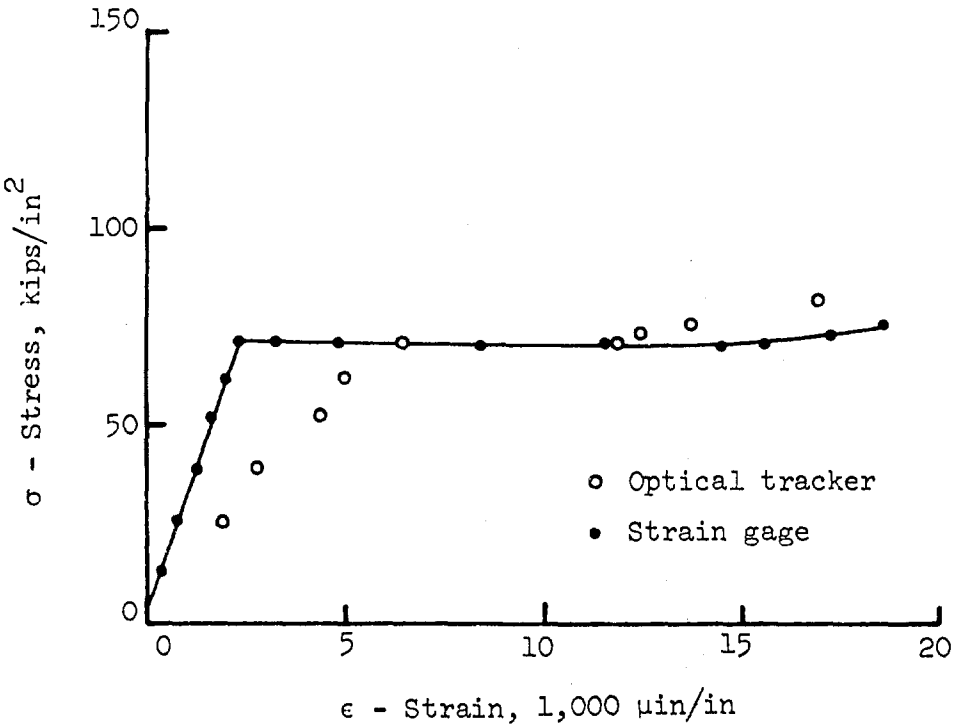

Figure 3.58 Cadweld splice, Grade 60, Test No. 192.

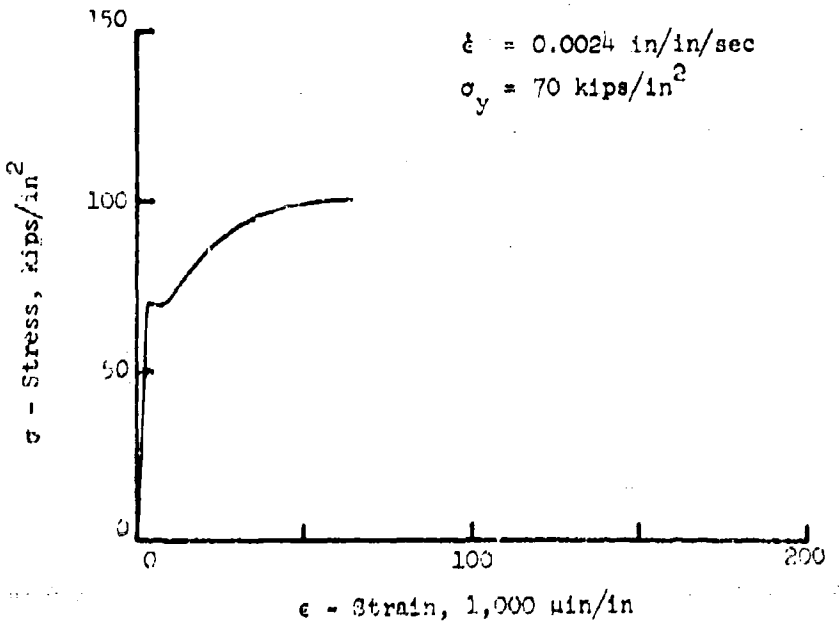

Figure 3.57 (Continued) Test No. 187.

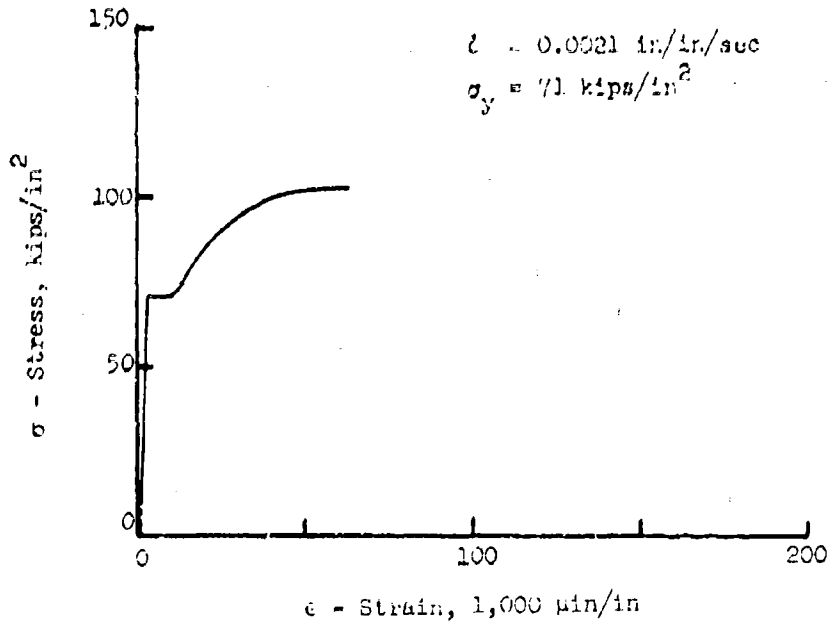

Figure 3.58 (Continued) Test No. 192.

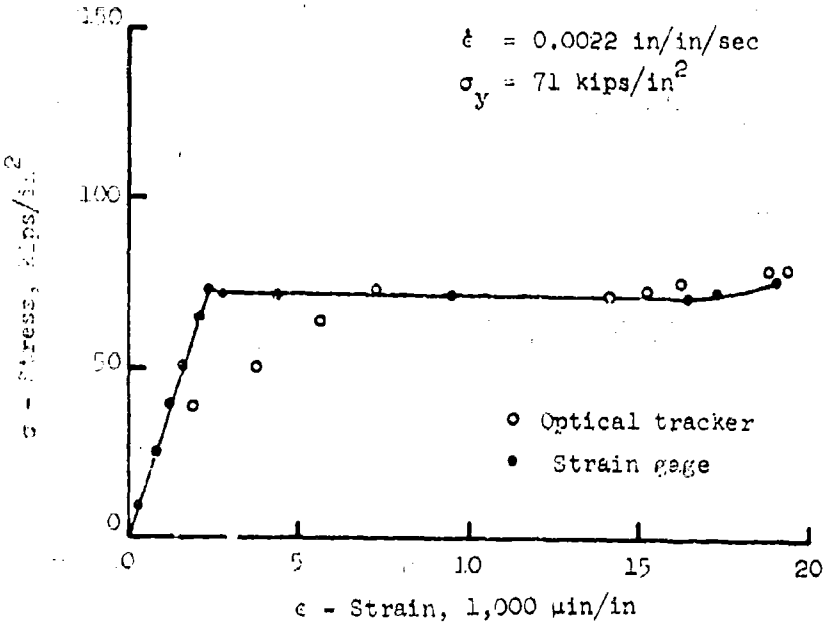

Figure 3.59 Cadweld splice, Grade 60, Test No. 196.

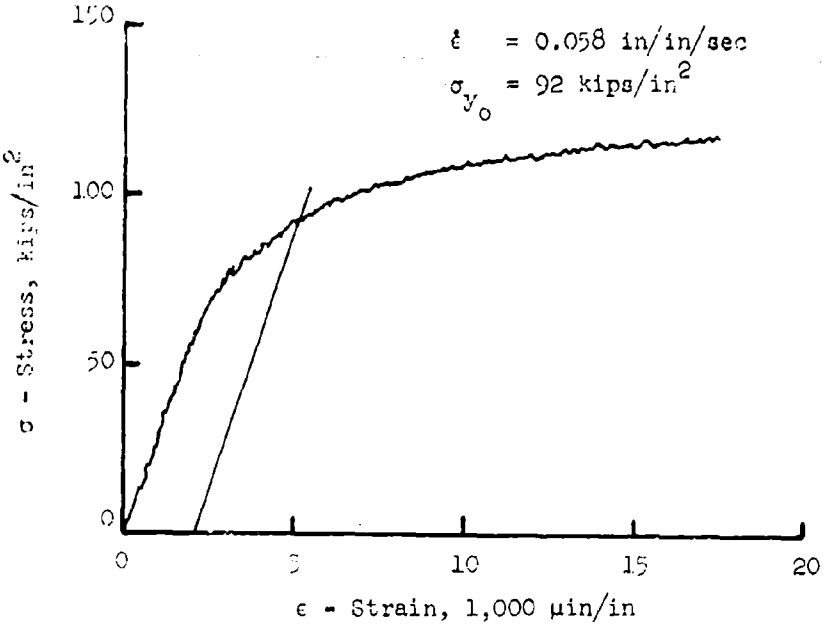

Figure 3.60 Cadweld splice, Grade 75, Test No. 175.

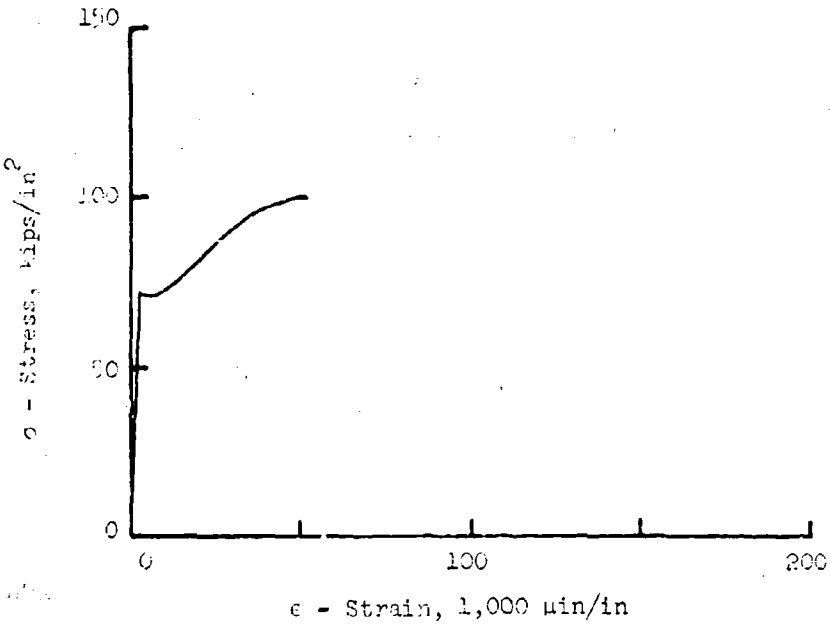

Figure 3.59 (Continued) Test No. 196.

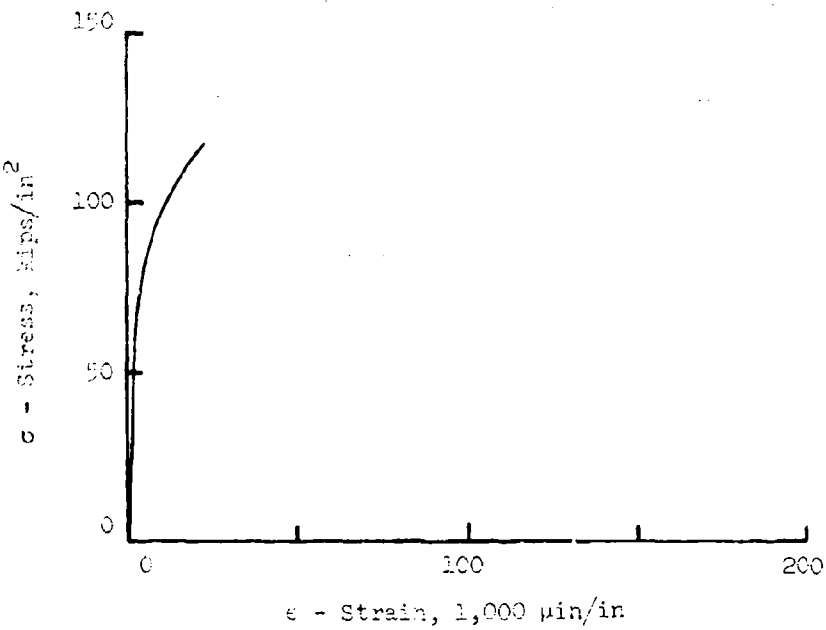

Figure 3.60 (Continued) Test No. 175.

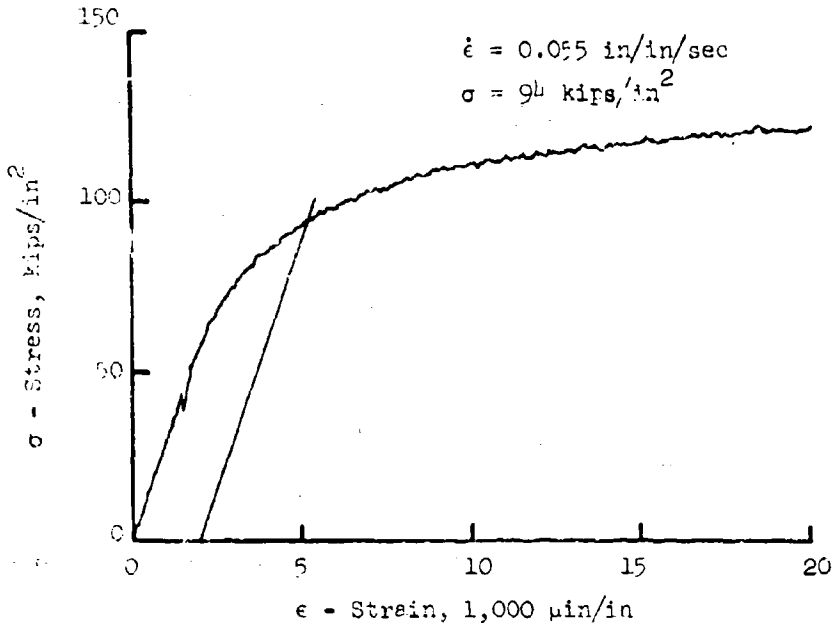

Figure 3.61 Cadweld splice, Grade 75, Test No. 179.

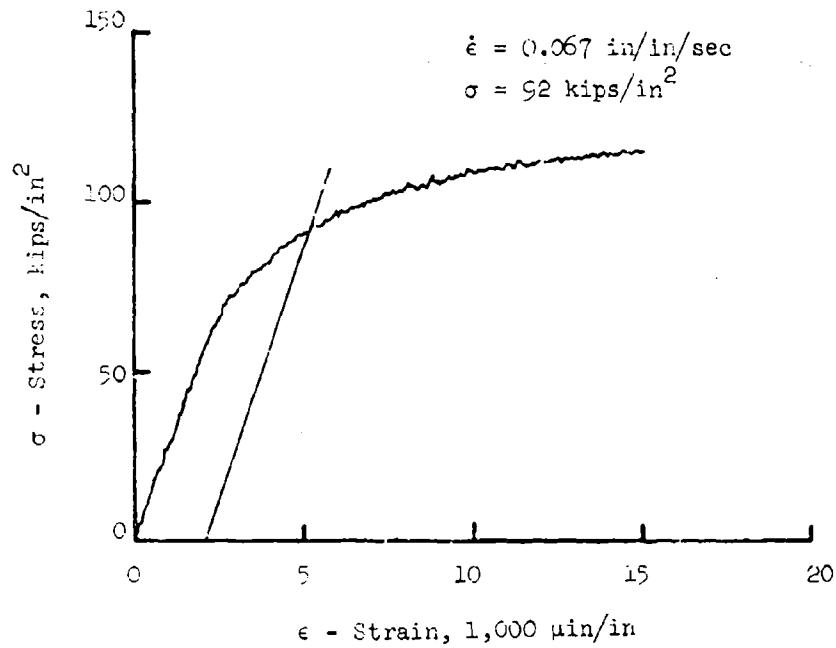

Figure 3.62 Cadweld splice, Grade 75, Test No. 183.

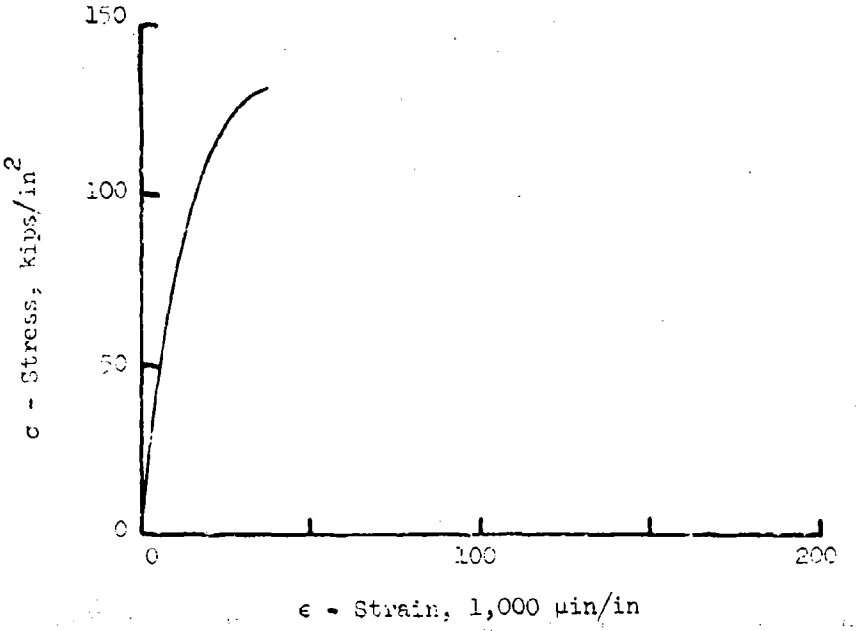

Figure 3.61 (Continued) Test No. 179.

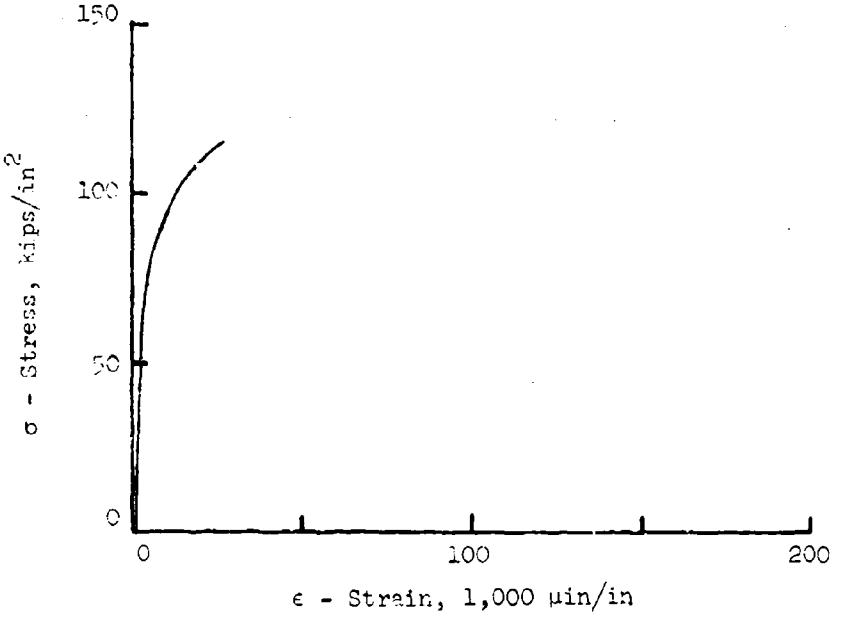

Figure 3.62 (Continued) Test No. 183.

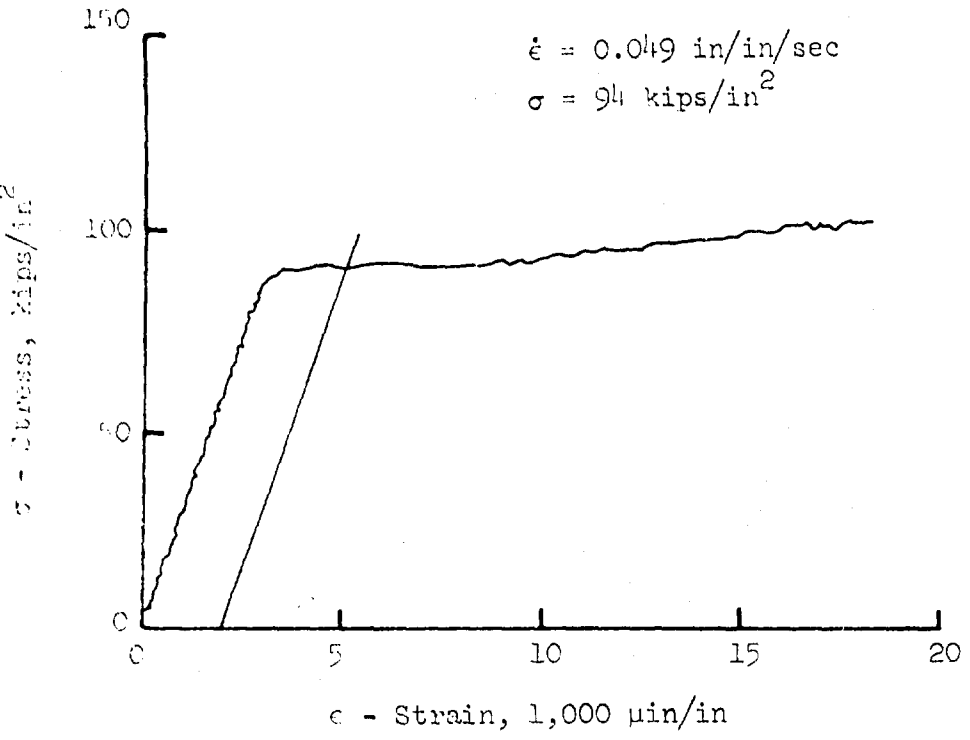

Figure 3.63 Cadweld splice, Grade 75 ("X" ribs), Test No. 201.

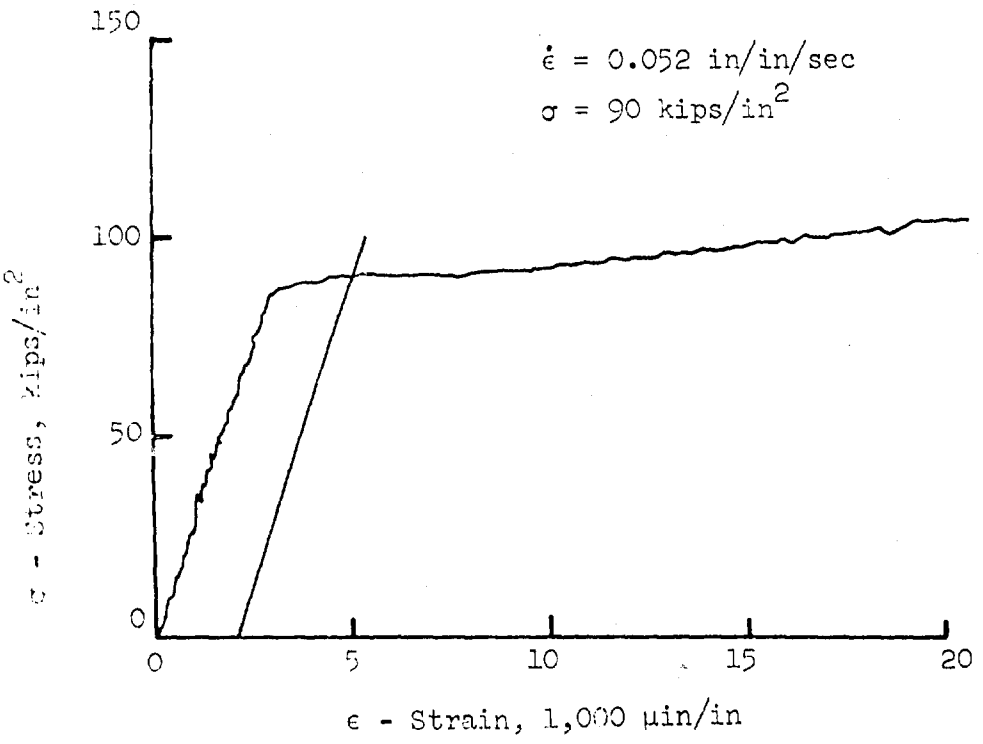

Figure 3.64 Cadweld splice, Grade 75 ("X" ribs), Test No. 202.

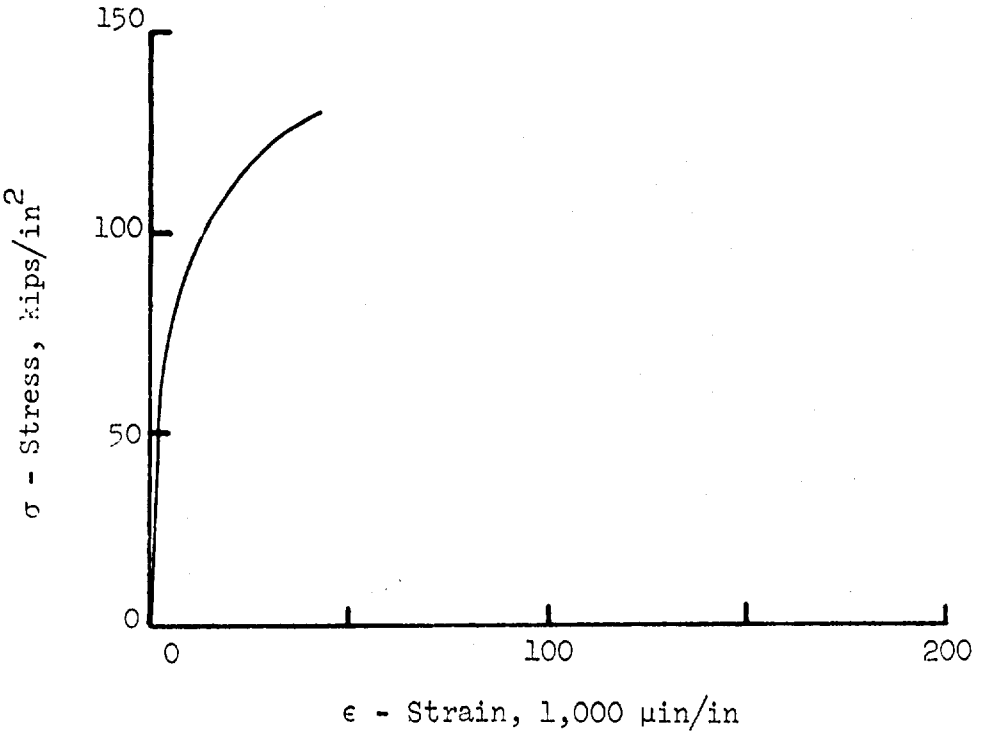

Figure 3.63 (Continued) Test No. 201.

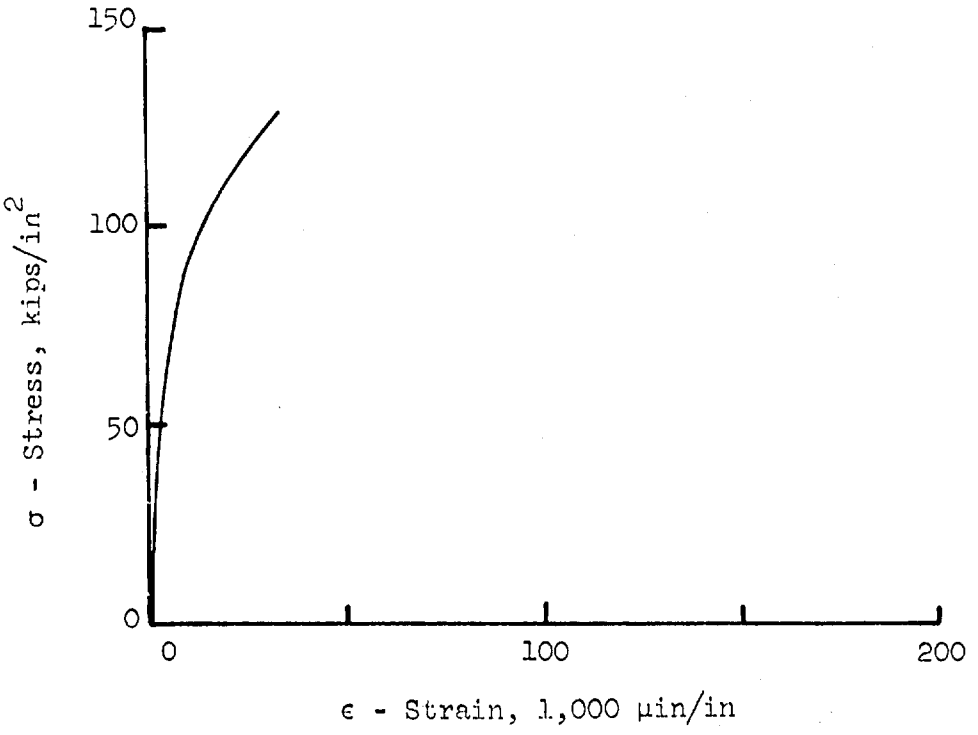

Figure 3.64 (Continued) Test No. 202.

CHAPTER 4

DISCUSSION OF RESULTS

The loading equipment, transducers, and electronic recording equipment appeared to function properly. The upper and lower load cells were recalibrated after all tests were completed, and the resulting calibration curves were identical with the pretest calibration curves. In most tension tests reviewed in the literature, only one load cell was used; in the tests reported herein, a lower and upper cell were used making it possible to compare applied forces with reactive forces. As shown in Tables 3.1 through 3.5, the upper and lower loads were approximately the same for intermediate and slow strain rate tests. However, for rapid strain rates, these loads were appreciably different because of inertial effects. By using the procedures described in Section 2.4, a corrected or so-called true load applied to the specimen was determined. The strains determined from the optical tracker data appear reasonable especially when compared with strains determined from strain gage data, as shown in the slow rate test results presented in Figures 3.9 through 3.64. However, the tracker data are valid within a band of approximately $\pm$1,200 μin/in of strain for a particular stress level. A study of the static stress-strain plots shows that in most cases the strains from tracker data are well within 1,000 μin/in of the corresponding strain determined from strain gage data at a particular stress level.

4.1 SPLICED BARS

Shown in Figures 4.1 through 4.3 are composite stress-strain curves

for butt-welded, Thermit, and Cadweld splices, respectively, that were determined by averaging the appropriate curves presented in Figures 3.9 through 3.64. The breaking strengths of all the spliced bars were greater than 125 percent of the nominal yield strengths as required by codes,[6,7,8] which are 75,000 and 94,000 psi for the Grades 60 and 75 bars, respectively; these values are also shown in Figures 4.1 through 4.3. The total areas (A_2) under the various stress-strain curves for the three general rates of strain, i.e., rapid, intermediate, and slow, were determined using a planimeter. The area under these curves represents the energy absorbed by the various spliced bars. The area (A_1) under the curve bounded by 1.25 times the nominal yield stress was determined. It is believed that a ratio of the two areas (A_2:A_1) is a good indication of the effectiveness of the splice, especially for dynamic loads. Such values are presented in Table 4.1 along with ratios of breaking stress to 125 percent of the nominal yield stress (σ_m:$1.25\sigma_y$) as well as ratios of strain at failure to 125 percent of the nominal yield strain (ϵ_m:$1.25\epsilon_y$). A comparison of the total area (A_2) under the stress-strain curves for the Grades 60 and 75 bars for the intermediate load rates shows that apparently the energy absorbing capacity for the Grade 60 bars is slightly greater. The Grade 60 spliced bars seem to be more ductile than the Grade 75 spliced bars; however, none of the spliced bars were as ductile as the machined or as-rolled bars. This can be observed by studying the stress-strain curves in Chapter 3 and by comparing the final elongation in percent shown in Tables 3.1 through 3.5. In general, it seems that the machined bars were approximately four times more ductile than the spliced bars. Based on this,

it would seem reasonable to assume that the heat produced by all three of the splicing techniques affects the metallurgical properties of the spliced bars, thereby reducing their ductility. The ASTM standards[15,16] for Grades 60 and 75 bars stipulate a minimum elongation of 7 and 5 percent, respectively, over an 8-inch gage length. Very few of the spliced bars met this requirement (see Figures 4.1 through 4.3). It should be noted that a 1 percent elongation represents a strain of 10,000 μin/in.

4.1.1 Butt-Welded Splices. The butt-welded splices all performed satisfactorily strengthwise; however, most of them did not meet ASTM elongation requirements.[15,16] Only four of the nine Grade 60 spliced bars had final elongations greater than 7 percent. One out of three Grade 75 spliced bars had an elongation greater than 5 percent. The Grade 75 butt-welded splices appeared to be more ductile than the Thermit or Cadweld splices made from Grade 75 bars. All the bars failed in the welded joint.

4.1.2 Thermit Splices. All of the splices performed satisfactorily strengthwise; however, only three out of the nine Grade 60 spliced bars had final elongations greater than 7 percent. The final elongations for the three Grade 75 spliced bars were much less than 5 percent. For the spliced Grade 60 bars, none failed in the splice except that in Test 189, which was a slow load rate test. This bar was in the elastic range of response when the splice failed. For the three Grade 75 bars tested, one broke in the splice and the others adjacent to the splice.

4.1.3 Cadweld Splices. All of the splices performed satisfactorily

strengthwise; however, the final elongations for all nine spliced Grade 60 bars were less than 7 percent. The final elongations for three Grade 75 spliced bars with the bamboo deformation pattern were less than 5 percent. For the two Grade 75 spliced bars having "X" deformations, the final elongation of one was about 5 percent, and that of the other was greater than 5 percent. All Grade 60 bars pulled out of the metal splicing sleeve. In Test 147, the bar remained elastic when the splice failed. For this test, only two deformations were within the sleeve of the Cadweld splice. Since the Cadweld splice depends upon the shearing resistance of the deformations on the reinforcing bar, its strength is dependent upon the total shearing area of the deformations within the splice. The spliced Grade 75 bars performed in the same manner except for those in Tests 201 and 202, which were the only two bars having an "X" deformation pattern (see Figure 3.8). More shear area for deformation per inch of bar length was available with this pattern than for the bamboo deformation pattern characteristic of all the other bars tested. Consequently, the spliced bars having the "X" deformations were more ductile and met the final elongation requirement stipulated by standards.[16] The width of the deformation for these bars was greater than the width of the deformation for the other bars. Based on the results of these tests, it is believed that the ASTM standards[15,16] should be changed to establish a minimum width for deformations on reinforcing bars.

Examination of Figures 3.57 through 3.59 shows a definite biased diversion of strain determined from optical tracker data from that determined from strain gage data for like stress levels. The strain gage

data were taken on the bar 5-1/2 inches below the center of the splice, whereas the optical tracker data were taken across the splice. The difference in these curves, even taking into account the error (±1,200 μin/in) in the optical tracker data, indicates that slippage occurred in these splices. Slippages showing similar values of stress and strain are discussed in References 14 (Holt) and 29 (Siess).

However, consideration should be given to tests made on a spliced bar surrounded by air when compared to a spliced bar tested in a reinforced concrete member. Tests (Siess and Sozen)[29,30] of reinforced concrete beams with and without Cadweld splices were conducted to determine the measured load and/or moment with respect to deflection for these two cases. Very little difference in load- (and moment-) deflection plots for the beams with and without spliced bars could be observed. It was interesting to note (in Reference 30) that the reinforcing bar in the beam with the Cadweld splice ruptured (rupture occurred in bar adjacent to splice) at a midspan deflection of about 14 inches. However, the bar in the unspliced beam did not rupture when loaded to produce the same deflection. Observation of tests on butt-welded, Thermit, and Cadweld splices in this study showed that the ductility of the parent bar was reduced appreciably by any of the three splicing techniques. This helps to explain why the beam with the spliced bar failed and the other did not.

4.2 DYNAMIC STRENGTH CHARACTERISTICS

An extensive series of tests (Sanders)[31] was conducted on No. 18 Grade 75 bars to determine differences in strength of as-rolled bars, bars with deformations removed, machined-bar specimens having diameters of 1/2 and 3/4 inch, and 1/2-inch-diameter specimens machined from different

quadrants of the circular cross section of the bar. In these tests, the average yield strengths for both the 1/2- and 3/4-inch-diameter machined bars were about 3 percent lower than that for the as-rolled bars. In another test series (Cowell),[12] the average yield strength of Grade 75 machined bars was 1 percent greater than that of as-rolled bars and the average yield strength of Grade 60 machined bars was 10 percent greater than that of as-rolled bars.

In order to detect some variation in the strength characteristics over the cross section of the bar types tested, Rockwell Hardness determinations were conducted. Cross sections were saw cut from untested specimens of Grade 60, Grade 75, Grade 75 with an "X" deformation pattern (Test 201), and a butt-welded splice. For each of the four specimens, seven separate Rockwell Hardness evaluations were made across a diameter of the specimen as shown in Table 4.2. The chemical analysis for these same four specimens is presented in Table 2.2. In all cases, the specimens appear to be stronger away from the center of the bar except for one reading for the butt-welded splice, which indicates that the weld at that location was poor. In general, however, based on the Rockwell Hardness numbers, the weld material appears to be as strong as or stronger than the Grade 75 bars tested. The stress-strain curves for the butt-welded splices also support this observation. It is also interesting to note that the average tensile strength approximated from Rockwell Hardness numbers[18] for the Grades 60 and 75 bars (shown in Table 4.2) corresponds closely to the measured tensile strength supplied by the manufacturer (shown in Table 2.1).

Relations of yield strength to strain rate for all the Grades 60

and 75 specimens are plotted in Figures 4.4 and 4.5, respectively.

In order to correlate the information on yield strength with respect to strain rate that can be expected for typical structures, References 32 through 35 were examined. The strain rate that a structure will undergo depends primarily on the shape of the structure, the stiffness, and the shape of the time-dependent load.

A model aboveground structure (Kennedy)[32] was subjected to the blast effects from the detonation of a 500-ton sphere of high explosives (HE). Based on the results of the model test, the prototype strain rates vary from 0.0015 to 0.004 in/in/sec. A 1/4-scale reinforced concrete model (Criswell)[33] of a nine-panel floor system having drop panels, column capitals, and four round columns was tested in the WES Blast Load Generator Facility up to a pressure of 27 psi. Predicted prototype strain rates based on the model results ranged from 0.05 to 0.10 in/in/sec. Deep reinforced concrete slabs (Albritton)[34] were subjected to high overpressures from the detonation of a 100-ton HE charge detonated during the MINE SHAFT Event. Strain rates of approximately 0.6 in/in/sec were recorded. A deep reinforced concrete beam (Balsara)[35] was tested dynamically using the WES 200-kip-capacity ram loader. Strain rates up to 0.2 in/in/sec were recorded.

4.2.1 Grade 60 Bars. For the slow load rate tests reported herein, the yield stresses for the as-rolled and machined Grade 60 bars were about the same. The yield stresses for the as-rolled bars at the intermediate and rapid strain rates appear to be 10 percent lower than the average stresses depicted by the curve shown in Figure 4.4. It was

postulated early in the test series that the recorded values of strain for the spliced bars would be approximately the same as the results from as-rolled bars. Consequently, for economic reasons only a minimum number of as-rolled bars were tested. The results of tests of the three as-rolled bars fell within the scatter band for the data recorded. The yield stress data determined for the spliced bars appeared to be about 5 percent greater than those for machined bars tested at slow rates of strain and about 2 percent greater for those tested at intermediate strain rates. At rapid rates of strain, no differences between the yield stresses for machined bars and spliced bars can be observed.

It is believed that the rapid rates of strain (up to 5 in/in/sec) achieved in this program extend the state-of-the-art in assessing the increase in yield strength with increase in strain rate. The yield stress at a strain rate of 5 in/in/sec is about 75 percent greater than the static yield stress of approximately 70,000 psi.

4.2.2 Grade 75 Bars. Spliced bars were tested at only intermediate rates of strain, whereas machined bars were tested at slow, intermediate, and rapid rates of strain. The yield stresses for the machined bars fell well within the band of data for the spliced bars. It can also be observed that the yield stresses for the Grade 75 bars are not as sensitive to strain rate effects as those for Grade 60 bars. At a strain rate of 4 in/in/sec, the yield strength is about 17 percent greater than the static yield strength.

The chemical and physical properties of the Grade 75 bars discussed in Reference 8 are very similar to those of Grade 75 bars tested in this

study; consequently, it was possible to compare directly the strain rate effects with respect to yield strength for machined test specimens (see Figure 4.6). The results from both these test series compare very favorably, a fact which tends to lend validity to the results of both test programs.

4.3 LOAD ANALYSIS

For all rapid load rate tests, it was necessary to correct the load applied to the test specimens to account for inertial effects. This procedure, however, was not necessary for the intermediate and slow load rate tests. For many of the machined bars tested, the upper and lower necked-down sections were instrumented with strain gages for the purpose of utilizing these sections as load cells. The values of load thus determined were compared with the upper and lower load cell values.

4.3.1 Rapid Load Tests. The analog records, as shown in Appendix A, were digitized at a sampling rate of 96 kc, which means that values of load, strain, and acceleration were recorded approximately every 0.01 msec. The loads applied to the test specimens were corrected according to procedures outlined in Section 2.4 at each time step utilizing the WES central processor. By use of a plot routine, stress-strain graphs were automatically plotted.

Shown in Table 4.3 are uncorrected and corrected values for a particular instant in time. The table is set up to correspond to Equation 2.4 of Section 2.4. In some instances, the corrected values for the upper load (P_{uc}) and the lower load ($P_{\ell c}$) do not compare favorably for the instant in time selected; this can be partially explained by

examining the analog records in Appendix A. For example, a study of Figure A.6 shows that the lower acceleration record extends from a finite value to a maximum value over a time interval so short that no real difference can be detected in the value for the lower load (P_ℓ). Such differences show up as variations in the stress-strain curves shown in Chapter 3.

4.3.2 Machined Specimens. The upper and lower machined-down sections for the tests whose results are shown in Table 4.4 were evaluated to determine the applied load. The average strain was determined and multiplied by the modulus of elasticity to determine the average stress from which load was determined. Also tabulated are the upper and lower load cell readings. However, for rapid load tests, these readings were adjusted to account for inertial effects. For the intermediate and slow load rate tests, the values of upper and lower load determined from strain readings on the bar compare very favorably with the load cell readings. For all the rapid load tests except Test 155, the differences in the upper and lower load values determined from load cells were about the same as the differences in the upper and lower load values determined from the strain gage readings on the upper and lower necked-down sections.

TABLE 4.1 COMPARATIVE EFFECTIVENESS OF THE VARIOUS SPLICED BARS

Splice Type	Load Rate	Grade	$1.25\sigma_y$	σ_m	$\frac{\sigma_m}{1.25\sigma_y}$	$1.25\epsilon_y$	ϵ_m	$\frac{\epsilon_m}{1.25\epsilon_y}$	A_1[a]	A_2[a]	$\frac{A_2}{A_1}$
			kips/in^2			1,000 μin/in					
Butt weld	Rapid	60	75	114	1.52	2.5	63	25.2	0.04	2.583	64.58
	Intermediate	60	75	103	1.37	2.5	72	28.8	0.04	2.677	66.93
	Slow	60	75	96	1.28	2.5	58	23.2	0.04	2.000	50.00
	Intermediate	75	94	126	1.34	11	48	4.36	0.283	2.020	7.14
Thermit	Rapid	60	75	123	1.64	2.5	56	22.4	0.04	2.380	59.50
	Intermediate	60	75	105	1.40	2.5	55	22.0	0.04	2.003	50.08
	Slow	60	75	96	1.28	2.5	44	17.6	0.04	1.393	34.83
	Intermediate	75	94	115	1.22	5	13	2.6	0.103	0.443	4.30
Cadweld	Rapid	60	75	106	1.42	2.5	23	9.2	0.04	0.893	22.33
	Intermediate	60	75	99	1.32	2.5	37	14.8	0.04	1.253	31.33
	Slow	60	75	100	1.33	2.5	58	23.2	0.04	2.033	50.83
	Intermediate	75	94	124	1.32	11	32	2.9	0.287	1.243	4.33

[a] Areas were determined with a planimeter, and no particular dimension was determined.

TABLE 4.2 APPROXIMATE RELATION OF ROCKWELL HARDNESS NUMBERS TO TENSILE STRENGTH

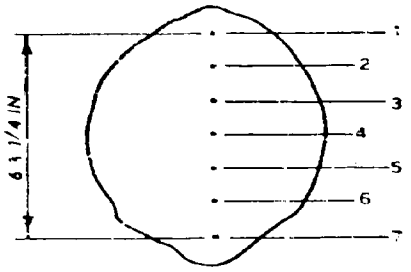

Point[a]	Grade 60		Grade 75		Grade 75 (Test 201)		Butt-Welded Splice	
	Rockwell No. (B) Scale	Tensile Strength	Rockwell No. (B) Scale	Tensile Strength	Rockwell No. (B) Scale	Tensile Strength	Rockwell No. (B) Scale	Tensile Strength
		kips/in^2		kips/in^2		kips/in^2		kips/in^2
1	92	92	102	124	103	127	105	134
2	89	88	100	116	103	127	106	138
3	90	89	100	116	100	116	103	127
4	85	82	99	114	99	114	100	116
5	92	92	99	114	102	124	103	1[illegible]
6	94	97	100	116	100	116	104	130
7	90	89	101	120	102	124	66	56
	Average	90		117		121		118

[a] See drawing above for location.

TABLE 4.3 LOADS CORRECTED FOR INERTIAL EFFECTS ON MACHINED-BAR SPECIMENS

Test No.	Grade	Upper Load					Lower Load				
		(P_u) or k_1x_1	M_1	(a_u) or $\ddot{x}_1$	$M_1\ddot{x}_1$	(P_{uc}) or $k_1x_1 + M_1\ddot{x}_1$	(P_ℓ) or $k_3(x_3 - x_2)$	M_2	(a_ℓ) or $\ddot{x}_2$	$M_2\ddot{x}_2$	$(P_{\ell c})$ or $k_3(x_3 - x_2) - M_2\ddot{x}_2$
		kips	lb/g	g	kips	kips	kips	lb/g	g	kips	kips
145	60	52.2	12.6	275	3.5	55.7	57.9	12.6	872	11.0	46.9
148	60	45.2	12.6	27	0.3	45.5	54.9	12.6	651	8.2	46.7
152	60	51.3	12.6	8	0.1	51.4	61.0	12.6	708	8.9	52.1
155	75	47.0	12.6	0	0	47.0	62.0	12.6	520	6.6	55.4
170	75	43.0	12.6	--	--	43.0	60.0	12.6	520	6.6	53.4

TABLE 4.4 UPPER AND LOWER LOADS DETERMINED FROM STRAIN GAGE READINGS ON MACHINED-BAR SPECIMENS

Test No.	Grade	Loading Rate	Strain Gages						Load Cell[a]	
			Upper Load			Lower Load			Upper P_u	Lower P_l
			$\frac{\epsilon_1 + \epsilon_2}{2} = \epsilon_a$	$\epsilon_a E = \sigma$	$\sigma A = P_u$	$\frac{\epsilon_7 + \epsilon_8}{2} = \epsilon_a$	$\epsilon_a E = \sigma$	$\sigma A = P_l$		
			1,000 μin/in	kips/in^2	kips	1,000 μin/in	kips/in^2	kips	kips	kips
145	60	Rapid	1.54	46.2	45.9	1.29	38.7	38.4	55.7	46.9
148	60	Rapid	1.27	38.1	38.1	1.37	41.1	41.3	45.5	46.7
152	60	Rapid	1.30	39.0	39.0	1.43	42.9	42.9	51.4	52.1
161	60	Intermediate	1.18	35.4	36.7	1.10	33.0	34.2	36.2	35.5
164	60	Intermediate	1.13	33.9	33.7	1.20	36.0	35.8	34.0	34.0
1[illegible]	60	Intermediate	1.00	30.0	29.5	1.08	32.4	31.9	32.[illegible]	34.0
1[illegible]	60	Slow	1.08	32.4	32.2	1.13	33.9	33.6	32.5	34.0
155	75	Rapid	1.60	48.0	47.7	1.69	50.7	50.4	46.6	62.2
170	75	Rapid	1.90	57.0	55.9	1.50	45.0	44.2	44.0	61.0

[a] For the rapid tests, the corrected load cell readings were used.

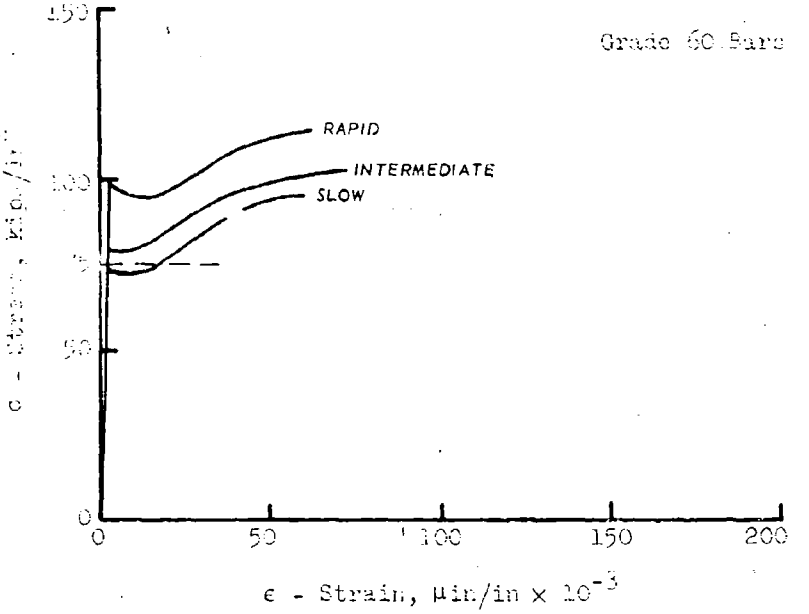

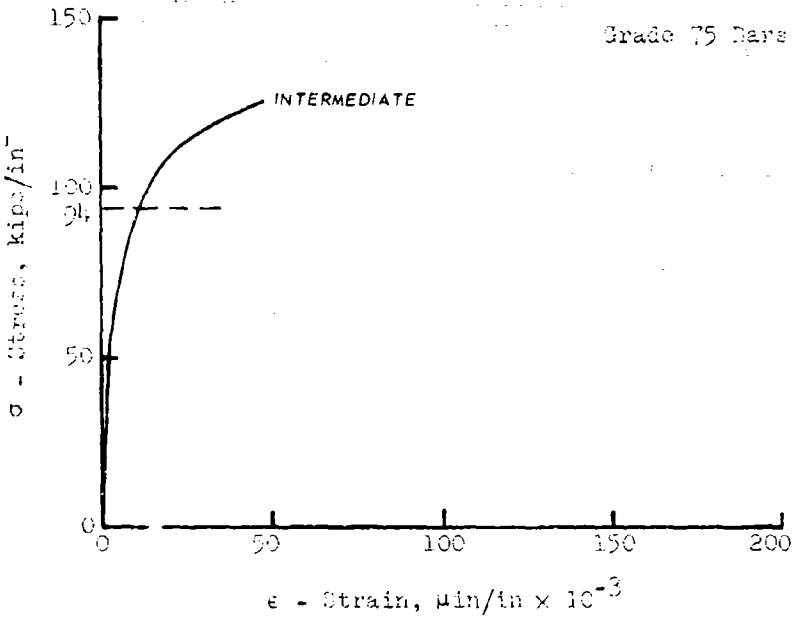

Figure 4.1 Composite stress-strain curves, butt-welded splices.

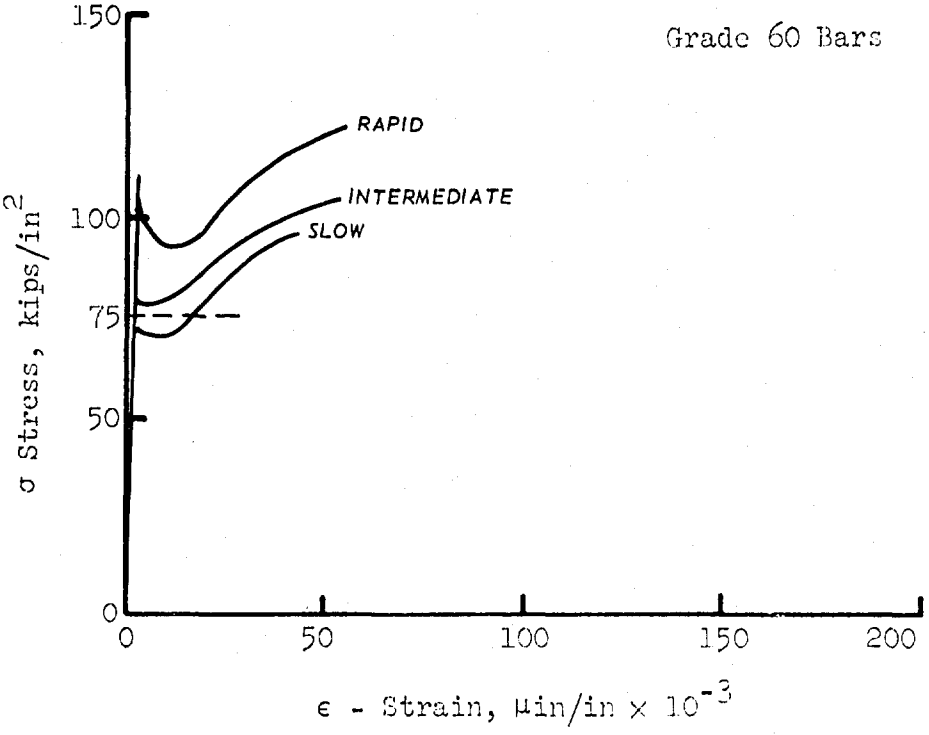

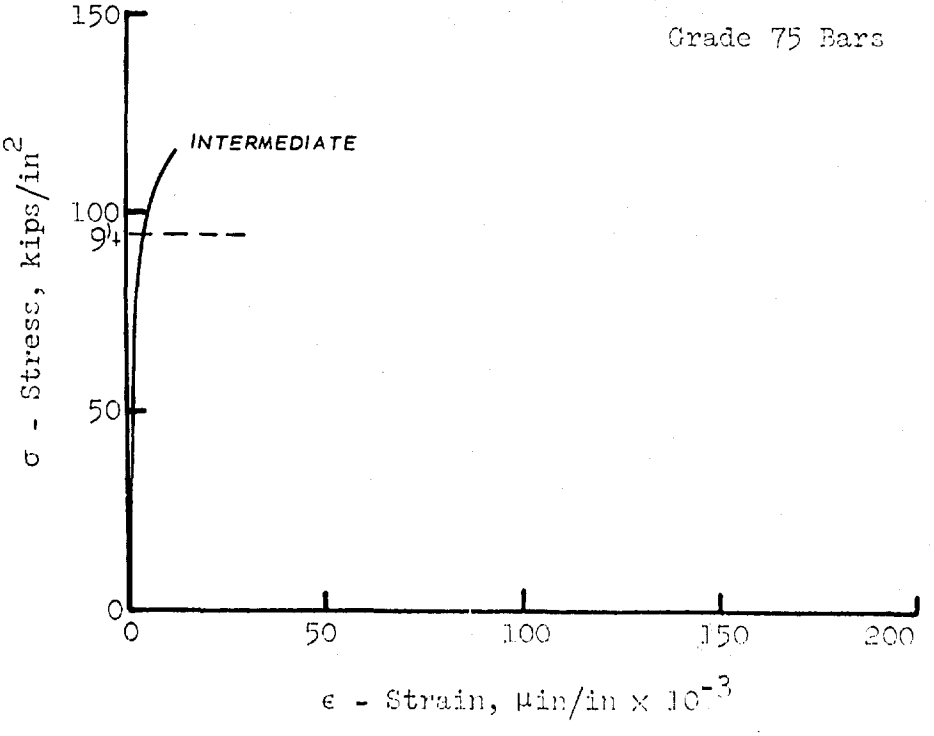

Figure 4.2 Composite stress-strain curves, Thermit splices.

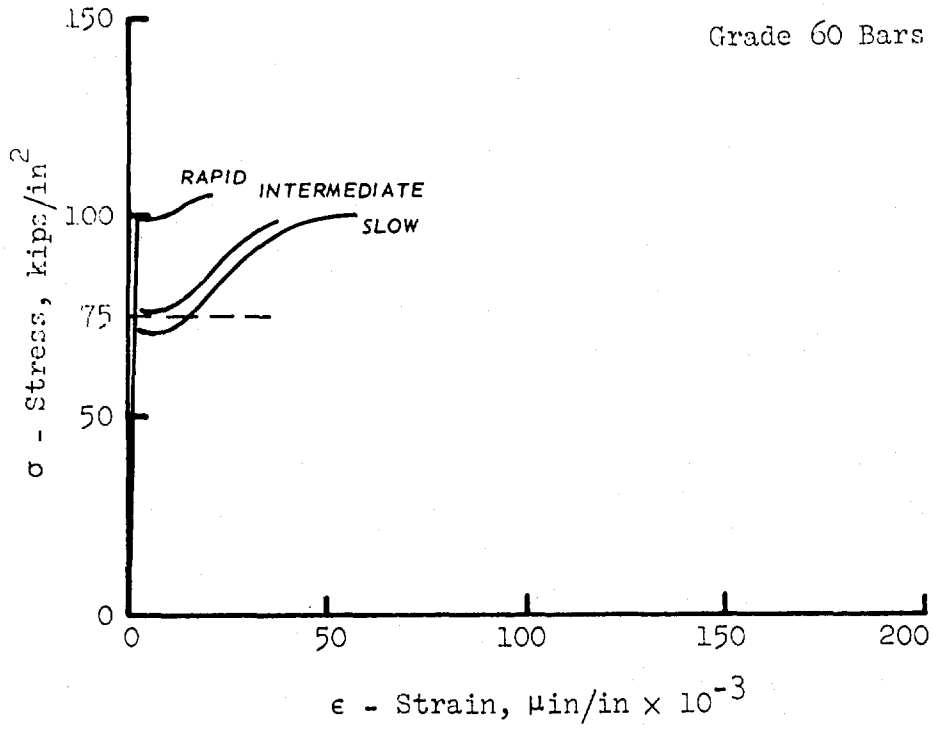

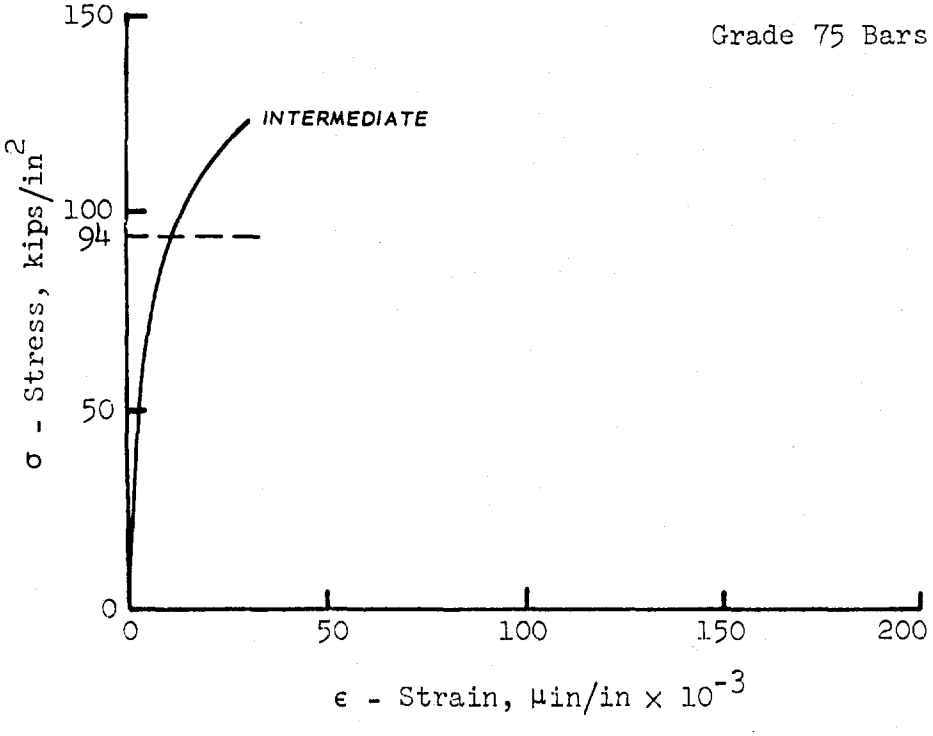

Figure 4.3 Composite stress-strain curves, Cadweld splices.

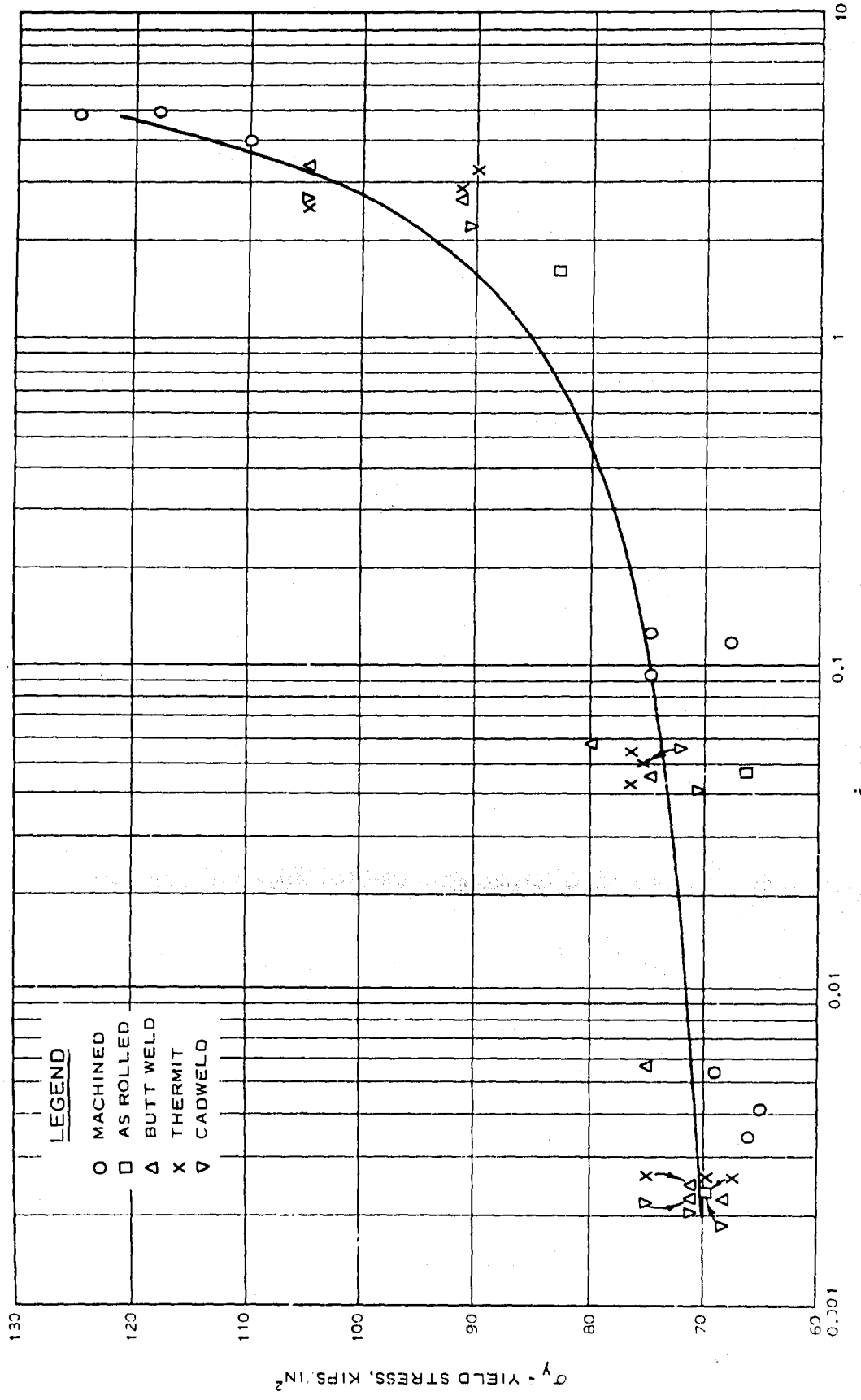

Figure 4.4 Yield stress versus strain rate, Grade 60 bars.

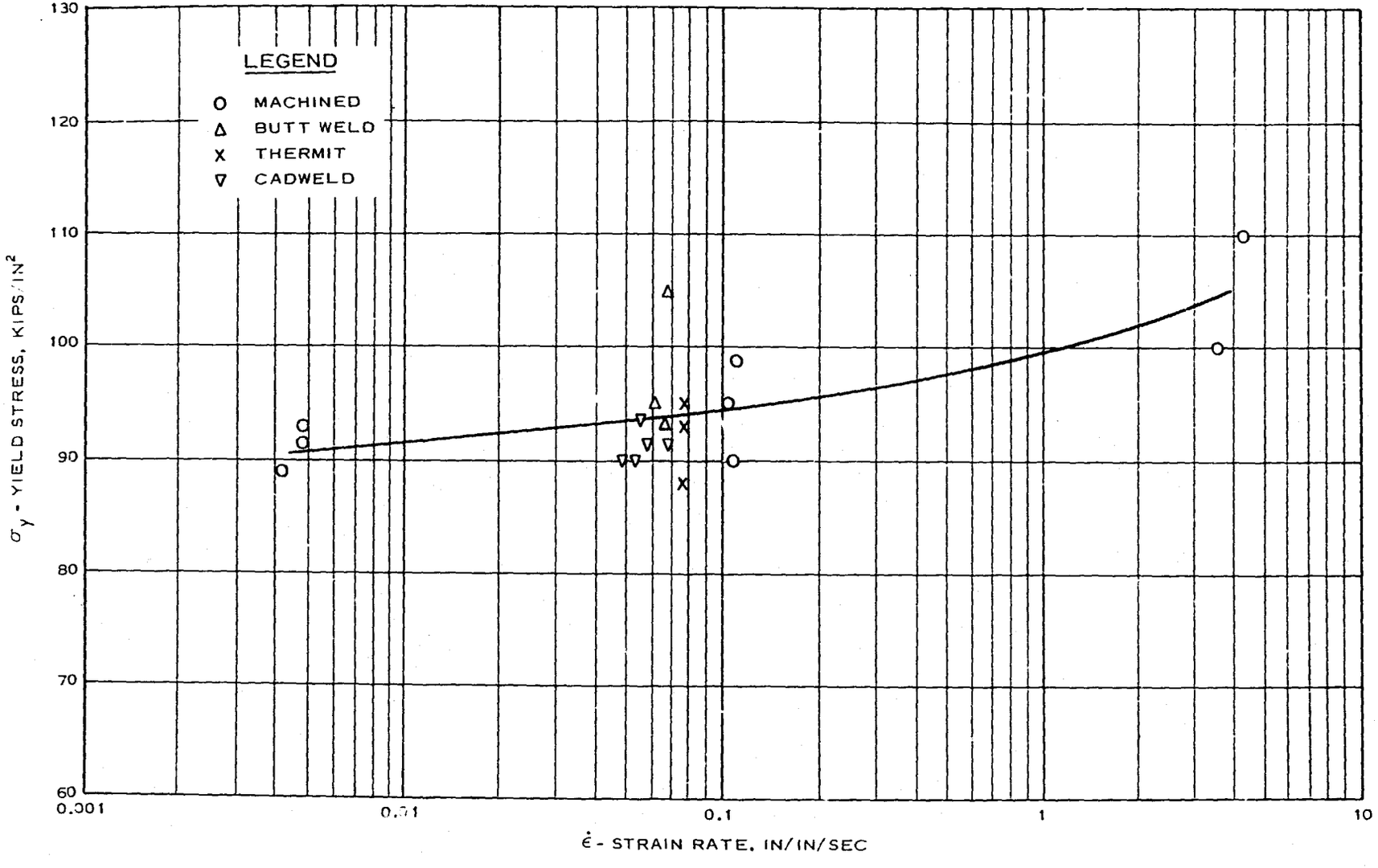

Figure 4.5 Yield stress versus strain rate, Grade 75 bars.

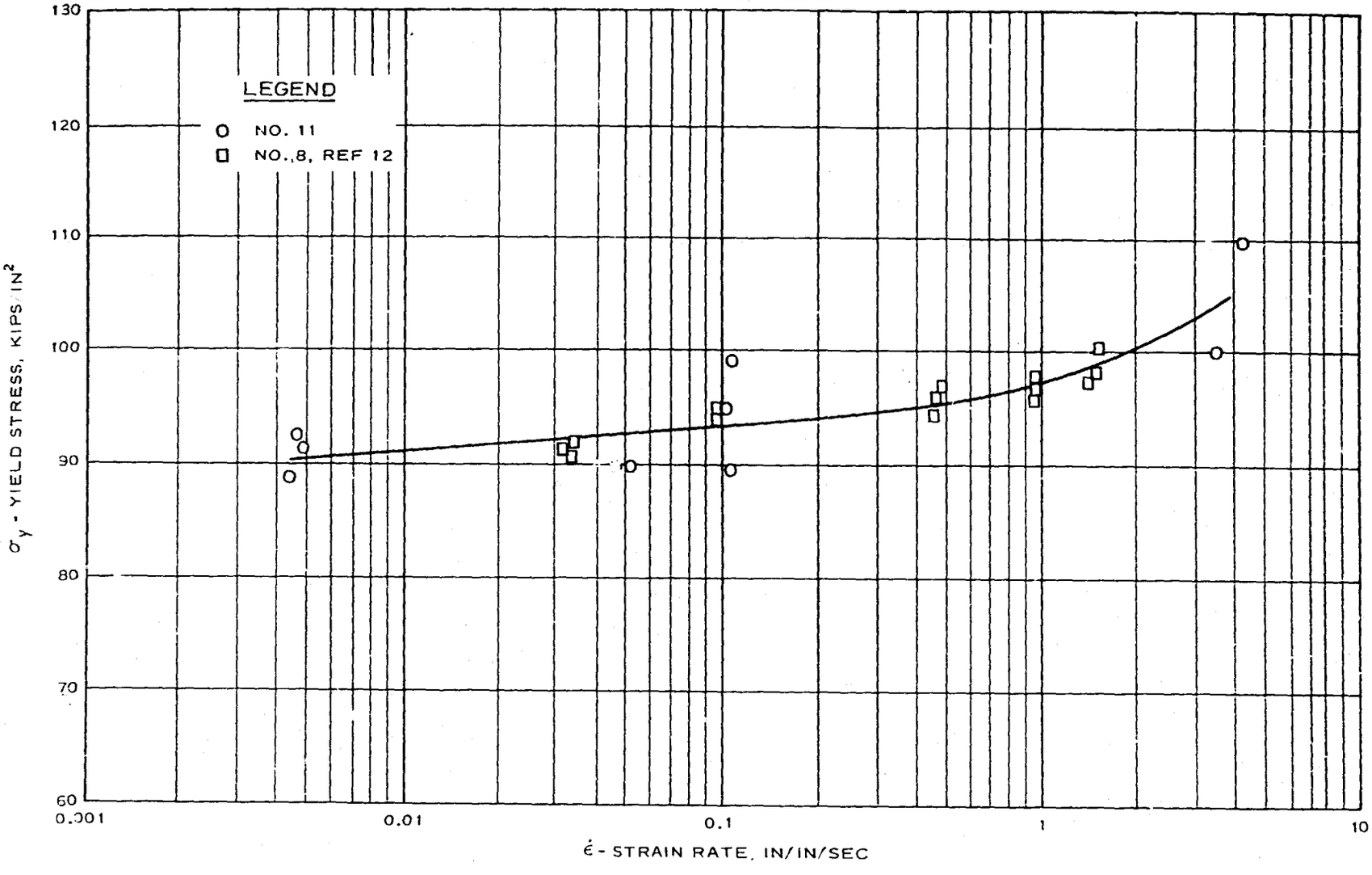

Figure 4.6 Yield stress versus strain rate, machined bars, Grade 75.

CHAPTER 5

SUMMARY OF RESULTS, CONCLUSIONS, AND RECOMMENDATIONS

5.1 SUMMARY OF RESULTS

The results of the study reported herein are summarized as follows:

1. The yield strength of the Grade 60 bars increased appreciably as the loading rate or strain rate application was increased. The yield strength of the Grade 75 bars did not increase so appreciably.

2. At strain rates of 4 to 5 in/in/sec, the dynamic yield strength for the Grade 60 bars was approximately 75 percent greater than the static yield strength, indicating an appreciably greater load-carrying capacity of the bars under dynamic load.

3. The Grade 60 bars, which might be termed more ductile than the Grade 75 bars, were more sensitive to strain rate increases.

4. The Grade 75 bars at high rates of strain, e.g., 4 to 5 in/in/sec, showed an approximate 17 percent increase in dynamic yield strength over static yield strength.

5. For high rates of strain, i.e., 3 in/in/sec and greater, inertial effects induced by the loading device were significant and need to be accounted for in determining the true load applied to a specimen in order to determine the stress. However, for practical rates of strain associated with most strategic structures, such inertial effects were insignificant when determining the true load applied to the tensile test specimen.

5.2 CONCLUSIONS

Based on the results of this study, the following conclusions are believed warranted:

1. All of the spliced bar types, i.e. butt-welded, Cadweld, and Thermit splices, will function satisfactorily under static and dynamic loading conditions for both Grades 60 and 75 billet steel bars conforming to ASTM specifications for A615 steel.

2. The load-carrying capacity of all the spliced bars will increase as the rate of loading increases just as do the load-carrying capacities of the as-rolled and machined bars.

3. For all three types of splice, the maximum strain achieved is only about one-fourth as great as the strain that develops in the as-rolled and machined bars.

4. The optical tracker used in this study appears to be a very workable and useful tool for assessing the postyield strain for spliced bars that have been tested to rupture.

5.3 RECOMMENDATIONS

Also based on the results of this study, the following recommendations are made:

1. Either the Cadweld or Thermit splice should be used in the field in lieu of the butt-welded splice because it is believed that the quality control for these two techniques is much better than that for the butt-welded technique. The variation in the results of the hardness test for the butt-welded splice tends to indicate an inconsistency in strength for butt-welded splices.

2. All torch cutting and tack welding on deformed bars in the field should be avoided if at all possible. These techniques produce heat that affects the ductility of the bars.

3. The strength characteristics of the Grade 60, and especially the Grade 75, bars should be assessed under controlled environmental conditions, i.e., such bars should be tested at elevated and subzero temperatures to determine how variations in temperature affect their strength. It is believed that severe temperatures could cause serious problems for the Grade 75 bars, which are more brittle in nature than the Grade 60 bars.

4. ASTM standards should be revised to include a minimum width for deformations on reinforcing bars to insure that adequate deformation shearing area per inch is provided.

BIBLIOGRAPHY

1. Headquarters, Department of the Army, Design of Structures to Resist the Effects of Atomic Weapons; Strength of Materials and Structural Elements. U. S. Army Technical Manual TM 5-856-2 (EM 1110-345-414), August 1965, Washington, D. C.

2. Sauer, F. M., Clark, G. B., and Anderson, D. C., Nuclear Geoplosics; Part IV, Empirical Analysis of Ground Motion and Cratering. Defense Atomic Support Agency, DASA-1285(IV), May 1964, Washington, D. C.

3. Newmark, N. M., and Haltiwanger, J. D., Air Force Design Manual; Principles and Practices for Design of Hardened Structures. Air Force Special Weapons Center, Technical Documentary Report No. AFSWC-TDR-62-138, December 1962, Kirtland Air Force Base, N. Mex.

4. Anderson, F. E., Jr., et al., Design of Structures to Resist Nuclear Weapons Effects. American Society of Civil Engineers Manuals of Engineering Practice No. 42, 1962, New York, N. Y.

5. U. S. Atomic Energy Commission, Design Manual for AEC Test Structures; Volume II, Structural Response Characteristics Under Dynamic Loads. Contract AT(29-2)-20 with Holmes and Narver, Inc., December 1961, Albuquerque, N. Mex.

6. American Concrete Institute, ACI Standard Building Code Requirements for Reinforced Concrete. ACI Committee 318, ACI 318-63, June 1963, Detroit, Mich.

7. American Welding Society, Recommended Practices for Welding Reinforcing Steel, Metal Inserts and Connections in Reinforced Concrete Construction. Committee on Welding Reinforcing Steel, AWS D12.1-61, 1961, New York, N. Y.

8. Concrete Reinforcing Steel Institute, Reinforcing Bar Splices. Engineering Practice Committee, Subcommittee on Splicing of Re-Bars, 1968, Chicago, Ill.

9. Concrete Reinforcing Steel Institute, Reinforced Concrete - Manual of Standard Practice. Nineteenth Edition, 1968, Chicago, Ill.

10. Keenan, W. A., and Feldman, A., Behavior and Design of Deep Structural Members; Part 6, The Yield Strength of Intermediate Grade Reinforcing Bars Under Rapid Loading. Air Force Special Weapons Center, AFSWC-TR-59-72, March 1960, Kirtland Air Force Base, N. Mex.

11. Siess, C. P., Behavior of High Strength Deformed Reinforcing Bars

Under Rapid Loading. University of Illinois, February 1962, Urbana, Ill.

12. Cowell, W. L., Dynamic Tests of Concrete Reinforcing Steels. U. S. Naval Civil Engineering Laboratory, DASA-13.0181, September 1965, Port Hueneme, Calif.

13. Huff, W. L., Test Devices, Blast Load Generator Facility. U. S. Army Engineer Waterways Experiment Station, CE, Miscellaneous Paper N-69-1, April 1969, Vicksburg, Miss.

14. Holt, R. E., Static Tensile Tests of Large Reinforcing Bar Splicing Techniques. Air Force Weapons Laboratory, Air Force System Command, Technical Report AFWL-TR-67-73, November 1967, Kirtland Air Force Base, N. Mex.

15. American Society for Testing and Materials, "Standard Specification for Deformed Billet-Steel Bars for Concrete Reinforcement with 60,000 psi Minimum Yield Strength," Designation: A432-66, 1968 Book of ASTM Standards, Part 4 (1968), Philadelphia, Pa., 598-602.

16. American Society for Testing and Materials, "Standard Specification for High-Strength Preformed Billet-Steel Bars for Concrete Reinforcement with 75,000 psi Minimum Yield Strength," Designation: A431-66, 1968 Book of ASTM Standards, Part 4 (1968), Philadelphia, Pa., 593-597.

17. American Society for Testing and Materials, "Standard Specification for Minimum Requirements for the Deformations of Deformed Steel Bars for Concrete Reinforcement," Designation: A305-65, 1968 Book of ASTM Standards, Part 4 (1968), Philadelphia, Pa., 368-370.

18. American Society for Testing and Materials, "Standard Methods and Definitions for Mechanical Testing of Steel Products," Designation: A370-67, 1968 Book of ASTM Standards, Part 4 (1968), Philadelphia, Pa., 440-493.

19. Manjoine, M. J., "Influence of Rate of Strain and Temperature on Yield Stresses of Mild Steel," Journal of Applied Mechanics, II, No. 4 (December 1944), A211-A218.

20. Jones, P. G., and Moore, H. F., "An Investigation of the Effect of Rate of Strain on the Results of Tension Tests of Metals," American Society for Testing and Materials, Proceedings, 40 (1940). 610.

21. Fry, L. H., "Speed in Tension Testing and Its Influence on Yield Point Values," American Society for Testing and Materials, Proceedings, 40 (1940), 625.

22. Vreeland, T., Jr., Wood, D. S., and Clark, D. S., "A Study of the

Mechanism of the Delayed Yield Phenomenon," American Society for Metals - Metal Progress, Preprint No. 33 (October 1952).

23. Massard, J. M., The Stress-Deformation Characteristics of Some Mild Steels Subjected to Various Rapid Uniaxial Stressing. University of Illinois, Ph. D. Thesis, 1955, Urbana, Ill.

24. Vigness, I., Krafft, J. M., and Smith, R. C., "Effect of Loading History Upon the Yield Strength of a Plain Carbon Steel," Proceedings, Conference on the Properties of Materials at High Rates of Strain, Institution of Mechanical Engineers, London (1957), 138.

25. Taylor, D. B. D., "Non-Uniform Yield in a Mild Steel Under Dynamic Straining," Proceedings, Conference on the Properties of Materials at High Rates of Strain, Institution of Mechanical Engineers, London (1957), 229.

26. Carlson, R. H., and Murtha, J. P., Operation Plumbbob; Comparison Test of Reinforcing Steels. Sandia Corporation, WT-1473, September 1960, Albuquerque, N. Mex.

27. Thermit Self Preheat Reinforcing Bar Welding, Thermex Metallurgical, Corp., Lakehurst, N. J.

28. Cadweld Rebar Splicing, Erico Products, Inc., Rebar Division, 1969, Cleveland, Ohio.

29. Siess, C. P., and Abbasi, A. F., Tests of Reinforced Concrete Beams with Cadweld Reinforcing Bar Splices. Erico Products, Inc., January 1967, Cleveland, Ohio.

30. Sozen, M. A., and Gamble, W. L., Two Tests of Reinforced Concrete Beams to Study the Performance of High Strength Bars with Cadweld Splices Subjected to Reversals of the Yield Load. Erico Products, Inc., September 1967, Cleveland, Ohio.

31. Sanders, W. W., Jr., and Siess, C. P., "Tension Tests of Large-Size Deformed Concrete Reinforcing Bars," American Society for Testing and Materials, Proceedings, 65 (1965), 654-660.

32. Kennedy, T. E., and Garland, J., Dynamic Response of Small Shear Wall Structures, Project LN316, Event Dial Pack (U). U. S. Army Engineer Waterways Experiment Station, CE (report in preparation), Vicksburg, Miss., SECRET.

33. Criswell, M. E., and Huff, W. L., Design and Testing of a Blast-Loaded Reinforced Concrete Slab System. U. S. Army Engineer Waterways Experiment Station, CE (report in preparation), Vicksburg, Miss.

34. Albritton, G. E., Balsara, J. T., and Bayer, D. M., Response of Deep Two-Way-Reinforced and Unreinforced Concrete Slabs to Static and Dynamic Loading; Mine Shaft Series, Mine Under Event; Program 3 - Structural Response, Deep-Slab Tests. U. S. Army Engineer Waterways Experiment Station, CE, Technical Report N-69-2, Report 4, November 1969, Vicksburg, Miss.

35. Balsara, J. T., and Roggenkamp, L. E., Similitude Study of Reinforced Concrete Deep Beams. U. S. Army Engineer Waterways Experiment Station, CE (report in preparation), Vicksburg, Miss.

APPENDIX A

TEST RECORDS

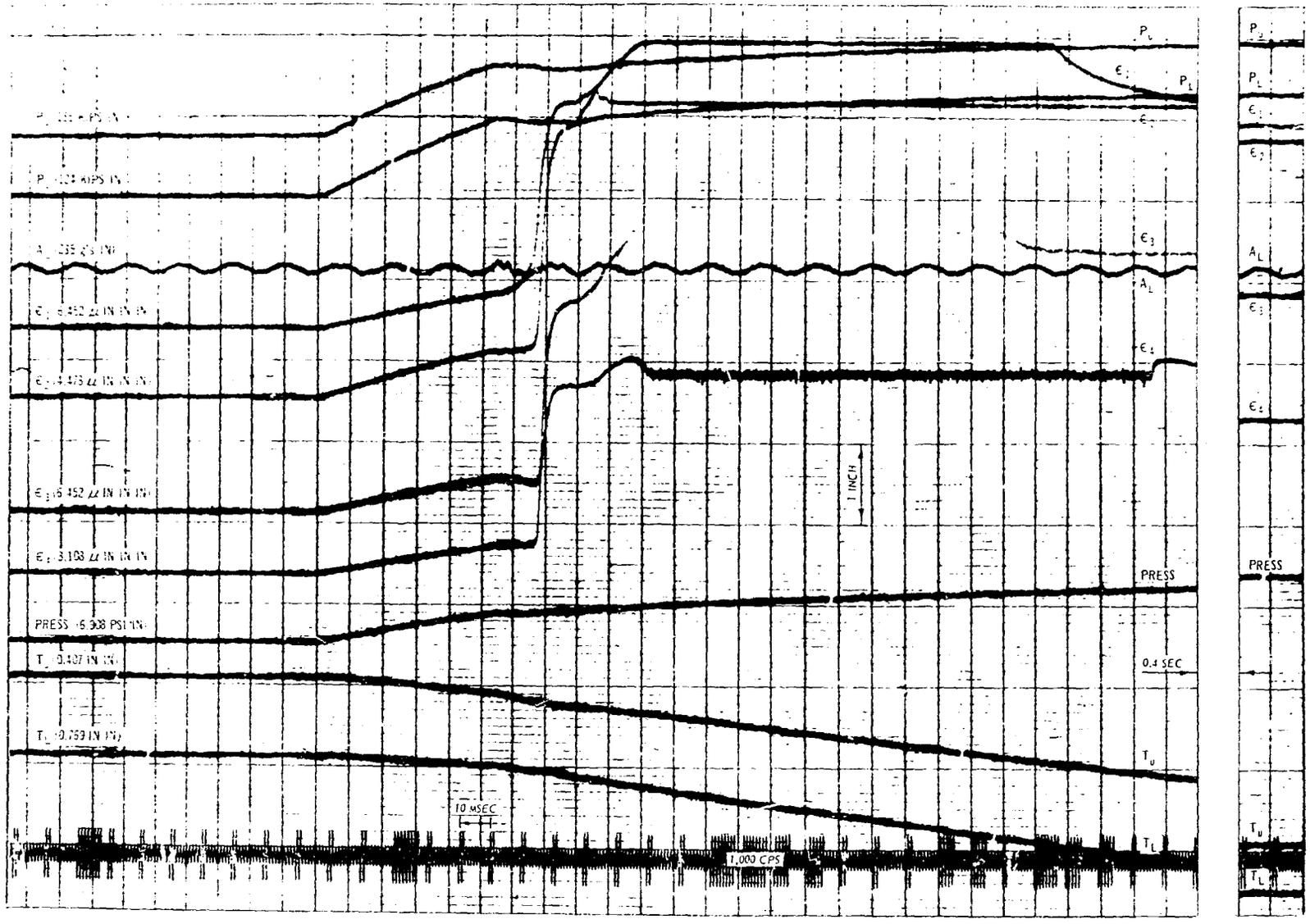

Figure A.1 As-rolled bar, Grade 60, intermediate load rate, Test 172.

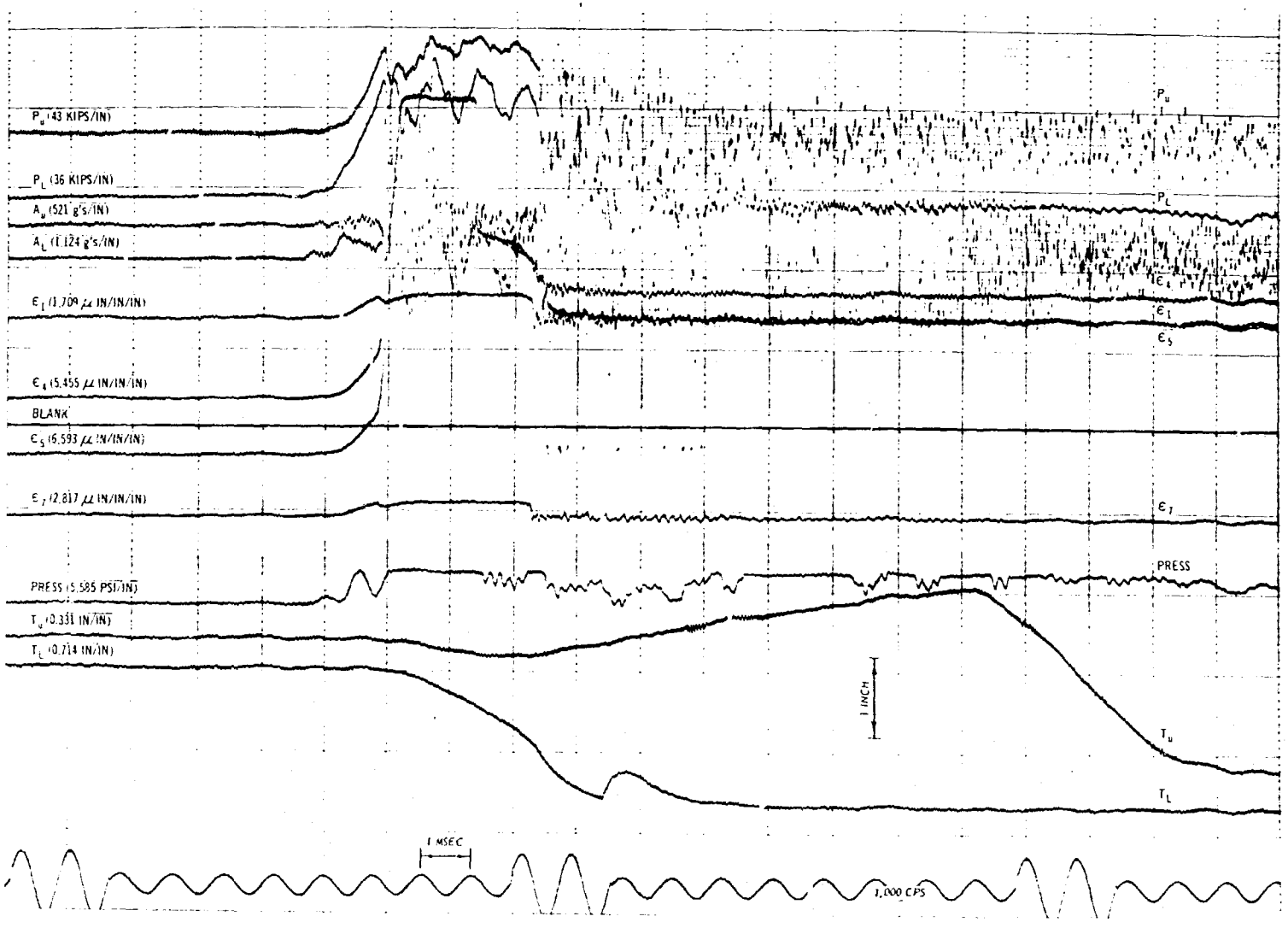

Figure A.2 Machined bar, Grade 60, rapid load rate, Test 148 (Sheet 1 of 2).

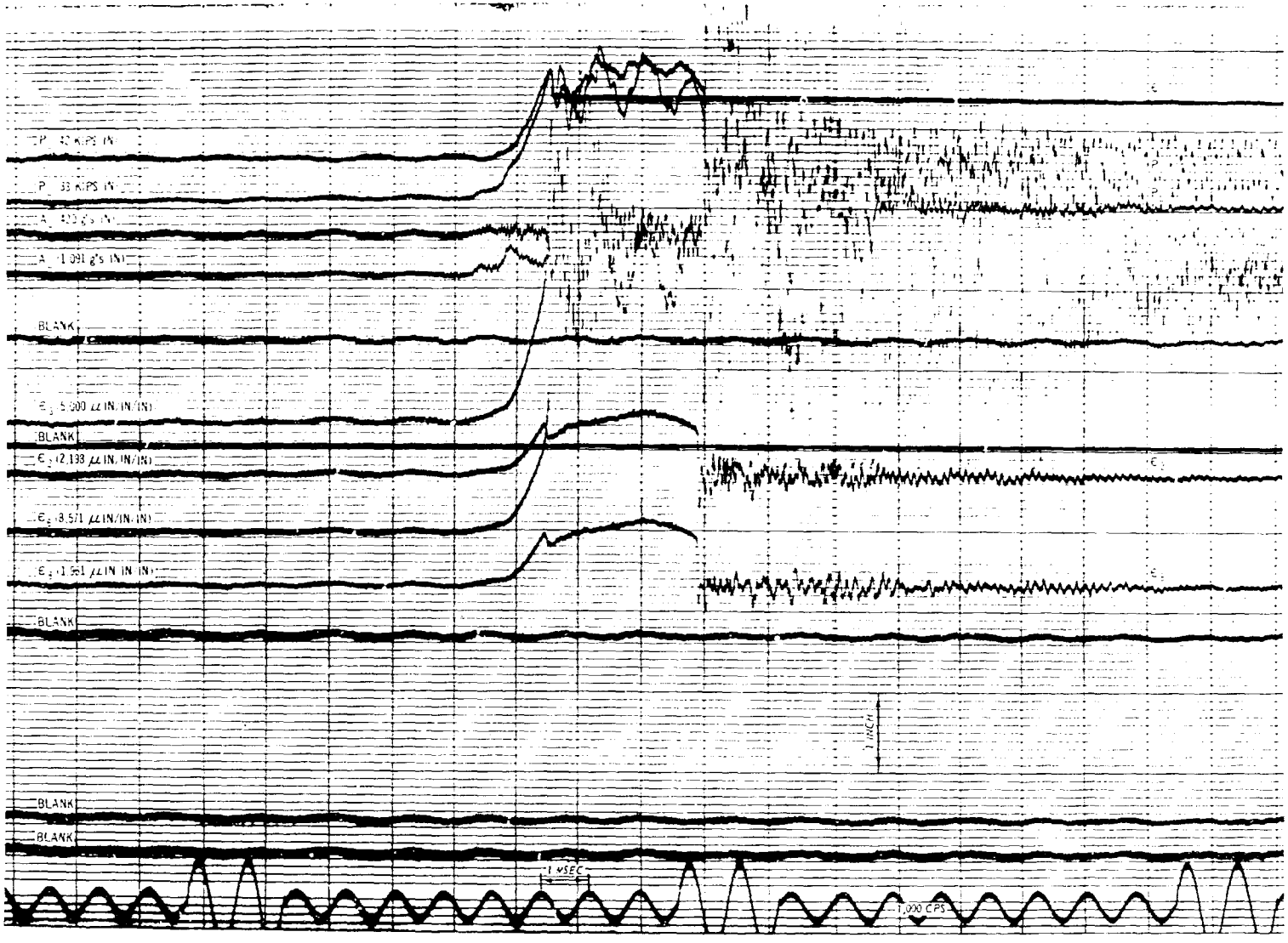

Figure A.2 (Sheet 2 of 2).

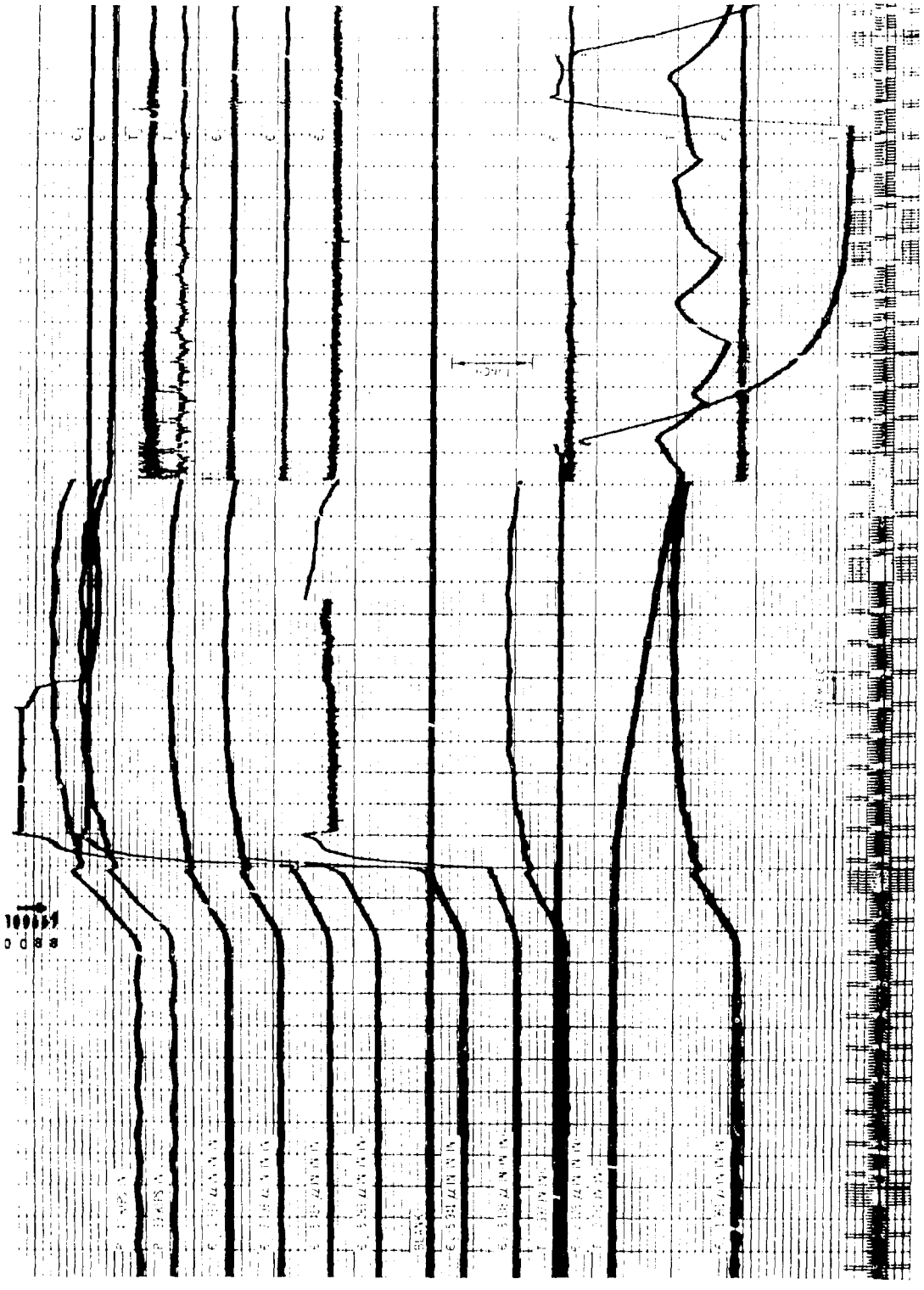

Figure A.3 Machined bar, Grade 60, intermediate load rate, Test 167.

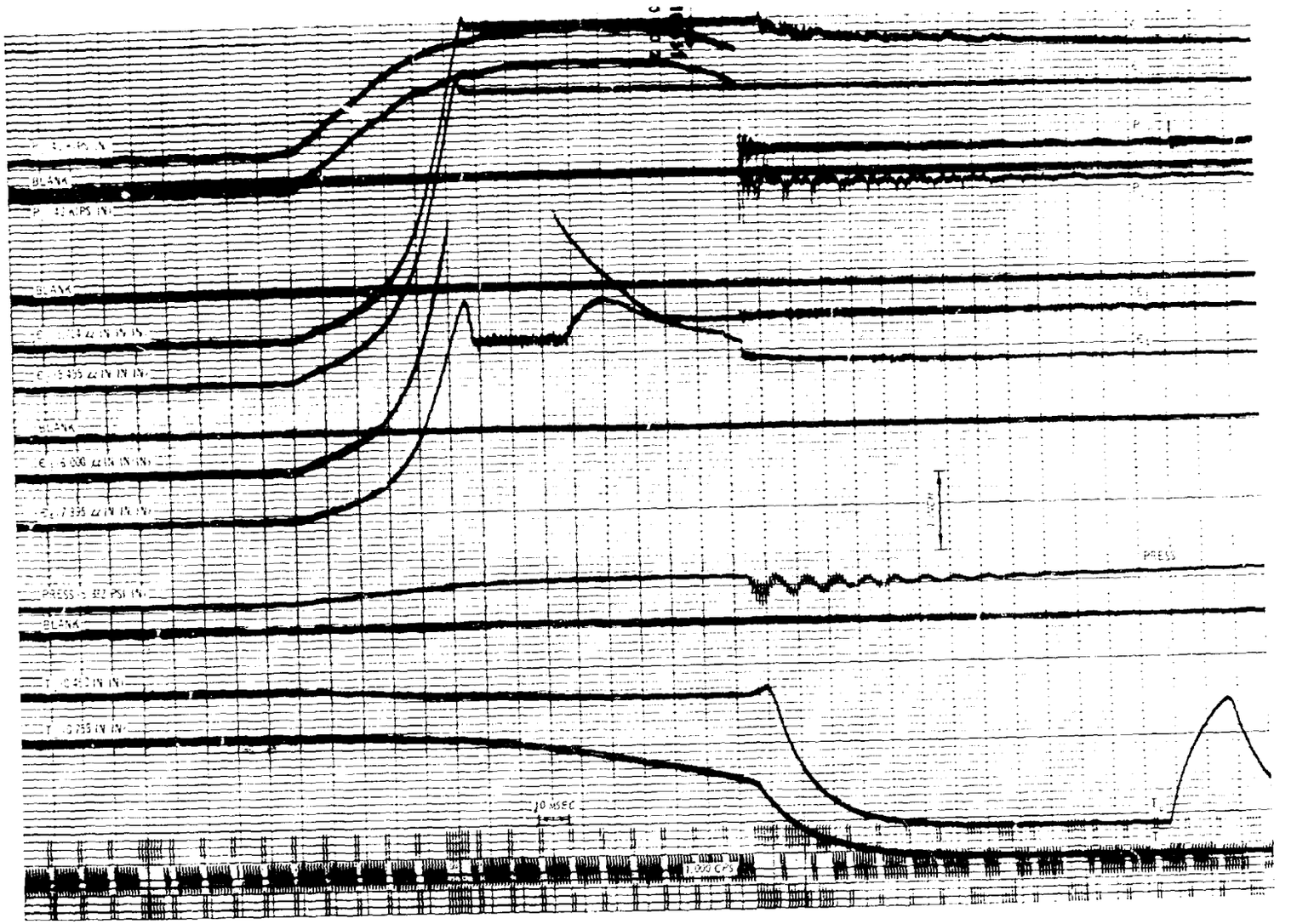

Figure A.4 Machined bar, Grade 75, intermediate load rate, Test 180.

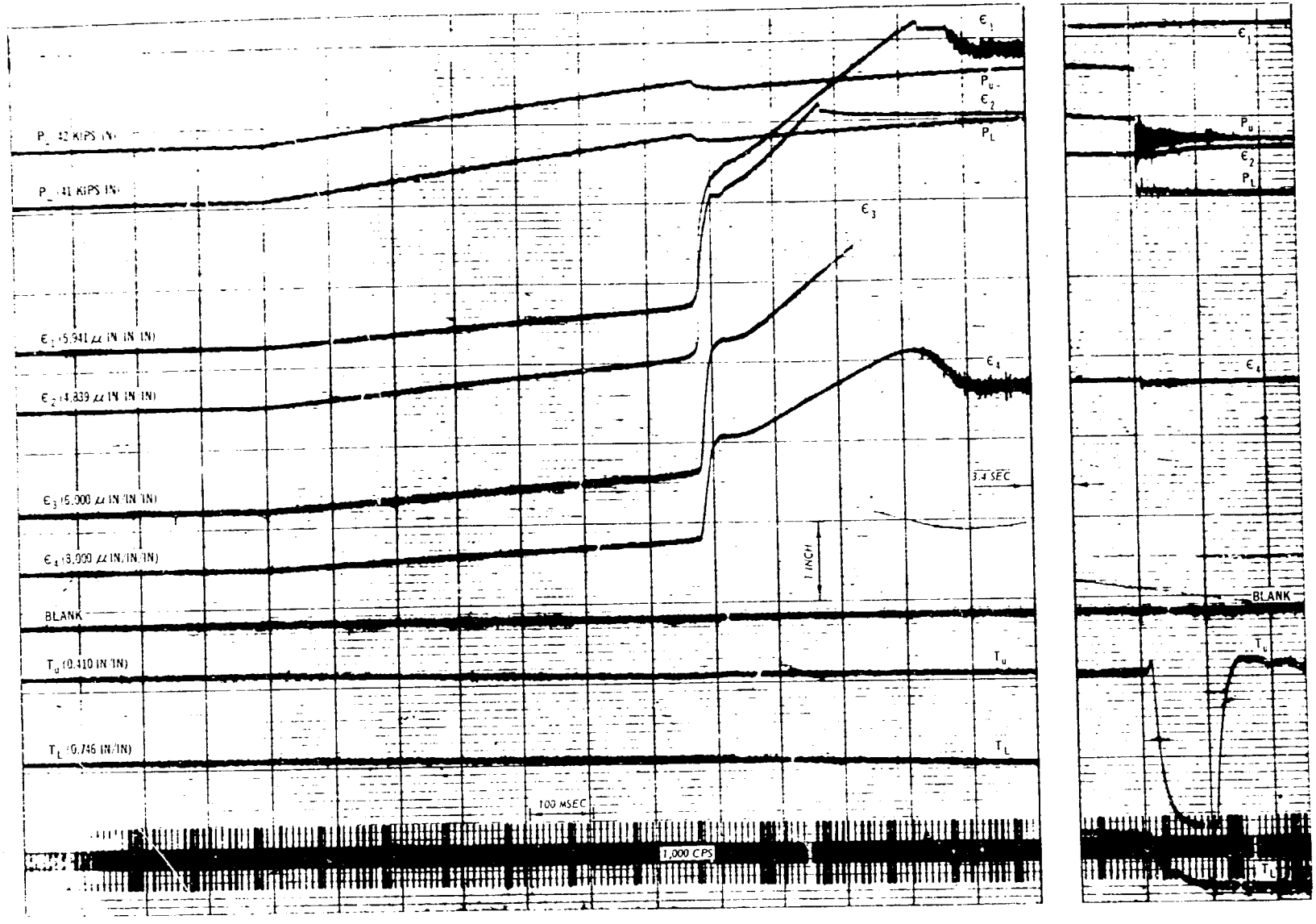

Figure A.5 Machined bar, Grade 60, slow load rate, Test 191.

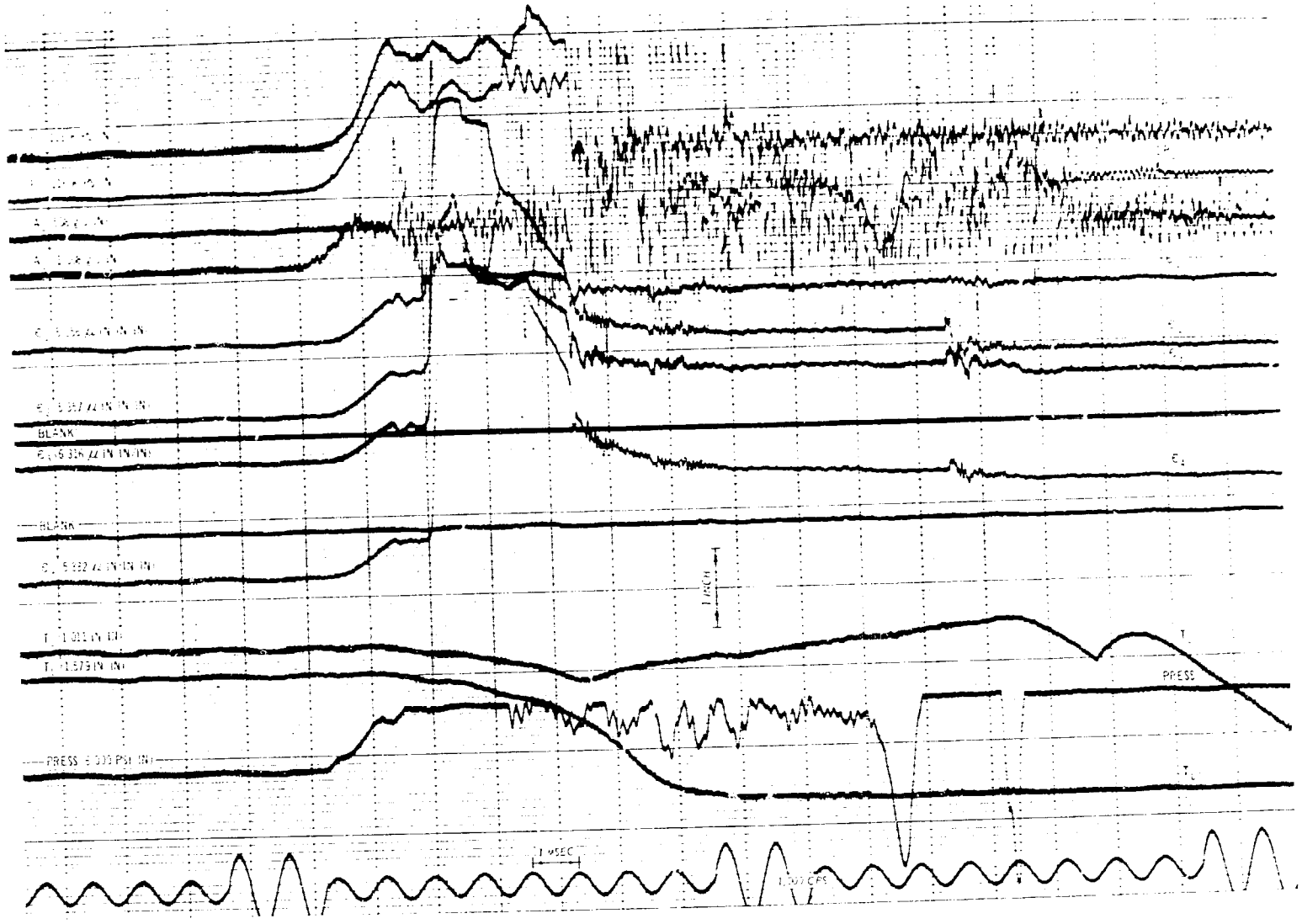

Figure A.6 Butt-welded splice, Grade 60, rapid load rate, Test 159.

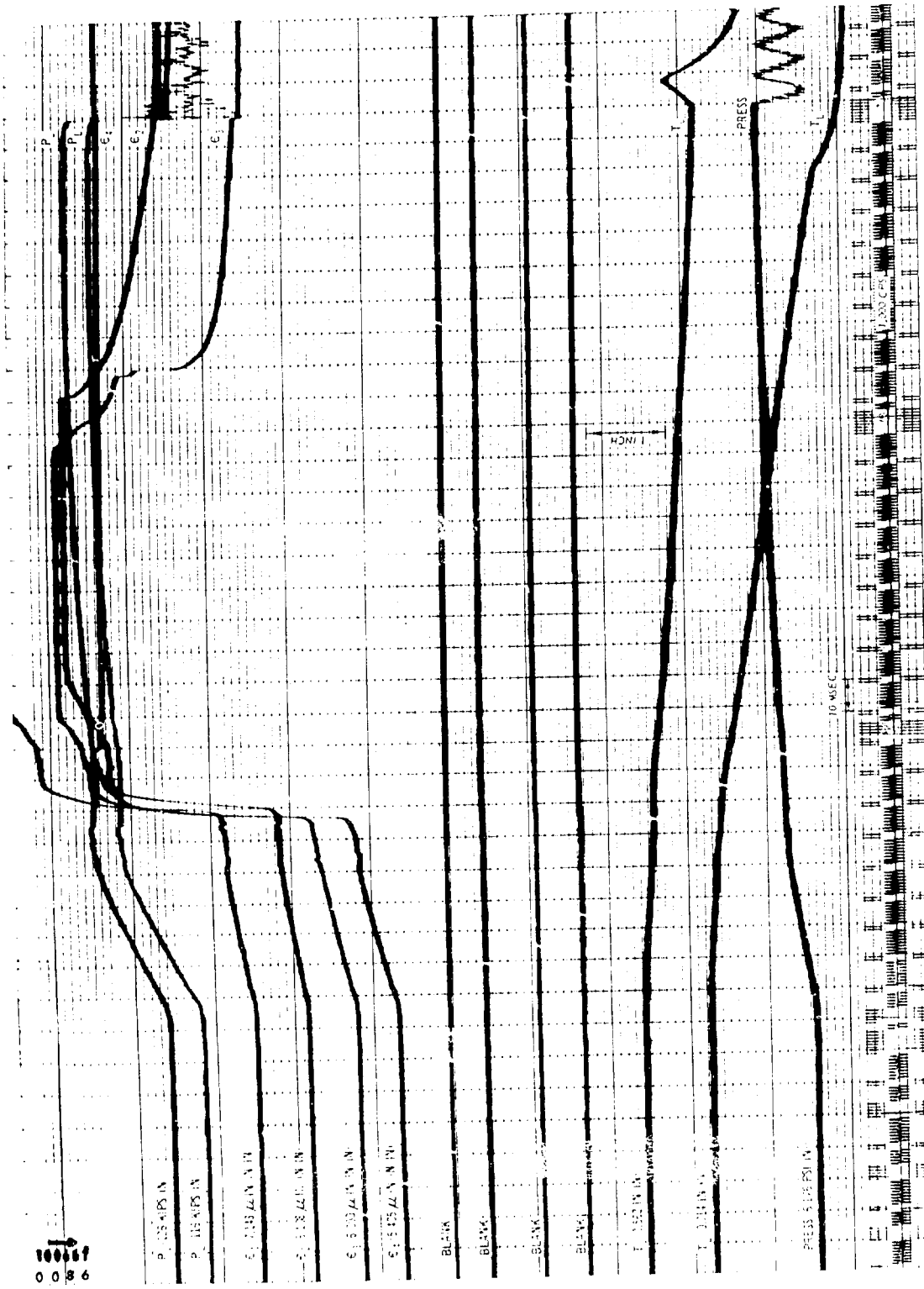

Figure A.7 Butt-welded splice, Grade 60, intermediate load rate, Test 163.

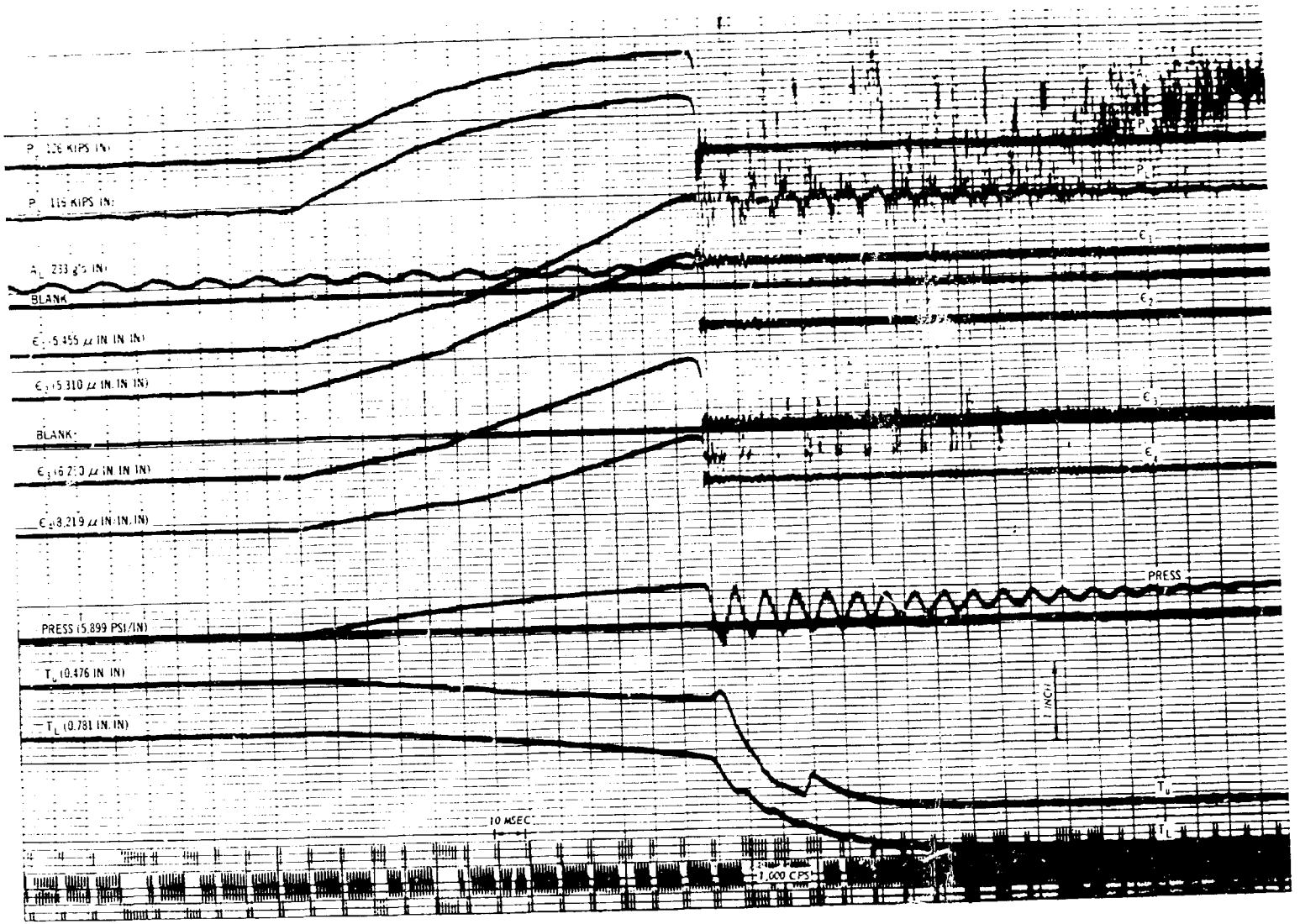

Figure A.8 Butt-welded splice, Grade 75, intermediate load rate, Test 174.

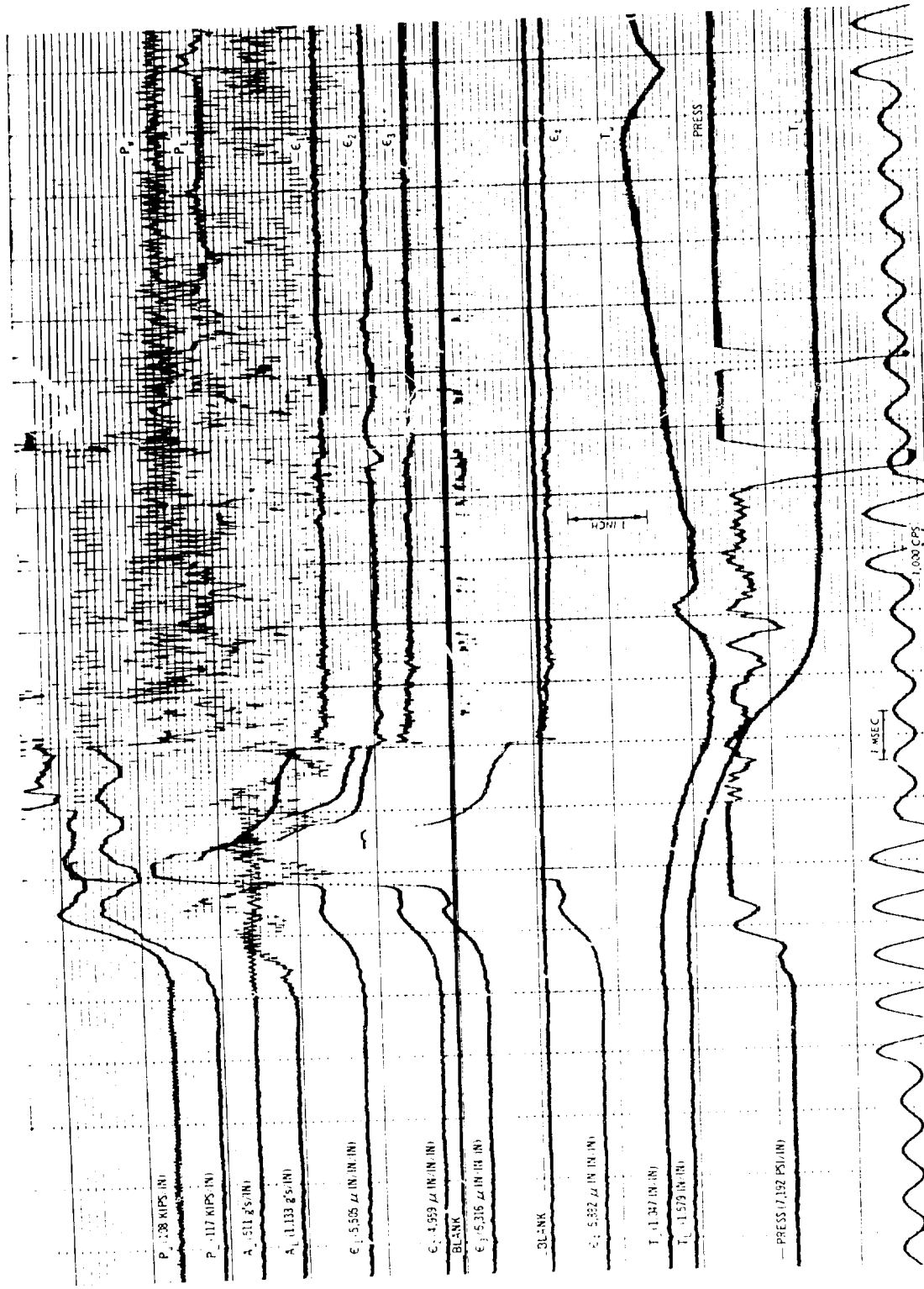

Figure A.9 Thermit splice, Grade 60, rapid load rate, Test 157.

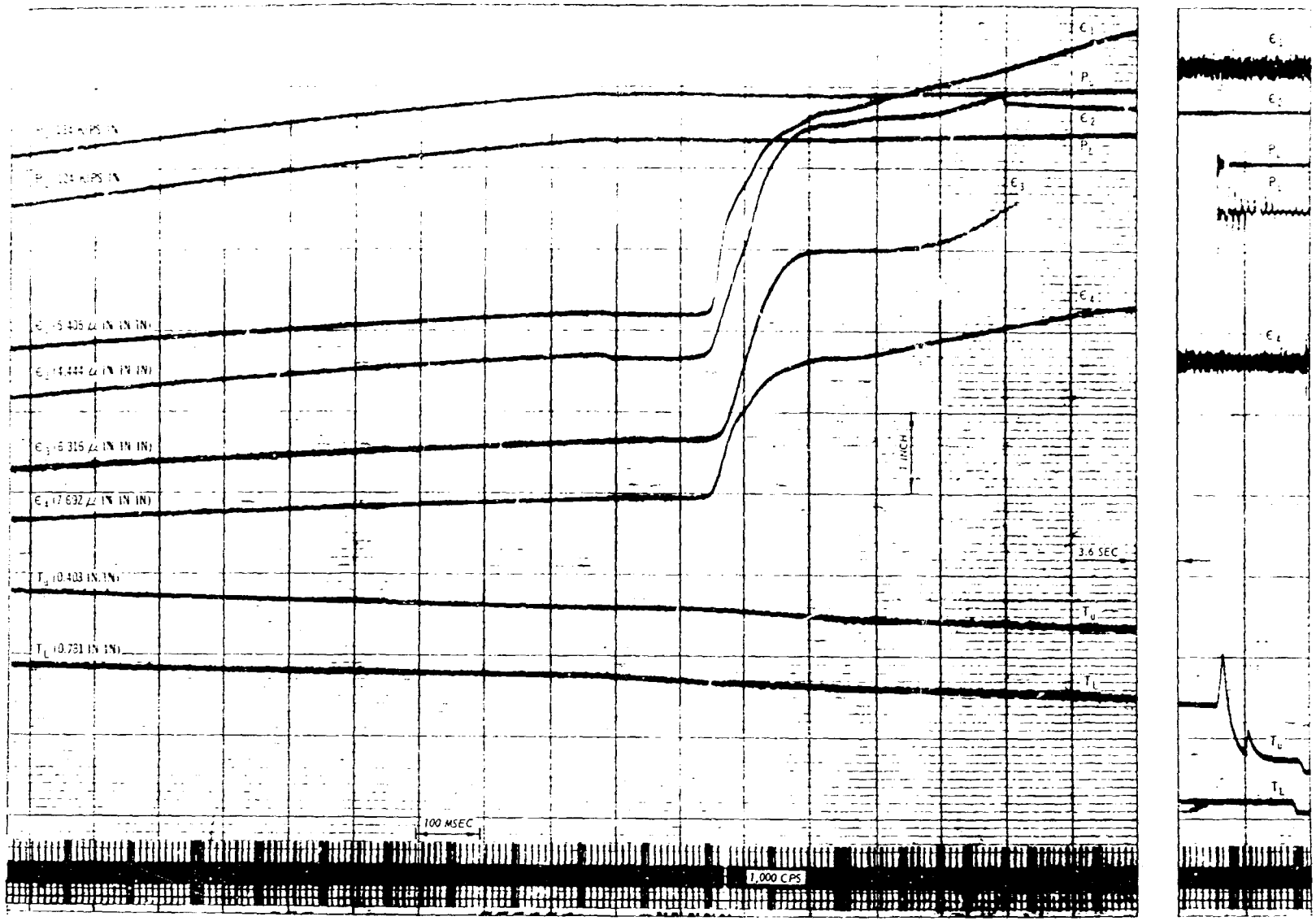

Figure A.10 Thermit splice, Grade 60, slow load rate, Test 198.

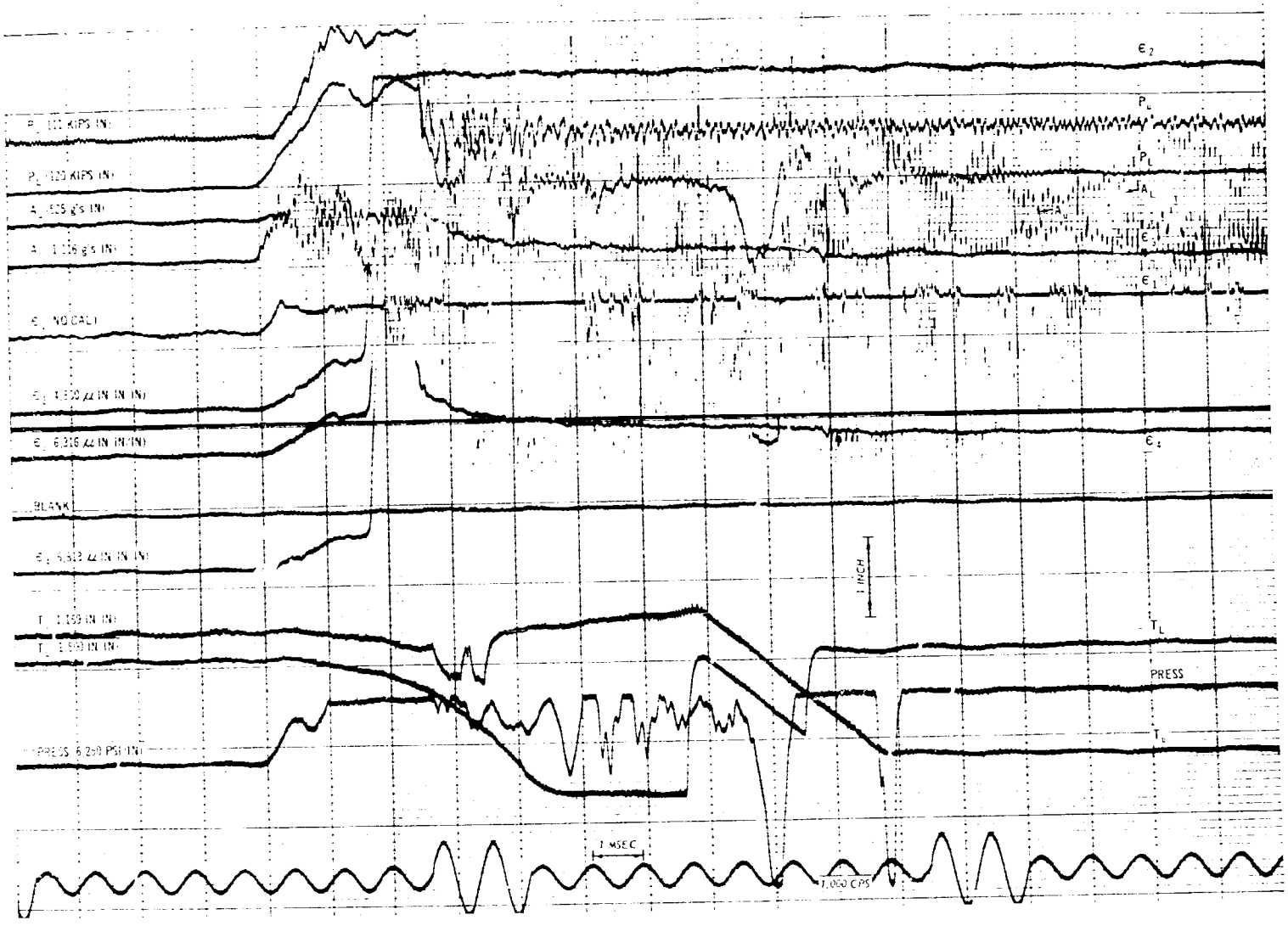

Figure A.11 Cadweld splice, Grade 60, rapid load rate, Test 156.

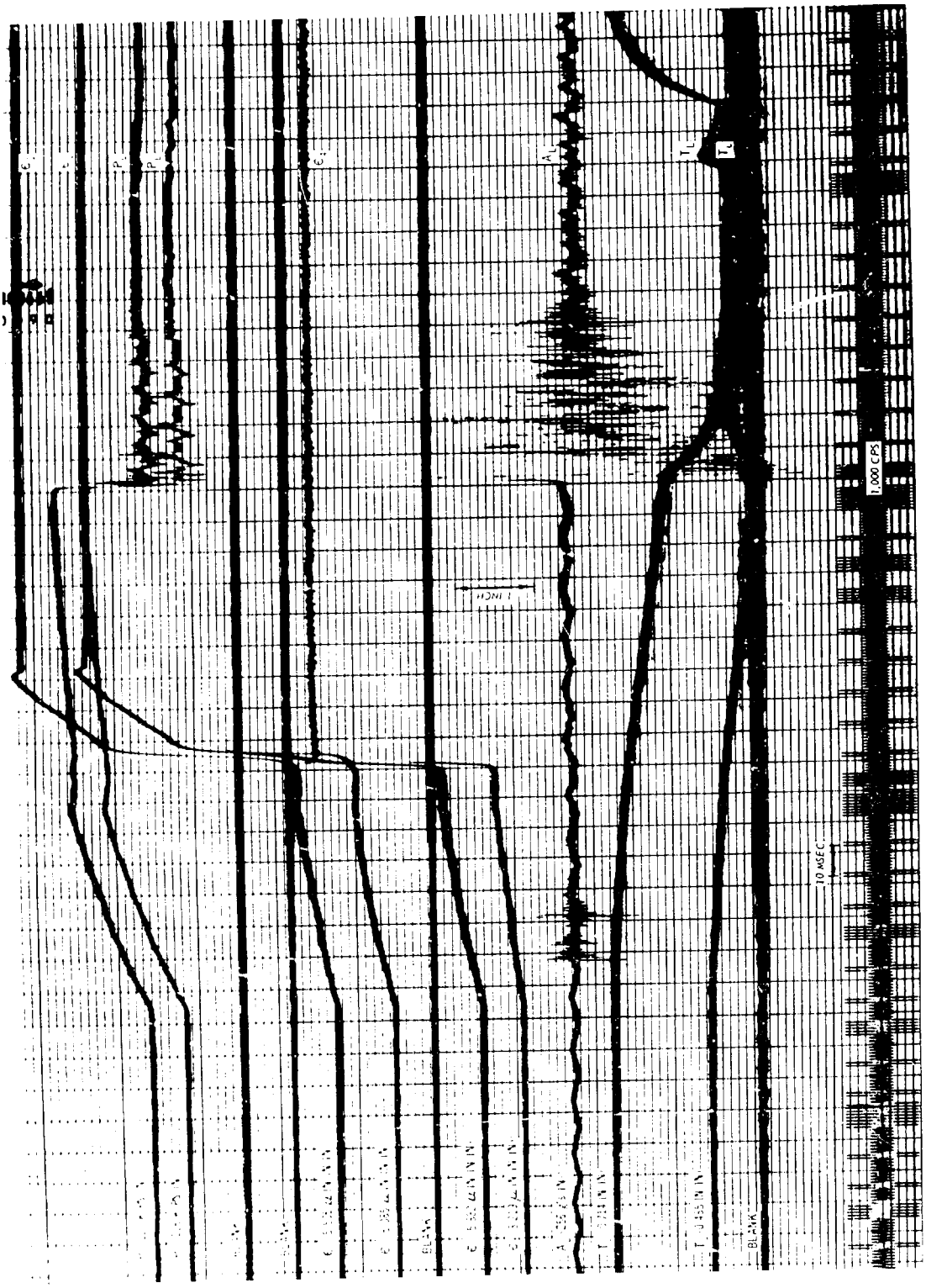

Figure A.12 Cadweld splice, Grade 60, intermediate load rate, Test 169.

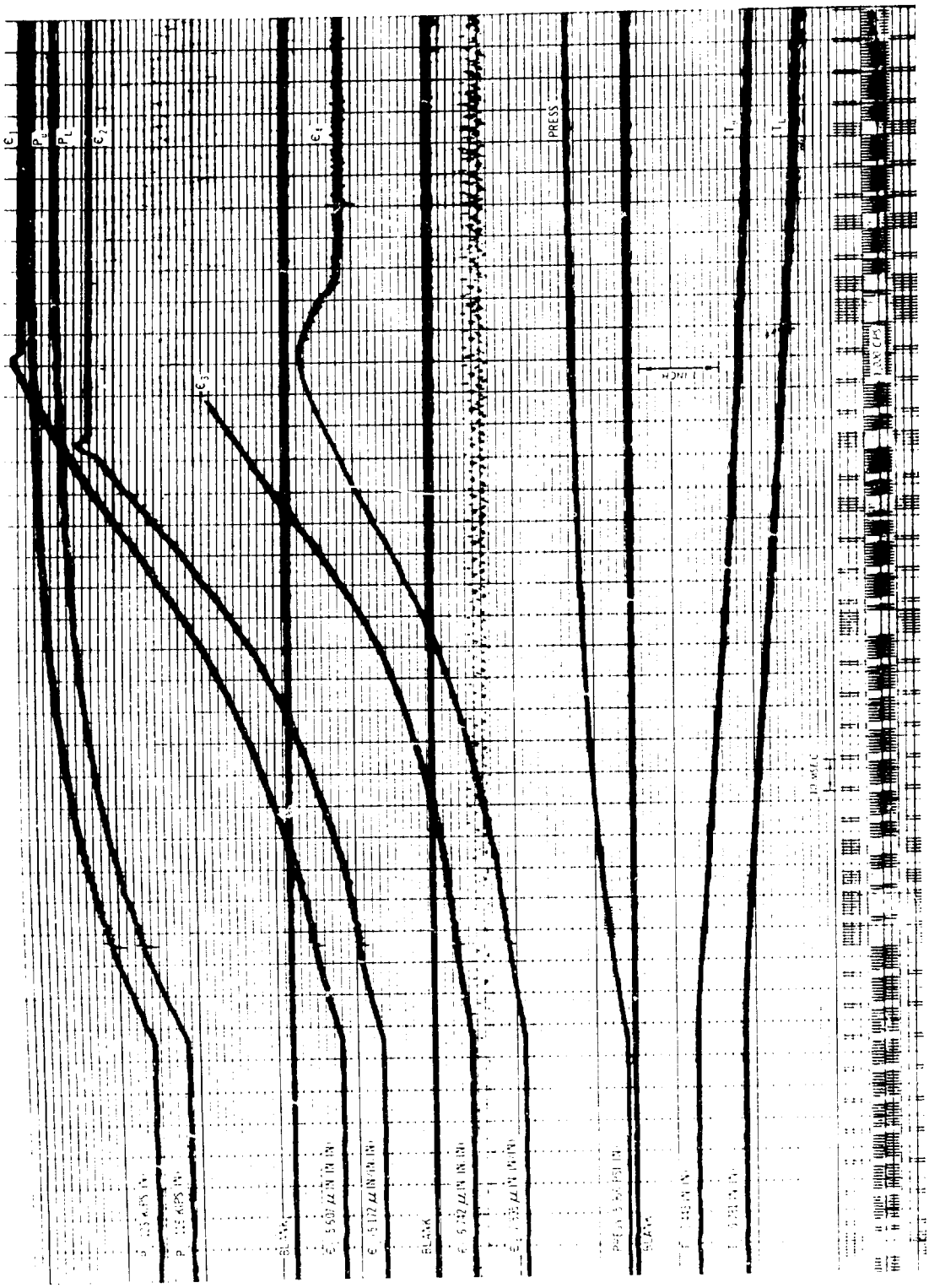

Figure A.13 Cadweld splice, Grade 75, intermediate load rate, Test 179.

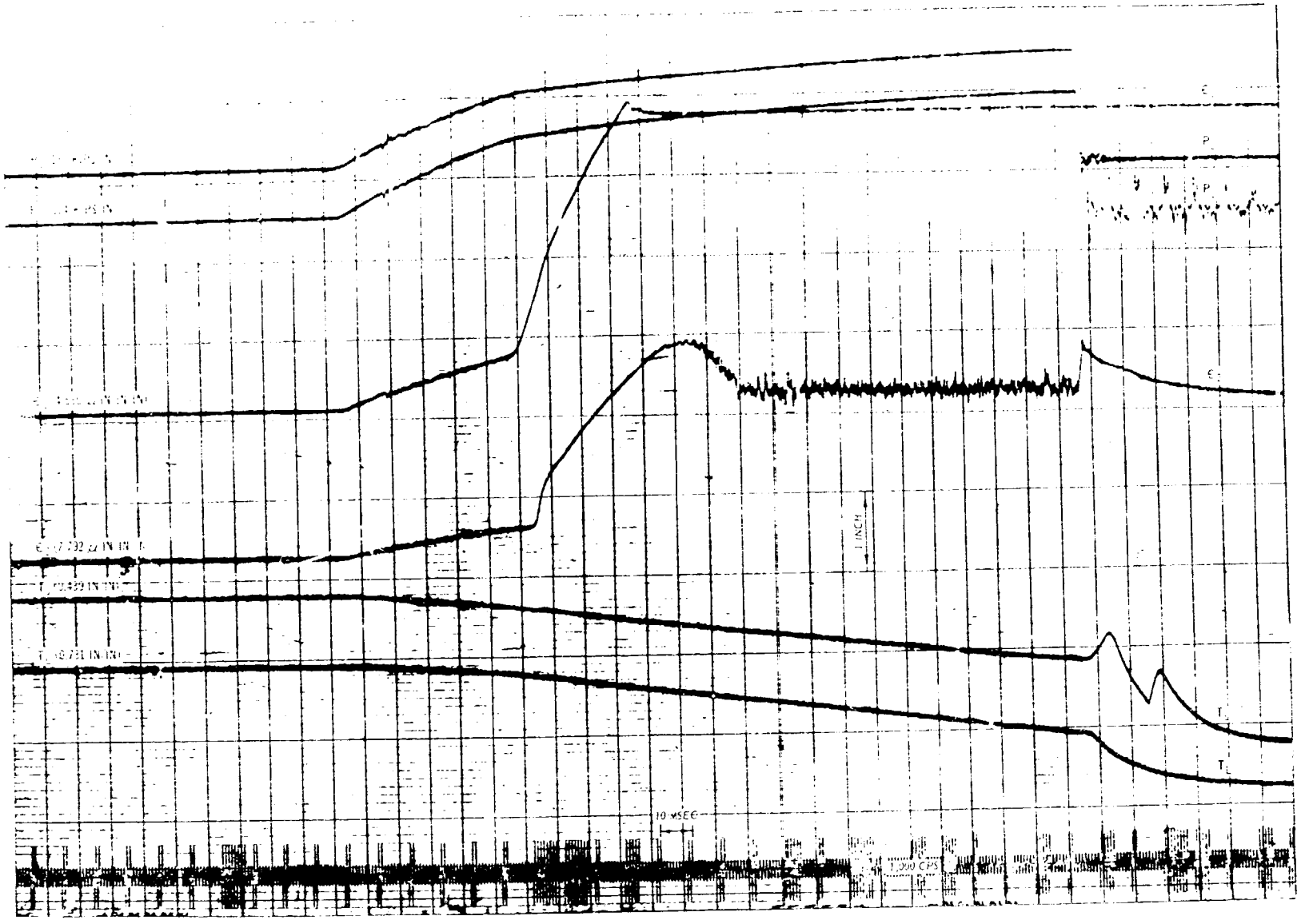

Figure A.14 Cadweld splice, Grade 75, intermediate load rate, Test 202.

Unclassified

Security Classification

DOCUMENT CONTROL DATA - R & D

(Security classification of title, body of abstract and indexing annotation must be entered when the overall report is classified)

1. ORIGINATING ACTIVITY (Corporate author)	2a. REPORT SECURITY CLASSIFICATION
U. S. Army Engineer Waterways Experiment Station Vicksburg, Mississippi	Unclassified
	2b. GROUP

3. REPORT TITLE

DYNAMIC TESTS OF LARGE REINFORCING BAR SPLICES

4. DESCRIPTIVE NOTES (Type of report and inclusive dates)

Final report

5. AUTHOR(S) (First name, middle initial, last name)

William J. Flathau

6. REPORT DATE	7a. TOTAL NO. OF PAGES	7b. NO. OF REFS
April 1971	190	35

8a. CONTRACT OR GRANT NO.	9a. ORIGINATOR'S REPORT NUMBER(S)
b. PROJECT NO.	Technical Report N-71-2
c.	9b. OTHER REPORT NO(S) (Any other numbers that may be assigned this report)
d.	

10. DISTRIBUTION STATEMENT

Approved for public release; distribution unlimited.

11. SUPPLEMENTARY NOTES	12. SPONSORING MILITARY ACTIVITY
Report also submitted to Mississippi State University, State College, Mississippi, as thesis for degree of Master of Science in Civil Engineering	U. S. Army Engineer Division, Huntsville Huntsville, Alabama

13. ABSTRACT

Dynamic tensile tests were conducted at rapid, intermediate, and slow rates of strain on specimens of No. 11 reinforcing bars of Grades 60 and 75 A615 billet steel. As-rolled bars, machined bars, butt-welded splices, Thermit splices, and Cadweld splices were prepared. The as-rolled and machined specimens were tested primarily to determine the tensile strength characteristics of the Grades 60 and 75 bars for use when assessing how effective the various spliced specimens were when tested. All tests were conducted in a 200,000-pound-capacity dynamic loader. Under all loading rates, the breaking strength for all three splice types was greater than the 125 percent of nominal yield required by standards set forth by the American Concrete Institute, the American Welding Society, and the Concrete Reinforcing Steel Institute. Apparently, however, the heat produced by the three splicing methods appreciably reduced the ductility of all spliced bars. The strains in the bars when any of the splice types failed were generally less than 25 percent of the maximum strain achieved by the as-rolled or machined bars at rupture. Very few of the spliced bars met ASTM standards for minimum elongations of 7 and 5 percent, respectively, for Grades 60 and 75 bars. The butt-welded splices, Thermit splices, and Cadweld splices all performed satisfactorily under rapid rates of loading. However, it is believed that better quality control can be achieved at a lesser cost using either a Thermit or Cadweld splice in lieu of a butt-welded splice. The Grade 60 bars were more ductile than the Grade 75 bars and were also more sensitive to the influence of strain rate on the dynamic strength of the bars tested. An optical tracker was used to measure postyield strains for all the specimen types. This device made it possible, especially in the rapid strain rate tests, to measure successfully the strains across the various spliced specimens.

DD FORM 1 NOV 1473 REPLACES DD FORM 1473, 1 JAN 64, WHICH IS OBSOLETE FOR ARMY USE.

Unclassified

Security Classification

14. KEY WORDS	LINK A		LINK B		LINK C	
	ROLE	WT	ROLE	WT	ROLE	WT
Bar splices						
Dynamic tests						
Reinforcing steels						
Splices						
Steel bars						